Dissertation

submitted to the
Combined Faculty of Natural Sciences and Mathematics
of the Ruperto Carola University Heidelberg, Germany
for the degree of
Doctor of Natural Sciences

Presented by

Lucia Cassella, M.Sc. in Biology
born in Como, Italy

Oral examination date:
27th of July, 2020

# Landscape and functions of RNA localization in the *Drosophila* follicular epithelium

Examiners:

Dr. Justin M. Crocker

Prof. Dr. Ana Martin-Villalba

*Et quid amabo nisi quod aenigma est?*

Giorgio de Chirico

# Table of contents

# Acknowledgements

When I started my PhD at EMBL, it was a bit of a shock. I was coming from a humble Italian University, and the only lab I was familiar with was incredibly unequipped, but run by people with a great heart, who instilled in me the passion for research. When I came to EMBL, I encountered a totally different world, with amazing facilities and services, and extremely intelligent people with a big passion for science. I felt part of a community and this made me grew immensely, from both scientific and personal point of view. I am deeply grateful to Anne, my supervisor, for giving me the opportunity to be part of this experience and for shaping my scientific personality. Thank you for always supporting me with great humanity.

I would like to thank all members of my TAC, Justin Crocker, Ana Martin-Villalba, Martin Beck, and Kathi Zarnack, for giving me useful feedbacks for my project. A special thank you goes to Kathi, who guided me in the murky world of bioinformatics. I am also grateful to Maria Leptin and Georg Stoecklin, who accepted to be in my defense committee.

The birth and the development of this project would have not been possible without the help of Stefan Terjung (ALMF) with the set-up of the LCM microscope at EMBL, and the GeneCore Facility for providing the sequencing of my libraries. Thanks to Juan Manuel Gomez-Elliff and Andre Schwartz, for making my experiments easier. Finally, thanks to Wolfgang Huber, Bernd Klaus, Charles Girardot for useful technical and scientific advice.

Last but not least, a big thank you to all past and present members of the Ephrussi lab I had the pleasure to encounter in my PhD, for giving me useful scientific feedbacks, guidance, and real friendship. I would like to thank in particular Anna, for all the help with the flies, and Ale, for being always helpful, and a true friend. Thank you both for all the effort spent taking care of my flies during the shutdown. Thanks to Simone, for correcting my summary in German, and for the wonderful time we had together with Jane at that crazy rodeo in the US. Thanks to Brana, Vaishali, and Jane for making my PhD a bit less serious.

I would have probably gone crazy without my favorite hobby: the kicker. However, if this has been my salvation, it was all because of a few friends that grew this passion with me: Luigi, Sharaz, Ewa, Kuba, Jacob, and many others that eventually were too scared to continue playing with us ☺

Grazie a tutta la comunità di italiani all'EMBL e per gli Italian party, in cui mi sono sentita a casa. Grazie a Sergio, Alessio, Matteo, Elisabetta, Federico, per aver condiviso insieme questo percorso. Un grazie anche al gruppo del wine tasting, anche se io non c'ho mai capito niente, venivo solo per la compagnia e l'alcol.

Infine, grazie alle persone che mi sono state più vicine. Poche righe non bastano per ringraziarvi per tutto quello che sono diventata grazie a voi. A Luigi, che è rimasto sempre al mio fianco, e mi ha salvato dal primo momento. Ai miei amici di una vita, ormai sparsi per il mondo, ma col cuore sempre al 35 di via Rovelli. A Sergio, un membro della famiglia. Infine, ai miei genitori, che nonostante la lontananza mi sono sempre vicini, e che mi hanno donato la curiosità, una mentalità aperta, e la passione per il mondo.

# Summary

The mechanisms and roles underlying the phenomenon of RNA localization in differentiated tissues are poorly characterized. *Drosophila* follicular epithelium represents a good model to study RNA localization in the context of an adult tissue, for several reasons. First, it expresses the dynein/BicD/Egl RNA localization machinery, which transports RNAs to the apical domain. Second, it is genetically tractable, offering the possibility to generate mutant clones for a gene of interest in a mosaic manner. So far, only a handful of mRNAs showing a subcellular localization pattern in the follicular epithelium have been reported, and the extent and significance of the phenomenon are not known. To address this, I applied a spatial transcriptomics approach to identify the mRNAs that show apical or basal localization patterns in this tissue. Laser-capture microdissection (LCM) followed by RNA-seq and bioinformatic analysis allowed the identification of 520 differentially enriched mRNAs in either the apical or the basal domain. Gene Ontology (GO) enrichment analysis showed a functional compartmentalization of mRNAs in different cellular domains, suggesting that mRNAs encoding components of the same organelle or pathway might be locally translated.

Next, I investigated the mechanisms that govern apical and basal RNA localization in the follicular epithelium, by knocking down components of known microtubule (MT) minus end- and plus end-directed RNA transport. I found that apical RNA localization is achieved mainly by the activity of the dynein/BicD/Egl RNA transport machinery, but that at least one mRNA (*BicD*) is localized apically by another MT-based mechanism. On the other hand, basal RNA localization is dependent on kinesin-1 and, in some cases, is regulated by the deposition of the Exon Junction Complex (EJC), reminiscent of the mechanisms that underlie *oskar* RNA localization to the posterior pole. Interestingly, disrupting kinesin-1 by *Khc* RNAi causes basal mRNAs to localize apically. Taking *zipper* (*zip*) mRNA as a model, I have shown that such apical mislocalization of a basal RNA depends on *egalitarian* (*egl*), but that the basal RNA's localization is not affected upon sole knock-down of *egl*. Based on this, I propose a model whereby the localization of basal mRNAs is

accomplished by kinesin-1, which counteracts a default apical RNA transport pathway by inhibiting the activity of the dynein/BicD/Egl machinery.

Finally, I investigated the role of Egl in apical localization of *Imp* mRNA by analyzing *eglRNAi* follicle cell clones and measuring the hatching rate of eggs generated from egg-chambers subjected to *egl* RNAi in the follicle cells. Upon *egl* RNAi, *Imp* mRNA is mislocalized without impact on Imp protein levels, suggesting that *Imp* mRNA is not translationally repressed while in transport by the dynein/BicD/Egl machinery. Furthermore, absence of Egl in the follicle cells caused only a small reduction in egg hatching rate. Taken together, these results suggest that the Egalitarian-mediated transport is necessary to enrich mRNAs apically and create an apical protein gradient, and that the mild phenotype observed in the egg hatching rate might be due to residual apical localization of Imp protein upon *egl* RNAi. It is possible that *egalitarian*-dependent apical localization of mRNAs in the follicular epithelium becomes important in conditions of stress encountered by fruit flies in a natural environment.

# Zusammenfassung

Die Mechanismen und Funktionen, die dem Phänomen der RNA-Lokalisation in differenzierten Geweben zugrunde liegen, sind schlecht charakterisiert. Das follikuläre Epithel von *Drosophila* ist aus mehreren Gründen ein gutes Modell zur Untersuchung der RNA-Lokalisation im Kontext eines adulten Gewebes. Erstens exprimiert es die Dynein/BicD/Egl-Lokalisationsmaschinerie, die RNAs zur apikalen Domäne transportiert. Zweitens ist es genetisch manipulierbar und bietet die Möglichkeit, mutierte Klone für ein Gen von Interesse auf mosaikartige Weise zu erzeugen. Bisher wurde nur über eine Handvoll mRNAs berichtet, die ein subzelluläres Lokalisationsmuster im Follikelepithel aufweisen, aber das Ausmaß und die Bedeutung des Phänomens sind nicht bekannt. Um dies aufzuklären, habe ich räumliche Transkriptomik angewendet, um mRNAs zu identifizieren, die apikale oder basale Lokalisationssmuster in diesem Gewebe aufweisen. Laser-Capture-Mikrodissektion (LCM), gefolgt von RNA-seq und bioinformatischer Analyse ermöglichte die Identifizierung von 520 entweder in der apikalen oder in der basalen Domäne differentiell angereicherten mRNAs. Die Gene Ontology (GO)-Anreicherungsanalyse zeigte eine funktionelle Kompartimentierung von mRNAs in verschiedenen zellulären Domänen, was darauf hindeutet, dass mRNAs, die Komponenten desselben Organells oder desselben Reaktions- oder Signalweges codieren, lokal translatiert werden könnten.

Als nächstes untersuchte ich die Mechanismen, die der apikalen und basalen RNA-Lokalisation im Follikelepithel zu Grunde liegen, durch Gen-Knock-downs bekannter Komponenten des Mikrotubuli (MT) minus-Ende- und plus-Ende-gerichteten RNA-Transports. Ich fand heraus, dass die Lokalisation apikaler RNA hauptsächlich durch die Aktivität der Dynein/BicD/Egl-RNA-Transportmaschinerie erreicht wird, aber dass mindestens eine mRNA (*BicD*) durch einen anderen MT-basierten Mechanismus apikal lokalisiert wird. Des Weiteren hängt die basale RNA-Lokalisation von Kinesin-1 ab und wird in einigen Fällen durch die Ablagerung des Exon Junction Complex (EJC) auf der RNA reguliert, was an die zugrundeliegenden Mechanismen der Lokalisation von *oskar*-RNA zum posterioren Pol der *Drosophila* Eizelle erinnert. Interessanterweise führt die Störung der Funktion von Kinesin-1

durch *Khc* RNAi dazu, dass basale mRNAs apikal lokalisiert werden. Anhand der *zipper* (*zip*) mRNA als Modell habe ich gezeigt, dass eine solche apikale Fehllokalisation einer basalen RNA von *egalitarian* (*egl*) abhängt, die Lokalisation der basalen RNA jedoch nicht durch den alleinigen Knock-down von *egl* beeinflusst wird. Auf dieser Grundlage schlage ich ein Modell vor, bei dem die Lokalisation basaler mRNAs durch Kinesin-1 bewirkt wird, welches einem apikalen Standardtransportweg für RNAs entgegenwirkt, indem es die Aktivität der Dynein/BicD/Egl-Maschinerie hemmt.

Schließlich untersuchte ich die Rolle von Egl bei der apikalen Lokalisation von *Imp* mRNA, indem ich *eglRNAi*-Follikelzellklone analysierte und die Schlupfrate von Eiern maß, die sich aus Eikammern mit *eglRNAi*-Follikelzellen entwickelten. Bei *egl* RNAi wird *Imp* mRNA ohne Einfluss auf die Imp-Proteinmengen falsch lokalisiert, was darauf hindeutet, dass *Imp* mRNA während des Transports durch die Dynein/BicD/Egl-Maschinerie nicht translatorisch unterdrückt wird. Darüber hinaus verursachte das Fehlen von Egl in den Follikelzellen nur eine geringe Reduzierung der Schlupfrate. Zusammengenommen legen diese Ergebnisse nahe, dass der durch Egl vermittelte Transport notwendig ist, um mRNAs apikal anzureichern und einen apikalen Proteingradienten zu erzeugen, und dass der milde Phänotyp, der bei der Schlupfrate der Eier beobachtet wird, möglicherweise auf trotz *egl* RNAi verbleibende, geringe Mengen an apikalem Imp-Protein zurückzuführen ist. Es ist möglich, dass die *egalitarian*-abhängige apikale Lokalisation von mRNAs im Follikelepithel unter Stressbedingungen wichtig wird, denen Fruchtfliegen in einer natürlichen Umgebung ausgesetzt sind.

# List of Abbreviations

| | | | |
|---|---|---|---|
| A | Apical domain | EJC | Exon Junction Complex |
| A-D | Anterior-Dorsal | FC | Follicle cell |
| A-V | Animal-Vegetal | FDR | False Discovery Rate |
| A/B | Apical-Basal | FE | Follicular epithelium |
| A/P | Anterior-Posterior | *ftz* | *fushi tarazu* |
| B | Basal domain | GLS | Gurken Localization Signal |
| *bcd* | *bicoid* | GO | Gene Ontology |
| bg | background | *grk* | *gurken* |
| *BicD* | *Bicaudal-D* | GSC | Germline stem cell |
| *BicD-RC* | *BicD*-isoform RC | *h* | *hairy* |
| BLE | Bicoid Localization Element | *insc* | *inscuteable* |
| BRE | Bruno Response Element | Khc | Kinesin heavy chain |
| *btsz* | *bitesize* | Klc | Kinesin light chain |
| CC1 | Coiled coil 1 | *Kr* | *Kruppel* |
| CC2 | Coiled coil 2 | LCM | Laser-Capture Microdissection |
| CC3 | Coiled coil 3 | LE | Localization Element |
| Chc | Clathrin heavy chain | *Lis-1* | *Lissencephaly-1* |
| *crb* | *crumbs* | m.f.i. | Mean fluorescence intensity |
| CTD | C-terminal domain | METRO | Message Transport Organizer |
| D/V | Dorsal-Ventral | MT | Microtubule |
| Dhc | Dynein heavy chain | MTOC | Microtubule organizing center |
| dm6 | Drosophila melanogaster release 6 | NGF | Nerve Growth Factor |
| DOL | Degree of labelling | NMD | Non-sense mediated decay |
| EGFR | Epidermal Growth Factor Receptor | *nos* | *nanos* |
| *egl* | *egalitarian* | OES | Oocyte Entry Signal |
| eIF4E | eukaryotic Initiation Factor 4E | *osk* | *oskar* |
| P-body | Processing body | | |

| | |
|---|---|
| PCA | Principal Component Analysis |
| *pcnt* | *pericentrin* |
| PGC | Primordial germ cell |
| *pros* | *prospero* |
| *Pym* | *Partner of Y14-MAGO* |
| RBP | RNA-binding protein |
| RNAi | RNA interference |
| ROI | Region of interest |
| *sdt* | *stardust* |
| shRNA | short hairpin RNA |
| smFISH | single-molecule Fluorescence in situ Hybridization |
| SOLE | Spliced Oskar Localization Element |
| SRE | Smaug Response Element |
| SSC | Somatic stem cell |
| *stau* | *staufen* |
| TdT | Terminal deoxynucleotidyl transferase |
| TGF-α | Transforming Growth Factor-α |
| *tj* | *traffic jam* |
| TLS | Transport/Localization Sequence |
| *Tm1-I/C* | Tropomyosin 1-isoform I/C |
| *upd* | *unpaired* |
| UTR | Untranslated region |
| *wg* | *wingless* |
| wt | wild-type |
| ZBP | Zipcode Binding Protein |
| *zip* | *zipper* |

# Chapter 1: Introduction

## 1.1 Overview of RNA localization

RNA localization is a type of post-transcriptional regulation that allows the spatial and temporal restriction of gene expression within a polarized cell. RNA molecules subjected to this type of regulation become localized in a precise subcellular compartment after nuclear export, while they are typically in a repressed state. Once they reach their final destination, translational inhibition is released and the protein can be locally produced.

Localized gene expression in the cell is thought to serve to several purposes. First, it allows the cell to save energy: localized mRNAs can undergo several rounds of translation, resulting in a more economical way to achieve local protein concentration than by localizing single proteins. Second, localized translation allows the restriction of protein activity to the specific subcellular compartment where the protein is needed. This can promote the local assembly of protein complexes and the local activation of signaling pathways. Third, RNA localization allows local subcellular concentration of proteins whose ectopic expression might be toxic. Fourth, localized transcripts that remain in a translationally repressed state may be quickly released from inhibition by an external signal, eliciting a rapid localized cellular response.

The first report of a localized RNA dates back to 1983, when *actin* mRNA was found to be preferentially accumulated in the myoplasm and ectoplasm of ascidian eggs and later distributed only in those cells giving rise to mesoderm (Jeffery et al., 1983). Later, a handful of mRNAs were shown to localize in different cell types and organisms, and it was realized that mRNA localization plays crucial roles during development. However, only until recently it became clear that RNA localization is a widespread phenomenon in polarized cells, thanks to the development of high-throughput technologies that allowed genome-wide screens (Shepard et al., 2003; Blower et al., 2007; Lecuyer et al., 2007; Mili et al., 2008; Jambor et al., 2015; Wilk et al., 2016). In particular, this led to the striking discovery that 70% of mRNAs expressed during early *Drosophila* embryogenesis are localized in a variety of

subcellular patterns (Lecuyer et al., 2007). This finding opened the possibility that RNA localization is a prevalent mechanism to regulate gene expression in space and time.

In the past years, the mechanisms and functions of RNA localization have been well characterized in oogenesis and early embryogenesis, when the subcellular deposition of polarity determinants is crucial to establish embryonic patterns. However, only little is known about the significance of RNA localization in later development and differentiated tissues, with the exception of neurons.

## 1.2 Roles of RNA localization in oogenesis and early embryogenesis

Most of the functions and mechanisms of RNA localization have been discovered through pioneering studies in eggs end early embryos. Oocytes are large cells that accumulate maternally-provided mRNAs, proteins and organelles. The deposition of maternal products in localized subcellular compartments is crucial for a correct patterning of the future embryo; localized determinants can be partitioned into selected blastomeres through cell division. For this reason, mRNA localization in early development likely evolved as a means to spatially restrict gene expression and form heterogenous specialized cytoplasmic domains that functionally differ within large cells. In parallel, the polarity of the cytoskeleton and its organization plays fundamental roles in directing RNA transport to different cell compartments. *Drosophila* and *Xenopus* early development illustrate these characteristics and, as models, have provided invaluable insights into the mechanisms and functions of RNA localization.

### *1.2.1* Establishment of embryonic axes in *Drosophila*

The best characterized examples of essential functions of RNA localization during development were discovered in *Drosophila*. Here, RNA localization is responsible for the establishment of the anterior-posterior (A/P) and dorsal-ventral (D/V) axes of the embryo, as well as the correct spatial patterning of embryonic structures and germ cell formation. The establishment of the future A/P and D/V axes of the embryo happens during oogenesis, and depends on the deposition of maternally produced RNA determinants in the developing oocyte. Subcellular targeting of *bicoid*

(*bcd*), *gurken* (*grk*), *oskar* (*osk*), and *nanos* (*nos*) mRNAs in the developing oocyte represents key events for a correct embryonic development (Figure 1.1).

*Drosophila* oogenesis consists of 14 stages, defined on the basis of morphological features of the developing egg-chambers within the ovary (Figure 1.1). Egg-chambers develop in ovarioles, the functional units of oogenesis, and are organized in developmental order from anterior to posterior. Egg-chambers are composed of two main tissues: the germline, a syncytium that comprises 15 nurse cells and one posteriorly-positioned oocyte, and the soma, a monolayer of follicular epithelium surrounding the germline. The function of nurse cells is to produce cellular components (mRNAs, proteins, organelles) that are transferred to the transcriptionally silent oocyte during oogenesis.

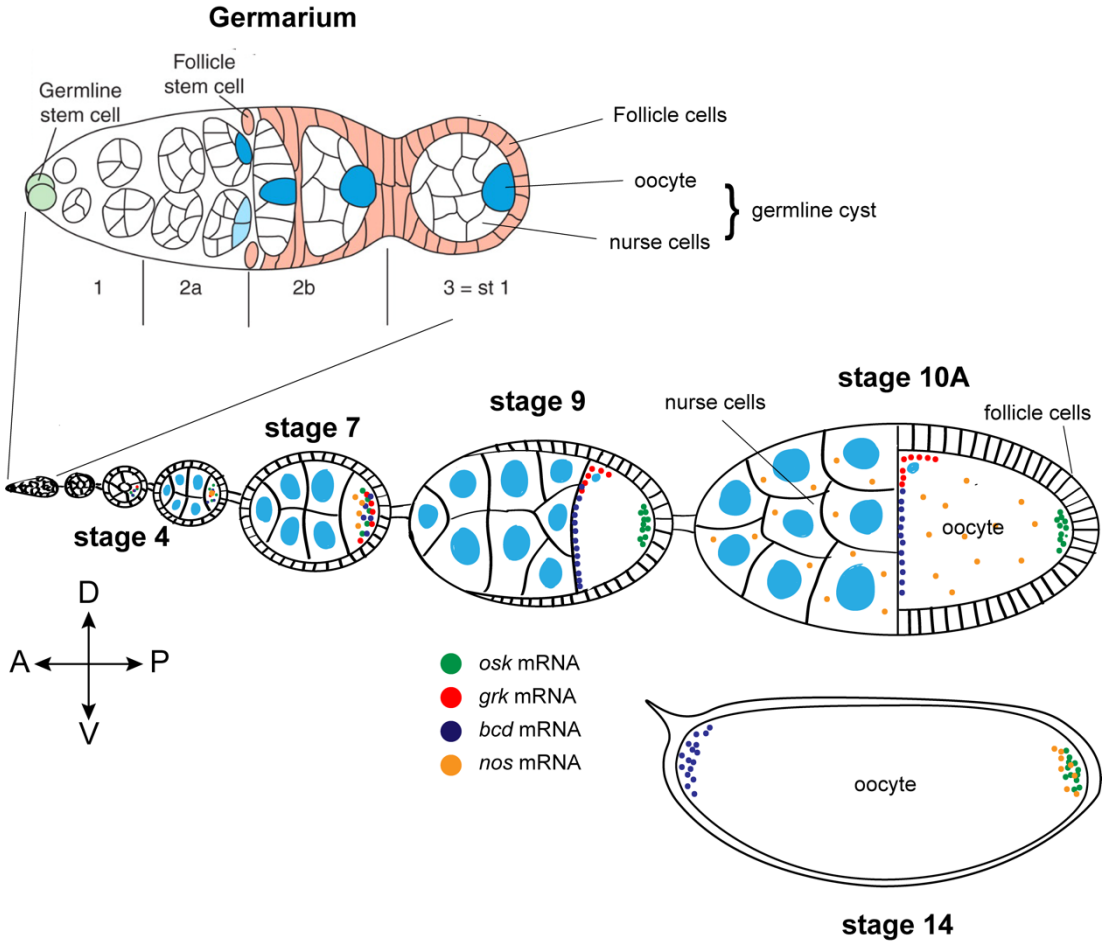


**Figure 1.1 - *Drosophila* oogenesis** (adapted from Roth and Lynch, 2009).

Oogenesis starts in the germarium (composed of region 1, 2a, and 2b), a structure that contains both the germline stem cells (GSCs, which will give rise to 15 nurse cells and the oocyte) and the somatic stem cells (SSCs, also called follicle cell stem cells),

which will generate all somatic cell types. In the germarium, the asymmetric division of the GSC gives rise to a cystoblast, which undergoes 4 rounds of cell division with incomplete cytokinesis; concomitantly, daughter cells produced from SSC divisions encapsulate the 16-cell cyst. Cyst encapsulation is completed in region 2b of the germarium, and a single egg-chamber with a posteriorly localized oocyte emerges, establishing the onset of stage 1 (also called region 3 of the germarium) of oogenesis (Figure 1.1).

The establishment of the A/P axis of the future embryo begins early during oogenesis, when *grk, bcd,* and *osk* mRNAs are transported from the nurse cells to the oocyte and are localized at the posterior-most part of the oocyte, between the nucleus and the overlying follicle cells. *grk* mRNA is then translated into Grk protein, a Transforming Growth Factor alpha (TGF-α)-like secreted protein. Here, Grk binds to Torpedo, an Epidermal Growth Factor Receptor (EGFR) expressed on the surface of the overlying follicle cells. This triggers a posteriorizing fate in the follicle cells, which send back to the oocyte a still unknown signal that induces reorganization of the oocyte cytoskeleton (Gonzalez-Reyes et al., 1995; Roth et al., 1995). The rearrangement of the cytoskeleton is crucial for the subsequent localization of *osk* to the posterior and of *bcd* mRNA to the anterior of the oocyte.

Loss-of-function mutants, as well as injection and targeting of maternal mRNAs to ectopic sites in the embryo, have been instrumental to understand the role of morphogenetic gradients initiated by RNA localization in embryonic patterning. For example, when *bcd* is ectopically expressed at the posterior, the embryo produces two heads and no tail; on the other hand, embryos lacking *bcd* do not develop a head, but posterior terminal structures (Frohnhoefer and Nüsslein-Volhard, 1986; Driever et al., 1990). Furthermore, when *osk* is ectopically expressed at the anterior, the embryo produces two tails and lacks anterior structures (also called “bicaudal” embryo). Conversely, embryos that are mutant for *osk* do not produce any posterior structures (Lehmann and Nüsslein-Volhard, 1986; Ephrussi and Lehmann, 1992). These and other experiments led to the discovery that the localization of *bcd* mRNA to the anterior of the oocyte allows the specification of head structures in the future embryo; conversely, the posterior accumulation of *osk* and *nos* mRNAs determine the specification of abdominal and posterior structures.

Importantly, *bcd*, *osk*, and *nos* mRNAs are translated in different time frames during development. While *bcd* is translationally silent during oogenesis, *osk* starts to be translated from stage 9 at the posterior of the oocyte (Ephrussi et al., 1991; Kim-Ha et al., 1991). On the other hand, Nos protein is dynamically expressed during oogenesis (Wang et al., 1994; Forrest et al., 2004). Translation of *nos* mRNA at the posterior of the oocyte requires Osk protein, which binds *nos* mRNA and activates its translation in the developing egg after ovulation and fertilization. At the same time, *bcd* is translated at the anterior (Salles et al., 1994). The defects associated to abdominal patterning observed in *osk* mutants represent an indirect effect due to a failure in either *oskar*-dependent localization of *nos* or expression of *nos* at the posterior (Gavis and Lehmann, 1994).

The establishment of the D/V axis of the future embryo is also dependent on *grk* RNA localization. Following reorganization of the microtubule cytoskeleton as a result of *grk* signaling to the posterior follicle cells, the nucleus and the associated *grk* mRNA move to the dorsal-anterior corner of the oocyte. Here, Grk protein binds to Torpedo/Egfr on the overlying follicle cells, which become specified to acquire a dorsal fate by repressing *pipe*; later in egg development, dorsal follicle cells will form specialized eggshell structures (dorsal appendages and micropyle). In parallel, absence of EGFR signaling in the ventral follicle cells allows activation of *pipe* expression. Expression of *pipe*, in turn, activates an extracellular serine protease cascade that eventually culminates with the expression of Dorsal, resulting in the ventralization of *pipe*-expressing follicle cells. Grk acts as a morphogen in establishing the D/V axis of the egg. Indeed, loss-of-function mutations in *grk* or *torpedo* cause ventralization of the egg, with reduced formation of dorsal appendages; conversely, mislocalization of *grk* mRNA to the oocyte anterior induces a dorsalized phenotype, with loss of ventral structures (Neuman-Silberberg and Schüpbach, 1993).

### 1.2.2 Increased nuclear uptake of pair-rule proteins in *Drosophila*

During the early stages of *Drosophila* embryogenesis a series of nuclear divisions occur in the absence of cell division, creating a syncytium called syncytial blastoderm. At stage 10, dividing nuclei that until this stage are distributed throughout the center of the embryo, start migrating to the cell periphery together with their associated cytoplasmic domain, where they continue dividing. Following stage 13, the

membrane of the embryo starts invaginating, creating a furrow between the nuclei positioned at the cell periphery and resulting in the formation of a single epithelial layer at the periphery of the embryo (cellular blastoderm).

During syncytial blastoderm stage, the localized expression of maternal effect genes results in the transcriptional activation of a set of zygotic genes (called "gap" genes) in partially overlapping embryonic domains. Different combinations and concentrations of gap gene products, in turn, allow the transcription of pair-rule genes and segment polarity genes in a striped expression pattern, that controls the segmentation hierarchy of the embryo.

While the mRNAs encoding gap genes are ubiquitously localized, pair-rule transcripts (*hairy*, *even-skipped*, *fushi tarazu*) are localized apically, in a narrow space between the nucleus and the plasma membrane (Hafen et al., 1984; Davis and Ish-Horowicz, 1991) (Figure 1.2). Apical localization of pair-rule mRNAs and subsequent apical translation was thought to restrict the lateral diffusion of the protein, allowing a precise spatial control of segmentation pattern (Davis and Ish-Horowicz, 1991). However, a later study showed that apical targeting of pair-rule mRNAs is required for efficient protein production. Indeed, disruption of their apical RNA localization causes reduced apical expression (Bullock et al., 2004). The segmentation defects observed in these embryos are related to a decrease in pair-rule activity rather than ectopic gene expression due to expansion of their expression domains. This led to the hypothesis that localized apical expression of pair-rule mRNAs increases nuclear uptake of the protein. Indeed, localization to the narrow apical cytoplasm would allow protein molecules to diffuse shorter distances in their way back to the nuclei, where they function as transcription factors (Bullock et al., 2004).

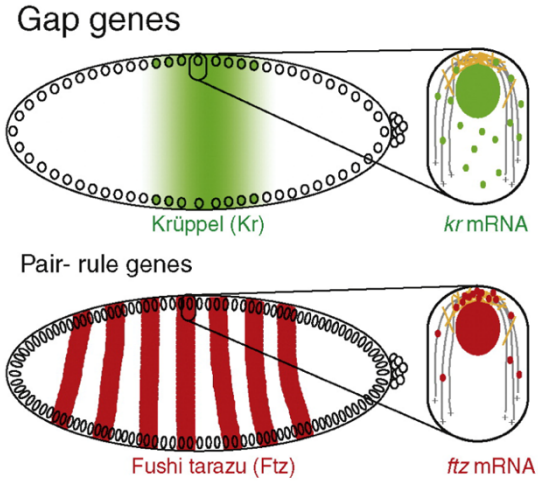


**Figure 1.2 - Subcellular localization of gap (*Kruppel*) and pair-rule (*fushi tarazu*) mRNAs in the blastoderm embryo** (adapted from Meignin and Davis, 2010).

### 1.2.3 Fate specification in *Xenopus*

As it does in *Drosophila*, RNA localization of axis determinants in *Xenopus* occurs during oogenesis. The first axis formed is the animal-vegetal (A-V) axis, which establishes structural cytoplasmic asymmetry. While the pigmented animal hemisphere contains the nucleus, the vegetal hemisphere contains mainly yolk. RNAs are differentially localized in the oocyte during early oogenesis, and this involves different developmentally regulated pathways (Kloc and Etkin, 1995). The early MEssage TRansport Organizer (METRO) pathway is activated in early stages (stages I-II), followed by the late pathway (stages III-IV). The METRO pathway is responsible for the localization of RNAs at the vegetal cortex encoding RNA-binding proteins (the *nanos*-related *Xcat2*, *Xdazl* and *DEAD-South*), that play a role in germ plasm specification later in development. Localized mRNAs that can be translationally silent for many months are stored in a cellular structure called mitochondrial cloud or Balbiani body, which contains ER and mitochondria. Similarly to *Drosophila* germ plasm, the *Xenopus* germ plasm determinants will be partitioned into the cells that become primordial germ cells (PGC), where they are required for PGC differentiation (Houston and King, 2000, Lai et al., 2011).

During the initial stages, *Vg1* (encoding a TGF-β growth factor) and *VegT* (encoding a T-box transcription factor) are ubiquitously distributed in the cytoplasm and excluded from the Balbiani body. Starting from stage III, *Vg1* and *VegT* mRNAs localize at the vegetal cortex of the embryo, where they are inherited by the vegetal blastomeres and are important for mesoderm and endoderm specification (Zhang et al., 1998; Birsoy et al., 2006).

## 1.3 Roles of RNA localization in later development and differentiated cells

In recent years, RNA localization was reported to occur in many differentiated cell types (Lecuyer et al., 2007) and its function in these tissues is starting to be uncovered. As in eggs and oocytes, RNA localization and localized translation has been reported to have important functions in large and highly polarized cells, such as neurons, which require to distribute cellular components long distances to accomplish spatially restricted and finely regulated functions, often in response to external stimuli. Indeed, many examples illustrate that localized gene expression is important in

different aspects of neuronal activity during development, plasticity, and regeneration. Interestingly, several studies showed that RNA and protein localization act synergistically or redundantly in ensuring localized protein accumulation, a phenomenon not well understood. Reported roles of RNA localization in later development include establishment/maintenance of cell polarity and epithelium integrity, efficient signaling and cell migration. Finally, changes in mRNA localization and local translation observed during nutritional stress in epithelial cells might underlie the ability to respond to an extracellular stimulus.

### 1.3.1 Stimulus-induced localized translation in neuronal function and cell migration

In *Alpysia* sensory-motor synapses, stimulation of the presynaptic neuron with serotonin induces the local translation of a neurite-localizing mRNA (*Sensorin*), whose activity is essential for long-term learning (Wang et al., 2009). Similarly, disruption of dendritic localization of *CamKIIα* mRNA resulted in long term-memory deficits in mice (Miller et al., 2002).

Development of sensory neurons induced by Nerve Growth Factor (NGF) triggers transcription of *bcl-w*, which prevents axonal degeneration *in vivo* (Courchesne et al., 2011). Upon NGF stimulation, newly transcribed *bcl-w* mRNAs are targeted to axons and translated upon continuous neurotrophin exposure. Here, locally translated Bcl-w prevents caspase-mediated axon degeneration (Cosker et al., 2013). Interestingly, NGF stimulates the translation of another mRNA localized in axons, *Par3*, which, in turn, promotes axon outgrowth (Hengst et al., 2009).

Local translation plays an important role in axonal growth cone guidance in *Xenopus* and mouse. *ß-actin* mRNA is transported to the growth cone in a translationally inhibited form by Zipcode-Binding Protein (*ZBP-1/IMP-1*); a guidance cue triggers a signal cascade that results in ZBP-1 phosphorylation and subsequent release of translation inhibition. Newly synthesized ß-actin enriched in microdomains is integrated into the growth cone, causing stimulus-dependent growth cone turning (Leung et al., 2006; Yao et al., 2006; Welshhans and Bassell, 2011) (Figure 1.3A). This is in accordance with the model proposed by Lin and Holt (2008), where growth cone steering results from the localized translation of a subset of mRNAs in the direction of the guidance cue.

Interestingly, localized translation of *ß-actin* mRNA is also required for cell migration (Kislauskis et al., 1997; Condeelis and Singer, 2005). In fibroblasts, *ß-actin* mRNA localizes to lamellipodia, actin-rich cell protrusions specialized for motility. Upon serum stimulation, newly-synthesized ß-actin promotes actin nucleation and contributes to cell migration. Interestingly, mRNAs encoding all seven subunits of the actin-regulator Arp2/3 complex have been found to be localized at cell protrusions together with *ß-actin* mRNA (Mingle et al., 2005), and their localization seems important for directional cell migration (Liao et al., 2011) (Figure 1.3B).

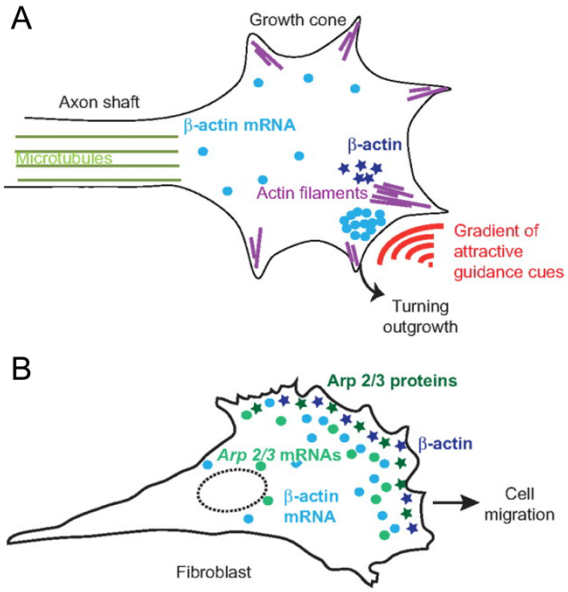


**Figure 1.3 – Localization of *ß-actin* mRNA in migrating cells.** A) Axonal growth cones. B) Migrating fibroblasts (adapted from Medioni et al., 2012).

### 1.3.2 Efficient signaling in *Drosophila*

A role of RNA localization in efficient apical secretion was identified in two different studies in *Drosophila* differentiated cells. Van De Bor and coworkers (2011) showed that down-regulation of components of the RNA transport machinery (dynein/BicD/Egl, see below) led to a decreased JAK/STAT signaling activity in border cells in the ovary, resulting in reduced cell migration. It has been proposed that efficient JAK/STAT signaling depends on the apical localization of *unpaired* (*upd)* mRNA in the neighboring polar cells, which, in turn, allows efficient translation of *upd* mRNA apically, where the protein is secreted (Van De Bor et al., 2011).

A direct role of RNA localization in regulating efficient signaling was discovered in a study on *wingless* (*wg*, ortholog of vertebrate WNT1) in *Drosophila*

embryonic epithelium. Here, Simmonds et al. (2001) found that the apical localization of *wg* mRNA is necessary for WNT signaling activity. By expressing different *wg* mRNA constructs differing in their ability localize along the apical-basal (A/B) axis of the cell, they found that only the apically-localized *wg* mRNA is able to efficiently induce autoregulatory-dependent increase in Wg expression levels and rescue cuticle defects observed in *wg* mutants. Interestingly, differently from pair-rule mRNAs, mislocalization of *wg* transcripts did not alter either the levels of the encoded protein, or its post-translational modifications. For this reason, the authors hypothesized that mRNA localization might be important to target *wg* transcripts to a specialized subcompartment (ER or Golgi) located in the apical domain for efficient Wg signaling (Simmonds et al., 2001).

### 1.3.3 Cell polarity and junction assembly in epithelia and neuroblasts

RNA localization was shown to contribute to A/B cell polarity in *Drosophila* follicular and embryonic epithelium. Both Crumbs (*crb*) and Stardust (*sdt*) are essential in the maintenance of polarity in the embryonic epithelium (Tepass and Knust, 1993) and are part of the same polarity complex. In two complementary studies it has been shown that apical localization of *crb* and *sdt* mRNAs contributes to the apical targeting of their encoded protein (Li et al., 2008; Horne-Badovinac and Bilder, 2008). In embryonic epithelia, the reduced apical targeting of *sdt* mRNA causes severe polarity defects. In contrast, although *sdt* mRNA is apically localized in the follicular epithelium, disruption of transcript localization only partially affects polarity (Horne-Badovinac and Bilder, 2008). On the other hand, targeting *crb* mRNA to the apical domain of the follicular epithelium is required to rescue the polarity phenotype observed in *crb* mutants (Li et al., 2008). Interestingly, endogenous wild-type *crb* gene activity is required for apical localization of exogenous Crb protein derived from a localization-defective *crb* mRNA. However, 1/3 of the cells expressing ubiquitously localizing *crb* RNAs in a *crb* mutant background still show apical Crb protein localization; thus, protein and mRNA localization appear to act redundantly in localization of Crb protein to the apical membrane (Li et al., 2008).

A/B polarity is essential for correct asymmetric cell division in neuroblasts, the neural stem cells in *Drosophila. Inscuteable* (*insc*) encodes an adaptor protein that binds to apical complex proteins and plays a role in inducing A/B spindle orientation. Additionally, it coordinates the basal sorting of cell fate determinants. Hughes and

colleagues (2004) found that *insc* mRNA is apically localized in interphase neuroblasts; disruption of *insc* mRNA apical localization through RNA interference (RNAi) against components of the RNA transport complex causes a reduction in apical Insc protein accumulation, which results in misorientation of neuroblast division and reduced spindle length (Hughes et al., 2004). Intriguingly, disruption of apical *insc* mRNA localization is not sufficient for a complete depletion of Insc protein apically, suggesting that additional mechanisms are involved to achieve Insc protein localization.

Interestingly, RNA localization and local translation are required for the assembly of epithelial junctions. In mammary epithelial cells, RNA localization of *ZO-1* mRNA is important for tight junction assembly (Nagaoka et al., 2012). *ZO-1* encodes a peripheral component of tight junctions and its mRNA is apically targeted by CPEB RNA binding protein. In the absence of CPEB, *ZO-1* mRNA is mislocalized and the protein randomly distributed; this causes defects in tight junction assembly and the subsequent loss of cell polarity. In another report, localized translation of *ß-actin* mRNA in MDCK epithelial cell line was shown to be required for adherens junction assembly but not maintenance (Gutierrez et al., 2014). Locally reduced levels of newly translated ß-actin monomers are insufficient to stimulate the linear filament polymerization that stabilizes adherens junction complex assembly at cell-cell contacts.

### 1.3.4 A role for RNA localization in the stress response?

Numerous studies in neurons have reported changes in RNA localization following external stimuli (Link et al., 1995; Rook et al., 2000; Tongiorgi et al., 1997; Grooms et al., 2006; Willis et al., 2007; Dictenberg et al 2008; Gumy et al., 2011; Steward et al., 1998; Steward and Worley, 2001; Smith et al., 2005; Yoon et al., 2016). Intriguingly, recent reports have linked changes in RNA localization with the nutrient stress response. Moor and colleagues (2017) found that the mouse intestinal epithelium shows a high degree of A/B mRNA asymmetry. When fasting mice are refed, transcripts encoding ribosomal subunits specifically enrich at the apical side of the enterocyte, where they elicit an increase in the translation rate of apically localized mRNAs. It was proposed that the higher efficiency of translation of apical mRNAs encoding nutrient transporters underlies the higher nutrient absorption observed upon re-feeding (Moor et al., 2017) (Figure 1.4).

Interestingly, the environmental availability of nutrients also impacts RNA localization in *Drosophila* oogenesis. Flies subjected to a protein-poor diet show a decrease in insulin levels that elicits the rearrangement of microtubule cytoskeleton in the germline within only a few hours from the onset of nutrient deprivation. This results in the formation of large RNP aggregates called Processing bodies (P-bodies) that are thought to store mRNAs in a silent form and thus escape transcript degradation (Shimada et al., 2011; Burn et al., 2016). P-bodies are rapidly disassembled once the fasting conditions are released or when insulin is provided in culture. Blocking formation of P-bodies in the germline during starvation is associated with reduced fecundity, suggesting that P-body formation maximizes egg production in conditions of nutritional shortage. P-bodies and stress granules form in many organisms upon different stress conditions, like starvation, heat-shock or osmotic stress (Schisa, 2013).

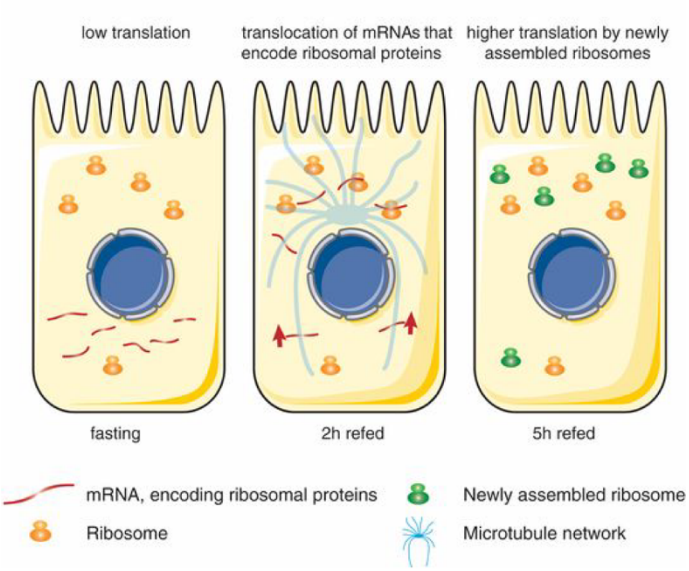


**Figure 1.4 - RNA localization in mouse intestinal epithelium** (adapted from Moor et al., 2017)**.**

## 1.4 Mechanisms of RNA localization

The processes involved in RNA localization are diverse and highly regulated by orchestrated events taking place from the time of transcription to arrival of the mRNA at its final destination. RNAs are in complex with *trans*-acting RNA-binding proteins (RBPs) that recognize *cis*-regulatory elements, often, but not exclusively, present in the mRNA 3'UTR (Kislauskis and Singer, 1992). The presence of *cis*-acting elements has been described to influence RNA fate in three ways (Martin and Ephrussi, 2009). First, it may be recognized by specific RBPs that are part of RNA transport complexes

for the active, directed transport of the mRNA. Second, it might influence the stability of the mRNA, or be a target for mRNA degradation. Third, it might be recognized by anchor proteins to tether the mRNA at its final destination. In addition, *cis*-acting sequences are also target of translational repressors, thus influencing the translational status of the mRNA.

The destination of a localizing mRNA can be established already in the nucleus through splicing, where both the differential inclusion of exons and the deposition of specific RBPs (i.e the EJC, see below) upon splicing can modify the mRNA's fate. In addition, once it reaches its final destination, the RNA can be anchored (usually by actin and dynein) and the translational inhibition released.

Three main mechanisms have been described to accomplish RNA localization: (1) selective degradation, whereby the transcript is degraded throughout the cell, with the exception of a site where it is locally protected (Figure 1.5A); (2) facilitated diffusion and entrapment, whereby the mRNA diffuses in the cytoplasm and is trapped by a localized anchor at its final destination (Figure 1.5B); (3) directed mRNA transport, whereby a transcript is actively transported in ribonucleoprotein (RNP) granules by motor proteins (dynein, kinesin, or myosin) on cytoskeletal tracks (microtubules or actin) (Figure 1.5C) (Martin and Ephrussi, 2009).

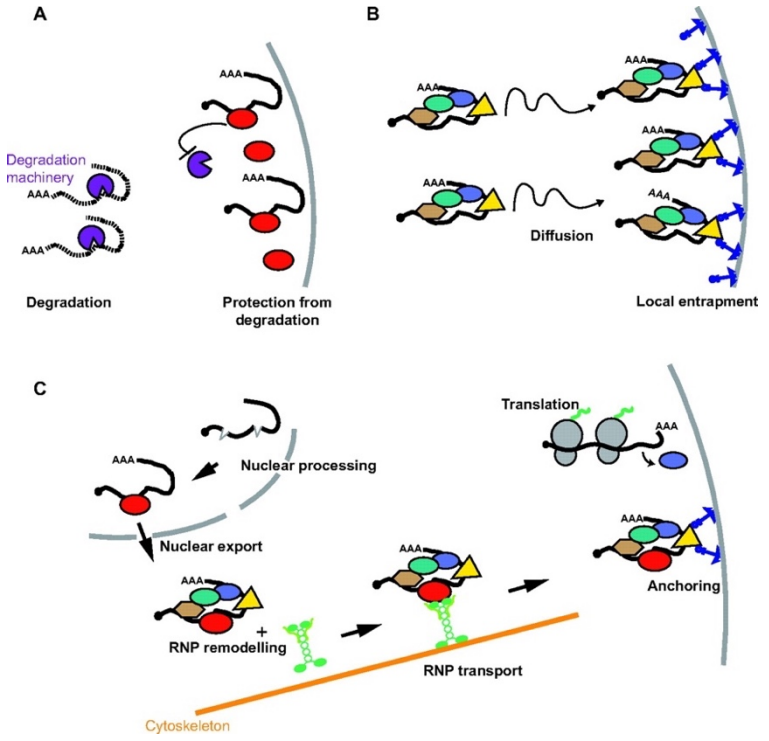


**Figure 1.5 - Mechanisms of RNA localization.** A) Localized protection from degradation. B) Facilitated diffusion and entrapment. C) Active transport (from Medioni et al., 2012).

Although directed RNA transport is the best-characterized mode of RNA localization, examples of all three mechanisms have been demonstrated in *Drosophila*.

### 1.4.1 *Cis*-acting determinants of RNA fate and localization elements (LEs)

mRNAs are characterized by the presence of untranslated regions (UTRs) upstream and downstream of their coding sequence (called 5' and 3'UTRs, respectively). Whereas the 5'UTR is primarily involved in translation regulation (Pickering and Willis, 2005), the 3'UTR typically regulates the stability, translational efficiency, subcellular localization, and nuclear export of the mRNA (Moore, 2005; Andreassi and Riccio, 2009; Mayr, 2016). Localized RNAs are targeted to cytoplasmic regions by *cis*-acting RNA elements called localization elements (LEs) or zipcodes. To date, only a few studies have reported the presence of LEs in the coding sequence; examples of transcripts carrying CDS-containing LE include *Drosophila stardust A* isoform and *gurken* mRNA (Horne-Badovinac and Bilder, 2008; Thio et al., 2000), and yeast mRNAs localized to the bud (Shepard et al., 2003).

LEs are relatively short stretches of nucleotides, with the majority being less than 1 Kb long (Jambhekar and DeRisi, 2007; Andreassi and Riccio, 2009). Typically, LEs form RNA stem-loop secondary structures through intra-molecular base-pairing. Secondary structures, rather than the primary sequence, seem largely responsible for the recognition by a particular RBPs.

To date, LEs have been identified in many subcellularly localizing mRNAs in *Drosophila*. The Transport/Localization Sequence (TLS) mediates the localization of *K10* and *orb* to oocytes (Cohen et al 2005; Serano and Cohen 1995). The Bicoid Localization Element (BLE) in *bcd* mRNA has a modular architecture, in which different regions of the LE specify sequential transport steps (Macdonald and Struhl, 1988; Macdonald et al., 1993; Ferrandon et al., 1997; Macdonald and Kerr, 1997). The Gurken Localization Signal (GLS) in *grk* mRNA mediates its localization to the dorsal-anterior corner of the oocyte (Van De Bor et al., 2005). In addition, LEs present in the mRNA mediate *Vg1* localization to the vegetal pole in *Xenopus* (Mowry and Melton, 1992), *Ash1* localization to the daughter cell in the budding yeast (Chartrand et al., 1999; Gonzalez et al., 1999), and localization of *ß-actin* to the cell protrusions of migrating fibroblasts (Kislauskis et al., 1994).

Several LEs can act sequentially in achieving different steps in the localization of an RNA. The dynein-dependent localization of *osk* mRNA to the oocyte in *Drosophila* egg-chambers represents a first step in its transport, and is dependent on a 67-nt stem-loop LE (Oocyte Entry Signal, OES) present in the *oskar* 3'UTR (Jambor et al., 2014). For the second, kinesin-dependent step of localization to the posterior pole of the oocyte, another stem-loop structure located in the *osk* CDS and formed upon splicing (Spliced Oskar Localization Element, SOLE) is necessary for posterior RNA localization (Ghosh et al., 2012).

In addition to LEs, 3'UTRs may also contain *cis*-acting elements that impact the translation of mRNAs. A sequence contained in the 3'UTR of vertebrate *ß-actin* mRNA is recognized by ZBP-1, which, upon binding, is responsible for both the transport and the translational inhibition of the transcript (Hüttelmaier et al., 2005; Patel et al., 2012). In *Drosophila*, the translational repressor Bruno recognizes multiple BREs (Bruno Recognition Elements) in the 3'UTR of *osk* mRNA, causing its translational silencing during transport (Kim-Ha et al., 1995).

### 1.4.2 Nuclear events that influence RNA localization

Splicing was reported to influence RNA localization is several ways. In the *Drosophila* follicular epithelium, two differentially spliced isoforms of *sdt* mRNA, *sdtA* and *sdtB*, are expressed. *stdA* differs from *sdtB* in the retention of an exon (exon 3). Horne-Badovinac and Bilder (2008) demonstrated that *sdtA* localizes in the apical domain of follicle cells, while *sdtB* shows a ubiquitous localization pattern and it is expressed later during oogenesis. However, the functional significance of such a developmental regulation of *sdt* expression by alternatively spliced mRNA isoforms with different localization abilities is unclear (Horne-Badovinac and Bilder, 2008).

Upon splicing, the Exon Juction Complex (EJC) composed of the core proteins eIF4AIII, MAGO, Y14, and MLN51 is deposited close to exon-exon junctions on the mRNA and is associated with non-sense mediated decay (NMD) in mammals (Wagner and Lykke-Andersen, 2002). The *Drosophila* orthologs of the four EJC core components are largely dispensable for NMD (Gatfield et al., 2003), but are required for *osk* mRNA localization (Mohr et al., 2001; Hachet and Ephrussi, 2001; Newmark and Boswell, 1994; van Eeden et al., 2001; Palacios et al., 2004). Consistent with a splicing-dependent deposition of the EJC on mRNAs, splicing was identified as an

essential step in conferring *osk* mRNA the ability to localize to the posterior pole (Hachet and Ephrussi, 2004). Specifically, *osk* requires the presence of the first intron to be correctly localized at the posterior, independently of the intron sequence. Splicing of the first intron causes the formation of a stem-loop structure (SOLE) at the junction between exon 1 and exon 2 in *osk* mRNA, which acts in concert with the EJC to accomplish *osk* RNA localization to the posterior pole (Ghosh et al., 2012; Ghosh et al., 2014). Moreover, the *Drosophila* ortholog of Partner of Y14-MAGO (*Pym*), when overexpressed, dissociates the EJC from *osk* mRNA and causes its mislocalization (Ghosh et al., 2014).

Alternative polyadenylation can also account for differences in RNA localization capacity, producing mRNA isoforms that differ in their 3'UTR. This is the case of *BDNF* mRNA isoforms produced in mouse brains (An et al., 2008). The long 3'UTR isoform is targeted to dendrites, where it is translated and regulates pruning and enlargements of dendritic spines. Instead, the short 3'UTR isoform remains in the soma and may be involved in sustaining neuronal survival and maintenance.

### 1.4.3 Anchoring the mRNA at its destination

In metazoans, RNA transport appears to be mostly mediated by kinesin and dynein motors in complex with RNPs, as a result of translocation on microtubule tracks. Conversely, anchoring of the mRNA at its final destination appears to be mostly mediated by the actin cytoskeleton. The actin cytoskeleton is involved in anchoring *ß-actin* mRNA in fibroblasts (Sundell and Singer, 1991), *Vg1* mRNA in *Xenopus* (Yisraeli et al., 1990), *arc* mRNA in neurons (Huang et al 2007), *osk* and *nos* mRNAs in *Drosophila* oocytes (Jankovics et al., 2002; Babu et al., 2004; Forrest and Gavis, 2006). In some cases, protein adaptors that mediate anchoring to microfilaments have been identified. For example, *osk* mRNA is trapped at the posterior pole by myosin V (encoded by *didum*) (Krauss et al., 2009). Interestingly, Osk protein itself is required for *osk* mRNA anchoring at the posterior pole (Rongo et al., 1995; Vanzo and Ephrussi, 2002).

In *Drosophila*, several reports have shown that cytoplasmic dynein may switch from an active motor to a static anchor. Delanoue and Davis (2005) have shown that pair-rule mRNAs, localized apically in the blastoderm embryo by dynein, require

dynein itself to be maintained at the apical domain. However, here dynein most likely becomes a static anchor, as ATPase activity inhibition with Vanadate does not affect the apical retention of RNAs. This suggests that the motor function of dynein is required for RNA transport to the apical domain, but the motor switches to a static RNA anchor at the destination (Delanoue and Davis, 2005). A similar mechanism accounts for anchoring of *grk* mRNA in sponge bodies at the anterior-dorsal (A-D) corner of the oocyte. Here, *grk* mRNA is transported in a dynein-dependent manner; once the RNP particles reach the sponge body at the A-D corner, dynein becomes a static anchor and is required for the maintenance of sponge body integrity (Delanoue et al., 2007).

### 1.4.4 Translational control of localized mRNAs

When they reach their final destination, most mRNAs are translationally silent. To ensure a tight control of localized expression, translational repression of RNAs must be relieved and the mRNAs translated. The transport of the pole plasm determinant *osk* must be transported to the posterior pole of the oocyte in a translationally repressed form to avoid deleterious effects in the embryo caused by ectopic expression of the mRNA. It has been shown that the RBP Bruno binds to multiple sites (BRE motifs) in the *osk* 3'UTR and represses *oskar* translation until the transcript reaches the posterior pole (Kim-Ha et al., 1995; Webster et al., 1997); repression of *osk* translation by Bruno was also confirmed *in vitro* (Lie and Macdonald, 1999; Castagnetti et al., 2000). Mutations in BREs impair Bruno's capacity to bind *osk* mRNA, causing its precocious translation (Kim-Ha et al., 1995). Bruno recruits Cup, an eukaryotic Initiation Factor 4E (eIF4E)-binding protein, which was proposed to act as a translational repressor by blocking eIF4G-eIF4E interaction and the recruitment of the small ribosomal subunit (Nakamura et al., 2004; Chekulaeva et al., 2006). However, later studies showed that Cup causes *osk* translational repression by polyA shortening through the recruitment of the CCR4 complex rather than binding with eIF4E (Igreja and Izaurralde, 2011); consistently, cytoplasmic polyadenylation is a translational activator of *Vg1* mRNA in Xenopus oocyte (Radford et al., 2008). Additionally, it was also proposed that *osk* mRNA is packaged into high order particles that prevent access to the translational machinery (Chekulaeva et al., 2006). However, translational control of *osk* mRNA is complex and requires the

activity of several regulators in both translational repression and activation (reviewed in Kugler and Lasko, 2009).

Several proteins involved in *osk* translational control have been found to play a role in the translational regulation of other maternally deposited mRNAs, in combination with specific RBPs. For example, translational inhibition of *nos* is mediated by Cup, which interacts with Smaug (Nelson et al., 2004). Smaug is functionally similar to Bruno, and binds Smaug Response Elements (SREs) in *nos* 3'UTR (Dahanukar et al., 1999; Smibert et al., 1999). Activation of *nos* translation requires also Oskar protein (Gavis and Lehmann, 1994).

In mammalian brain, FMRP has been linked to both RNA transport and translation regulation (Darnell et al., 2011; Dictenberg et al., 2008). In *Drosophila*, both the gene (encoded by *FMRP*/*Fmr1*) and its neuronal functions are conserved. FMRP effectively represses translation by first binding to the target mRNA, then to elongating ribosomes; the arrest in translation is caused by an interaction between the KH domain of FMRP with the P-site on the ribosome, creating a steric conflict with the P-site tRNA (Chen et al., 2014).

Finally, post-translational modifications of the translational inhibitor can cause conformational or affinity changes and lead to the release of the translational repression. This scenario was described for ZBP-1, which binds *ß-actin* mRNA in a translationally repressed form in migrating fibroblasts. At the cell protrusion, Src kinase-mediated activity phosphorylates ZBP-1 causing its dissociation from *ß-actin* mRNA and translational activation (Hüttelmaier et al., 2005).

## 1.5 Mechanisms of RNA localization in *Drosophila*

Most of what we know about the mechanisms governing RNA localization come from in-depth studies of localizing RNAs during *Drosophila* oogenesis, when the transcripts encoding embryonic determinants, such as *bcd*, *grk*, *osk*, become localized in the oocyte through microtubule-based active RNA transport. Importantly, the study of the mechanisms involved in the apical localization of pair-rule mRNAs in the syncytial blastoderm was instrumental to identify the dynein-dependent RNA transport machinery, the dynein/BicD/Egl complex. Apart from active RNA transport, other modes of RNA localization have been identified, although seemingly restricted to specific developmental phases and cellular compartments. In addition, mRNAs such

as *nos* can be localized through different mechanisms during development: during late oogenesis, it is localized at the posterior through facilitated diffusion and entrapment, while during early embryogenesis it gets restricted to the pole cells by localized protection from degradation.

### 1.5.1 Active RNA transport

Active RNA transport is mediated by mechanoenzymes that translocate on either microtubules (MTs) or microfilaments (actin). Cytoplasmic dynein and kinesin-1 motors transport cargoes on MTs in opposing directions; actin-based transport is performed by myosin V, which moves towards actin plus ends (Figure 1.6). Actin-based RNA transport has been well characterized in the budding yeast in the context of of *Ash1* mRNA localization (Bobola et al., 1996; Jansen et al., 1996; Heym and Niessing, 2012). In contrast, in *Drosophila*, actin-based transport has been associated mainly with cortical anchoring of mRNAs, whose transport to their site of localization is achieved via microtubules. It has also been proposed that transport of *osk* mRNA by long-range microtubule-based RNA transport might switch to short-range actin-based

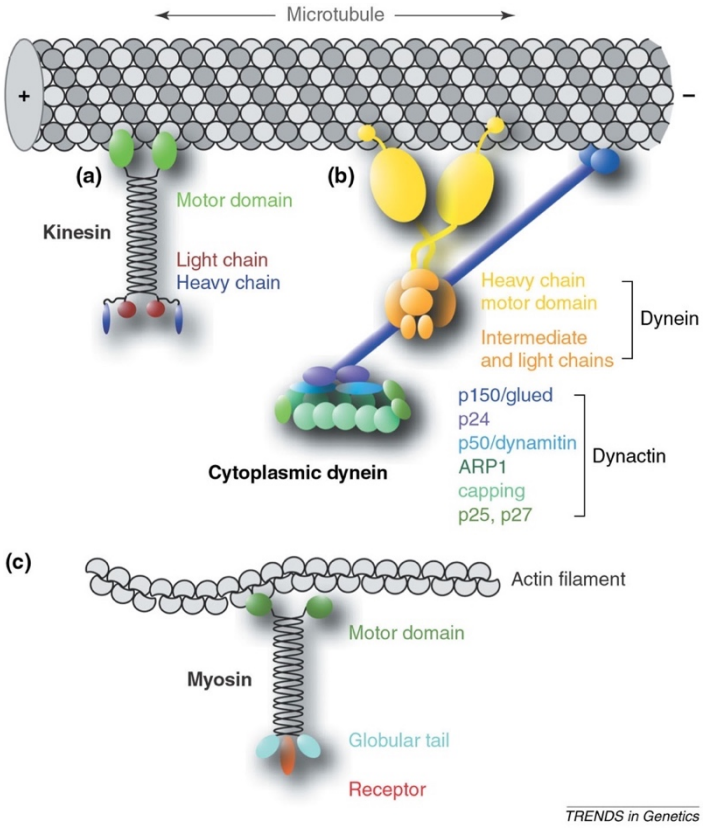


**Figure 1.6 - Molecular motors.** Kinesin (a) and dynein (b) move cargoes on MT tracks; myosin (c) moves cargoes on actin tracks (from Tekotte and Davis, 2002).

transport, eventually mediating entrapment of the mRNA at the final destination (Krauss et al., 2009).

The direction of travel of RNP cargoes transported on microtubules depends on the type of motor used to accomplish their transport. Cytoplasmic dynein transports its cargoes towards microtubule minus ends, whereas kinesins have been described to move primarily towards microtubule plus ends, with a few exceptions (Walker et al., 1990).

During *Drosophila* oogenesis, maternal mRNAs transcribed in the nurse cells are transported to a transcriptionally silent oocyte on a microtubule cytoskeleton. Therefore, the dynamic changes in organisation of the microtubule cytoskeleton in the germline cyst during oogenesis plays an essential role in determining the final destination of RNAs in the oocyte. In the germline syncytium, microtubules nucleate from a microtubule organizing center (MTOC) that forms in the oocyte at stage 1 and reach towards and into the 15 nurse cells, which are interconnected with the oocyte (stage 2-6) by ring canals (Theurkauf et al., 1993). Therefore, during early oogenesis, the MT minus ends are concentrated in the oocyte, and plus ends are concentrated at the oocyte anterior and in the nurse cells (Figure 1.7A). During these stages, proteins and mRNAs (such as *grk*, *bcd*, *osk*), are transported from the nurse cells to the oocyte in a dynein-dependent manner (Clark et al., 2007). During stage 7, a Gurken-dependent signalling event between the oocyte and the overlying follicle cells triggers repolarization of the MT cytoskeleton in the oocyte and establishment of the anterior-posterior axis (Roth et al., 1995; Gonzales-Reyes et al., 1995). MT minus ends now nucleate from the lateral and anterior cortex and plus ends become weakly biased towards the posterior of the oocyte (Theurkauf et al., 1992; Zimyanin et al., 2008) (Figure 1.7B). This event allows the oocyte-enriched mRNAs to acquire their final destination: *bcd* is localized at the anterior of the oocyte in a dynein-dependent manner, while *osk* localization to the posterior is kinesin-dependent (Duncan and Warrior, 2002; Januschke et al., 2002; Brendza et al., 2000; Weil et al., 2006; Zimyanin et al., 2008). At the same time, the oocyte nucleus migrates to the anterior-dorsal corner of the oocyte together with *grk* mRNA (Guichet et al., 2001). Here, *grk* RNA is translated, leading to a second burst of Grk signalling that induces the formation of the D/V axis. Throughout oogenesis, the transport of RNAs and nutrients from the nurse cells allows the continuous growth of the oocyte. During late stages of

oogenesis, the nurse cells deposit their contents into the oocyte, a phenomenon called "nurse cell dumping". At the same time, kinesin-directed sliding of subcortical microtubules in the oocyte cause the emergence of bulk cytoplasmic movements called "cytoplasmic streaming" that promote the mixing of nurse cell cytoplasm and ooplasm (Forrest and Gavis, 2003; Lu et al., 2016). This phenomenon is essential for facilitating the diffusion of *nos* and several other mRNAs to the posterior pole, where they are trapped.

Similarly, later on, in the blastoderm embryo and after cellularization, MTs are highly polarized and distributed along the A/B axis of the cortical nuclei. Microtubules nucleate from centrosomes positioned apically between the nucleus and the plasma membrane, with their minus ends concentrated at the apical side and plus ends basally (Figure 1.7C). At stage 14, MTs extend in the basal direction, and help direct the ingression of membrane furrows that encapsulate each nucleus in the process of cellularization (Mazumdar and Mazumdar, 2002). While dynein directs the transport of cargoes towards the apical domain, kinesin is speculated to direct cargoes towards the basal domain, although not experimentally proven (Mazumdar and Mazumdar, 2002).

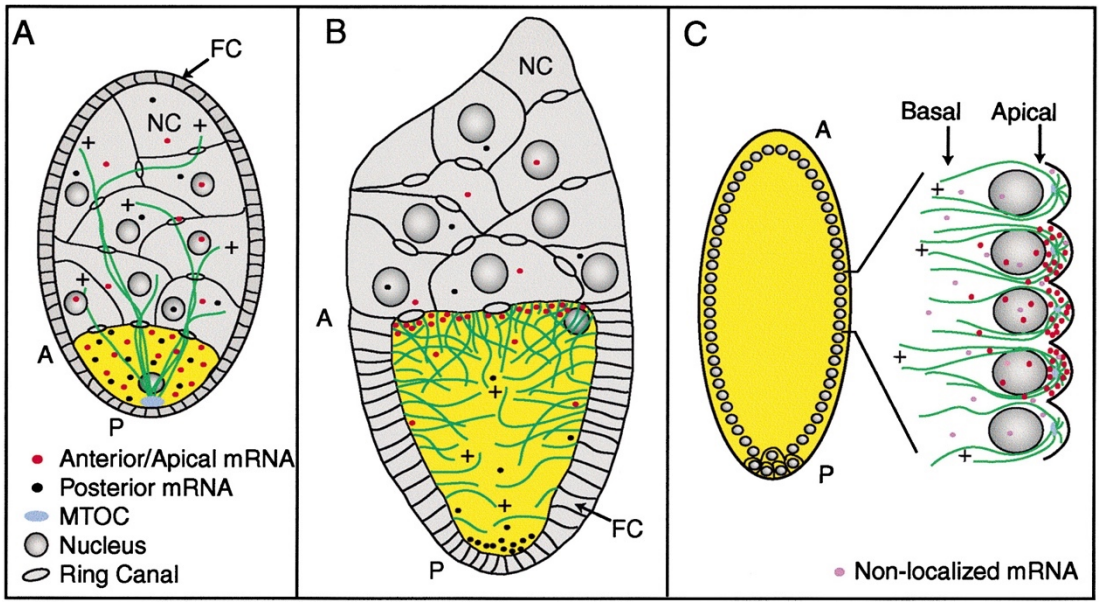


**Figure 1.7 - Polarity of the microtubule network in stage 6 (A) and stage 10 (B) egg-chambers and blastoderm embryo (C).** A=anterior; P=posterior; FC=follicle cells; NC=nurse cells (from Saxton, 2001)**.**

### 1.5.2 Facilitated diffusion and entrapment

Live imaging experiments showed that injected *osk* mRNA molecules in late stage oocytes are localized at the posterior by diffusion facilitated by ooplasmic streaming, followed by trapping by a localized anchor (Glotzer et al., 1997). This mechanism was also shown to contribute to *nos* localization to the posterior pole during the late stages of oogenesis (Forrest and Gavis, 2003), where, once at the posterior of the oocyte, *nos* mRNA is trapped by the actin cytoskeleton and associates with the germ plasm (Forrest and Gavis, 2003) (Figure 1.8).

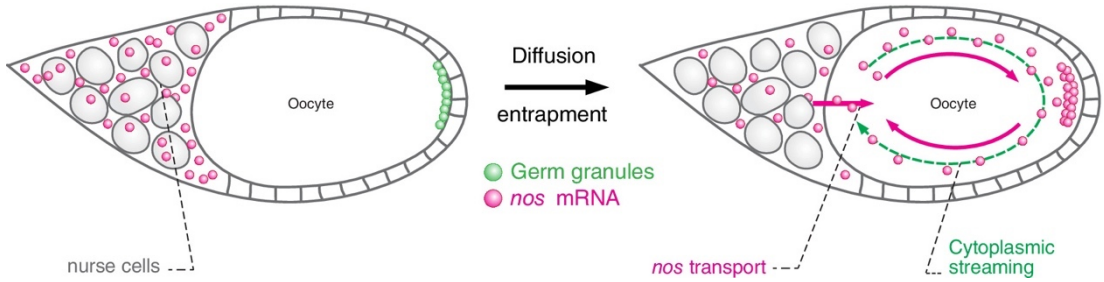


**Figure 1.8 - *nos* mRNA localization by facilitated diffusion and entrapment in late stages of oogenesis** (from Trcek and Lehmann, 2019)**.**

### 1.5.3 Localized protection from degradation

*Hsp83* mRNA is a component of the pole plasm and is maternally deposited. At stage 10B of oogenesis, nurse cell dumping causes the deposition of *Hsp83* mRNA transcribed in the nurse cells in the oocyte. During early embryogenesis, *Hsp83* mRNA is distributed ubiquitously in the embryo; however, its expression pattern becomes gradually restricted to the pole cells at syncytial blastoderm stage (Ding et al., 1993). The changes in *Hsp83* mRNA expression pattern over time results from a generalized degradation of the maternal mRNA everywhere in the embryo, with the exception of an area including the pole cells, where it is protected from degradation (Ding et al., 1993). *nos* mRNA is subjected to the same mechanism of localized protection from degradation during embryogenesis and becomes restricted as well to the pole cells (Bashirullah et al., 1999). *nos* and *Hsp83* are characterized by the presence of *cis*-acting elements in their 3'UTR recognized by Smaug (Smibert et al., 1999; Dahanukar et al., 1999; Semotok et al., 2008); once bound, Smaug recruits the CCR4-NOT deadenylase complex, which triggers RNA degradation (Semotok et al., 2005). At the posterior pole, Osk interferes with Smaug binding, resulting in the local protection of the maternal mRNAs from decay (Ding et al., 1993; Zaessinger et al., 2006) (Figure 1.9).

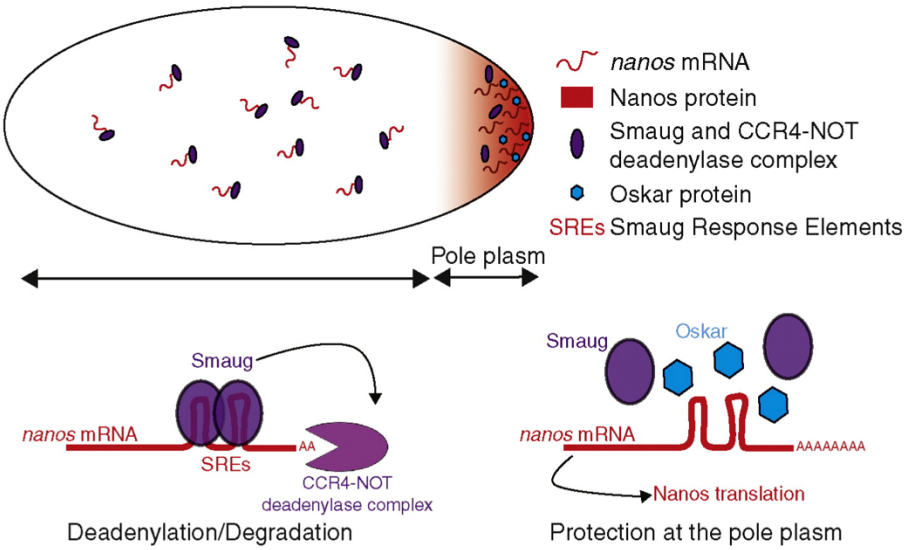


**Figure 1.9 - *nos* mRNA localization by localized protection from degradation during early embryogenesis** (adapted from Meignin and Davis, 2010).

### 1.5.4 Unconventional mechanisms of RNA transport

In addition to the mechanisms described above, several novel mechanisms have been recently reported to mediate RNA localization, such as hitch-hiking on other RNAs or vesicles and co-translational RNA transport.

*osk* mRNA dimerizes through RNA-RNA interaction with other *osk* mRNA molecules (Jambor et al., 2011). *osk* mRNA localization to the posterior pole of the oocyte requires both the presence of its 3'UTR and splicing, which renders the mRNA competent for posterior transport (Hachet and Ephrussi, 2004). However, intronless transgenic constructs containing only *osk* 3'UTR can localize to the posterior pole when wild-type, transport-competent *osk* mRNAs are also present. This observation led to the hypothesis that intronless *osk* mRNA could assemble with endogenous *osk* transcripts and "hitch-hike" to the posterior pole (Hachet and Ephrussi 2004). A later study showed that *osk* mRNA dimerizes both *in vitro* and *in vivo* through RNA-RNA interactions that involve base-pairing *in trans* of a stem-loop structure situated in the 3'UTR (Jambor et al., 2011). Hitch-hiking seems only to apply to posterior localization within the oocyte, but not to nurse-cell to oocyte transport (Jambor et al., 2011).

In other systems, several mRNAs were reported to hitch-hike on organelles and vesicles that move on microtubule tracks to reach their final destination. This mechanism has been well characterized in the transport of hyphae-localized mRNAs

in the fungus *Ustilago maydis*, where RNPs travel in complex with vesicles (Baumann et al., 2012). Recently, this mechanism was also found to be responsible for the transport of some mRNAs in vertebrate neurons, with RNA particles hitch-hiking on lysosomes (Liao et al., 2019) or endosomes (Corradi et al., 2020).

Interestingly, a new mechanism underlying the localization of *ABP40* mRNA in the budding yeast was proposed that involves mRNA co-translational transport (Kilchert and Spang, 2011). According to the model, the N-terminal domain of nascent ABP140 protein interacts with actin cables; the whole complex, composed of the *ABP140* mRNA, the translating ribosome, and the nascent protein, would then move by actin retrograde flow. A similar mechanism has been described to account for the localization of *pericentrin* (*pcnt*) mRNA to centrosomes of early zebrafish embryos and cultured HeLa cells (Sepulveda et al., 2018). Here, nascent PCNT binds to dynein and is co-translationally transported on microtubules. It is unclear is if similar mechanisms also exist for *Drosophila* RNA localization.

## 1.6 *Trans*-acting factors regulating MT-based RNA transport in *Drosophila*

The process of RNA transport relies on the formation of RNP complexes through binding of one or more RBPs to specific LEs on the mRNA. RNP complexes are transported on microtubule tracks as cargoes by dynein or kinesin motors whose RNP-motor association is usually accomplished by adaptor molecules. However, the mechanisms that underlie RNA transport are often difficult to dissect. A single RNA may bind to many different RBPs, and a single RBP may recognize LEs on several RNAs. Although machineries active in the polarized transport of some RNAs have been elucidated, it is likely that the final destination of an mRNA is determined by specific combinations of *trans*-acting factors that might be spatially and/or developmentally regulated. For example, although *bcd*, *osk*, and *grk* mRNA enter the oocyte in a dynein-dependent manner, their final destination within the oocyte differs, with *bcd* positioning at the anterior, *grk* at the dorsal-anterior, and *osk* at the posterior of the oocyte.

In addition to RBPs, the different activity, number, and composition of molecular motors associated with an RNA impact its final destination and localization

pattern, and it is often a combination of these factor that determines the subcellular localization of the transcripts (Gagnon and Mowry, 2011).

Dyneins and kinesins use the energy derived from ATP hydrolysis to move directionally towards the minus and the plus end of microtubules, respectively. In *Drosophila* and most metazoans, cytoplasmic dynein and kinesin-1 (also called conventional kinesin) are responsible for the movement of cellular cargoes through the cytoplasm, including RNPs, organelles, and proteins; the binding of different adaptors and RBP proteins usually determines cargo specificity.

### 1.6.1 MT minus end-directed transport

Cytoplasmic dynein (hereafter referred to as dynein) is composed of several subunits. The dynein heavy chain (Dhc) subunit, encoded by *Dhc64C*, forms a homodimer, hydrolizes ATP and contains the MT-binding domain. The other subunits mediate the interaction with cargoes and include the intermediate, light intermediate and light chains (Neisch et al., 2017). To effectively transport cargoes, dynein engages in interactions with a large multi-subunit complex, called dynactin, which in turn interacts and regulates binding with cargoes and adaptors. For example, overexpression of the dynactin subunit dynamitin (*DCTN-p50*) causes dissociation of the dynactin complex (Echeverri et al., 1996; Eckley et al., 1999). Cytoplasmic dynein activity can also be regulated by additional sets of proteins. For instance, Lissencephaly-1 (*Lis-1*) binds to dynein heavy chain and promotes the recruitment of transported RNPs to the dynein/dynactin complex (Dix et al., 2013).

#### *The dynein/BicD/Egl complex*

The RNA transport complex responsible for minus end-directed transport in *Drosophila* oogenesis and embryogenesis has been extensively characterized by several groups and represents one of the few examples where the complete link between the motor and the RNA cargo is understood. The complex is composed of the dynein-dynactin motor complex, the adaptor protein Bicaudal-D (BicD), and the atypical RNA-binding protein Egalitarian (Egl) (Figure 1.10A) (Mach and Lehmann, 1997; Dienstbier et al., 2009). The dynein/BicD/Egl complex was shown to transport pair-rule mRNAs to the apical domain of the blastoderm embryo and is thought to be responsible for transporting RNAs from the nurse cells to the oocyte during oogenesis (Ran et al., 1994; Suter and Steward, 1991; Navarro et al., 2004; Clark et al., 2007;

Bullock and Ish-Horowicz, 2001). The movement of dynein/BicD/Egl in complex with mRNAs was recently reconstituted *in vitro* (McClintock et al., 2018; Sladewski et al., 2018).

*BicD* and *egl* were first identified by genetic screens for maternally-required genes. Both mRNAs and protein encoded by *BicD* and *egl* localize to the presumptive oocyte during early oogenesis. Disruption of their function causes a 16 nurse cell-phenotype, where the oocyte fails to be specified and, instead, becomes a nurse cell (Ran et al., 1994; Suter and Steward, 1991; Schüpbach and Wieschaus, 1991) (Figure 1.10B). Subsequently, oogenesis is arrested at early stages, resulting in rudimentary ovaries. Disruption of the MT cytoskeleton, in *Dhc64C* or in *Lis-1* mutants, causes a similar phenotype (Koch and Spitzer, 1983; Therkauf et al., 1993; McGrail and Hays, 1997; Liu et al., 1999). In addition, loss-of-function mutations in *BicD* cause lack of accumulation of oocyte mRNAs, including *osk*, *orb*, *fs(1)K10* and *BicD*, suggesting that the failure to transport might contribute to a loss of oocyte differentiation (Ran et al., 1994; Suter and Steward, 1991).

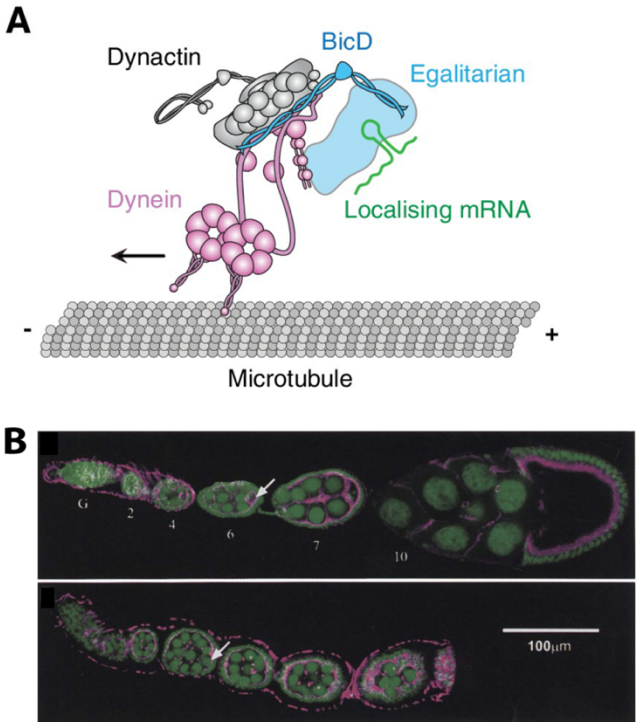


**Figure 1.10 - A) dynein/BicD/Egl RNA transport machinery. B) 16-nurse cell phenotype caused by the null allele *eglWU50* that disrupts Egl expression.** Upper panel: wild-type ovariole; lower panel: *egl* null ovariole. The arrow indicates the oocyte (upper panel) and the posterior-most cell differentiated as a nurse cell (lower panel) (adapted from McClintock et al., 2018; adapted from Mach and Lehmann, 1997).

In blastoderm stage embryos, injection of activity-disrupting antibodies against Dhc, Egl, and BicD was shown to disrupt apical accumulation of injected pair-rule and maternal mRNAs, providing the first direct evidence of their role in RNA transport (Wilkie and Davis, 2001; Bullock and Ish-Horowicz, 2001). Egl and BicD localize

ectopically expressed maternal RNAs in the blastoderm embryo; similarly, pair-rule transcripts expressed during oogenesis become localized in the oocyte. These experiments showed that the BicD/Egl transport machinery recognizes and transports to the minus end of microtubules both embryonic and germline mRNAs, suggesting that the machinery is conserved and active in both tissues (Bullock and Ish-Horowicz, 2001). Furthermore, the BicD/Egl complex is expressed and active in the localization of RNAs in other *Drosophila* tissues, such as neuroblasts and ovarian follicle cells (Hughes et al., 2004; Van De Bor et al., 2011; Vazquez-Pianzola et al., 2017) and of *gurken* mRNA within the oocyte (Delanoue et al., 2007).

Egl is a non-canonical RNA-binding protein that binds BicD through its N-terminal domain (residues 1-79), while a larger region encompassing residues 1-814 is required to bind RNAs (Dienstbier et al., 2009). Although several maternal and pair-rule mRNAs (*ftz*, *h*, *grk*, *wg*, *bcd*, *I-factor*, *osk, K10*) are thought to be localized by recruiting the complex through a LE in their 3'UTR, no common motif in their primary sequence was found. Structural analysis of a LE located in the *K10* 3'UTR revealed that it forms a stem-loop structure, with the stem region adopting an "A'-form" helical conformation due to the stacking interactions between purine bases (Bullock et al., 2010) (Figure 1.11A). Two spatially registered widened major grooves in the A' form helix are the presumed sites of interaction of Egl with the TLS. It is possible that other LEs, some of which also contain contiguous purines, could adopt the same conformation and be recognized by Egl (Bullock et al., 2010; Jambor et al., 2014) (Figure 1.11B).

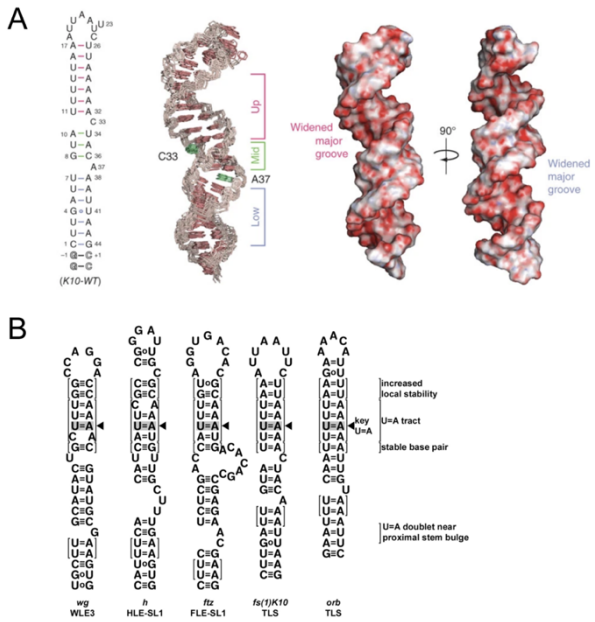


**Figure 1.11 – A) A'-form structure of *K10* TLS. B) Shared features (in brackets) of different LEs that mediate transport to the apical domain of the blastoderm embryo** (adapted from Bullock et al., 2010; adapted from dos Santos et al., 2008).

BicD is an adaptor protein that links the dynein/dynactin complex to RNPs and other cellular cargoes. In mammals, it is encoded by the *BICD1* and *BICD2* genes and its adaptor function is conserved (Hoogenraad et al., 2001). Studies of mammalian BICD2 have shown that it interacts with dynein/dynactin with its N-terminal domain, while the C-terminus (called CTD) interacts with cargoes such as Rab6, linking its function with vesicular trafficking (Hoogenraad et al., 2001; Hoogenraad et al., 2003; Matanis et al., 2002; Splinter et al., 2012). BICD activity is regulated such that, in the absence of cargo, the BICD N-terminus and the CTD interact, resulting in an inactive conformation of the protein (Hoogenraad et al., 2003). Both the dynein-binding and cargo-binding domains seem to be conserved in *Drosophila* BicD, as well as the autoinhibitory activity of the protein (Dienstbier et al., 2009; Liu et al., 2013) (Figure 1.12). In addition, a single residue substitution (K730M) in the BicD CTD completely abolishes binding of two BicD adaptor proteins, namely Egl and Rab6, suggesting that binding of Egl and Rab6 to BicD CTD might be mutually exclusive. This is supported by the finding that overexpression of Egl reduces the apical accumulation of lipid droplets, whose transport is dependent on BicD/Rab6 (Dienstbier et al., 2009). In addition to Egl and Rab6, BicD was also shown to interact with Fmr1 and with Clathrin Heavy Chain (Chc), which are involved in neuronal RNA localization (Bianco et al., 2010) and synaptic vesicle recycling (Li et al., 2010). Further BicD functions include transport of lipid droplets (Larsen et al., 2008) and movement of the nucleus in oocytes and photoreceptor cells (Swan and Suter, 1996; Swan et al., 1999).

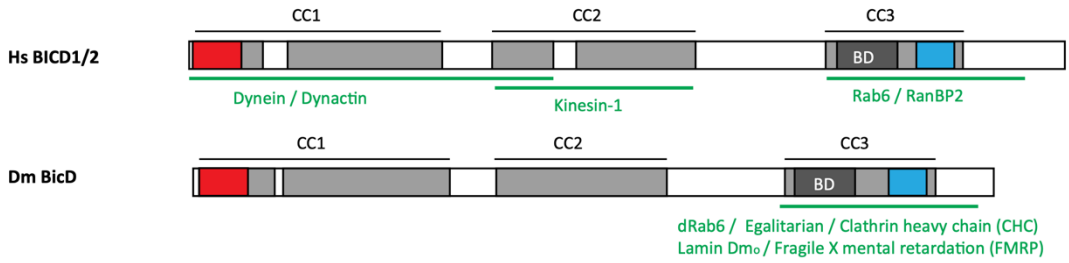


**Figure 1.12 - Conservation of human and Drosophila BicD.** Hs: *H. sapiens*; Dm: *D. melanogaster*. Green lines highlight known interaction domains with other proteins. Red and blue boxes indicate conserved regions. CC= Coiled coil; BD = BICD domain (adapted from Hoogenraad and Akhmanova, 2016).

***Dynein-dependent RNA localization within the oocyte and other cell types***

Although the dynein/BicD/Egl complex has been implicated in nurse cell-to-oocyte during oogenesis and and apical transport in embryogenesis, not much is known about the complex(es) that mediate minus end-directed localization of mRNAs within the oocyte and in other *Drosophila* tissues. Dynein is responsible for both *bcd* and *grk* localization to the anterior and dorsal-anterior corners of the oocyte, respectively (Schnorrer et al., 2000; Duncan and Warrior, 2002; Weil et al., 2006; MacDougall et al., 2003, Trovisco et al., 2016). In addition, dynein is required for apical localization of *sdt* and *crb* in the follicular epithelium, although requirement of the Egl/BicD machinery for localization of these mRNAs has not been investigated. Interestingly, despite being localized by facilitated diffusion and local entrapment during late oogenesis, *nos* mRNA transport is dynein-dependent in the *Drosophila* nervous system (Xu et al., 2013).

### 1.6.2 MT plus end-directed transport

Kinesin-1, the founding member of the kinesin superfamily of motor proteins, transports cargoes towards the plus end of MTs. Other members of the kinesin superfamily include kinesin-2, which plays a role in sensory cilia assembly and axonal transport, and the minus end-directed kinesin (*ncd*) (Miki et al., 2005).

In Drosophila, kinesin-1 is a hetero-tetramer composed of two heavy chains (Khc) and two light chains (Klc). Similarly to Dhc, the Khc N-terminal motor domain is involved in ATP hydrolysis and production of the energy required for translocation of the motor on microtubules. Beyond that, the mechanism(s) by which kinesin-1-mediates RNA transport in *Drosophila* is poorly characterized. *Khc* is required for transport of *osk* mRNA to the posterior pole of the oocyte (Brendza et al., 2000; Zimyanin et al., 2008; Micklem et al., 2000). However, *Klc* seems to be dispensable in this process (Palacios and St Johnston, 2002), suggesting that other Klc-like proteins might link kinesin to its cargoes. One such Klc-like adaptor has been identified in Pat1, which functions together with Khc in *osk* posterior localization (Loiseau et al., 2010).

To date, localization of *osk* mRNA represents the best characterized example of plus end-directed RNA transport. As described above, *osk* mRNA is first transported into the oocyte in a dynein-dependent process that likely involves the BicD/Egl transport machinery and its interaction with a stem-loop structure in the *osk* 3'UTR

(OES). Once in the oocyte and starting from stage 9 of oogenesis, *osk* switches motors and moves towards the posterior pole, where the plus end of microtubules are enriched (Zimyanin et al., 2007). Although the molecular mechanism underlying the switch from dynein to kinesin based transport is not understood, a number of factors have been identified to play important roles in *osk* posterior localization. For example, the SOLE element formed upon splicing of the first intron and the EJC are required for *osk* mRNA localization at the posterior of the oocyte. Another regulator of *osk* posterior transport is Staufen (Stau), a double-stranded RNA-binding protein (Ephrussi et al., 1991; Kim-Ha et al., 1991; St Johnston et al., 1991), which is also involved in the basal localization of *prospero* (*pros*) mRNA in neuroblasts (Li et al., 1997). Moreover, Stau is also involved in *osk* translational activation and anchoring at the posterior (Markussen et al., 1995; Rongo et al., 1995), as well as in the anchoring of *bcd* at the anterior of the oocyte (St Johnston et al., 1989).

Interestingly, two recent publications provided a link between the EJC, kinesin-1 and an atypical RNA-binding protein, the unconventional Tropomyosin 1-isoform I/C (*Tm1-I/C*). Loss of function mutations in *Tm1-I/C* cause *osk* to mislocalize at the anterior, suggesting that Tm1-I/C plays a role in plus end-directed transport of *osk* mRNA (Erdelyi et al., 1995; Gaspar et al., 2016; Veeranan-Karmegam et al., 2016). Tm1-I/C is found in a complex with Stau, Khc and *osk* RNA (Gaspar et al., 2016) and binds directly to Khc (Veeranan-Karmegam et al., 2016). Moreover, Tm1-I/C seems to recruit inactive Khc upon nuclear export, while the EJC/SOLE appear to be required for Khc activation of kinesin for *osk* RNA transport (Gaspar et al., 2016). Interestingly, although in *Khc* mutant egg-chambers *grk* and *bcd* mRNAs are delocalized, in *Tm1-I/C* null oocytes their localization is reported to be unaffected, which suggest that Tm1-I/C might have a specific function in regulating *osk* RNA transport (Erdelyi et al., 1995; Veeranan-Karmegam et al., 2016).

### 1.6.3 Bidirectional transport and cross-talk between dynein and kinesin

The switch from minus end- to plus end-directed transport of *osk* mRNA in mid-oogenesis implies that RNA transport must be tightly regulated and might involve the cooperation of the dynein and kinesin motors. Zimyanin and colleagues (2008) tested the requirement of known *osk* transport regulators by live imaging of *osk* mRNA transport. This revealed that *osk* mRNAs move in an almost random walk, with a slight bias towards the posterior that reflects the weakly polarized MT network in the oocyte

at mid-oogenesis. Interestingly, in *mago*, *barentsz*, and *Tm1-I/C* mutant oocytes, *osk* mRNA is mislocalized towards the anterior of the oocyte, where the minus ends of microtubules are enriched, suggesting that mutation in these genes cause a switch to dynein-dependent *oskar* transport. However, in a hypomorphic *Dhc* mutant background, neither minus end-movement nor net posterior *osk* transport was affected; in addition, in hypomorphic *Khc* mutants, the velocity of the mRNA particles was lower in both anterior and posterior directions. Therefore, it was proposed that, once *osk* enters the oocyte, the EJC and Tm1-I/C might be required to inhibit the activity of the dynein/BicD/Egl complex used for nurse cell-to-oocyte transport, allowing activation of plus end-directed, kinesin-based transport and posterior localization. However, the molecular mechanisms that underlie this phenomenon are not clear.

In the *Drosophila* embryo, both apically-localizing and uniformly distributed mRNAs undergo bidirectional movements. *hairy* (*h*) mRNA is apically localized in early embryos by the dynein/BicD/Egl complex which recognizes a stem-loop structure that functions as LE (Bullock et al., 2003). Bullock et al. (2006) have shown that injected fluorescently labelled *h* mRNA undergoes bidirectional movements, with longer runs towards the minus ends, resulting in a net apical transport. The observed bidirectional movement suggested that *h* might bind opposite polarity motors, and that net transport might result from differences in the activity of the opposing motors. Surprisingly, Injected *Kruppel* (*Kr*) mRNA, which is evenly distributed in the cytoplasm, showed short motor-dependent bidirectional movements and can occasionally make use of the Egl/BicD machinery for long minus end-directed runs.. The authors therefore suggested that the *h* LE is not required for motor recruitment; rather, that it increases the probability and maintenance of minus end-directed movements, through recruitment of additional copies of the dynein/BicD/Egl machinery (Bullock et al., 2006; Amrute-Nayak and Bullock, 2012) (Figure 1.13). A following study revealed that the plus end-directed movements of apical mRNAs are not dependent on kinesin-1 or kinesin-2 activity. Indeed, it was proposed that dynein itself is responsible for plus end-directed movements; in addition, dynactin seems to be required to repress plus end movements and accomplish a net minus end transport of apical mRNAs (Vendra et al., 2007).

Several publications have reported that transported mRNAs and other cargoes could be bound simultaneously by both dynein and kinesin motors. Through

alternating movements towards the plus and the minus ends, this phenomenon was hypothesized to help cargoes overcome obstacles within the crowded cytoplasmic environment (Hancock et al., 2014). The net movement of the cargo towards a specific direction is considered to be the result of a mechanical competition between two motors that pull the cargo towards opposite directions, with one of the two winning over the other; this model is called "tug of war" and was first used in the context of bidirectional microtubule transport by Welte et al. (1998) to describe the motion of lipid droplets in *Drosophila* embryos. According to this model, inhibition of one of the two molecular motors engaged in transport would result in the accumulation of the cargo in the direction established by the active motor. Although several studies have reported such a phenomenon, others have shown that inhibition of one motor causes a seemingly paradoxical decreased motility in the opposite direction (Hancock et al., 2014). As *Khc* mutants exhibit reduced anterior localization of *bcd* and *grk* mRNAs, which require dynein activity for their localization to the anterior, it was proposed that *Khc* mutants indirectly affect dynein-dependent processes as a result of the role of kinesin-1 in transporting dynein to the posterior, presumably for motor recycling (Brendza et al., 2002; Duncan and Warrior, 2002; Januschke et al 2002). A similar co-dependence phenotype was observed in the movement of cargoes in *Drosophila* axons upon disruption of dynein function (Martin et al., 1999).

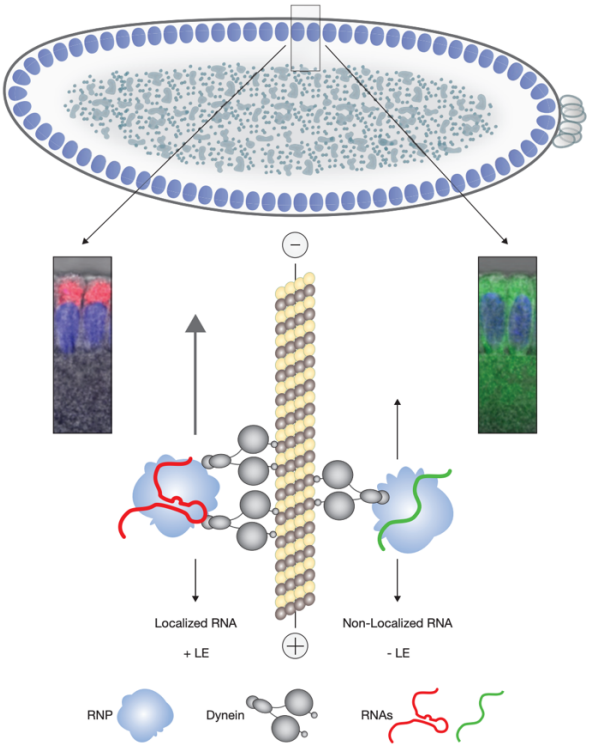


**Figure 1.13 – Mechanistic characterization of *h* (red) and *Kr* (green) mRNA transport.** *h* mRNA undergoes bidirectional movements, with longer runs towards the minus ends, resulting in a net apical transport; *Kr* shows short motor-dependent bidirectional movements resulting in no net direction of transport (from Doyle and Kiebler, 2012).

## 1.7 The follicular epithelium as a model to study RNA localization

The follicular epithelium (FE) is a monolayer of polarized somatic cells, also called follicle cells (FCs), that encapsulate the germline cyst. The FE delimits the egg-chamber and represents the interface between the germline and the environment and play an important role in the formation of the eggshell structures. In addition, through extensive communication with the underlying oocyte during early and mid-oogenesis, the FE contributes to establishment of both the A/P and the D/V axis of the future embryo, and participates in the synthesis and delivery of yolk proteins stored in the oocyte and production of chorion proteins. Finally, the FE is able to sense the nutrient status of the fly, which is communicated to the oocyte through the insulin/TOR pathway; this signaling event is fundamental to activate the germline starvation response upon nutrient deprivation.

The FE has long been used as a model to study tissue morphogenesis, establishment/maintenance of epithelial cell polarity and cell-cell communication. Recently, a few studies have reported the phenomenon of RNA localization in this tissue, although the mechanisms that govern it and its functional significance are largely unknown. As a tissue ideally suited to sophisticated genetic manipulation, for instance generation of mosaics, and with the advent of high-resolution imaging, the FE represents an excellent model to study the mechanisms and functions of RNA localization in a somatic tissue.

### 1.7.1 Follicle cell types and morphogenesis

During oogenesis, the oocyte grows thanks to the continuous transfer of proteins, RNAs and organelles produced by the nurse cells; concomitantly, the FCs, which surround the germline, undergo extensive morphogenetic movements to form specialized structures and deposit eggshell components necessary for the survival and hatching of the developing embryo in the environment. After eggshell deposition, FCs degenerate undergoing programmed cell death.

At stage 2, three follicle cell types compose the egg-chamber: the stalk cells, which connect each egg-chamber and are organized in a thick cluster of 6-8 cells; the polar cells, which are present in pairs and delimit the anterior and the posterior termini of the egg-chamber; and the epithelial FCs, which surround each egg-chamber as a

cuboidal monolayer. The epithelial FCs proliferate until stage 6, when they cease to divide and switch to an endoreplicative state and become polyploid, with a concurrent increase in size. After completing three rounds of endoreplication (stage 7-10A), epithelial FCs selectively amplify chromosomal regions that include cluster of genes required for eggshell production (Duhart et al., 2017).

The transition between stage 8 and 9 marks the onset of vitellogenesis (production and uptake of yolk proteins) and it is accompanied by dramatic morphogenetic movements and changes in cell shape (Figure 1.14). Starting from stage 9, the majority (~95%) of epithelial FCs start compacting towards the posterior of the egg-chamber and align over the oocyte; this movement is accompanied by the transition from a cuboidal epithelium to a columnar epithelium (main body FCs). The remaining ~50 FCs stretch over the nurse cells and are called stretch cells or squamous FCs. At stage 10A, the oocyte anterior is aligned with the border between the main body FCs and the stretch cells, and takes up half of the volume of the egg-chamber. At this stage, columnar FCs start producing eggshell components (vitelline membrane and chorion) which they secrete apically. Concomitant with the migration of the epithelial FCs towards the posterior, a cluster of 4-8 anterior FCs, called border cells, and the two anterior polar cells begin to move towards the posterior of the egg-chamber, migrating between the tightly packed nurse cells. At stage 10A, the cell cluster reaches the anterior of the oocyte.

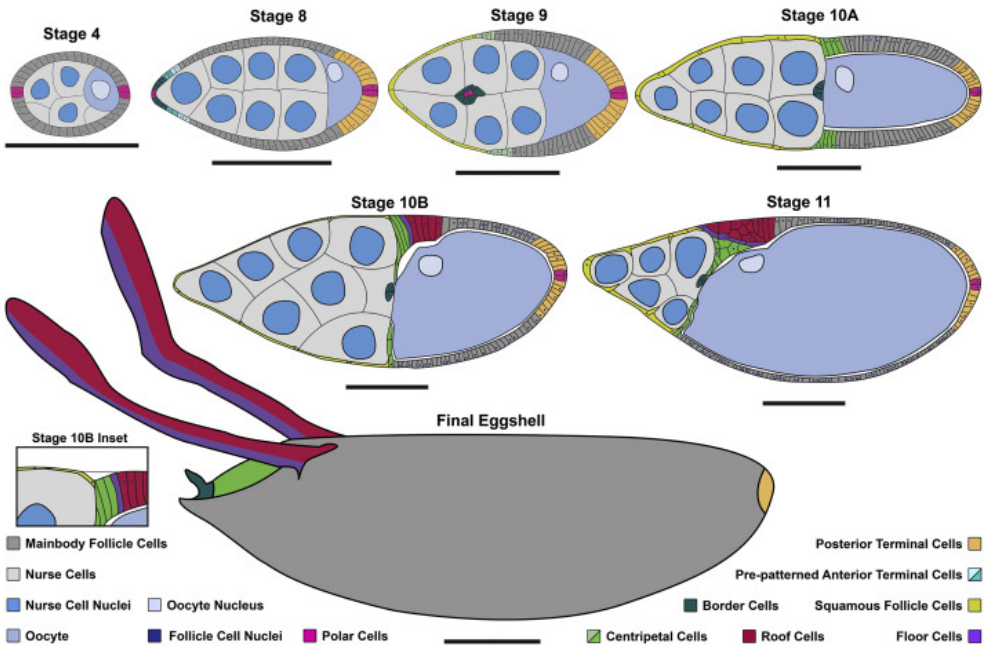


**Figure 1.14 - Follicle cell types.** Colors show the contribution of each follicle cell population to each eggshell structure (from Duhart et al., 2017).

Stage 10B marks another transition. At this time, the oocyte occupies the majority of the egg-chamber volume and the nurse cells start initiate the transfer of their entire content into the oocyte (nurse cell dumping). The border cells, together with the polar cells, migrate towards the nucleus of the oocyte, positioned at the dorsal-anterior corner of the oocyte. A group of anterior main body columnar FCs differentiate into centripetal cells and starts migrating inward, eventually covering the anterior side of the oocyte. Two patches of dorsal-anterior columnar FCs are responsible for the reorganization that results in formation of the dorsal appendages, elongated dorsal-anterior chorionic structures that facilitate gas exchange. The anterior-most dorsal columnar FCs are responsible for the formation of the operculum and contribute, together with the border cells and the anterior-most ventral columnar FCs, to the formation of the micropyle. The micropyle is a narrow channel and functions as the sperm entry site; the operculum is a fragile anterior region of the eggshell from which the hatching larva later escapes. The dorsal appendages, the operculum and the micropyle are therefore the result of chorion deposition and their morphology reflects the shape of the cells that deposited these components (Figure 1.15). Eventually, the FCs and the nurse cells will degenerate by programmed cell death.

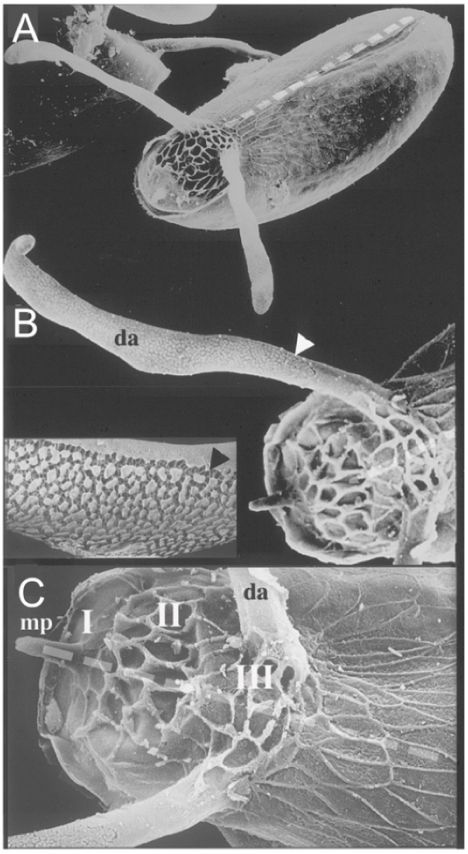


**Figure 1.15 – *Drosophila* egg and eggshell structures.** A) Egg. Dashed line marks the dorsal midline. B) Structure of a dorsal appendage (da). Inset shows the exochorionic structures specialized for respiratory functions. C) Anterior eggshell showing the micropyle (mp), dorsal appendages (da) and three regions of distinct cell imprints (I–III) (adapted from Dobens and Raftery, 2000).

### 1.7.2 Functions of the follicular epithelium

As mentioned above, the columnar FE plays an important role in the synthesis and deposition of the eggshell structures and the vitelline membrane. These structures are essential for fertilization, the survival of the embryo in the environment, and hatching. In addition, the columnar FE provides the oocyte yolk proteins that sustain early embryonic development.

The FE plays additional essential roles through extensive signalling communication with the oocyte during the course of oogenesis. During early oogenesis, the positioning of the oocyte at the posterior of the egg-chamber is considered the first polarization event. The posterior position is thought to be achieved through a direct cell-cell interaction between the oocyte and the posterior FCs which involves expression of DE-cadherin in both tissues. Germline and FC clones mutant in DE-cadherin or its intracellular interactor Armadillo cause mispositioning of the oocyte (Gonzalez-Reyes and St Johnston, 1998).

The posterior positioning of the oocyte is essential for establishment of the A/P axis of the future embryo, which, in turn, is key for the specification of D/V axis later in oogenesis (stage 7). Both A/P and D/V axes are specified by interactions between the oocyte and the FCs. This interaction is dependent on Grk protein secreted locally by the oocyte and activation of EGFR signalling in a subset of FCs by binding to the EGFR receptor Torpedo (Roth et al., 1995; Gonzales-Reyes et al., 1995). The first EGFR signalling event imparts posterior fate to the neighboring FCs, which send an unknown signal back to the oocyte that results in the reorganization of the oocyte cytoskeleton and the establishment of the A/P axis. The second EGFR signalling event induces dorsal fate in the FCs close to the dorsal-anterior corner of the oocyte, a key event for the formation of eggshell structures and establishment of the D/V axis.

Finally, the FE plays a role in monitoring the nutritional status of the fly. In conditions of low nutrient diet, oogenesis is arrested, and vitellogenic egg-chambers undergo apoptosis (Drummond-Barbosa and Spradling, 2001). Interestingly, the FE acts as a sensor of the insulin signal from the environment; the information is transduced to the oocyte via an unknown signal that involves activation of the insulin/TOR pathway in the FCs (Burn et al., 2015). As a result of low insulin levels, the germline starvation response is activated in the oocyte, which involves the formation of P-bodies (sites of RNA storage).

### 1.7.3 Polarity of the follicular epithelium

Epithelial cells exhibit a strong polarization of cellular components (protein complexes, organelles, cytoskeleton) along their A/B axis, which define an apical domain and a basolateral domain. In the FE, the apical domain is closely apposed to the germline, and the basolateral domain faces a basement membrane and the circular muscle layers that surround the egg-chamber. During their transition from a cuboidal to columnar epithelium (stage 9), mitotic FCs switch to endoreplicative cycles, stop dividing and mature into a differentiated secretory epithelium.

The microtubule cytoskeleton of the epithelial FCs is organized in parallel MT arrays that run along the A/B axis of the cell, with minus ends at the apical side, and plus ends basally (Bacallao et al., 1989; Clark et al., 1997) (Figure 1.16). In cuboidal FCs (stage 2-9), microtubules nucleate from centrosomal MTOCs; at stage 10, the centrioles disappear and the cells acquire a columnar morphology (Mahowald et al., 1979). In columnar FCs, non-centrosomal microtubules are tethered to an apical spectrin array by Shot (*short stop*) and Patronin (Khanal et al., 2016).

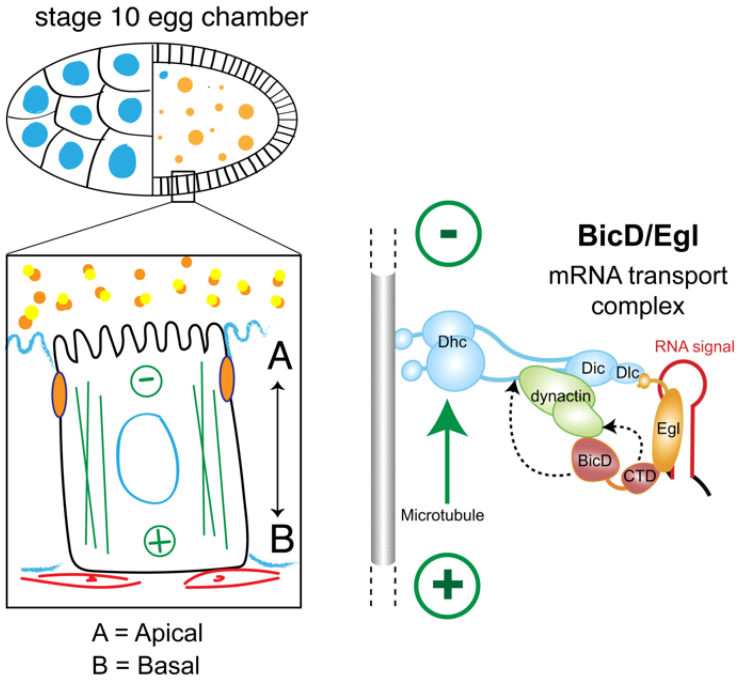


**Figure 1.16 – Microtubule polarity of columnar follicle cells and direction of the dynein/BicD/Egl RNA transport complex.** MTs are in green (adapted from Dienstbier et al., 2009).

Cell polarity and the integrity of the epithelium are maintained by polarity protein complexes that localize subapically, such as the Crumbs complex (Crumbs/Stardust/Patj) and the PAR complex (Bazooka/Par6/aPKC), and baso-laterally, by the Scribble complex (Scrib/Lgl/Dlg). Loss of epithelial integrity results in polarity defects such as multi-layering, cell rounding and mislocalization of the nucleus (Tanentzapf et al., 2000; Bilder et al., 2000; Cox et al, 1996). It is noteworthy that mutations in dynein heavy chain (*Dhc64C*) and a component of dynactin (*Glued/p150*) show multilayering of the posterior FCs after stage 6 (Li et al., 2008), probably due to a failure in targeting *crumbs* mRNA (Li et al., 2008) and/or protein (Aguilar-Aragon et al., 2020) to the apical domain.

### 1.7.4 RNA localization in the follicular epithelium

RNA localization in the *Drosophila* germline is extensively characterized, both mechanistically and functionally. In recent years, some reports have begun to elucidate these aspects of RNA localization in the context of the FCs. High-throughput *in situ* hybridization experiments identified 30 apically- and 9 basally-localizing mRNAs in FCs (Jambor et al., 2015). Investigations into the functional significance of the apical targeting of *crb* and *sdt* mRNAs have shown that localization of these transcripts contributes to the maintenance of cell polarity (Li et al., 2008; Horne-Badovinac and Bilder, 2008); in addition, apical localization of *upd* mRNA in polar cells is important for efficient JAK/STAT signaling and cell migration (Van De Bor et al., 2011). However, RNA localization of these transcripts does not fully account for the apical targeting of the encoded protein, suggesting that RNA and protein localization might act redundantly in this tissue.

Maternal mRNAs such as *oskar*, *bicoid*, and *K10* are recognized by the dynein/BicD/Egl RNA transport machinery. When these mRNAs are ectopically expressed in the FE, they localize in the apical domain, towards the minus ends of microtubules (Karlin-McGinness et al., 1996, Jambor et al., 2014) (Figure 1.16). These experiments suggest that the BicD/Egl machinery is active in the FCs, and localizes transcripts carrying a localization signal recognized by Egl. In addition, Egl pull-down experiments from ovarian lysates identified 3 additional mRNAs (*CG33129*, *Uba1*, *egl*) that are apically localized in the FE, and their localization was shown to depend on BicD activity (Vazquez-Pianzola et al., 2017). Finally, *upd* mRNA localization was shown to be dependent on BicD and Egl and, when ectopically expressed in the

columnar FCs, localizes apically (Van De Bor et al., 2011). Altogether, these studies show that the dynein/BicD/Egl machinery is expressed in the FE and directs the apical localization of transcripts carrying a localization signal, a phenomenon that is conserved during both oogenesis and embryogenesis. Other transcripts, such as *crb* and *sdt*, are apically localized in FCs in a dynein-dependent fashion; however, it has not been tested whether their localization requires BicD/Egl or is mediated by other dynein-dependent mechanisms (Li et al., 2008; Horne-Badovinac and Bilder, 2008).

Four more RNAs were shown to display subcellular localization in the FE: *bitesize* (*btsz*) mRNA (encoding a a synaptotagmin-like protein) is apically localized; *mew* (encoding the alpha subunit of PS1 integrin), *Grasp65* and *Gos28* (involved in Golgi transport) are basally localized (Schotman et al., 2008; Serano and Rubin, 2003). However, the mechanisms underlying their subcellular localization have not been addressed.

Interestingly, the subcellular localization of several mRNAs expressed in the FCs (*btsz*, *sdt*, *Grasp65*, *upd*) requires elements present in the coding sequence. Considering that and only a few examples of LEs present in the CDS have been described, it is surprising that such a relatively high number of mRNAs containing LEs in their CDS are present in the FCs. This might suggest that novel mechanisms/RNA localization machineries may be involved in RNA localization in the FCs.

To conclude, the follicular epithelium of *Drosophila melanogaster* represents an ideal system with which to investigate the mechanisms and the roles of RNA localization in the context of a differentiated tissue. First, it is ideally suited to genetic manipulation, including generation of genetic mosaics composed of wild-type and mutant cells within the same tissue; second, the development of high-resolution imaging approaches allows the visualization and precise quantification of RNA and protein molecules; third, while the conserved BicD/Egl RNA localization machinery is clearly active in the follicular epithelium, additional unknown mechanisms may also be involved in RNA localization in this somatic tissue.

# Aim

Although the phenomenon of RNA localization is well characterized in eggs and early embryos, not much is known of the mechanisms and the functions of RNA localization in differentiated polarized tissues. In the *Drosophila* follicular epithelium only a handful of mRNAs have been described to show subcellular localization. In some cases, the apical localization of follicle cell mRNAs appears to be mediated by the dynein/BicD/Egl machinery, however nothing is known concerning the mechanisms underlying basal RNA localization. Finally, previous reports indicate that RNA and protein localization in this tissue have redundant roles in achieving subcellular gene expression, leaving open the question of the significance of RNA localization in the follicular epithelium. With the work presented in this thesis, I aim at gaining a deeper understanding of both the mechanisms and the functions of RNA localization in the context of a differentiated tissue. I first characterized the genome-wide landscape of apically and basally localizing RNAs in the columnar follicle cells by applying spatial transcriptomics. Then, I investigated at a mechanistic level how apical and basal localization are achieved, as well as the interplay between the two processes and novel modes of apical RNA localization. Finally, I initiated a genetic investigation of the functional significance of RNA localization in this tissue.

# Chapter 2: Materials and Methods

## 2.1 Materials

### 2.1.1 Enzymes

| Name | Application | Source (Catalog #) |
|---|---|---|
| Terminal Deoxynucleotidyl Transferase (TdT), 20 U/µl | smFISH probe labelling | EP0161 |

### 2.1.2 Antibodies

| Name | Dilution | type | Application | Source (Catalog #) |
|---|---|---|---|---|
| Rabbit α-Egl | 1:2,500 | Primary | Western blot | Gift from R. Lehmann |
| Mouse α-Tub | 1:20,000 | Primary | Western blot | T5168 |
| α-rabbit-HRP | 1:10,000 | Secondary | Western blot | GENA934 |
| α-mouse-HRP | 1:10,000 | Secondary | Western blot | GENA931 |

### 2.1.3 Chemicals

| Name | Application | Source (Catalog #) |
|---|---|---|
| 2-Methylbutane | Ovary embedding | 277258-1L |
| Histogene Staining Solution | Cryosection staining | KIT0415 |
| Ribolock RNase inhibitor, 40 U/µl | Lysis (LCM-seq)<br>Dissolution Buffer (Geo-seq)<br>Smart-seq2 | EO0381 |
| GlycoBlue co-precipitant 15 mg/ml | Precipitation Buffer (Geo-seq) | AM9515 |
| 10 mM dNTP mix | LCM-seq and Geo-seq | R0191 |
| Betaine solution 5 M | Smart-seq2 | B0300-1VL |
| $MgCl_2$ 1 M | Smart-seq2 | AM9530G |
| AMPure XP beads | Purification of cDNA | Aliquote kindly donated by GeneCore facility |
| 16% Formaldehyde, methanol-free | Ovary fixation (smFISH) | 50-980-487 |
| Formamide, deionized | smFISH | S4117 |
| Ribonucleoside Vanadyl Complexes (VRC), 200 mM | smFISH | R3380-5ML |

| | | |
|---|---|---|
| Salmon sperm DNA solution, 10 mg/ml | smFISH | 15632011 |
| Dextran sulfate sodium salt | smFISH | 42867-5G |
| Bovine Serum Albumin (BSA) | smFISH | A3294-10G |
| 2,2'-thiodiethanol (TDE) | smFISH | 166782 |
| cOmplete protease inhibitor cocktail | Ovary lysis (western blot) | 11697498001 |
| 5X Bradford Reagent | Measurement of protein concentration (western blot) | 39222.01 |

### 2.1.4 Additional commercial material

| Name | Application | Source (Catalog #) |
|---|---|---|
| Tissue-Tek Cryomolds | Ovary embedding | SA62534-10 |
| Tissue-Tek OCT Compund | Ovary embedding | SA62550-01 |
| Zeiss MembraneSlide NF 1.0 PEN | Cryosectioning and LCM | 415190-9081-000 |
| Zeiss AdhesiveCap 200 opaque | LCM | 415190-9181-000 |
| Invitrogen NuPAGE 4-12% precasted gels | SDS-PAGE | NP0321BOX |
| Immobilon PVDF Transfer membrane | Western blotting | T831.1 |
| Immobilon Western HRP substrate peroxide solution | Western blotting | WBKLSO500 |

### 2.1.5 Kits

| Name | Source (Catalog #) |
|---|---|
| SuperScript II Reverse Transcriptase | 18064014 |
| KAPA HiFi HotStart ReadyMix | KR0370 |

### 2.1.6 Buffers, solutions and mixes

| Name | Composition | Application |
|---|---|---|
| PBS (Phosphate Buffered Saline) | Prepared in house | Ovary dissection |
| Lysis buffer | 0.4% TritonX-100<br>2 U Ribolock RNase inhibitor | Lysis (LCM-seq) |
| GuSCN solution | 4 M Guanidine Thyocianate<br>50 mM Tris-HCl pH 7.5 | Lysis (Geo-seq) |

| | | |
|---|---|---|
| | 25 mM EDTA | |
| Precipitating Buffer | 78 % Ethanol<br>0.04 M Sodium Acetate pH 6.5<br>20 µg GlycoBlue coprecipitant | RNA precipitation (Geo-seq) |
| Dissolution Buffer | 1 µM oligo-dT<br>1 mM dNTP mix<br>2 U Ribolock RNase inhibitor | RNA dissolution and denaturation (Geo-seq) |
| Reverse Transcription Mix | 100 U SuperScript II reverse transcriptase<br>10 U Ribolock RNAse inhibitor<br>1X Superscript II first-strand buffer<br>5 mM DTT<br>1 M Betaine<br>6 mM MgCl2<br>1 µM TSO oligo | Smart-seq2 |
| PCR Mix | 1X KAPA HiFi HotStart ReadyMix<br>0.1 µM ISPCR primers | Smart-seq2 |
| Schneider's Medium | S2 cell medium<br>15% Fetal Bovine Serum<br>0.6% Penicillin/Streptavidin<br>200 µg/ml insulin | *ex vivo* culture for colchicine treatment |
| ddUTP-ATTO-633 labelling mix | 1000 pmol oligo mix<br>200 µM ddUTP-ATTO-633<br>24 U TdT<br>1X Buffer TdT | smFISH probe labelling |
| ddUTP-ATTO-565 labelling mix | 1000 pmol oligo mix<br>300 µM ddUTP-ATTO-565<br>24 U TdT<br>1X Buffer TdT | smFISH probe labelling |
| PBSTX(0.1%) | 0.1% Triton X-100/PBS | smFISH |
| 2% PFA/PBSTX(0.1%) | 2 % PFA/PBS<br>0.05% Triton X-100/PBS | smFISH |
| Pre-hybridization/Washing Buffer | 2X SSC<br>10% deionized formamide<br>0.1% Tween20 | smFISH |
| Hybridization Buffer | 2X SSC<br>10% deionized formamide<br>0.1% Tween20<br>2 mM VRC<br>0.1 mg/ml salmon sperm DNA<br>100 mg/ml (10%) dextran sulfate<br>20 µg/ml RNAse-free BSA | smFISH |
| PBST(0.1%) | 0.1% Tween20/PBS | smFISH |

| | | |
|---|---|---|
| 80%TDE/PBS | 80% 2,2'-thiodiethanol/PBS | smFISH |
| RIPA Buffer | 150 mM NaCl<br>1% NP-40<br>0.5% Sodium Deoxycholate<br>0.1% SDS<br>50 mM Tris-HCl pH 8.0<br>1X cOmplete protease inhibitor | Ovary lysis (western blot) |
| Transfer Buffer (Towbin Buffer) | 25 mM Tris<br>192 mM Glycine<br>20% (v/v) Methanol | Western blot |
| TBS | 20 mM Tris-Cl pH 7.6<br>150 mM NaCl | Western blot |
| Blocking Buffer | 5% Milk/TBS | Western blot |
| TBST(0.1%) | 0.1% Tween20/TBS | Western blot |

### 2.1.7 Primers and smFISH probes

#### *Primers*

| Name | Sequence | Application |
|---|---|---|
| oligo-dT | AAGCAGTGGTATCAACGCAGAGTACT$_{(30)}$VN | LCM-seq, Geo-seq |
| TSO oligo | AAGCAGTGGTATCAACGCAGAGTACATrGrG+G | Smart-seq2 |
| ISPCR primers | AAGCAGTGGTATCAACGCAGAGT | Smart-seq2 |

#### *smFISH probe sets*

smFISH probe sets are listed in the Supplementary Material section.

### 2.1.8 Fly stocks

#### *Parental lines*

| Genotype | ID# | Description | Source/Publication |
|---|---|---|---|
| *w$^{1118}$* | 1 | wild-type | Ephrussi lab |
| *HsFlp; arm>f$^{+}$>Gal4; UAS-CD8-mCherry* | 2 | UAS/Gal4 "flip-out" system; expresses Gal4 and CD8-mCherry in a subset of cells upon heat-shock | Gift from J. M. Gomez-Elliff |
| *y[1] sc[*] v[1]; P{y[+t7.7]v[+t1.8]=TRiP.GL00330}attP2* | 3 | Expresses dsRNA for RNAi of *Khc* under UAS control | Bloomington stock #35409 |

| | | | |
|---|---|---|---|
| *If/CyO; ΔC-Pym-GFP/Tm3Ser* | 4 | Expresses ΔC -Pym-GFP under UAS control | Ghosh et al., 2014 |
| *y[1] sc[*] v[1] sev[21]; P{y[+t7.7]v[+t1.8]=TRiP.HMS01587}attP2* | 5 | Expresses dsRNA for RNAi of *Dhc64C* under UAS control | Bloomington stock #36698 |
| *y[1] v[1]; P{y[+t7.7] v[+t1.8]=TRiP.HM05180}attP2* | 6 | Expresses dsRNA for RNAi of *egl* under UAS control | Bloomington stock #28969 |
| *w[*]; P{w[+mC]=UAS-mCherry.NLS}2; MKRS/TM6B, Tb[1]* | 7 | Expresses nuclear-localized mCherry under UAS control | Bloomington stock #38425 |
| *yw; $egl^{WU50}$ bw sp/SM1* | 8 | Null allele (*egl*) | Mach and Lehmann, 1997 |
| *yw; $egl^{PR29}$/SM6a* | 9 | Null allele (*egl*) | Mach and Lehmann, 1997 |
| *w;+;osk-Gal4/TM3,Sb* | 10 | Expresses Gal4 under the control of *osk* promoter | Ephrussi Lab |
| *+; +; UAS-Egl* | 11 | Expresses Egl under the control of UAS | Ephrussi Lab |
| *+; +; Jupiter-GFP[PTT]* | 12 | Expresses Jupiter-GFP under the endogenous *Jupiter* promoter | Karpova et al., 2006 |
| *+; tj-Gal4; +* | 13 | Expresses Gal4 under the control of *tj* promoter | Gift from J. M. Gomez-Elliff |
| *y,w,;+; UASp-BicD-3xEGFP* | 14 | Expresses BicD tagged with 3 copies of GFP under the control of UAS | Gift from S.Bullock |
| *Imp-GFP[PTT]; +; +* | 15 | Expresses Imp-GFP under the endogenous *Imp* promoter | Gift from F. Wippich |
| *y[1] sc[*] v[1] sev[21]; P{y[+t7.7] v[+t1.8]=TRiP.GL00094}attP2* | 16 | Expresses dsRNA for RNAi of *w* under UAS control | Bloomington stock #35573 |
| *If/Cyo; Sb/TM3Ser* | 17 | Double balancer line | Ephrussi lab |
| *If/CyO; TM2/TM6B,Tb* | 18 | Double balancer line | Ephrussi lab |
| *w ; + ; vasa-Gal4/TM3,Sb* | 19 | Expresses Gal4 under the control of *vasa* promoter | Ephrussi lab |
| *w[*]; P{w[+mC]=matalpha4-GAL-VP16}V37* | 20 | Expresses Gal4-VP16 under the control of the *αTub67C* promoter | Bloomington stock #7063 |

### *Lines used in experiments*

| Name | Genotype | Parental lines |
|---|---|---|
| wild-type | *w*$^{1118}$ | #1 |
| *Khc* RNAi (HS-induced clones) | *HsFlp/+; arm>f*$^{+}$*>Gal4/+; UAS-mCherry/KhcRNAi* | #2, #3 |
| *ΔC-Pym-GFP* (HS-induced clones) | *HsFlp/+; arm>f*$^{+}$*>Gal4/+; UAS-mCherry/UAS-ΔC-Pym-GFP* | #2, #4 |
| *Dhc64C* RNAi (HS-induced clones) | *HsFlp/+; arm>f*$^{+}$*>Gal4/+; UAS-mCherry/Dhc64CRNAi* | #2, #5 |
| *egl* RNAi (HS-induced clones) | *HsFlp/+; arm>f*$^{+}$*>Gal4/+; UAS-mCherry/eglRNAi* | #2, #6 |
| *Khc* RNAi (HS-induced clones) | *HsFlp/+; arm>f*$^{+}$*>Gal4/UAS-NLS-mCherry; KhcRNAi/MKRS* | #2, #3, #6, #7, #18 |
| *egl* RNAi (HS-induced clones) | *HsFlp/+; arm>f*$^{+}$*>Gal4/UAS-NLS-mCherry; eglRNAi/TM6B,Tb* | #2, #3, #6, #7, #18 |
| *egl* RNAi + *Khc* RNAi (HS-induced clones) | *HsFlp/+; arm>f*$^{+}$*>Gal4/UAS-NLSmCherry; eglRNAi/KhcRNAi* | #2, #3, #6, #7, #18 |
| *egl*$^{NULL}$*FC + osk>Egl* | *w; egl*$^{WU50}$*/egl*$^{PR29}$*; osk-Gal4/UAS-Egl* | #8, #9, #10, #11, #17 |
| *Jupiter-GFP* | *+; +; Jupiter-GFP[PTT]* | #12 |
| *tj>BicD-3xEGFP* | *+; tj-Gal4/+; UAS-BicD-3xEGFP/+* | #13, #14 |
| *Imp-GFP* | *Imp-GFP[PTT]; +; +* | #15 |
| *egl* RNAi (HS-induced clones) in *Imp-GFP* background | *HsFlp/Imp-GFP[PTT]; arm>f*$^{+}$*>Gal4/Cyo; UAS-mCherry/eglRNAi* | #2, #6, #15, #17 |
| *tj>wRNAi* | *+; tj-Gal4/+; wRNAi/+* | #13, #16 |
| *tj>eglRNAi* | *+; tj-Gal4/+; eglRNAi/+* | #13, #6 |
| *egl*$^{NULL}$*FC + vasa>Egl* | *w; egl*$^{WU50}$*/egl*$^{PR29}$*; vasa-Gal4/UAS-Egl* | #8, #9, #11, #18, #19 |
| *egl*$^{NULL}$*FC + αTub67C>Egl* | *w; egl*$^{WU50}$*/egl*$^{PR29}$*; αTub67C-Gal4/UAS-Egl* | #8, #9, #11, #18, #20 |

### 2.1.9 Software, algorithms and online resources

| Name | Reference | Source |
|---|---|---|
| Galaxy | Afgan et al., 2018 | https://galaxy.embl.de/ |
| FastQC (Galaxy) | Andrews, 2010 | http://www.bioinformatics.babraham.ac.uk/projects/fastqc |
| Trimmomatic (Galaxy) | Bolger et al., 2014 | http://www.usadellab.org/cms/index.php?page=trimmomatic |
| SortMeRNA (Galaxy) | Kopylova et al., 2012 | https://bioinfo.lifl.fr/RNA/sortmerna/ |
| RNA STAR (Galaxy) | Dobin et al., 2013 | https://code.google.com/archive/p/rna-star/ |
| Picard tools (Galaxy) | Broad Institute | http://broadinstitute.github.io/picard/ |
| featureCounts (Galaxy) | Liao et al., 2014 | http://bioconductor.org/packages/release/bioc/html/Rsubread.html |
| R Studio | R Studio Team, 2015 | https://rstudio.com/ |
| ggplot2 (R package) | Wickham, 2016 | https://ggplot2.tidyverse.org/ |
| DESeq2 (R package) | Love et al., 2014 | https://bioconductor.org/packages/release/bioc/html/DESeq2.html |
| org.Dm.eg.db (R package) | Carlson, 2019 | https://bioconductor.org/packages/org.Dm.eg.db/ |
| clusterProfiler (R package) | Yu et al., 2012 | https://bioconductor.org/packages/clusterProfiler/ |
| FlyFISH database | Lecuyer et al., 2007<br>Wilk et al., 2016 | http://fly-fish.ccbr.utoronto.ca/ |
| Dresden Ovary Table (DOT) database | Jambor et al., 2015 | http://tomancak-srv1.mpi-cbg.de/DOT/main |
| FIJI | Schindelin et al., 2012 | https://fiji.sc/ |

## 2.2 Methods

### 2.2.1 Generation of LCM samples

***Ovary embedding and cryosectioning***

$w^{1118}$ virgin females were kept for 24 h with males and at 25ºC on yeast-supplemented fly food. Ovaries were dissected in PBS and rapidly placed in the center of small plastic cryomolds containing PBS. PBS was then carefully removed with a pipette and the bottom of the ovary-containing mold was snap-frozen in cold 2-Methylbutane. The cryomold was then filled with OCT and snap-frozen again. The block was kept at -80°C for several days and equilibrated at -20ºC for 1 h before cryostat sectioning.

OCT-embedded ovaries were cut with a Leica CM3050S cryostat at a thickness of 10 µm. Several sections were carefully placed on a Zeiss MembraneSlide NF 1.0 PEN and kept at -20°C. After sectioning, slides were briefly thawed at RT and processed for staining and dehydration. Slides were first fixed in 75% Ethanol RF (30 s), washed to remove OCT in $ddH_2O$ RF (40 s, dipping), stained in 100 µl Histogene staining solution (20 s), washed again in $ddH_2O$ RF to remove the excess solution and dehydrated in increasing Ethanol concentrations (75%, 95%, 100%; 30 s each). Finally, slides were briefly air-dried and LCM immediately performed.

***Laser-Capture Microdissection procedure***

LCM was performed with a Zeiss PALM MicroBeam with a 63X objective. Laser power was carefully adjusted to avoid RNA damage; micro-dissected fragments were collected into the cap of a Zeiss AdhesiveCap tube. A total of 10 fragments of either apical or basal domains of micro-dissected columnar follicle cells from stage 9-10A egg-chambers were pooled for each replicate (~3000-4000 $\mu m^2$), with a total of 5 replicates for each of the apical and basal sample types.

***LCM-seq sample preparation***

LCM-seq samples were lysed according to the protocol described in Nichterwitz et al. (2016) with minor modifications. Briefly, 2.4 µl of lysis buffer (see Material section) were placed on the cap of the tube containing the LCM fragments and carefully lysed by pipetting up and down several times. Lysates were centrifuged briefly to collect the liquid into the bottom of the tube, and the cap was visualized under the microscope to check that lysis was successful. Lysates were immediately snap-frozen in dry ice and kept at -80°C until further processing. On the day of Smart-seq2 reaction, samples were thawed and incubated with 1 µl of 10 mM dNTP mix and 1 µl of 5 µM oligo-dT primer at 72°C for 3 min, and immediately placed on ice. Samples were then processed following the Smart-seq2 protocol for cDNA library preparation.

***Geo-seq sample preparation***

Geo-seq samples were lysed according to the protocol described in Chen et al. (2017) with minor modifications. Immediately after collection of LCM fragments, 50 µl of GuSCN solution (see Materials) was placed in the bottom of the AdhesiveCap tube. Next, the tube was inverted allowing the solution to cover the LCM fragments

present on the cap surface, sealed with parafilm and placed in a water bath heated at 42°C for 15 min to allow for the dissolution of the fragments. Samples were then centrifuged at 7000xg for 30 s with a tabletop centrifuge pre-cooled at 4°C. 771.3 µl of freshly-prepared precooled Precipitating Buffer (see Materials) were added to each sample, mixed thoroughly, and incubated o/n at -80°C. The following day, samples were thawed and centrifuged at 12,000xg for 30 min in a tabletop centrifuged pre-cooled at 4°C. The pellet was washed at 4°C with 75% ethanol RF for 10 min at 12,000xg and air dried. Finally, the RNA pellet was resuspended in 4.56 µl Dissolution Buffer (see Materials), incubated in a thermocycler at 72°C for 3 min, and immediately chilled on ice. Samples were then further processed for Smart-seq2 cDNA library preparation.

***Preparation of cDNA libraries***

cDNA libraries were prepared according to the Smart-seq2 protocol described by Picelli et al. (2014) (Figure 2.1). Following oligo-dT annealing, the Reverse Transcription Mix (see Materials) was added to each sample an incubated in a thermocycler according to the following program:

| Cycle | Temperature | Time |
|---|---|---|
| 1 | 42°C | 90 min |
| 2 | 70°C | 15 min |
| 3 | 4°C | hold |

For cDNA amplification, 15 µl of PCR Mix (see Materials) was added to each sample and the thermal cycle was programmed as follows:

| Cycle | Temperature | Time |
|---|---|---|
| 1 | 98°C | 3 min |
| 2-19 | 98°C<br>67°C<br>72°C | 20 s<br>15 s<br>6 min |
| 20 | 72°C | 5 min |
| 21 | 10°C | hold |

Bead purification was performed with AMPure XP beads with a ratio of 0.8:1 to the PCR product, mixed and incubated 15 min at room temperature to bind DNA. Beads were then washed 2x 30 s with 75% ethanol and eluted in 15 µl H2O. The cDNA concentration was measured with a fluorometer (QBIT) following the manufacturer's instructions. The quality of the cDNA was analyzed with capillary electrophoresis (Bioanalyzer).

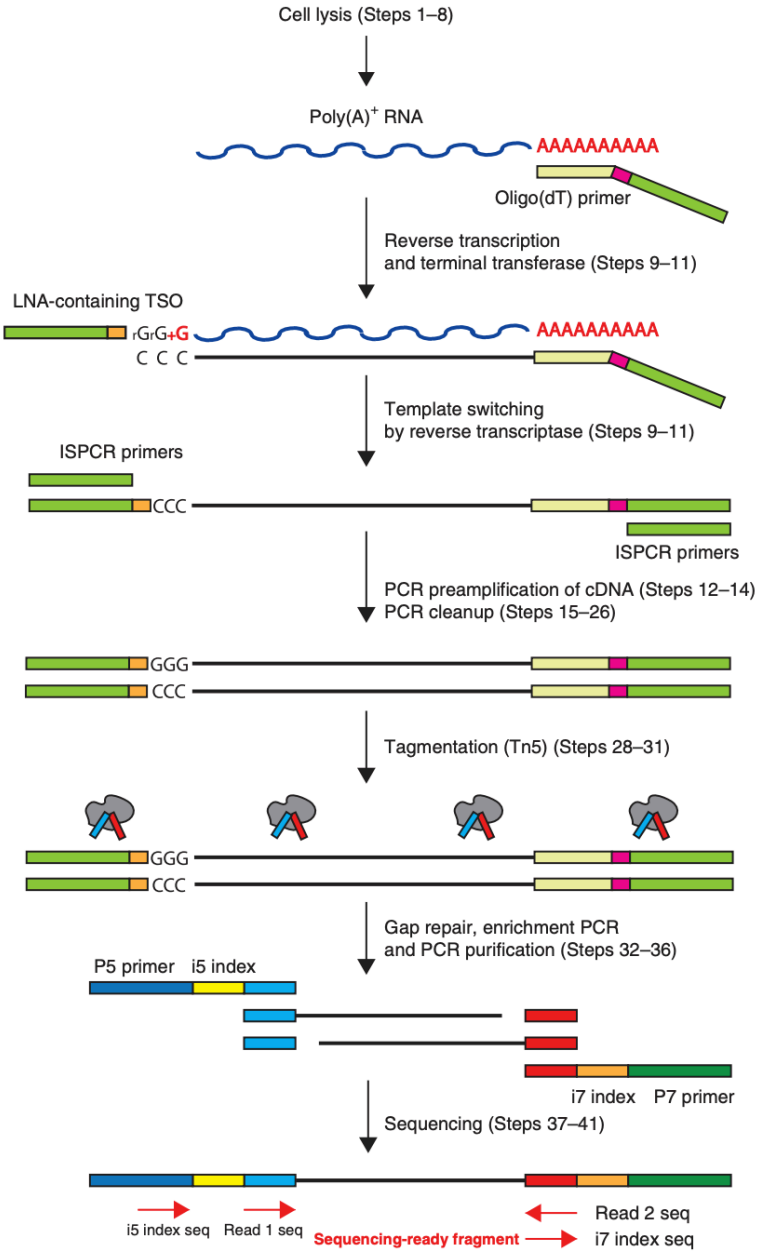


**Figure 2.1 - Smart-seq2 reaction** (from Picelli et al., 2014).

***Illumina sequencing***

The preparation of Nextera XT DNA sequencing libraries and Illumina sequencing was performed the GeneCore Facility at EMBL Heidelberg. Samples were multiplexed and simultaneously sequenced on a single lane using the NextSeq500 system.

### 2.2.2 Computational procedures

***Pre-processing and mapping***

Pre-processing of demultiplexed raw reads was performed on EMBL's instance of Galaxy platform. Read quality was checked after each processing step with FastQC. Briefly, raw reads were first processed with Trimmomatic to remove low-quality bases and adapter sequences. Trimmed reads were filtered from rRNA contaminant reads with SortMeRNA and mapped via STAR against *D. melanogaster* Release 6 (dm6) reference genome. Normalized transcript coverage of the uniquely mapping reads was calculated with CollectRNAseqMetrics (part of Picard tools). Finally, featureCount was used to count reads that mapped uniquely to genes.

***Quality control of RNA-seq data and differential gene expression analysis***

Quality control of RNA-seq libraries was performed with R Studio. Read counts were normalized with DESeq2 R package through the median of ratios method. Euclidean distances and PCA plots were generated with DESeq2 as part of the library quality control. Replicates A5 and B5 showed a higher dissimilarity among apical and basal replicates respectively, and were excluded from further analysis.

Differential gene expression analysis was performed with DESeq2 by comparing the mean read counts of the Apical and Basal samples. Positive $\log_2$FoldChange values identified apically-enriched RNAs ("Apical dataset") and negative $\log_2$FoldChange values identified basally enriched RNAs ("Basal dataset"). The threshold for statistical significance was set to a FDR < 0.1. Quality control of the differential gene expression analysis was performed by evaluating the dispersion estimates, Cook's distances and p-value frequency plots generated with DESeq2.

***Comparison with public collections of subcellularly localized RNAs***

The lists of genes composing the apical and basal datasets generated by the differential gene expression analysis were compared with publicly available resources of subcellularly localized RNAs generated by high-throughput FISH experiments

(FlyFISH and Dresden Ovary Table). Subcellularly localizing mRNAs were queried for "subcellular localization pattern" in all embryonic tissues listed in FlyFISH database and compared with significantly enriched genes (merged Apical and Basal datasets). Next, genes annotated as "apical" or "basal" were queried in both FlyFISH and DOT and compared with the gene composition of the Apical and Basal dataset respectively.

***Filtering of contaminant reads***

Filtering of contaminant mRNAs was performed with R Studio. After selecting the significantly enriched genes (FDR < 0.1), genes with a $\log_2$FoldChange > 3 ("Apical contaminants") and genes with a $\log_2$FoldChange < -3 ("Basal contaminants") were analyzed separately with Gene Ontology (GO) enrichment analysis.

***Gene Ontology enrichment analysis***

GO enrichment analysis was performed in R Studio, before and after contaminant filtering. Genes were annotated with the org.Dm.eg.db and GO analysis was performed with clusterProfiler on the apical and basal dataset separately considering the Biological Process ontology.

### 2.2.3 Fly procedures

**Drosophila *maintenance***

All fly stocks were maintained at 18°C on standard fly food. For crosses, virgin females were kept with a few males at 25°C on food supplemented with yeast. Before all experiments, newborn females of the desired genotype were incubated with $w^{1118}$ males on a yeast-supplemented medium at 25°C to stimulate the emergence of vitellogenic stage egg-chambers.

***Clonal analysis***

The UAS-Gal4 "flip-out" system was used to generate marked mutant clones in a wild-type background (Pignoni and Zipurski, 1997). Male flies homozygous for an allele that carried a Gal4-inducible promoter (UAS) upstream of the desired hairpin RNA (to perform *Khc* RNAi, *egl* RNAi, or *Dhc64C* RNAi) or gene construct (for ΔC -Pym-GFP expression) were crossed with *hsFlp; arm>$f^+$>Gal4; UAS-CD8-mCherry* virgins. Upon heat-shock, the expression of the flippase is induced in all cells; the short duration (1 h) of heat shock allows the flippase-mediated excision of the $f^+$ cassette

upstream of Gal4 in a small subset of cells by recognition of FRT sites flanking the cassette (indicated with the symbol ">"). The excision of the $f^+$ cassette allows the induction of Gal4 expression by the ubiquitous promoter *arm*. In these cells, Gal4 activates the expression of the transgene of interest (*m*) and the fluorescent membrane marker CD8-mCherry by binding to the UAS promoter, generating marked mutant clones in a wild-type unmarked background (Figure 2.2). The same system was used to generate single (*eglRNAi* or *KhcRNAi*) and double (*eglRNAi* + *KhcRNAi*) knock-down mutant clones to measure the change in *zip* RNA localization, with the substitution of the *UAS-CD8-mCherry* allele on the 3rd chromosome with the *UAS-NLS-mCherry* allele on the 2nd chromosome.

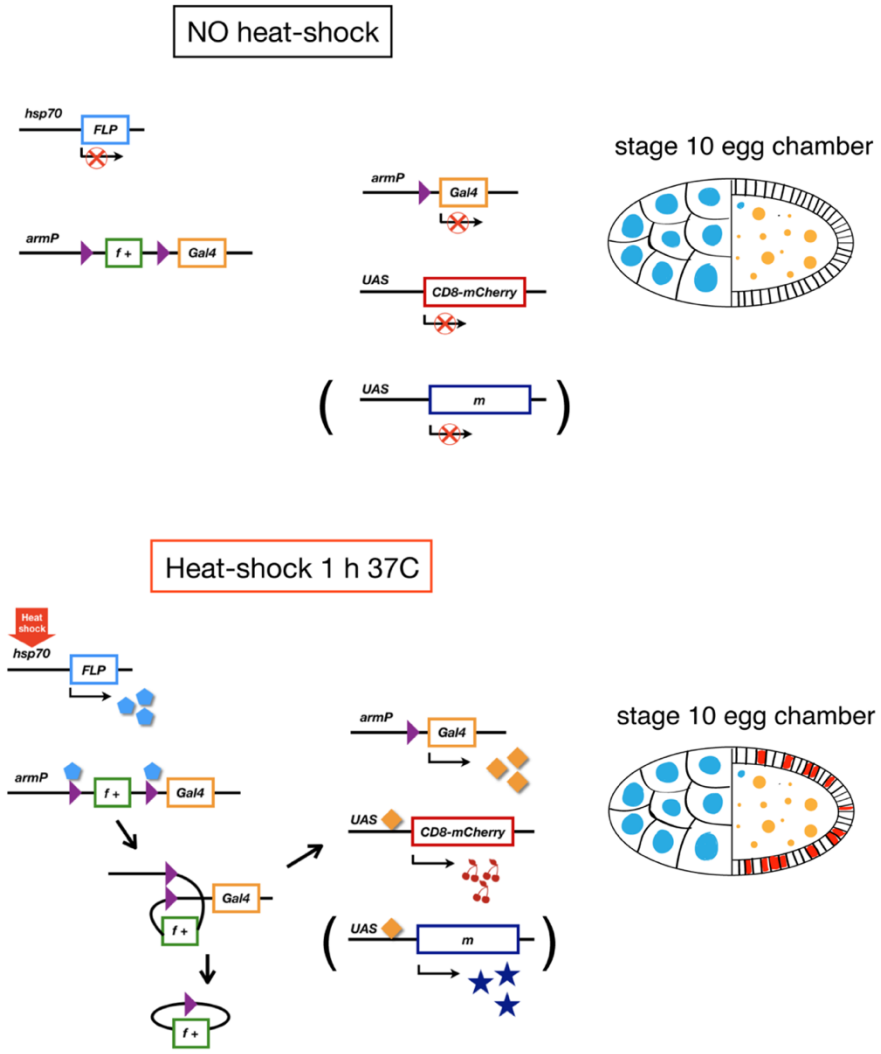


**Figure 2.2 - Generation of CD8-mCherry-marked mutant clones with the UAS-Gal4 "flip-out" system.**

The protocol described by Gonzales-Reyes and St Johnston (1998) was followed to generate follicle cell clones. This protocol allows one to create mutant clones at stage ~ 5 of oogenesis and visualize the phenotypic effect in stage 10 egg-chambers by controlling the timing between the heat shock and the dissection (39 h). Briefly, newborn females resulting from each cross were collected and mated with $w^{1118}$ males for 24 h at 25°C on food supplemented with yeast. Flies were heat-shocked for 1h in a water bath heated at 37°C; then, they were kept for 39 h at 25°C with males on yeast. Flies were flipped every day in new vials containing yeast until the day of dissection.

***Colchicine treatment***

Young *Jupiter-GFP* protein trap female flies were incubated with males for 24 h at 25°C on fly food supplemented with yeast. Ovaries were dissected in PBS and immediately incubated in Schneider's medium supplemented with insulin (200 µg/ml) and either 100% ethanol (control condition) or colchicine (200 µg/ml for 1 h or 100 µg/ml for 2 h) at RT before dissection.

***Egg hatching rate***

*wRNAi* (control) and *eglRNAi* female flies were crossed with *tj-Gal4* male flies to induce the expression of shRNA against *w* and *egl* respectively. Female flies resulting from these crosses were incubated with $w^{1118}$ males for 24 h at 25°C on fly food supplemented with yeast. Single females were then kept with 3 males on apple plates supplemented with yeast paste for 24 h at 25°C to allow the deposition of eggs. The next day, the number of eggs laid was counted and kept for 24 h at 25°C to allow eggs to hatch.

### 2.2.4 smFISH procedures

***Probe design***

smFISH antisense oligonucleotides were designed in R Studio with an algorithm developed by Imre Gaspar. With the exclusion of probes annealing to *BicD-RC* isoform, all probes were designed using as a template a region on the RNA common to all transcript isoforms, most frequently the CDS. For the specific detection of *BicD-RC* isoform, probes were designed using as a template the region of *BicD-RC* 3'UTR that does not overlap with the other *BicD* RNA isoforms. Non-overlapping probes of 18-30mer DNA oligonucleotides were designed complementary to *AdipoR*, *baz*, *BicD*, *Bsg25D*, *CG3308*, *CG33129*, *Cortactin*, *crb*, *CycG*, *Dlic*, *egl*, *Fkbp14*, *Imp*, *msps*, *qtc*,

*rho-4*, *Rtnl1*, *Sara*, *tud*, *vkg*, *zip* (apical and basally localizing mRNAs), *Act57B*, *Mhc*, *wupA* (muscle cell markers), *BicD(CDS)* (annealing to the CDS region of all *BicD* RNA isoforms), *BicD(RC)* (recognizing specifically *BicD-RC* RNA isoform), and *EGFP*. Probes were selected with the following criteria: 45-60% CG content, similar melting temperature (max 5°C difference). Probe sets were ordered in plates desalted-purified from Sigma-Aldrich, and dissolved in water in a final concentration of 250 µM/oligo.

***Probe labelling***

Probe sets were labelled with dye-conjugated ddUTPs according to the protocol described by Gaspar et al. (2017) to generate single-labelled oligonucleotides at their 3'. ATTO-565-NHS esters and ATTO-633-NHS esters were conjugated to $NH_2$-ddUTP by Imre Gaspar to create ddUTP-ATTO-565 and ddUTP-ATTO-633 respectively.

All probe sets were labelled with ddUTP-ATTO-633, with the exception of *BicD(RC)*, which was labelled with ddUTP-ATTO-565. In addition to the probe sets labelled with ddUTP-ATTO-633, a different aliquote of *crb* and *BicD(CDS)* probe sets were labelled with ddUTP-ATTO-565. The oligonucleotides composing each probe set were mixed in equal proportions, and 1000 pmol of the oligo mix was added to a reaction mix that included the terminal deoxynucleotidyl transferase (TdT), ddUTP-ATTO-633 (or ddUTP-ATTO-565), TdT buffer, and water to a final volume of 15 µl (see Materials). The reaction mixture was incubated o/n in a thermocycler set at 37°C; labelled probes were subjected the following day to ethanol precipitation for 1h at -80°C followed by 20 min centrifugation at 16,000xg in a in a tabletop centrifuge pre-cooled at 4°C. Labelled probes were then washed 3x with 80% ethanol at 16,000xg for 5 minutes. The pellet was air-dried and resuspended in 25 µl $H_2O$. The absorbance of unlabelled and dye-ddUTP-labelled probe sets was measured with UV-Vis spectroscopy at 260 nm and at the dye absorption maximum using a Nanodrop spectrophotometer. The degree of labelling (DOL, % of labelled oligos) and concentration of the labelled probe sets was measured according to the published algorithm. Only probe sets with a DOL > 70% were used in smFISH experiments.

***smFISH***

5-10 pairs of ovaries were dissected from flies of the desired genotype in PBS. Dissected ovaries were immediately fixed in 2% PFA/PBSTX(0.1%) on a nutator for

20 min at RT. In case of *ex vivo* colchicine incubation, dissected ovaries were incubated in Schneider's medium with ethanol or colchicine before proceeding with fixation, as described above. Fixed ovaries were rinsed and washed twice with PBSTX(0.1%) for 10 min gently shaking at RT and dehydrated by replacing PBSTX(0.1%) with increasing concentrations of ethanol/PBSTX(0.1%) (50%, 75%, 87%, 93%, 96%, 100%). Fixed and dehydrated ovaries were kept in 100% ethanol at -20°C for up to 10 days until the day of the experiment.

An optimized version of smFISH protocol was provided by Andre Schwarz and applied with some modifications. Ovaries were first re-hydrated by replacing 100% Ethanol with PBSTX(0.1%) and allowed to soak for 10 min, followed by two washes of 15 min each with PBSTX(0.1%) shaking at RT. PBSTX(0.1%) was then replaced with Pre-hybridization Buffer (see Materials) and kept shaking at RT for at least 30 min. The Pre-hybridization Buffer was replaced with 250 µl of Hybridization Buffer (see Materials) pre-warmed at 37°C in which smFISH probes were added to a final concentration of 1 nM/probe. Ovaries were kept hybridizing in the dark for 16 h on a heat block set at 37°C shaking at 1000 rpm. Ovaries where then washed 3x 10 min with Washing Buffer (of the same composition of Pre-hybridization Buffer) at 37°C. During the second wash, 1:10,000 DAPI was added to the Washing Buffer. Finally, ovaries were rinsed 4x in PBST(0.1%) and kept in 100 µl of 80% TDE/PBS o/n before mounting on microscope slides.

Z-stacks of images were acquired on a Leica TCS SP8 confocal microscope with 405nm, 488 nm, 552 nm and 640 nm fixed excitation laser lines using a 63× 1.3 NA glycerol immersion objective. A suitable range for spectral detection was carefully chosen for each channel to avoid cross-talk of fluorescence emission. Images were automatically restored by deconvolution with the Lightning module.

### 2.2.5 Western blotting

***Preparation of ovarian lysates***

$w^{1118}$, $egl^{NULL}FC$ + *osk>Egl*, $egl^{NULL}FC$ + *αTub67C>Egl*, and $egl^{NULL}FC$ + *vasa>Egl* ovaries were dissected in PBS and transferred to RIPA Buffer supplemented with protease inhibitor (see Materials). Ovaries were then mashed with a pestle and centrifuged for 5 min at max speed in a tabletop centrifuge pre-cooled at 4°C. The supernatant was transferred into a new tube and kept at -80°C.

***Measurement of the protein concentration (Bradford assay)***

The total protein concentration in the lysate was measured with the Bradford assay using the 5X Bradford Reagent (SERVA Electrophoresis) following the manufacturer's instructions (section: Micro assay). The standard curve was generated with the following BSA dilutions (in duplicate) of a 100 µg/ml BSA stock solution:

| | BSA (µl of stock) | RIPA Buffer (µl) | ddH20 (µl) |
|---|---|---|---|
| Blank | 0 | 2 | 798 |
| 1 µg/ml BSA | 10 | 2 | 788 |
| 5 µg/ml BSA | 50 | 2 | 748 |
| 10 µg/ml BSA | 100 | 2 | 698 |
| 15 µg/ml BSA | 150 | 2 | 648 |
| 20 µg/ml BSA | 200 | 2 | 598 |
| 25 µg/ml BSA | 250 | 2 | 548 |

2 µl of samples of unknown protein concentration were added to 2 µl RIPA Buffer and 798 µl $ddH_20$ (in duplicate). 200 µl of 5X Bradford was added to each blank, standard, and sample; tubes were vortexed and incubated for 5 min at RT. The absorbance was measured with UV-Vis spectroscopy at 595 nm using an Eppendorf Biophotometer Plus spectrophotometer.

***SDS-PAGE and western blotting***

20 µg of proteins for each samples were resolved in 4-12% polyacrylamide pre-casted gels. Proteins were transferred to methanol-activated PVDF membranes at 15 V for 1 h in a Trans-Blot SD semi-dry transfer cell soaked in Transfer Buffer (see Materials). After the transfer, proteins were visualized with Ponceau S staining. Membranes were incubated with Blocking Buffer (see Materials) for 1 h at RT, followed by incubation with primary antibodies diluted in Blocking Buffer o/n at 4°C on a nutator. Membranes were then washed 5x 5 min with TBST(0.1%) and incubated with HRP-conjugated secondary antibodies diluted in Blocking buffer for 1h at RT. Finally, membranes were washed 5x 5 min with TBST and 5x 5 min with TBS. Signal detection on X-ray film was performed by enhanced chemiluminescence with Immobilon Western HRP substrate peroxide solution according to the manufacturer's instructions.

### 2.2.6 Signal quantification and statistical analyses

***Quantification of RNA localization for validated RNAs***

To quantify the smFISH fluorescence as a proxy for relative transcript abundance, Z-projections of deconvolved image stacks acquired at the confocal microscope were analyzed with FIJI software. For each gene, a region of interest (ROI) was drawn encompassing the apical or the basal domain of 5-10 adjacent follicle cells (with the exclusion of nuclei) and the mean fluorescence intensity (m.f.i.) measured for each ROI; in addition, a ROI was drawn in an area of the image were no signal was present (background, *bg*) and measured the *bg* m.f.i. (Figure 2.3A). The $log_2$FoldChange of smFISH signal for each gene was measured by applying the formula:

$$log_2(FoldChange) = log_2\left(\frac{Apical_{m.f.i.} - bg_{m.f.i.}}{Basal_{m.f.i.} - bg_{m.f.i.}}\right)$$

For each gene, the $log_2$FoldChange of at least two different stacks was measured. The mean $log_2$FoldChange of each validated gene was plotted against the $log_2$FoldChange measured in the RNA-seq; linear regression was performed using R Studio. The adjusted $R^2$ was calculated to evaluate the goodness-of-fit of the model.

***Quantification of* zip *RNA localization in different conditions***

The $log_{10}$FoldChange between the apical and basal m.f.i. of *zip* mRNA in wild-type and RNAi conditions was calculated as described above with some modifications. For each cell type in the image (wild-type or *RNAi*), a ROI was drawn encompassing the apical or the basal domain of 2-5 adjacent follicle cells of the same type (with the exclusion of nuclei) and the m.f.i. measured for each ROI; in addition, a ROI was drawn in an area of the image were no signal was present (background, *bg*) and measured the *bg* m.f.i. (Figure 2.3B). The $log_{10}$FoldChange of *zip* smFISH signal was measured as follows:

$$log_{10}(FoldChange)_{(t,c)} = log_{10}\left(\frac{Apical_{m.f.i.(t)} - bg_{m.f.i.}}{Basal_{m.f.i.(t)} - bg_{m.f.i.}}\right)_c$$

Where *t* represents the cell type (wild-type or *RNAi*) and *c* the experimental condition (*egl* RNAi, *Khc* RNAi or *egl* RNAi + *Khc* RNAi). The mean $log_{10}$FoldChange of the wild-type and *RNAi* cells was calculated for each of the 3 experimental conditions on at least 3 different images (n = 3; n= 5; n=7 respectively).

Independent t-test was used to compare means within wild-type and *RNAi* cells for each of the 3 experimental conditions.

To calculate the change between the *RNAi* and wild-type (wt) *zip* enrichment in each experimental condition ($c$), the following formula was applied:

$$change_{RNAi/wt(c)} = \left(\frac{Apical_{m.f.i.(RNAi)} - bg_{m.f.i.}}{Basal_{m.f.i.(RNAi)} - bg_{m.f.i.}}\right)_c / \left(\frac{Apical_{m.f.i.(wt)} - bg_{m.f.i.}}{Basal_{m.f.i.(wt)} - bg_{m.f.i.}}\right)_c$$

The change(RNAi/wt) was measured for each image, and the average change(RNAi/wt) was calculated for each experimental condition. To determine whether the average change(RNAi/wt) measurements for each experimental condition significantly differ globally and with each other, one-way ANOVA followed by Tukey post-hoc statistical tests were used to compare means.

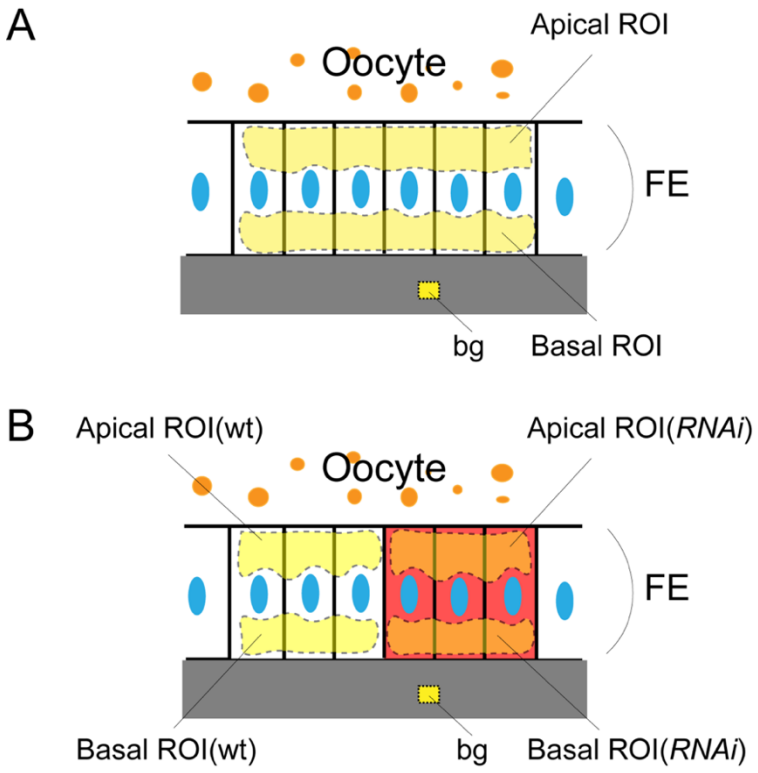


**Figure 2.3 - Analysis of signal intensity of apical and basal mRNAs.** A) analysis on wild-type follicle cells. B) Analysis on wildtype (wt, white cells) and *RNAi* (red cells) follicle cell clones. FE=Follicular epithelium; ROI=Region of interest; bg=background.

### *Quantification of Imp-GFP and Imp RNA fluorescence*

The $\log_{10}$FoldChange between the apical and basal m.f.i. of Imp-GFP and *Imp* RNA was calculated as described above with some modification. For each cell type in

the image (wild-type or *eglRNAi*), a ROI was drawn encompassing the apical or the basal domain of 2-5 adjacent follicle cells (with the exclusion of nuclei) and the m.f.i. measured for each ROI in each channel (RNA or GFP); in addition, a ROI was drawn in an area of the image were no signal was present (background, *bg*) and measured the *bg* m.f.i. for each of the two channels. The $\log_{10}$FoldChange of *Imp* RNA and Imp-GFP signal was measured as follows:

$$log_{10}(FoldChange)_{(t,ch)} = log_{10}\left(\frac{Apical_{m.f.i.(t)} - bg_{m.f.i.}}{Basal_{m.f.i.(t)} - bg_{m.f.i.}}\right)_{ch}$$

Where *t* represents the cell type (wild-type or *eglRNAi*) and *ch* the channel (RNA or GFP). The mean $\log_{10}$FoldChange of the wild-type and *eglRNAi* cells was calculated for each channel on 4 different images. Independent t-test was used to compare means between wild-type and *eglRNAi* cells for each RNA and GFP channel.

To calculate the total intensity signal the following formula was applied:

$$(A+B)_{m.f.i\,(t,ch)} = \left(Apical_{m.f.i(t)} - bg_{m.f.i}\right) + \left(Basal_{m.f.i(t)} - bg_{m.f.i}\right)_{ch}$$

Paired t-test was used to compare the mean (A+B)m.f.i. of wild-type and *eglRNAi* cells for each channel.

***Egg hatching rate analysis***

The egg hatching rate relative to eggs laid by a single fly was measured as follows:

$$egg\ hatching\ rate = \frac{n\ hatched\ eggs}{n\ total\ eggs}$$

The mean egg hatching rate was calculated by averaging the hatching rate of flies of the same genotype (*tj>wRNAi* or *tj>eglRNAi*). Independent t-test was used to compare means between the two groups.

***Quantification of driver strength***

Quantification of protein bands on western blot was done in FIJI. A single ROI was drawn in order to include the largest band. The same ROI was used to measure the intensity of each Egl and Tub bands present on the image and adjusted for background signal. The ratio between Egl and Tub intensities was calculated for each genotype and compared with the mean Egl/Tub ratio calculated by quantifying signal from two western blots.

# Chapter 3: Results

## 3.1 Part I: LCM followed by RNA-seq identifies apically- and basally-localizing mRNAs in the *Drosophila* follicular epithelium

### 3.1.1 The "Geo-seq" protocol produces good quality sequencing libraries

With the aim to identify transcriptome-wide mRNAs that localize apically and basally in the follicular epithelium (FE), I first established a procedure that allowed me to micro-dissect the ovarian tissues while preserving both the RNA quality and the egg-chamber morphology (Figure 3.1). Laser-Capture Microdissection (LCM) allows one to collect sub-population of cells in a heterogeneous tissue visualized under the microscope. When coupled with RNA-seq, LCM is a powerful tool to identify transcriptome-wide mRNAs present in the micro-dissected cell fragments without losing their spatial information. After LCM optimization, I micro-dissected and pooled several fragments consisting of either the apical half ("Apical domain", A) or the basal half ("Basal domain", B) of adjacent follicle cells of stage 9-10B egg-chambers.

To obtain good quality sequencing libraries from the LCM fragments, I sequenced and compared follicle cell cDNA libraries prepared with two different protocols, namely "Geo-seq" (Chen et al., 2017) and "LCM-seq" (Nichterwitz et al., 2016), with minor modifications. Although both protocols are based on the application of the Smart-seq2 technique (Picelli et al., 2014) to reverse-transcribe the mRNA into cDNA, they differ in the lysis treatment of the LCM samples. To evaluate which protocol works better for *Drosophila* ovarian tissue, I sequenced and mapped to the *Drosophila* genome LCM samples prepared with the two protocols. Then, I analyzed the normalized read coverage with respect to the relative transcript position for each library (Figure 3.2**)**. This test allowed me to spot the presence of possible mRNA degradation, characterized by an overrepresentation of reads in the 3' of transcripts. I found that the "Geo-seq" protocol performs better in preserving RNA integrity, showing only a slight 3'-end bias along the normalized transcript, which is expected from oligo dT-based reverse-transcription protocols. In contrast, libraries prepared following the "LCM-seq" protocol displayed a pronounced 3'-end bias, probably due to RNA degradation during the lysis procedure; this, in turn, could introduce a

systematic error in the downstream bioinformatic analysis. For this reason, I decided to follow the "Geo-seq" protocol for the preparation of the sequencing libraries. In total, I submitted for sequencing 5 biological replicates for each of the apical and basal samples.

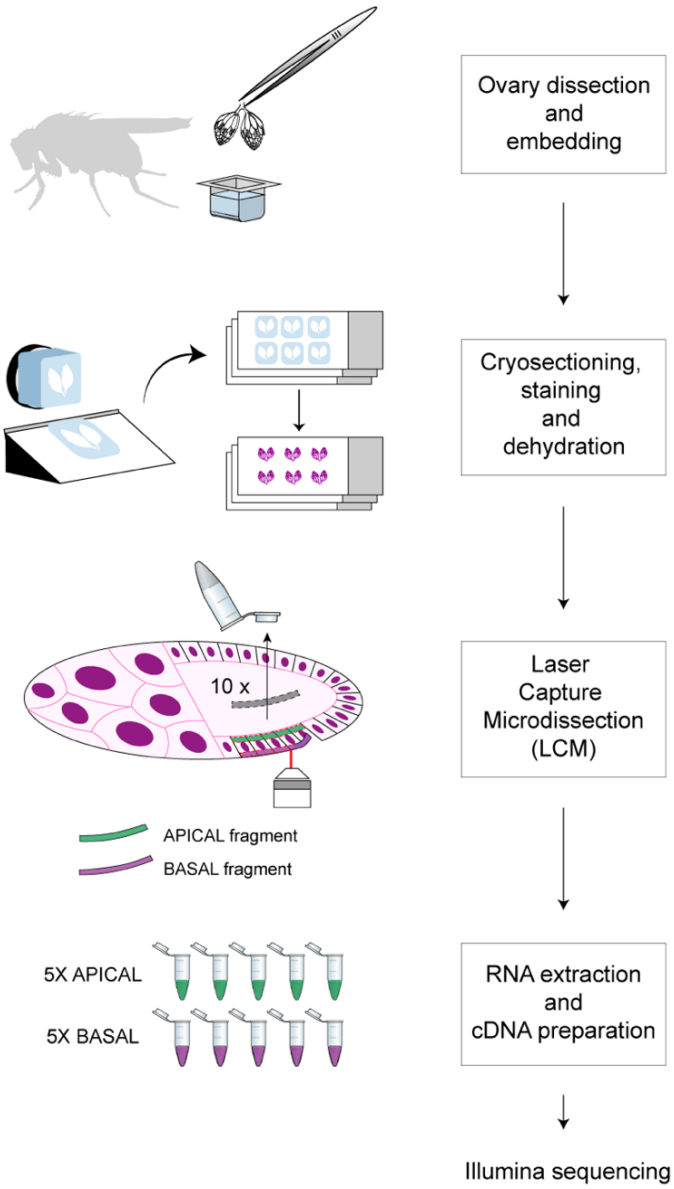


**Figure 3.1 - Overview of the LCM sample preparation procedure.**

Analysis of the total sequencing read distribution revealed that the average unique mappability across samples ranged between 27-56% (7.3-15.4 Million reads) (Supplementary Figure 1A, Supplementary Table 1). Despite the relatively low mappability, the amount of uniquely-mapping reads is considered adequate for downstream RNA-seq analysis (Conesa et al., 2016). The low percentage of mapping

reads was mainly due to the presence of a considerable proportion of reads that failed to map to the *Drosophila* genome ("unmapped reads"), which, instead, aligned with the sequence of the LNA-TSO oligo used in the template-switching step of the Smart-seq2 reaction. This revealed the presence of TSO concatemers seen also by Picelli et al. (2014) and generally considered to be due to the low amount of input material.

To have a deeper look into the quality of the sequencing libraries, I analyzed the composition of uniquely mapping reads in terms of mapping to genomic features (Supplementary Figure 1B, Supplementary Table 2). I found that the majority of reads (> 96%) mapped to transcribed regions of the genome (CDS + UTRs), confirming that the RNA-seq was successful.

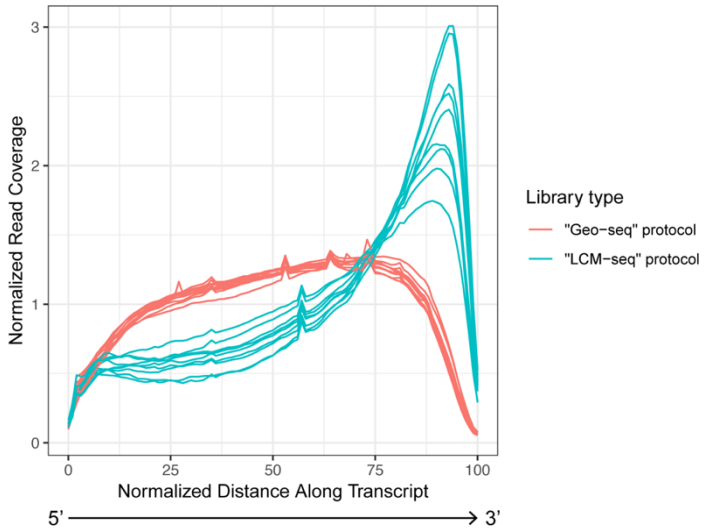


**Figure 3.2 - Normalized Transcript Coverage of RNA-seq libraries produced with "Geo-seq" (n=10) and "LCM-seq" (n=9) protocols.**

### 3.1.2 Differential gene expression analysis identifies the apical and basal transcriptomes of follicle cells

Quality control of normalized read counts is an essential step in defining which and how many of the sequenced libraries can be used for downstream differential gene expression analysis. To analyze the dissimilarity between the apical and basal datasets, I performed a pairwise comparison between replicates of the same type of biological sample (apical or basal) analyzing the Pearson coefficient as a proxy for correlation. In addition, I performed hierarchical clustering on the datasets by measuring the Euclidean distance among all samples. Finally, the Principal Component Analysis (PCA) allowed me to have an overview of the variability of the datasets.

The Pearson correlation coefficient ($r$) computed by pairwise replicate comparisons showed that the samples A5 and B5 were the least correlated replicates ($r < 0.92$) among the apical and basal samples, respectively (Supplementary Figure 2). Hierarchical clustering and the PCA analysis confirmed the dissimilarity, with the A5 and B5 samples clustering outside the main apical and basal groups (Supplementary Figure 3A,B). For these reasons, I excluded the A5 and B5 samples from further analysis. By comparing the apical and basal samples through differential gene expression analysis, I found that 306 mRNAs were enriched in the apical domain ("Apical dataset") and 249 mRNAs were enriched in the basal domain ("Basal dataset") (adjusted p-value < 0.1) (Figure 3.3 and Supplementary Figure 4A-F for quality control).

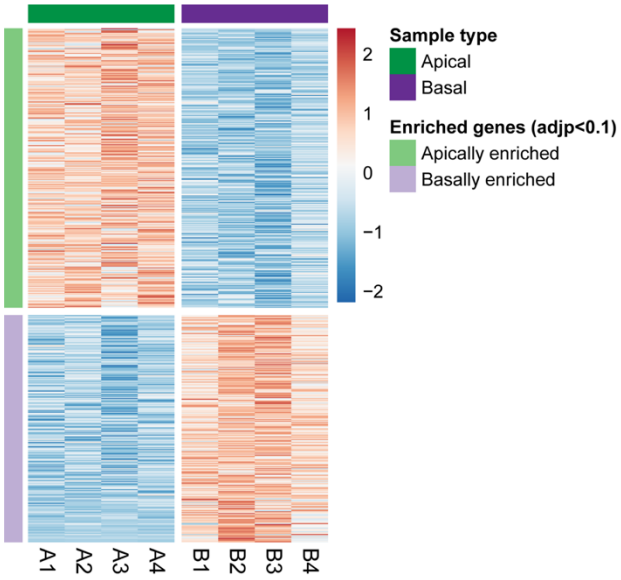


**Figure 3.3 - Significantly enriched genes (adjusted p-value: p < 0.1) in the apical and basal datasets.** The legend indicates the row Z-score for each gene across samples. A1-A4: apical samples; B1-B4; basal samples.

### 3.1.3 *In silico* comparison of the Apical and Basal datasets with published collections of *Drosophila* localizing RNAs reveals a high proportion of novel localizing RNAs

To have an overview of the apical and basal datasets, I compared their gene composition with published lists of subcellularly localizing RNAs in *Drosophila* embryonic tissues (FlyFISH, Lecuyer et al., 2007 and Wilk et al., 2016) and ovary (Dresden Ovary Table, Jambor et al., 2015), as determined by high-throughput FISH experiments. First, I analyzed what proportion of significantly enriched genes (either

apical or basal, n = 555) was included in a subset of the FlyFISH gene collection filtered for those genes annotated with the term "Subcellular localization" in any tissue (including embryonic, larval and adult tissues). Next, I analyzed separately the apical and basal datasets, by comparing each dataset with the lists of genes annotated as "apical" or "basal" from both the FlyFISH and the Dresden Ovary Table databases. I found that 44.9% of significantly enriched genes showed a subcellular localization pattern in other *Drosophila* tissues (Figure 3.4 top chart), indicating that the mechanisms that mediate RNA localization of these transcripts might be conserved throughout development. Conversely, only a small proportion (15.4% of apical and 6.8% of basal) of mRNAs that are significantly enriched in either domain was previously identified to be apically- or basally-localizing by high-throughput screens (Figure 3.4 middle and bottom chart). This suggests that the proportion of mRNAs that localize along the apical-basal (A/B) axis in different cell types might have been underestimated in previous high-throughput studies.

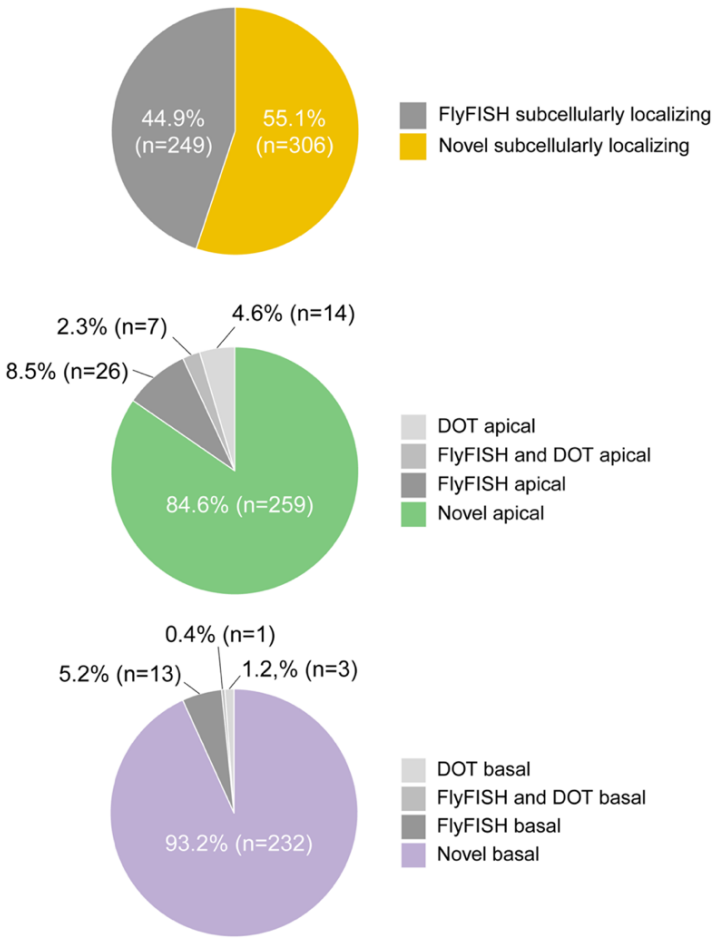


**Figure 3.4 - Comparison of significantly enriched genes with known gene sets of localizing mRNAs.** DOT: Dresden Ovary Table.

### 3.1.4 Validation of the RNA-seq through smFISH indicates that the apical and basal datasets are reliable

To validate the RNA-seq results, I performed single-molecule Fluorescence *In Situ* Hybridization (smFISH) experiments on wild-type fixed ovaries of selected apical and basal mRNA candidates (Figure 3.5A,B). Of 23 candidate genes tested, only 2 were not validated, showing that the apical and basal datasets obtained by RNA-seq of micro-dissected follicle cells are highly reliable. In addition, for each transcript I measured the ratio between the apical and basal mean fluorescence intensity and compared it to the gene's mean read fold-change obtained by differential gene expression analysis (both parameters converted to $\log_2$FoldChange) (Figure 3.6). This resulted in a good correlation between the smFISH and RNA-seq results (adjusted $R^2$= 0.65).

Among the validated genes, I could identify 2 categories of mRNAs: the first category includes those mRNAs which are excluded from one of the two domains, and present almost exclusively in the other (*CG33129*, *BicD*, *Bsg25D*, *qtc*, *CG3308*, *baz*); the second category comprises mRNAs that are enriched in one of the two domains, but are present in both (*egl*, *Imp*, *zip*, *Sara*, *vkg*, *Fkbp14*, *Dlic*, *tud*, *rho-4*, *CycG*, *AdipoR*, *msps*, *Cortactin*, *SerRS*, *Rtnl1*). This might be an indication of different modes of mRNA localization.

Interestingly, the localization pattern of the validated mRNAs in each domain is heterogeneous, with some mRNAs being localized in proximity of the cell periphery (*BicD*, *CG33129*, *Bsg25D*, *zip*, *CG3308*), while others seemingly associated with organelles (*vkg*), or exhibiting an expression pattern that resembles that of the endoplasmic reticulum (*Rtnl1*, *Fkbp14*). It is also interesting to note that mRNAs encoding putative or known transmembrane proteins (*CG33129*, *AdipoR*), as well as endosomal (*Sara*), ER- and Golgi-resident (*Fkbp14*, *qtc*), and nuclear (*CycG*) proteins show a clear subcellular localization pattern, suggesting the presence of subcellular compartments with specialized functions. Finally, 3 genes encoding components of the apical mRNA transport complex dynein/BicD/Egl (*Dlic*, *BicD*, *egl*) show, in turn, apical localization of their encoded mRNA. This hints at the possibility that components of the complex might be (co-)translated and assembled in the apical domain.

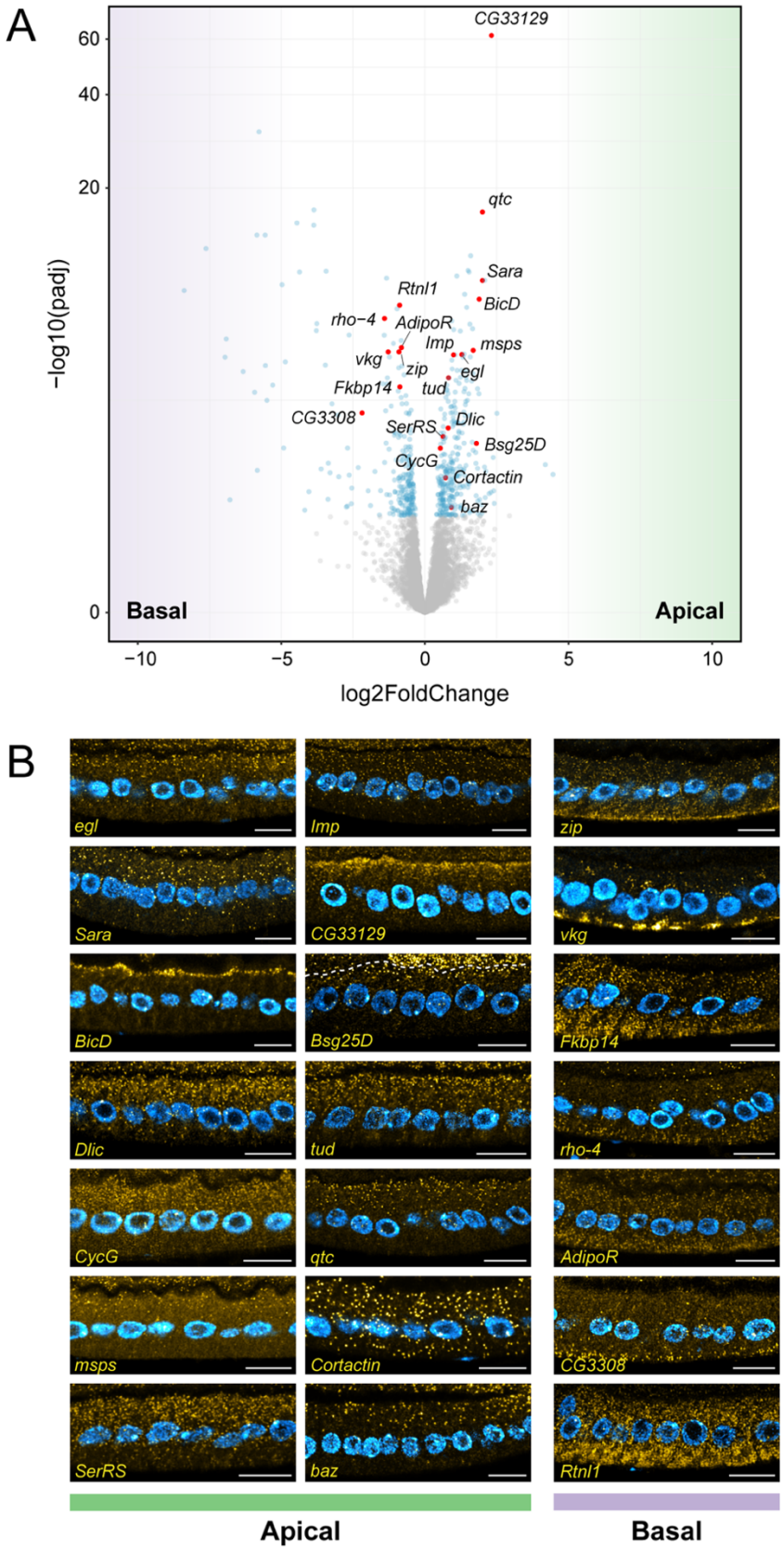


**Figure 3.5 – Validation of candidate apical and basal mRNAs by smFISH**. A) Volcano plot of significantly enriched genes (blue dots, padj <0.1). Candidate mRNAs chosen for validation are highlighted in red. B) smFISH validation of candidate mRNAs. The dashed line in *Bsg25D* panel delimits FCs and the germline. Apical is on the top. Nuclei are stained with DAPI. Scale bars 10 µm.

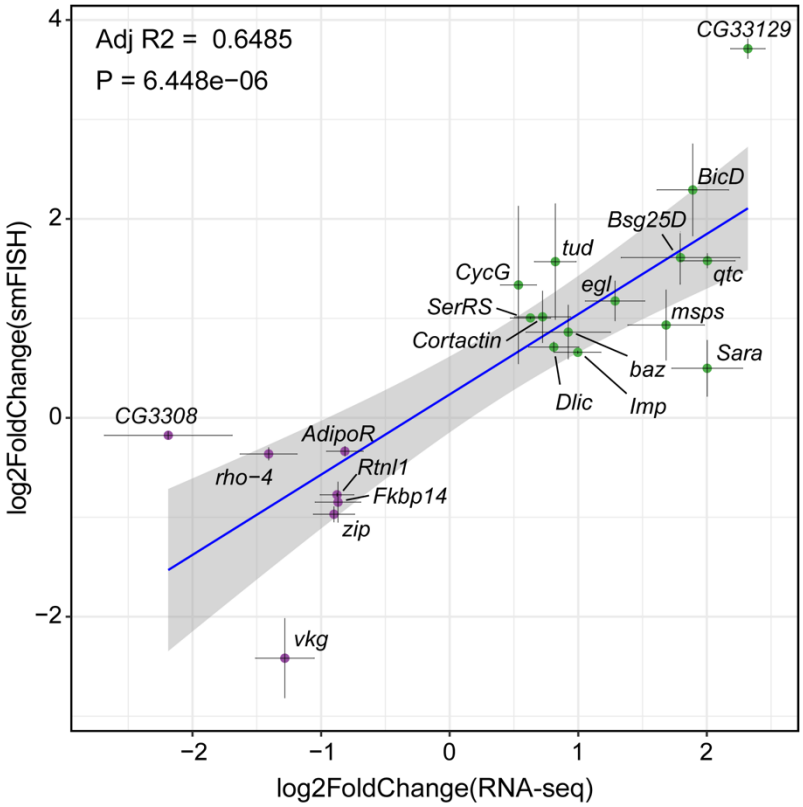


**Figure 3.6 - Correlation between RNA-seq and smFISH $log_2$Fold Change for validated candidate genes.** Lines indicate the standard error.

### 3.1.5 Bioinformatic analysis indicates that tissue contamination is limited

The FE is flanked by the oocyte on the apical side and by a thin layer of muscle fibers on the basal side. For this reason, LCM is particularly challenging in producing samples devoid of contaminating mRNA species from surrounding tissues. Therefore, I attempted to identify the apical and basal gene contaminants through a combination of functional analysis and fold change-based filtering. Throughout ovary development, many different mRNA species are deposited in the oocyte to function during oogenesis and/or early embryogenesis, creating a high degree of complexity and making it almost impossible to identify oocyte-specific contaminants. However, the muscle tissue is composed of terminally differentiated cells expressing a small subset of "hallmark" genes specialized for contractile functions. Therefore, contaminant genes from the muscle tissue could be easily identified by functional analysis.

Gene Ontology (GO) enrichment analysis of the apical and basal datasets highlighted which functional categories of genes were overrepresented in each dataset, compared to a "universe" of expressed genes. By looking at the biological processes

enriched in each dataset, I found that the basal dataset showed an over-representation of muscle-related terms (Figure 3.7), hinting at a possible contamination from the surrounding muscle tissue. Although it is tempting to consider as "contaminants" all genes falling into the categories of muscle-related terms, this strategy might lead to the filtering of genes expressed in the FE and annotated to have a function also in muscles (e.g. actin, myosinII, etc).

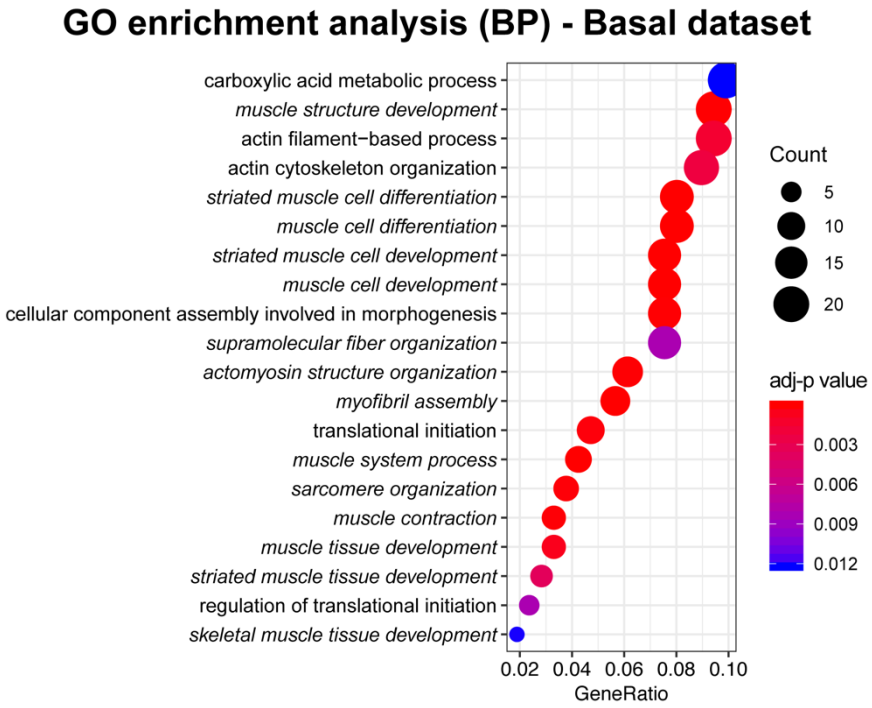


**Figure 3.7 - Gene Ontology (GO) enrichment analysis showing the over-representation of muscle-related terms (italic) in the basal dataset.**

For this reason, I attempted to find a strategy that would allow me to filter out contaminant genes in an unbiased way. By looking at the fold-change distribution of significantly enriched genes in the basal dataset, I noticed that genes with high fold change (> 3) were also likely to be annotated as muscle-related. The relatively high fold change can be explained by a characteristic read distribution in which reads mapping to these genes are found almost only in the basal dataset (Supplementary Figure 5). Thus, as a proxy for tissue contamination, I analyzed genes with $|\log_2 \text{FoldChange}| > 3$ in the apical and the basal datasets. I found that 2 genes in the apical dataset and 33 genes in the basal dataset satisfied this condition. Among the 33 basal contaminants, 2/3 (n=22) were annotated in Flybase as expressed or having a function in muscle tissues (Figure 3.8A). As highlighted by the MA plot, the majority

of contaminant genes (n=21) had a small mean count (baseMean < 100). Some 14 contaminant genes were more abundant (baseMean < 1000); however, their high abundance might reflect a combination of tissue contamination and expression in the follicle cells.

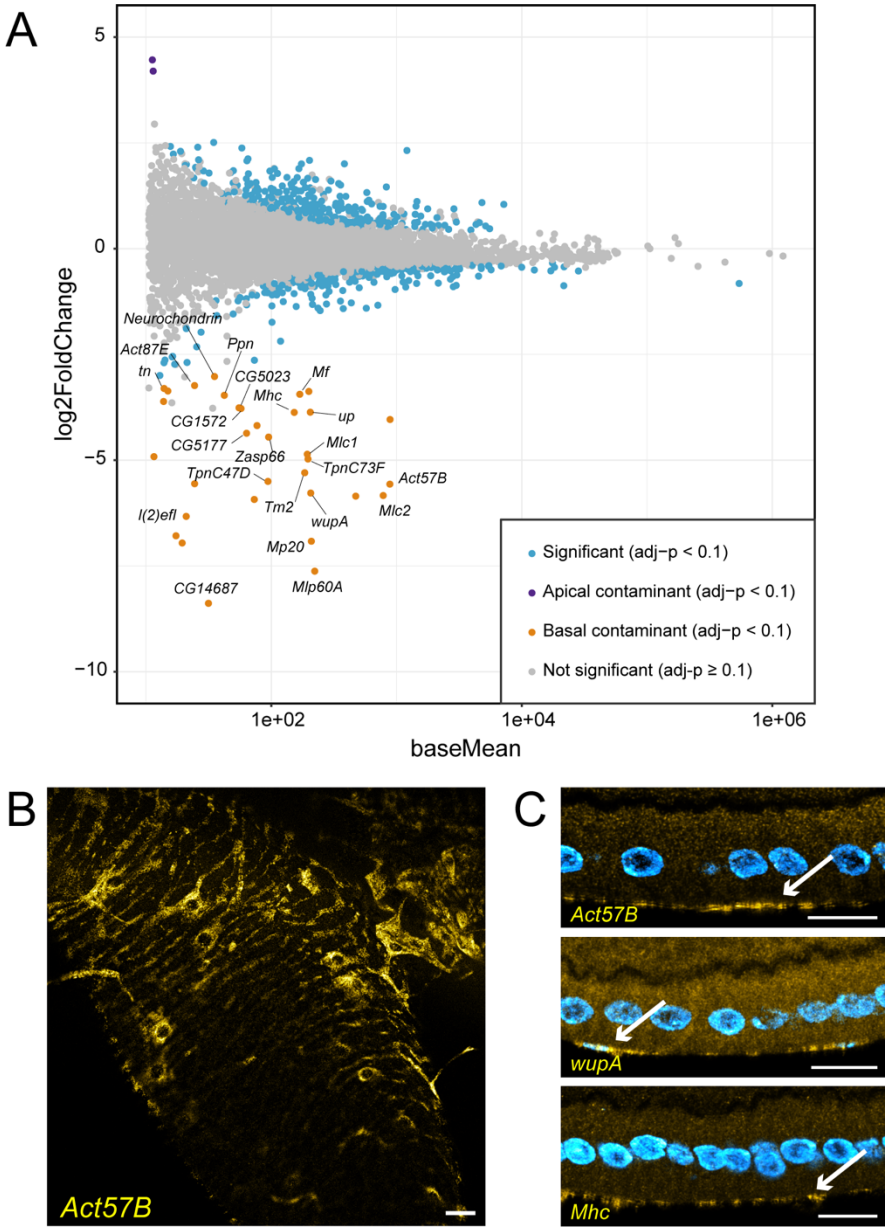


**Figure 3.8 - Evaluation of muscle contamination.** A) MA plot highlighting putative apical and basal contaminant genes, with labels indicating genes with known muscle-related functions and/or expression pattern. B) Upper view of an egg chamber stained for *Ac57B* mRNA showing expression in circular muscle fibers surrounding it. C) smFISH validation of candidate muscle mRNA contaminants. Arrows indicate signal from muscle fibers. Nulcei are stained with DAPI. Scale bars 10 µm.

To validate this analysis, I selected 3 significantly enriched genes in the basal dataset identified as putative muscle contaminants (*Act57B*, *Mhc*, *wupA*) and performed smFISH experiments on whole-mount fixed ovaries (Figure 3.8B,C). I found that all 3 genes were expressed in the muscle layer surrounding the follicle cells; in addition, *Act57B* was also expressed in the follicle cells, although the transcripts did not show a basal enrichment. This confirms that contamination from the muscle tissue results in the appearance of false-positive significant hits in the basal dataset. Importantly, a gene annotated as muscle-related (*zip*, encoding myosinII heavy chain) was validated as a true basally enriched transcript (Figure 3.5), highlighting how an unbiased, $log_2$FoldChange-based filtering is preferable to functional category-based contaminant filtering.

### 3.1.6 Gene Ontology enrichment analysis reveals functionally different apical and basal datasets

GO enrichment analysis on the apical and basal datasets filtered for contaminant genes might give an indication of functionally-related mRNAs enriching in the same domain. The comparison of the enriched biological processes shows that the two datasets differ significantly from each other in terms of overrepresented functional categories (Figure 3.9). The apical dataset is enriched for epithelium-specific processes, endosomal-mediated transport, and cell migration, whereas the basal dataset is characterized by an enrichment in metabolic and ER- and Golgi-related processes. This suggests that mRNA localization in follicle cells might play a role in locally concentrating mRNAs encoding functionally-related proteins.

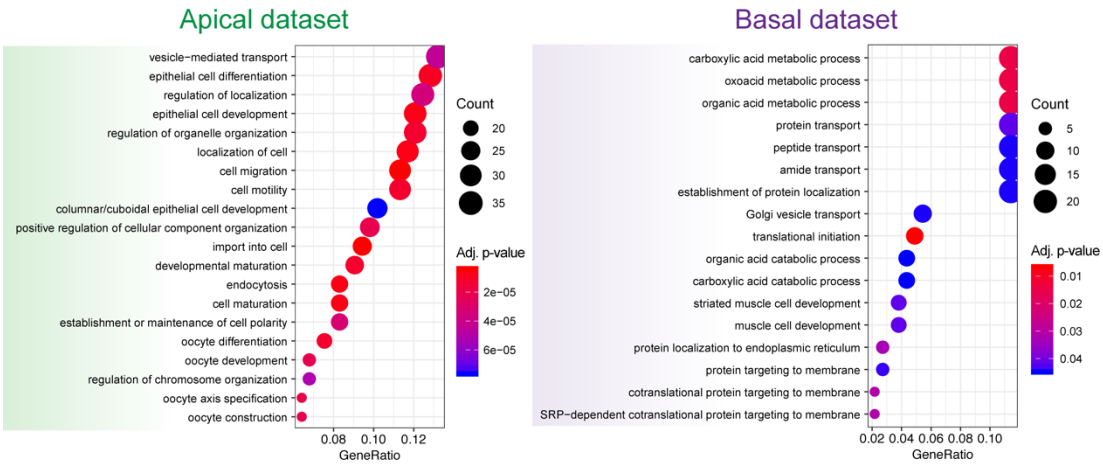


**Figure 3.9 - Gene Ontology (GO) enrichment analysis (Biological Process) on the contaminant-filtered apical and basal datasets.**

## 3.2 Part II: Apical and Basal RNA localization is finely regulated by different components of RNA transport machineries

The FE displays a highly polarized array of microtubules (MTs) that are organized in parallel bundles along the A/B axis of the cell, with their minus ends facing the apical side, and their plus ends concentrated at the basal side. Several studies have reported MT-dependent RNA localization for apical RNAs in the follicle cells (Horne-Badovinac and Bilder, 2008; Li et al., 2008). However, it is not known to which extent RNA localization in the FE is mediated by this mechanism.

To investigate the mechanisms active in the FE driving apical and basal localization, I selectively silenced key components of known RNA transport machineries by transgenic RNA interference (RNAi) (Dietzl et al., 2007) and assessed changes in RNA localization with smFISH of apically- and basally-localizing mRNA validated previously. To do so, I decided to use the UAS-Gal4 "flip-out" genetic system, which allows one to induce RNAi against a target gene by stably expressing the corresponding short hairpin RNA (shRNA) in a subset of cell clones in a tissue upon the activation of a heat shock-inducible promoter (see Materials and Methods). In this way, CD8-mCherry-marked *RNAi* mutant clones will be adjacent to wild-type control cells in a genetic mosaic fashion, allowing direct comparison of control and mutant cells within the same tissue. Finally, the use of genetic mosaics has the advantage to analyze the effect of mutations that otherwise would severely affect the ovarian development and/or tissue morphology.

I began the analysis by disrupting the activity of key components of the MT plus end-directed and MT minus end-directed RNA transport machineries. Next, I analyzed more in details how the two machineries are coordinated to regulate RNA transport. Finally, I performed an initial characterization of the mechanisms that underlie the apical localization of an *egalitarian*-independent mRNA.

### 3.2.1 Disruption of MT plus end-directed RNA transport affects basal RNA localization

To investigate the effect of disrupting MT plus end-directed RNA transport, I first knocked down the expression of the MT plus end-directed molecular motor kinesin-1 by performing RNAi against *Khc,* followed by smFISH of four apical (*crb*,

*CG33129*, *qtc*, *msps*) and four basal (*Fkbp14*, *CG3308*, *Rtnl1*, *zip*) mRNAs (Figure 3.10). The localization of the apical RNAs is not affected by *Khc* RNAi, suggesting that MT plus end-directed RNA transport plays little or no role in apical RNA localization. In contrast, localization of basal mRNAs was disrupted upon *Khc* RNAi, showing that the plus end-directed kinesin-1 motor plays a role in localizing basal RNAs towards the MT plus ends.

Interestingly, disruption of the basal RNA localization machinery results in a spectrum of RNA localization patterns. For example, *Khc* RNAi caused *CG3308* mRNA to become evenly distributed throughout the cytoplasm; in contrast, *Fkbp14*, *Rtnl1*, and *zip* mRNAs switched from basal to apical enrichment.

Previous reports have shown that the Exon Junction Complex (EJC) is required for kinesin-dependent transport of *oskar* mRNA to the posterior pole of the oocyte (Ghosh et al., 2014; Gaspar et al., 2016). To investigate if the same mechanism applies to basally-localizing mRNAs in the follicle cells, I expressed the EJC-disrupting protein ΔC-Pym tagged with GFP (Ghosh et al., 2014) in follicle cell clones, and carried out smFISH experiments of two apical mRNAs (*crb*, *CG33129*) and the same set of basal mRNAs (*Fkbp14*, *CG3308*, *Rtnl1*, *zip*) (Figure 3.11). The successful expression of ΔC-Pym was confirmed by the appearance of GFP signal in CD8-mCherry-expressing clones. EJC disruption resulted in the clear mislocalization of *Fkbp14* mRNA to the apical domain and, to a lesser extent, of *zip* and *CG3308* mRNAs. The subcellular localization of *Rtnl1*, *crb*, and *CG33129* mRNAs showed no change in enrichment compared to wild-type control cells. This suggests that EJC disruption affects kinesin-1-dependent RNA localization. However, the lack of change in *Rtnl1* mRNA localization in *ΔC-Pym-GFP* mutant clones suggests that the localization of only a subset of basal mRNAs is regulated by EJC deposition.

Importantly, it is unlikely that *Khc* RNAi and ΔC-Pym expression might have caused the apical enrichment phenotype of basal RNAs by affecting cell or MT polarity for two reasons. First, *KhcRNAi* and *ΔC-PYM* cells do not show any morphological polarity phenotype (mislocalization of the nucleus, cell rounding, multi-layering); secondly, apical RNA localization was not affected in the mutant clones, suggesting that the cell still possesses a clear A/B polariy.

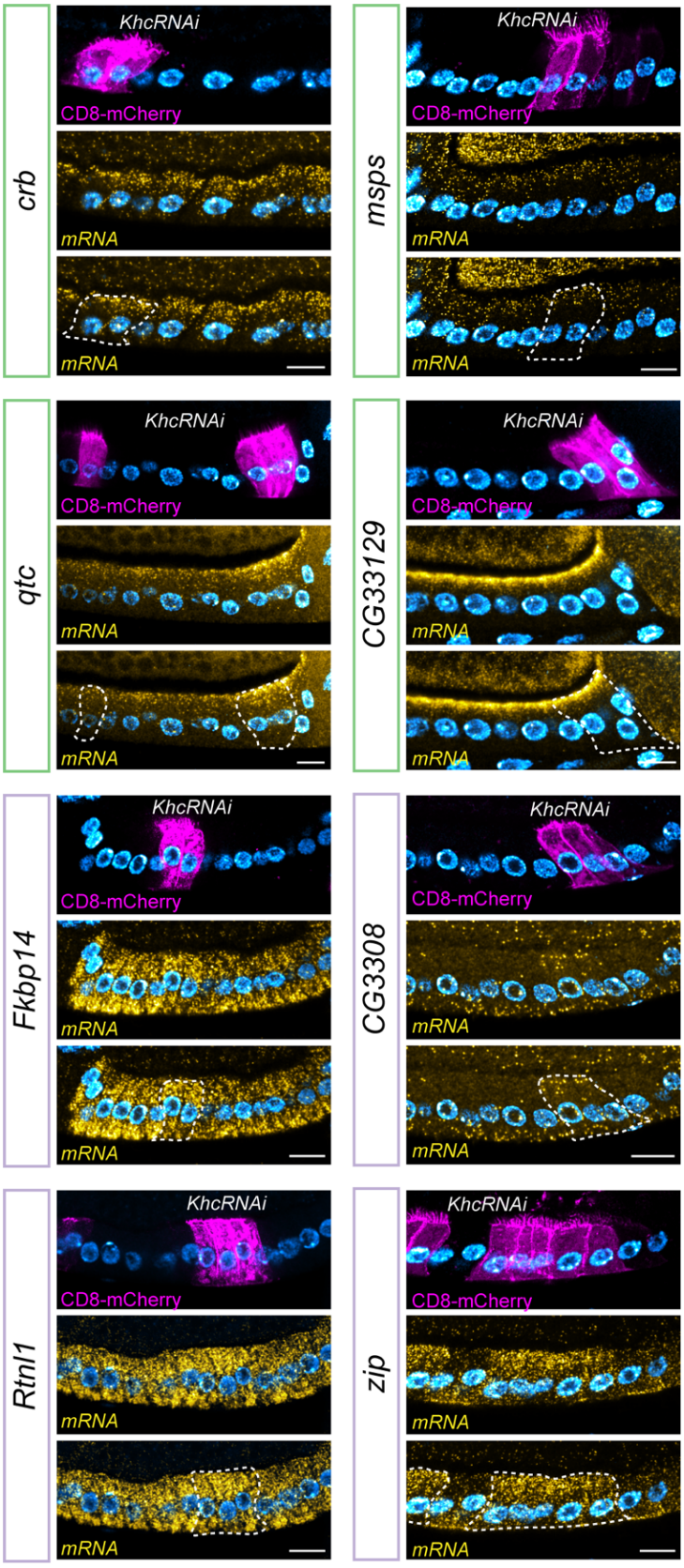


**Figure 3.10– Effects of *Khc* RNAi on the localization of apical and basal mRNAs revealed by smFISH.** Mutant *KhcRNAi* clones are identified by CD8-mCherry expression (dashed line in third panel down). Nuclei are stained with DAPI. Scale bars 10 µm.

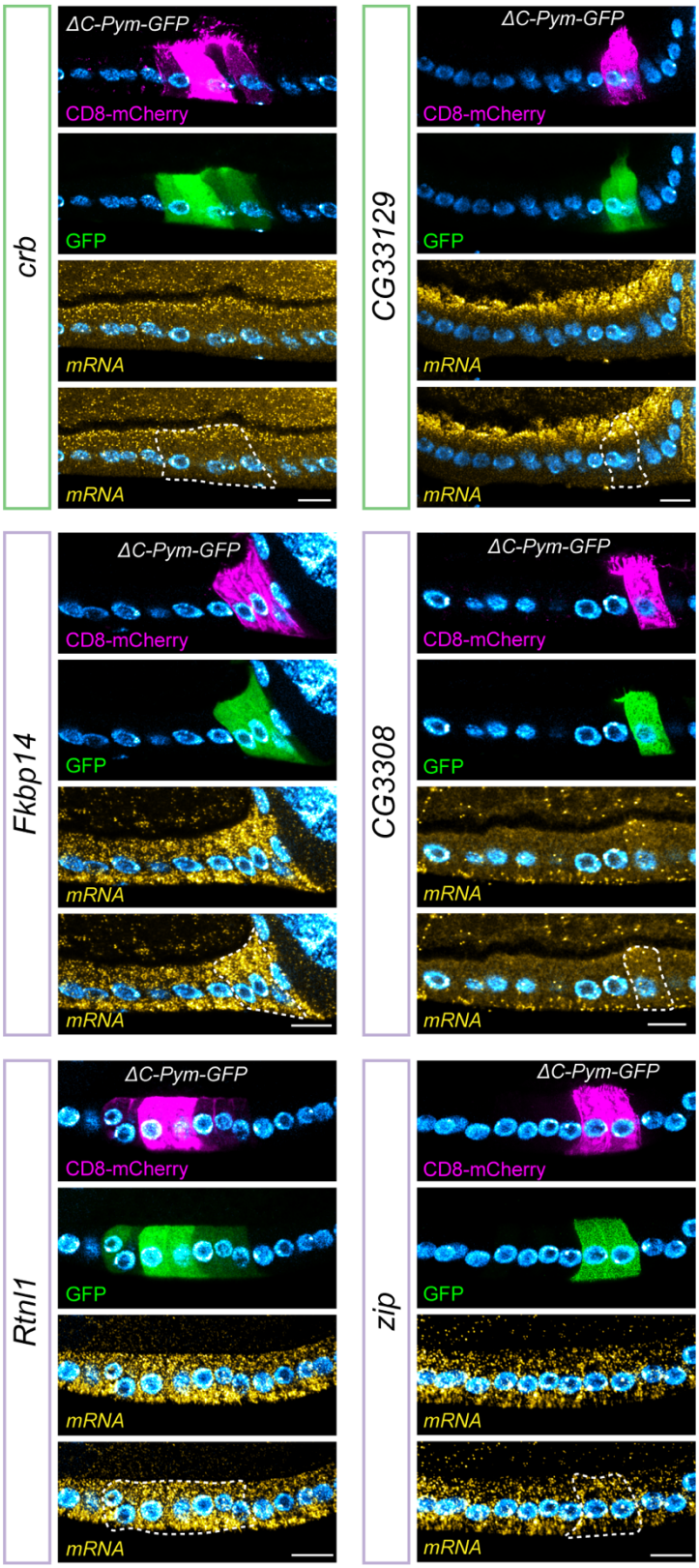


**Figure 3.11 - Effects of EJC disruption on the localization of apical and basal mRNAs revealed by smFISH.** Mutant *ΔC-Pym-GFP* clones are identified by CD8-mCherry expression (dashed line in fourth panel down) and ΔC-Pym-GFP expression. Nuclei are stained with DAPI. Scale bars 10 μm.

### 3.2.2 Disruption of MT minus end-directed RNA transport affects apical RNA localization

MT minus end-directed RNA localization has been better characterized than MT plus end-directed RNA localization in *Drosophila*. The dynein/BicD/Egl RNA localization machinery is responsible for transporting RNAs towards MT minus ends in both the oocyte and blastoderm embryos (Mach and Lehmann 1997, Bullock and Ish-Horowicz, 2001) and has been found to play a role in the apical localization of *inscuteable (insc)* mRNA in neuroblasts (Hughes et al., 2004). Dynein-dependent RNA transport in the follicle cells has been described for *crumbs* (*crb*) (Li et al., 2008) and *stardust* (*sdt*) (Horne-Badovinac and Bilder, 2008); moreover, three mRNAs expressed in the apical domain of the FE (*egl*, *CG33129*, *Uba1*) were enriched in Egalitarian protein pull-downs from ovarian tissues (Vazquez-Pianzola et al., 2017). Although these studies suggest that the dynein/BicD/Egl machinery is responsible for MT minus end-directed RNA transport in the follicle cells, it is not known whether this mechanism applies to only a small subset of mRNAs or is a common mechanism to achieve apical RNA localization in this tissue.

To have a deeper insight into MT minus end-directed RNA localization in follicle cells, I first knocked down the expression of cytoplasmic dynein by performing RNAi against *Dhc64C* in clones and evaluated changes in the localization of four apical (*crb*, *CG33129*, *qtc*, *msps,* with *crb* taken as a positive control) and four basal (*Fkbp14*, *CG3308*, *Rtnl1*, *zip*) mRNAs by smFISH (Figure 3.12). Down-regulation of dynein activity caused severe changes in localization patterns for all four apical mRNAs analyzed. Interestingly, unlike *Khc* RNAi, *Dhc64C* RNAi caused the apical mRNAs to become ubiquitously distributed in both domains, rather than becoming enriched in the basal domain. Disruption of dynein activity also partially affected the localization of basal mRNAs. However, *Dhc64CRNAi* cells often displayed morphological defects linked with cell polarity phenotypes, consistent with previous studies reporting that disruption of dynein activity might affect cell polarity (Horne-Badovinac and Bilder, 2008). For this reason, although the severe impairment of apical localization speaks in favor of a role of dynein in mediating apical RNA localization, it cannot be ruled out that the RNAs are mislocalized as a result of polarity disruption upon dynein down-regulation.

To investigate whether apical mRNA localization is dependent on the dynein/BicD/Egl transport machinery in the follicle cells, I performed RNAi against *egalitarian* (*egl*, encoding the RNA-binding protein in the complex) and analyzed changes in apical and basal localization in the same sets of apically- and basally-localizing RNAs by smFISH (Figure 3.13), as in the previous *Dhc64C* RNAi experiment. Similar to dynein disruption, *egl* RNAi causes the loss of apical enrichment for all apically-localizing mRNAs (*crb*, *CG33129*, *qtc*, *msps,* with *CG33129* taken as a positive control), leading to ubiquitous distribution of transcripts in both apical and basal domains, whereas the knock-down of Egalitarian did not visibly affect basal localization. Importantly, different from dynein disruption, *eglRNAi* clones did not show any cell polarity phenotypes, suggesting that the defects observed in apical RNA localization are directly linked to a decrease in Egl activity.

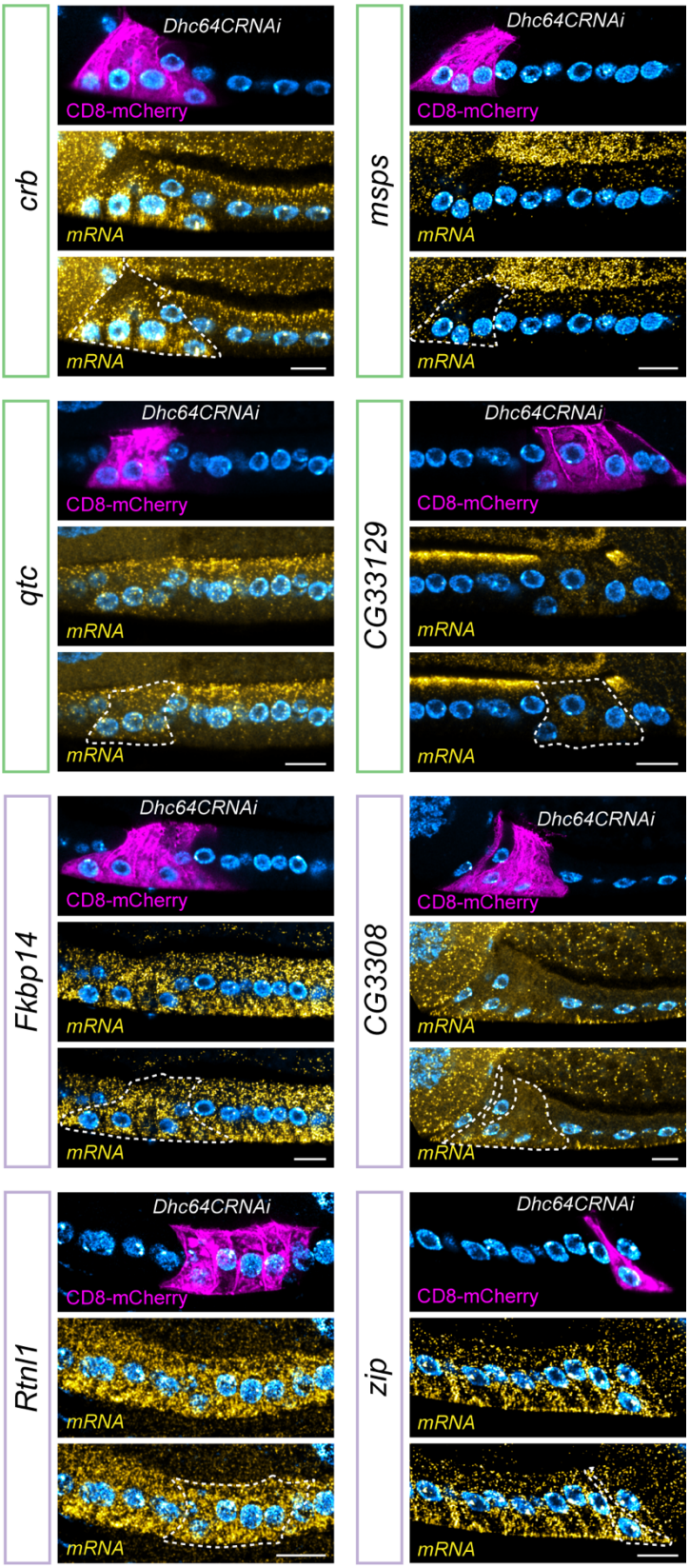


**Figure 3.12 - Effects of *Dhc64C* RNAi on the localization of apical and basal mRNAs revealed by smFISH.** Mutant *Dhc64CRNAi* clones are identified by CD8-mCherry expression (dashed line in third panel down). Nuclei are stained with DAPI. Scale bars 10 µm.

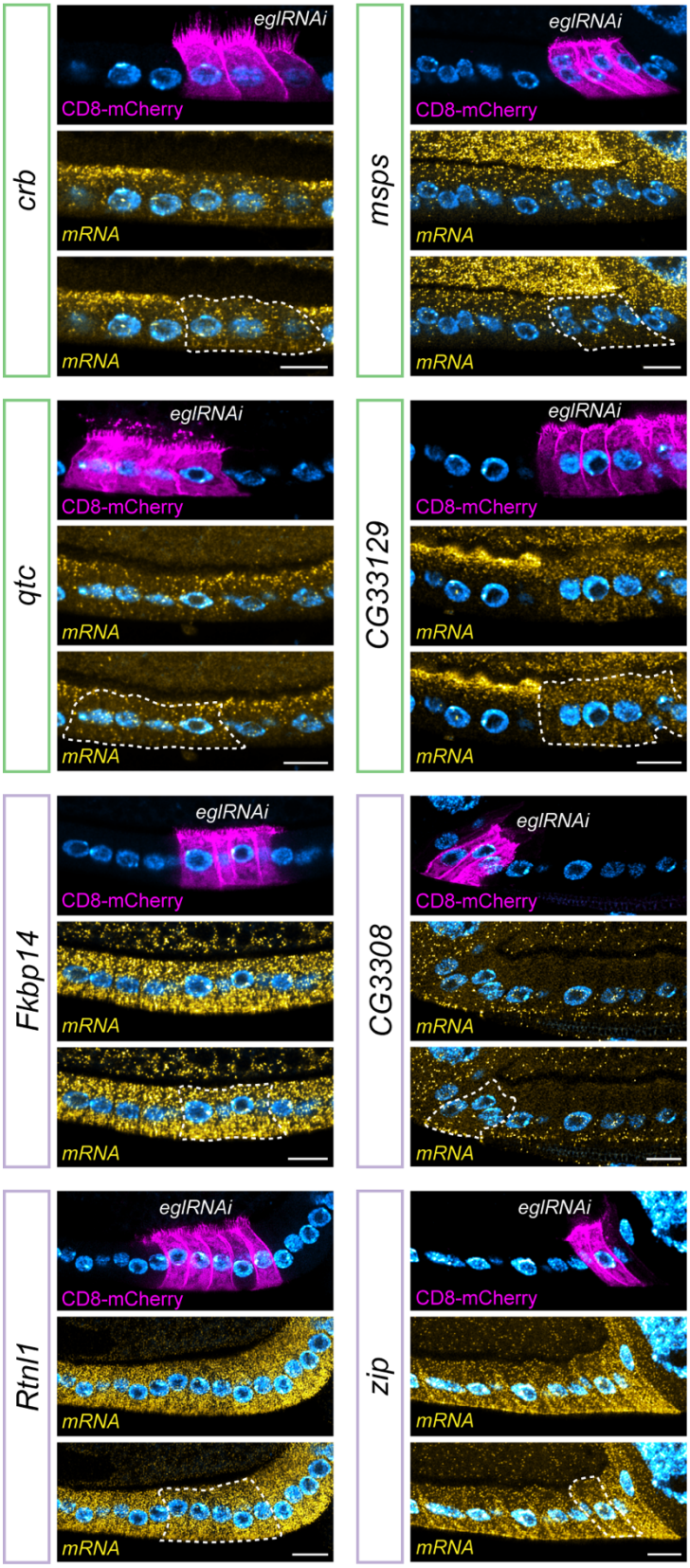


**Figure 3.13 - Effects of *egl* RNAi on the localization of apical and basal mRNAs revealed by smFISH.** Mutant *eglRNAi* clones are identified by CD8-mCherry expression (dashed line in third panel down). Nuclei are stained with DAPI. Scale bars 10 µm.

### 3.2.3 Apical mislocalization of *zip* mRNA upon *Khc* RNAi is partially rescued by simultaneous knock-down of Egalitarian

*zipper* (*zip*) mRNA localizes in a gradient-like manner along the A/B axis of stage 10 egg chambers, enriching close to the basolateral cell periphery (see Figure 3.5). Upon *Khc* RNAi, *zip* mRNA changes its localization, switching from basal-enriching to apical-enriching, almost mirroring the localization pattern seen in wild-type cells. Considering the established role of the dynein/BicD/Egl complex in transporting mRNAs to the minus ends of MTs, I hypothesized that this complex might be responsible for the mislocalization of *zip* mRNA to the apical domain when kinesin-1 activity is diminished. To test this, I attempted to simultaneously silence both *Khc* and *egl,* by generating *Khc* RNAi + *egl* RNAi double mutant clones, and performed smFISH to evaluate changes in *zip* mRNA localization. Single *Khc* RNAi and *egl* RNAi knock-down controls were also included in the analysis. For this experiment, I made use of the UAS-Gal4 "flip-out" genetic system described above, with the only difference that I substituted the allele expressing CD8-mCherry (3$^{rd}$ chromosome) with an allele expressing mCherry-NLS (mCherry carrying a nuclear localization signal, 2$^{nd}$ chromosome) to mark the mutant clones. This allowed me to combine single *eglRNAi* and *KhcRNAi* lines that carry their respective shRNA transgene on the 3$^{rd}$ chromosome, to obtain *eglRNAi/+*, *KhcRNAi/+*, and *eglRNAi/KhcRNAi* genotypes (abbreviated with "*eglRNAi*", "*KhcRNAi*", "*eglRNAi + KhcRNAi*"). Next, I applied the heat-shock treatment to these flies to induce the mutant phenotype in a mosaic manner in the FE and performed smFISH of *zip* mRNA (Figure 3.14A).

To quantitatively evaluate changes in RNA localization, I measured the apical (A) and basal (B) mean intensity fluorescence (m.i.f.) of *zip* signal in both mutant and wild-type cells for each experimental condition, and plotted the respective A/B m.f.i. ratio measured in this way (Figure 3.14B). With the A/B m.f.i. converted to logarithmic scale, the apical enrichment of the mRNA is characterized by positive values, while negative values correspond to basal enrichment; a value close to 0 represents a ubiquitous distribution of the mRNA. The results show that single knock-down treatments of *egl* RNAi and *Khc* RNAi recapitulate what was already observed with previous experiments (Figure 3.10 and Figure 3.13), showing that silencing *egl* alone does not lead to significant changes in *zip* mRNA localization, whereas silencing kinesin-1 activity causes the emergence of a strong apical localization pattern.

Simultaneous knock-down of *egl* and *Khc* still causes a significant, albeit less strong, change in localization compared to wild-type, with only a slight apical enrichment of *zip* mRNA in the double-mutant cells.

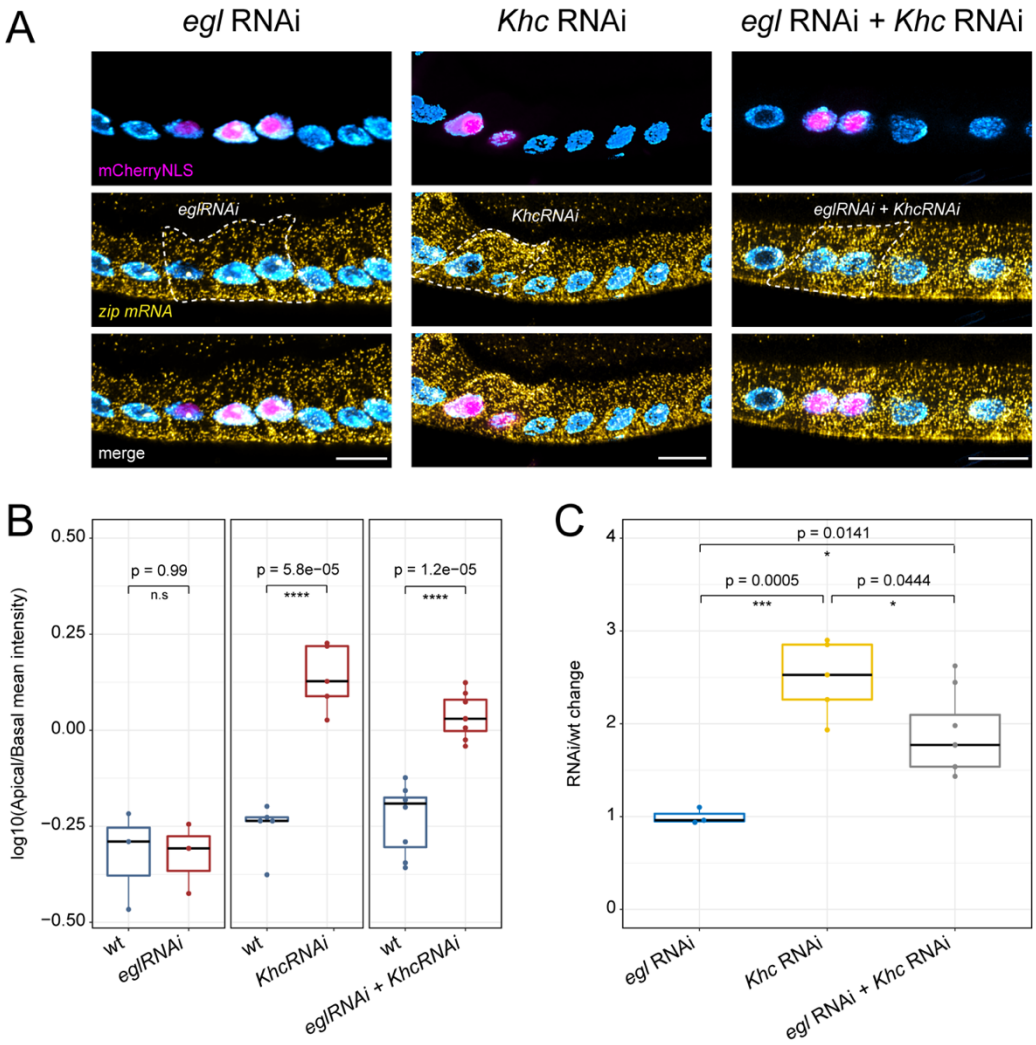


**Figure 3.14 - Apical localization of *zip* mRNA upon *Khc* RNAi is partially rescued by *egl* RNAi.** A) smFISH of *zip* mRNA in *egl* RNAi, *Khc* RNAi and *egl* RNAi + *Khc* RNAi conditions. Mutant clones are identified by nuclear expression of mCherry (dashed line). Nuclei are stained with DAPI. Scale bars 10 µm. B) Quantification of A/B mean fluorescence intensity (m.f.i.) of *zip* mRNA signal in wild-type (wt) and RNAi-treated cells. Independent t-test was used to compare means. C) Change between RNAi-treated and wt A/B m.f.i. values in the three experimental conditions. One-way ANOVA followed by Tukey post-hoc tests were used to compare means.

To assess if the changes in *zip* mRNA localization observed for each *egl* RNAi, *Khc* RNAi, and *egl* RNAi + *Khc* RNAi condition differ significantly from each other, I measured the change in localization pattern as the ratio between the A/B m.f.i. of mutant and control cells for each of the 3 experimental conditions, then performed one-way ANOVA followed by Tukey post-hoc tests to compare differences in their means (Figure 3.14C). These analyses show that changes observed in all conditions

significantly differ globally ($p = 0.00067$, ANOVA) and from each other ($p < 0.05$ for each pairwise comparison, Tukey tests). This shows that the apical localization of *zip* mRNA observed upon *Khc* RNAi can be partially rescued by simultaneous knock-down of Egalitarian and kinesin-1, suggesting that in the absence of kinesin-1 the dynein/BicD/Egl machinery mediates *zip* mRNA transport to the apical domain. The partial rescue of localization might be due to the fact that, as shown for apical RNAs in *egl* RNAi experiments (Figure 3.13), *egl* RNAi generally causes apical mRNAs to become ubiquitously distributed in the cytoplasm. Finally, it is interesting to note that *egl* RNAi alone does not seem to affect *zip* mRNA localization. This suggests that the dynein/BicD/egl complex might compete with kinesin-1 (or other associated kinesin-1-dependent co-factors) for binding to the same sites on *zip* mRNAs. Alternatively, kinesin-1 might play a role in dynein inhibition.

### 3.2.4 Apical localization of *BicD* mRNA requires microtubules but not Egalitarian activity and *BicD* 5' and 3' UTRs

Among the significantly apically-enriched mRNAs revealed by RNA-seq, *BicD* was among the most enriched transcripts, and it maintains its apical localization throughout all stages of oogenesis. To investigate if *BicD* mRNA localization in the apical domain is dependent on the activity of the dynein/BicD/Egl RNA transport machinery, I analyzed if the localization of *BicD* was affected in *eglRNAi* follicle cell clones. Surprisingly, no change in *BicD* localization pattern was observed in *eglRNAi* mutant cells at any stage of oogenesis (Figure 3.15A).

To exclude the possibility that apical localization of *BicD* mRNA resulted from residual Egl activity in the RNAi-mediated knock-down, I aimed at creating a fly line with no Egl protein expression in the follicle cells. To do so, I combined two reported *egl* protein null alleles ($egl^{WU50}$ and $egl^{PR29}$, Mach and Lehmann, 1997); in addition, as $egl^{NULL}$ fly lines fail to specify an oocyte and produce rudimentary ovaries, I rescued oogenesis by expressing an *egl* transgene under the control of the germline-specific *oskar* promoter (for full genotypes, see Material and Methods). This allowed me to analyze mid-oogenesis stage egg-chambers that would otherwise not develop in the $egl^{NULL}$ situation. The resulting fly line, called $egl^{NULL}FC$, expresses Egl in the nurse cells and oocyte, but not in the follicle cells. smFISH experiments of *BicD* RNA in the $egl^{NULL}FC$ ovaries generated in this way showed that *BicD* transcripts were still apically, thus confirming the results obtained with *egl* RNAi (Figure 3.15B).

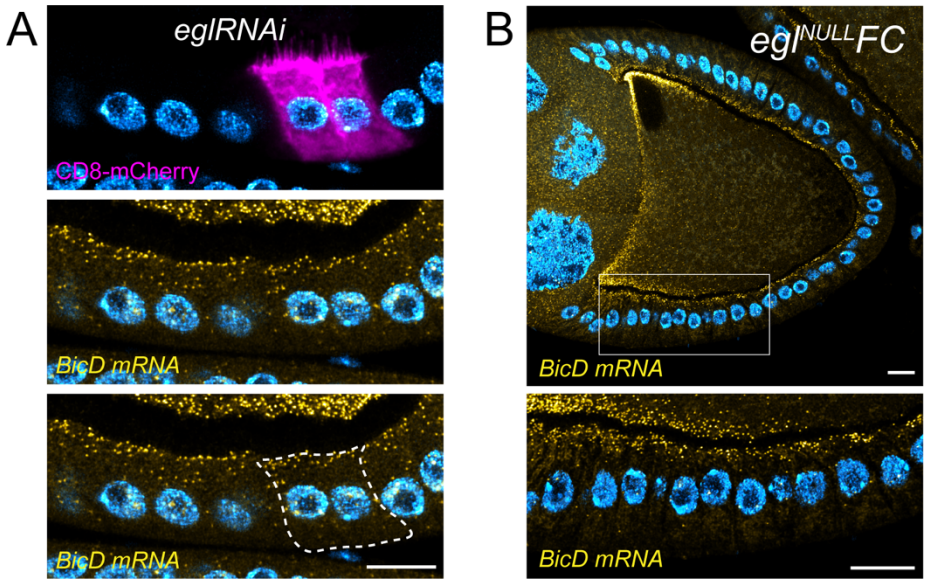


**Figure 3.15 - Apical localization of *BicD* mRNA does not depend on Egl.** A) smFISH of *BicD* mRNA in *eglRNAi* mosaic follicular epithelium. Mutant *eglRNAi* clones are identified by CD8-mCherry expression (dashed line in third panel down). B) smFISH of *BicD* mRNA in $egl^{NULL}FC$ egg chambers. Lower panel: magnified view of follicle cells. Nuclei are stained with DAPI. Scale bars 10 µm.

In *Drosophila*, active RNA transport requires an intact cytoskeleton on which dynein and kinesin motors travel with their RNP cargoes to their final destination. However, mechanisms of "passive" RNA localization have been described which do not make use of MT tracks to localize RNAs, namely (1) facilitated diffusion and local entrapment and (2) local protection from degradation (Medioni et al., 2012). To determine if *BicD* mRNA localization is MT-dependent, I perfomed smFISH of *BicD* mRNA in ovaries treated with colchicine, a MT-depolymerizing agent, and compared its localization pattern with ethanol-treated (solvent) control ovaries. To visualize MTs, I performed the experiment on a protein-trap fly line expressing an endogenously GFP-tagged MT-associated protein (Jupiter-GFP), which was described in previous reports to fluorescently mark MTs (Karpova et al., 2006). Dissected ovaries were incubated for different lengths of time in insulin-supplemented Schneider's medium with colchicine (200 µg/ml for 1 h and 100 µg/ml for 2 h), or with 100% ethanol for 1 h. Next, I performed a double smFISH of both *BicD* and *crb* mRNAs, the latter previously described as having a MT-dependent apical localization pattern (Li et al., 2008), thus representing the positive control for a complete MT depolymerization (Figure 3.16).

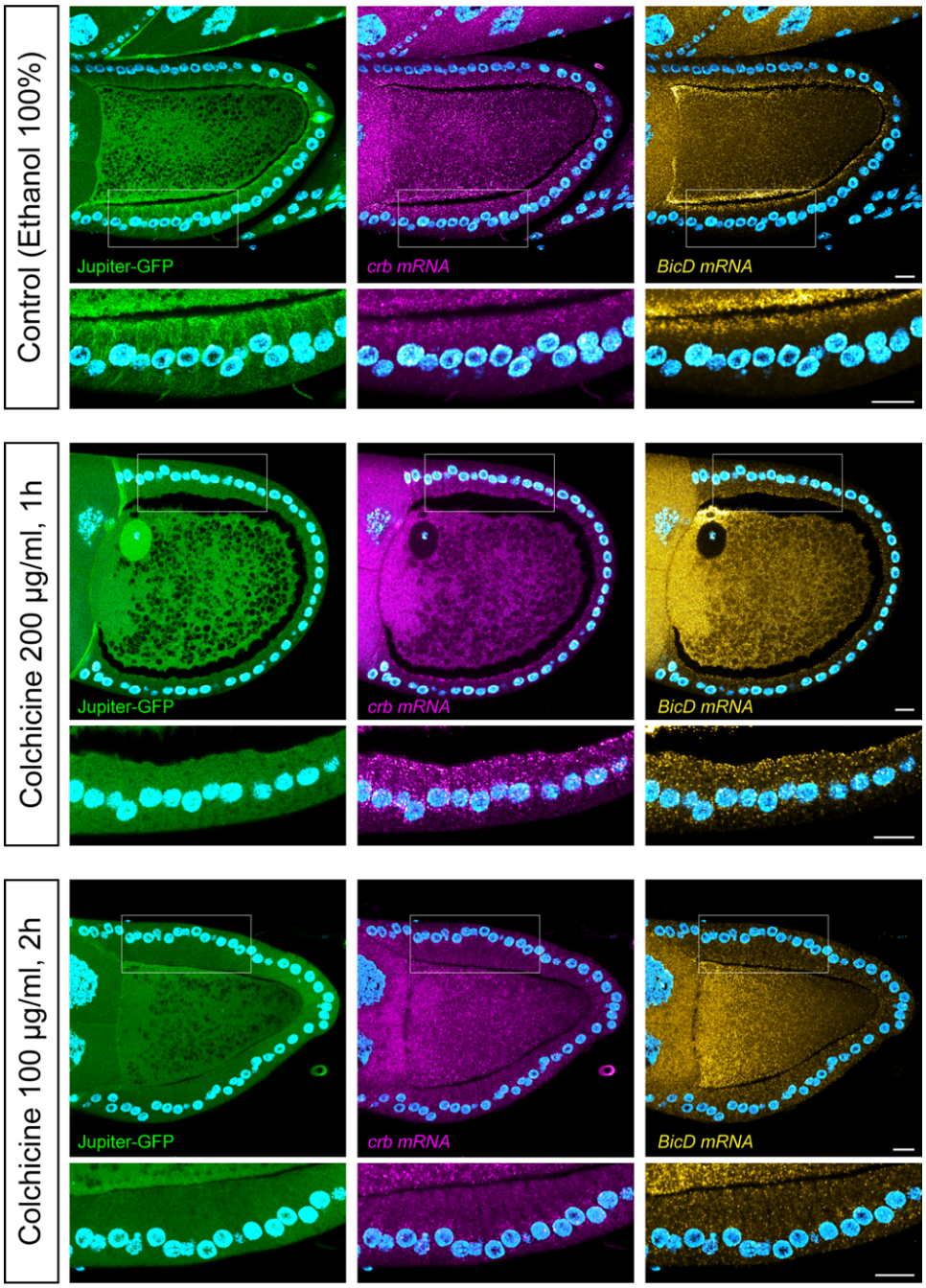


**Figure 3.16 - Disruption of microtubules abolishes apical localization of *BicD* mRNA.** Panels depict double smFISH experiments of *crb* and *BicD* mRNAs on Jupiter-GFP flies treated with ethanol 100% (control, upper panel) or colchicine at different concentrations and lengths of time (middle and lower panels). Nuclei are stained with DAPI. Scale bars 10 µm.

Results show that upon colchicine treatment, both *crb* and *BicD* mRNAs progressively lose their apical enrichment, although to different degrees, depending on the duration of incubation with the drug. This can be appreciated from the residual GFP fluorescence visible in the whole egg-chamber, and deduced from the partial maintenance of both anterior localization of *BicD* mRNA in the oocyte and apical

localization of *crb* mRNA in the follicle cells. In contrast, a 2-h colchicine treatment at a concentration of 100 µg/ml resulted in a sharp decrease in Jupiter-GFP signal and completely abolished both *BicD* and *crb* apical RNA localization. These results show that *BicD* mRNA localization is dependent on the presence of intact MTs. Although it cannot be ruled out that MT depolymerization might exert an indirect effect on *BicD* mRNA localization (for example by failing to transport a protein/mRNA that anchors *BicD* mRNA to the apical domain), the changes observed upon such a short acute treatment of colchicine might speak in favor of *BicD* mRNA being actively transported on MTs.

The *BicD* gene has four annotated mRNA isoforms (Flybase), which differ from each other in their 3' end, in particular regarding the length of the 3'UTR (Supplementary Figure 6). As RNA transport is mediated by cis-regulatory localization elements usually found in the 3'UTR of transcripts (Andreassi and Riccio, 2009), I sought to investigate whether the *BicD* 3'UTR is necessary for apical localization of the mRNA. First, I hypothesized that the isoform with the longest 3'UTR (*BicD-RC*) could be the one that gets localized to the apical domain. To test this possibility, I performed a double smFISH with probe sets that recognize different regions of the *BicD* transcript models. One set, labelled with ATTO-633, recognized a region encompassing part of the CDS of all 4 *BicD* isoforms (*BicD(CDS)-ATTO-633*), while the other set, labelled with ATTO-565, annealed to the 3'UTR region specific to the isoform RC (*BicD(RC)-ATTO-565*) (Supplementary Figure 6A). In this way, specific signal coming from *BicD-RC* transcripts could be easily recognized as sharp puncta showing expression in both the 633 and 565 channels. Conversely, background signal due to unspecific hybridization of *BicD(RC)-ATTO-565* probes to other RNAs would show signal only in the 565 channel. Surprisingly, the isoform *BicD-RC* appeared to be transcribed and present in both somatic and germline tissues, but was only detected in a few cytoplasmic foci (Figure 3.17A). This shows that *BicD-RC* is not the predominant *BicD* mRNA isoform expressed in the ovary. However, the *BicD-RC* isoform appears to be transcribed in the FE (as shown by the presence of nuclear foci associated with active transcription) and undergo post-transcriptional down-regulation in the cytoplasm.

Unfortunately, discrimination of other *BicD* mRNA isoforms is not possible by smFISH, because they lack long tracks of unique nucleotide sequence (>200 nt) on

which probes can be designed. However, one way to investigate a requirement of the *BicD* 3'UTR in apical localization is to take advantage of a transgenic fly line that expresses only the CDS of *BicD,* fused in frame with 3 copies of EGFP (Li et al, 2010). I hypothesized that, if (any) *BicD* 3'UTR were necessary for apical localization, then smFISH of the GFP nucleotide sequence of *BicD-3xEGFP* transcripts would reveal ubiquitous distribution of the transgenic mRNA. Importantly, the *BicD-3xEGFP* construct was cloned into pUASp vectors which contain a partial 3'UTR derived from *K10*, but lacks the *K10* localization signal (TLS) (S. Bullock personal communication) which would interfere with apical localization. Similarly to the previous experiment, I performed double smFISH on flies expressing the *BicD-3xEGFP* transgene in the follicle cells under the control of *traffic jam* (*tj*) promoter using two different probe sets: one set (*BicD(CDS)-ATTO-565*) recognized mRNAs encoded by both the endogenous and transgenic *BicD* loci, and the other set (*EGFP-ATTO-633*) specifically recognized the *EGFP* mRNA sequence of *BicD-3xEGFP* mRNAs (Supplementary Figure 6B). In addition, I checked if the BicD-3xEGFP protein was successfully translated by looking at GFP fluorescence. Results of the experiment show that *BicD-3xEGFP* mRNA, which lacks both *BicD* UTRs, reflects the RNA localization pattern of wild-type *BicD*, suggesting that these regions of the mRNAs are not essential for its apical localization. In addition, *BicD-3xEGFP* mRNA is correctly translated into protein (Figure 3.17B).

Interestingly, the transgenic construct was derived from *BicD* cDNA (Li et al, 2010), excluding the possibility that splicing is essential in conferring the ability to localize to the mRNAs, as it does in *oskar* mRNA localization (Hachet and Ephrussi, 2004). However, as it is the case for *oskar* localization, it cannot be ruled out that the mRNA encoded by the *BicD-3xEGFP* transgene could hitch-hike with localization-competent endogenous *BicD* mRNAs (Hachet and Ephrussi, 2004, Jambor et al., 2011).

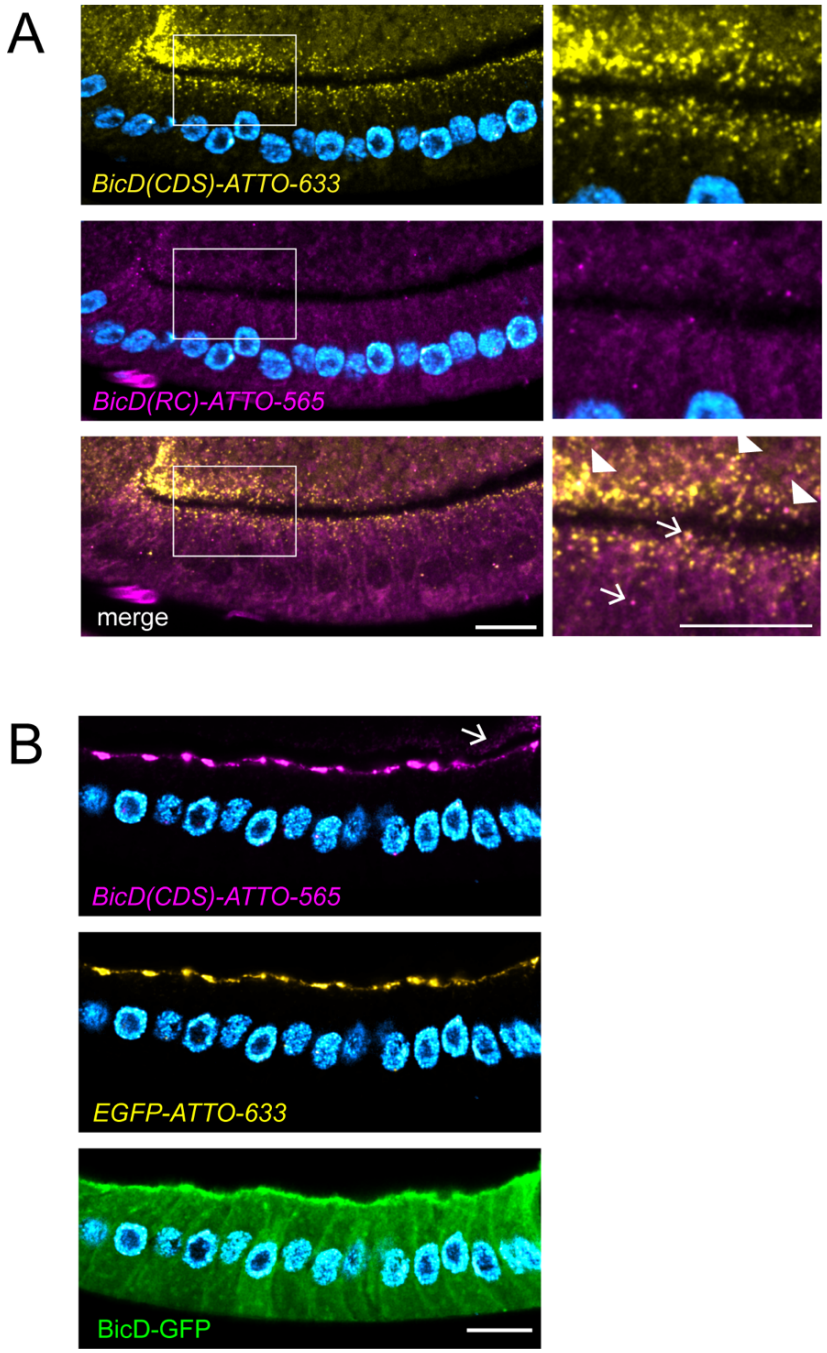


**Figure 3.17 – Double smFISH experiments on *BicD* RNA.** A) *BicD-RC* is not predominantly expressed in egg-chambers among the *BicD* mRNA isoforms. *BicD-RC* is expressed at low levels in both follicle cells (arrows) and oocyte (arrowheads). B) smFISH showing that the 5'- and 3'-UTR of *BicD* mRNA are not necessary for its apical localization. The arrow indicates endogenous expression of *BicD* mRNA in the oocyte. Most of the follicle cell signal from *BicD(CDS)-ATTO-565* probes comes from *tj*-driven expression of *BicD-3xEGFP* transgene. Nuclei are stained with DAPI. Scale bar 10 µm.

## 3.3 Preliminary results: Disruption of *egl*-dependent apical RNA localization affects Imp distribution and the proper egg chamber development

The experiments illustrated above show that the FE displays a diverse landscape of mechanisms employed to finely regulate RNA localization. However, it is poorly understood what is the function of mRNA localization in this tissue. Given the importance of Egalitarian in directing apical RNA localization, I began investigating whether *egalitarian*-dependent mRNA localization is important to achieve localized translation. Next, I evaluated the effects associated with a reduction in Egl activity in the follicle cells by measuring the hatching rate of eggs developed from egg-chambers lacking Egl in the FE.

### 3.3.1 RNAi against *egalitarian* affects the A/B distribution of *Imp* mRNA and protein

RNA localization promotes localized translation of the transcripts, and this is usually coupled with translational repression of the transported mRNA until it reaches its destination. Therefore, I sought to examine how the localization pattern observed in apical and basal mRNAs relate with the distribution of their encoded protein. Due to the unavailability of serological reagents, I took advantage of commercially available transgenic fly lines that express an endogenously GFP-tagged version of a gene of interest ("protein-trap" lines, Morin et al., 2001). The use of endogenously-tagged lines allows one to limit artifacts of protein expression patterns often observed when genes are expressed from transgenes at non-physiological levels.

The expression of Imp-GFP protein examined in *Imp-GFP[PTT]* line showed that the localization pattern of *Imp* mRNA closely resembles that of the encoded protein, both enriching in the apical domain in a gradient-like manner (Figure 3.18).

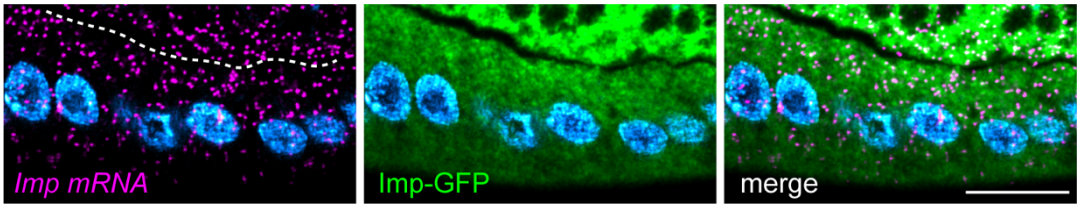


**Figure 3.18 – smFISH of *Imp* mRNA combined with GFP detection show that both mRNA and protein encoded by *Imp* exhibit a similar localized expression pattern.** The dashed line delimits the border between the follicular epithelium and the oocyte. Nuclei are stained with DAPI. Scale bar 10 μm.

To investigate whether apical enrichment of Imp-GFP is dependent on the localization of *Imp* mRNA, I performed RNAi against *egl* in follicle cell clones and assessed the presence of any changes in both *Imp* mRNA and Imp-GFP protein distribution through smFISH and detection of GFP fluorescence (Figure 3.19). Results show that, concomitantly with a loss of apical enrichment of *Imp* mRNA due to knock-down of Egl, Imp protein significantly changes its A/B distribution. This is particularly evident when looking at Z-projections taken at different depths within the FE (Figure 3.19A, top view and bottom view, corresponding to the basal domain and apical domain, respectively). Quantification of changes in both mRNA and protein localization though comparison of their A/B m.f.i. ratios in wildtype and *eglRNAi* cells confirmed that the change in localization pattern is significant (Figure 3.19B). In addition, the total intensity of both mRNA and GFP fluorescence does not seem to change in *eglRNAi* follicle cells compared to wild-type, suggesting that the reduction in apical enrichment does not result from mRNA degradation or reduced apical translation (Figure 3.19C). The fact that perturbation of *Imp* RNA localization is paralleled by a re-distribution of Imp protein suggests that the apical localization of *Imp* mRNA might serve to locally concentrate Imp protein in this domain.

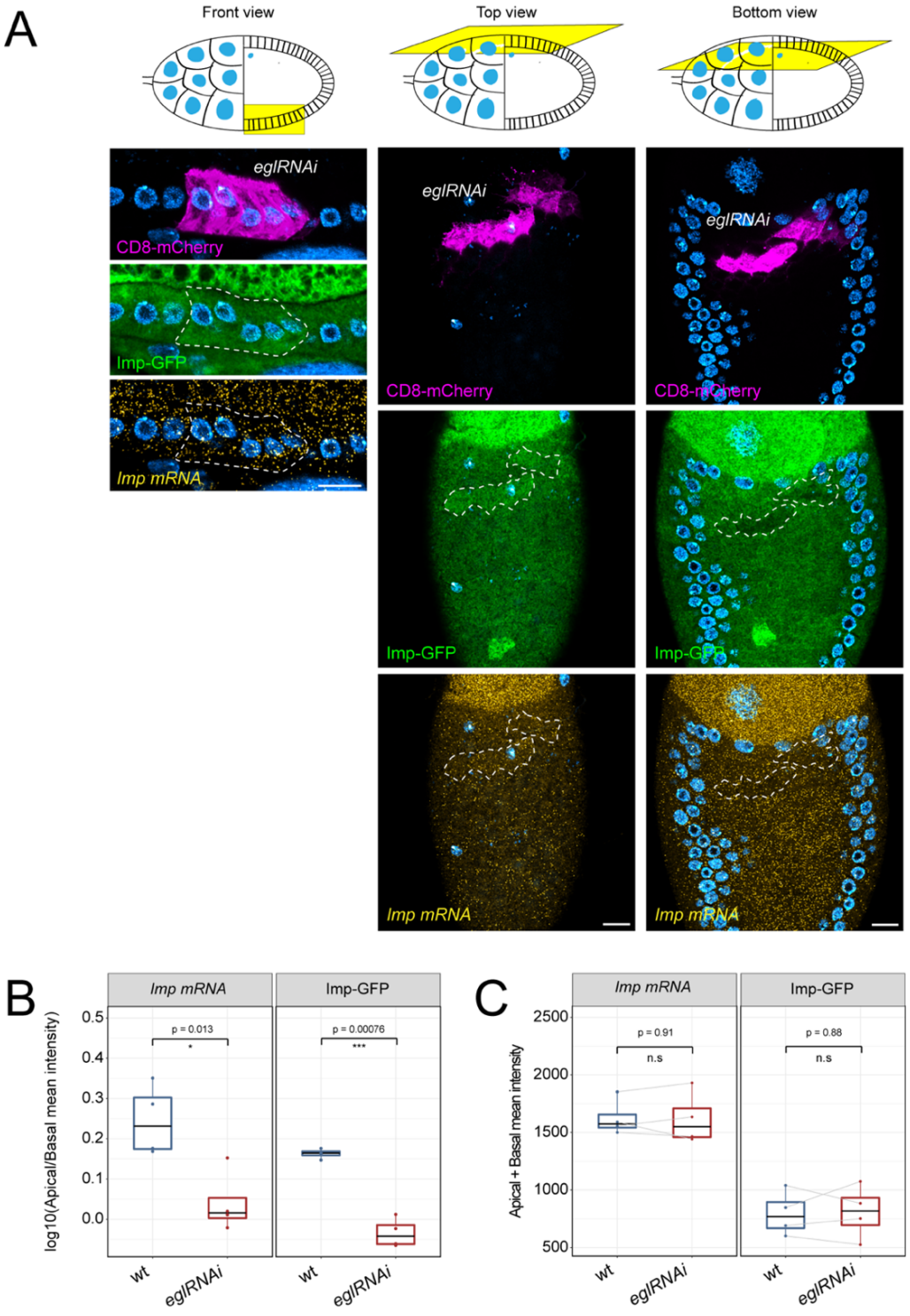


**Figure 3.19 – *egl* RNAi affects the distribution of Imp protein along the A/B axis of follicle cells.** A) smFISH of *Imp* mRNA and GFP detection in *eglRNAi* mosaic egg chambers. Nuclei are stained with DAPI. Scale bar 10 µm. B) Quantification of *Imp* mRNA and GFP fluorescence in wild-type (wt) and *eglRNAi* cells. Independent t-tests were used to compare A/B m.f.i. ratios. C) Quantification of total *Imp* mRNA and GFP fluorescence in wt and *eglRNAi* cells. Paired t-tests were used to compare the A+B mean intensity values.

### 3.3.2 Follicle cell-specific RNAi against *egalitarian* causes a small but significant reduction on the egg hatching rate

One way to assess a gene's function is to score the phenotypes resulting from mutations that impair gene activity. Null mutations are the most powerful to completely disrupt the production of the encoded protein. However, if the gene is normally expressed by different tissues in an organ, this usually raises difficulties in uncoupling the contribution of the individual tissues to the final phenotype. In addition, null mutations can be deleterious and cause an arrest of organ growth, sterility or lethality, often hindering a complete phenotypical analysis. This is the case of *egl* null mutations, which cause a failure in oocyte specification and premature arrest of oogenesis. Therefore, it is equally challenging to evaluate the role of *egl* played after early oogenesis and to establish the follicle cell-specific contribution of *egl* function.

To overcome this problem, I made use of the UAS-Gal4 system to specifically knock down Egl expression, by driving the expression of shRNA against *egl* specifically in the follicle cells through the use of the follicle cell-specific promoter *tj*. I hypothesized that, if *egalitarian*-dependent processes are involved in important developmental functions performed by the FE, a phenotype would manifest in the ability of the eggs to hatch. Therefore, I collected female flies of either *tj>eglRNAi* or *tj>wRNAi* (control) genotypes (see Materials and Methods for the full genotypes) and scored the hatching rate of the eggs they deposited after being fertilized (Figure 3.20). Although most of the eggs managed to hatch, the overall hatching rate of eggs developed from egg-chambers with follicle cells deficient in *egl* was significantly lower than control eggs (86% vs. 91% of eggs from control flies). This indicates that, under laboratory conditions, *egalitarian*-dependent RNA localization in the FE plays only a modest role in egg-chamber development. However, as it is often the case in the emergence of mild phenotypes, it will be important to investigate whether *egl* function might be essential under stress conditions that mimic life in a fruit fly's natural environment.

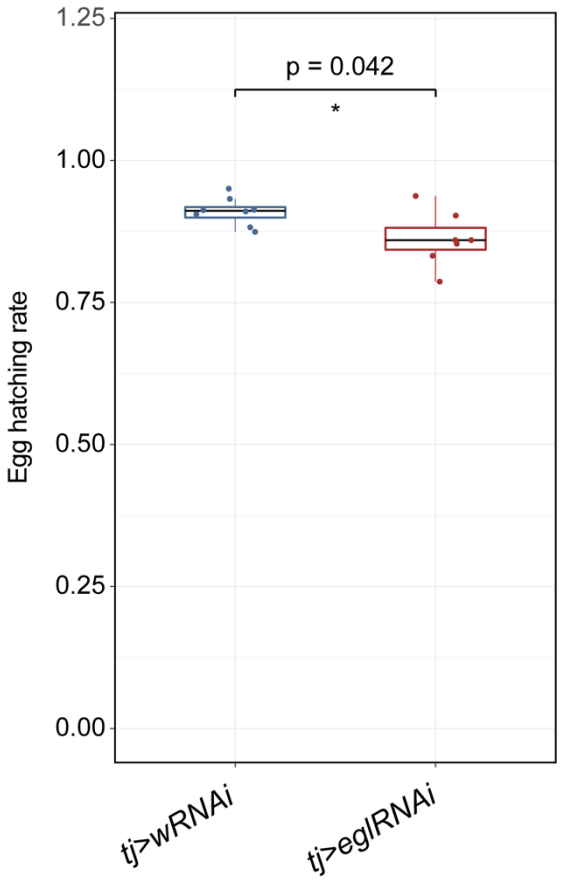


**Figure 3.20 - Hatching rates of *tj>wRNAi* (control) and *tj>eglRNAi* eggs.** Independent t-test was used to compare means between the two groups. For full genotypes see Materials and Methods.

### 3.3.3 Future perspectives

The preliminary result of the effect of *egl* RNAi on egg hatching rate indicates that *egalitarian*-dependent RNA localization in the follicle cells does not play a significant role in oogenesis. However, this contrasts with the observation that all apical mRNA tested (*CG33129*, *crb*, *qtc*, *msps*, *Imp*) but one (*BicD*) completely lose their apical enrichment when *egl* is silenced. In addition, disruption of *Imp* mRNA localization through *egl* RNAi is associated with a change in Imp protein distribution, suggesting that *egalitarian*-dependent localization of *Imp* mRNA might serve to create a gradient of Imp protein expression along the A/B axis of follicle cells.

Tissue-specific RNAi has the advantage of knocking down the expression of selected gene(s) only in the subset of cells in which the desired driver is active, disentangling the contributions of genes to each tissue. However, the disruption of

gene activity accomplished by RNAi is often only partial. For this reason, I plan to assess the phenotype(s) associated with Egl function in the follicle cells in the *egl*$^{NULL}$*FC* line (in which oogenesis is rescued by expressing *egl* under the control of *oskar* promoter through the use of the UAS-Gal4 system) described previously.

Surprisingly, preliminary results of the hatching rate of eggs deposited by *egl*$^{NULL}$*FC* flies revealed a value close to 0%. To investigate more in details the phenotype, I analyzed the cuticle preparations of embryos that failed to hatch. I found that 44% exhibited a posteriorization phenotype (ranging from head defects to complete bicaudal embryos), which is associated with excess or mislocalized *oskar* expression (Ephrussi and Lehmann, 1992). Mislocalization of *oskar* mRNA at the anterior occurs upon Egl overexpression in the germline (Gaspar et al., in preparation), suggesting that the the posterior defects seen in *egl*$^{NULL}$*FC* flies are due to an excess of Egl in the oocyte. Therefore, I compared the expression levels of Egl protein in wild-type and *egl*$^{NULL}$*FC* ovaries by western blotting. As anticipated, I found that *oskar*-driven rescue of oogenesis produced more than a 4-fold overexpression of Egl compared to wild-type levels. To avoid overexpression phenotypes, I am currently testing different drivers that should allow me to express Egl in the germline at close to wild-type levels.

Preliminary results represented in the western blot in Supplementary Figure 7 show the expression levels of Egl measured in *egl*$^{NULL}$*FC* lines that differ in the germline-specific promoters used to rescue oogenesis through Egl expression (*vasa*, *αTub67C, oskar*). Although all seem to be stronger than the endogenous *egl* promoter, *vasa* seems a promising driver, causing only a 2-fold increase in Egl expression over wild-type levels. Considering that the UAS-Gal4 system used to accomplish Egl expression was shown to be temperature-dependent (Brand et al., 1994), it should be possible to reduce the expression levels of Egl by growing *egl*$^{NULL}$*FC* flies at lower temperatures (18°C).

I also plan to perform several experiments to assess which phenotypes are associated with a loss in Egl expression in the follicle cells. First, I will repeat the hatching rate experiment, conducting in parallel cuticle preparations of unhatched embryos and evaluating eggshell phenotypes of the eggs (investigating the morphology of the dorsal appendages and chorionic structures). These experiments will be accompanied by control experiments performed in the *egl*$^{NULL}$*FC* lines

including (1) smFISH of *osk* to exclude anterior mislocalization, (2) Gurken immunostaining to rule out possible phenotypes due to incorrect Gurken expression in the oocyte, (3) double smFISH of mRNAs whose expression is induced by Gurken in the ventral and the dorsal follicle cells (*pipe* and *kekkon1*, respectively), as an additional control for correct EGFR signaling by Gurken.

Finally, to test whether Egalitarian in the FE might be important during the stress response, I will subject wild-type and $egl^{NULL}FC$ or *tj>eglRNAi* flies to different sources of stress (e.g temperature, starvation) and assess the associated phenotypes. Being epithelia the interface with the environment, they play important roles in sensing and transducing the information present in the surrounding environment to neighboring tissues. Among stress responses, the starvation response is one of the best characterized in *Drosophila* female germline, where the oogenesis is arrested in response to a nutrient-poor diet. Interestingly, follicle cells have been shown to function as sensors of the nutritional status of the fly and responsible for the initiation of the so-called "germline starvation response" in the oocyte (Burn et al., 2015). When insulin levels are low, germline mRNAs and proteins drastically change their expression pattern and aggregate in large RNP structures called P-bodies. However, this phenomenon can be reversed when insulin levels are restored by a protein-rich diet (Shimada et al., 2011). Therefore, it is thought that P-bodies in the germline function to protect mRNAs from degradation when the oogenesis is temporarily arrested. It will be interesting to see if, in such starvation-induced conditions, RNA localization in the follicle cells plays an important role in regulating the germline starvation response.

# Chapter 4: Discussion

### *The apical and basal transcriptomes of* Drosophila *follicular epithelial cells*

RNA localization in somatic differentiated tissues such as epithelia is poorly characterized. To address this, I investigated the prevalence, the mechanisms and the possible roles of RNA localization in the *Drosophila* follicular epithelium, a highly polarized monolayer of somatic cells that surrounds the germline component of the ovary.

Laser-capture Microdissection (LCM) followed by RNA-seq of the apical and basal domains of stage-10 follicular epithelium identified 306 apically- and 249 basally-localizing mRNAs. This extends the results obtained in a previous high-throughput *in situ* hybridization screen for ovarian subcellularly-localized mRNAs that identified 30 apically- and 9 basally-enriched mRNAs in the follicular epithelium (Jambor et al., 2015). Subsequent smFISH experiments validated 91% of the tested mRNAs (21/23) to be apically or basally enriched. The A/B fluorescent intensity fold change measured by smFISH showed a good correlation with the A/B read fold change of the RNA-seq (Adj. $R^2$=0.65).

Gene Ontology (GO) enrichment analysis of the apical and basal dataset filtered from tissue contaminants showed that the two datasets differ significantly. Interestingly, the GO term analysis highlighted a functional compartmentalization of the RNAs along the A/B axis of the cell. The apical domain is enriched in mRNAs that code for proteins involved in the establishment/maintenance of epithelial integrity/cell polarity (*baz*, *ena*, *dlg1*, *yrt*, *Traf4*, *bbg*, *crb*), suggesting that their apical localization might be important for their local function as polarity regulators. In follicle cells, the requirement for apical localization of *crb* and *sdt* (components of the Crb/Sdt/Patj polarity complex) mRNAs was addressed by previous reports, which showed that disruption of their apical RNA localization caused cell polarity defects (Li et al., 2008; Horne-Badovinac and Bilder, 2008). Therefore, it is possible that RNA localization evolved as a general means to ensure and/or restrict the apical targeting of cell polarity regulators.

The GO enrichment analysis also highlighted a functional compartmentalization of mRNAs encoding organelle components or acting in the same organelle-associated pathway. For example, the apical dataset is enriched in genes that participate in the endocytic pathway (*BicD*, *Sara*, *hook*, *Rme-8*, *Dap-160*, *Nak*, *AP-2α*); conversely, the basal domain is enriched in mRNAs encoding proteins that take part in ER/Golgi processes (*Papst2*, *KdelR*, *betaCOP*, *zetaCOP*, *Sar1*) and mitochondrial processes (*Gdh*, *mAcon1*, *Men*). Importantly, the apical domain of the follicular epithelium was shown by a previous study to be enriched in markers of the endocytic pathway (Rab4, Rab5, Rab7, Rab11) (Dunst et al., 2015). The apical localization of mRNAs encoding endocytic components and the apical enrichment of markers of the endocytic pathway suggests that they might co-localize in the apical domain. Therefore, I speculate that, in *Drosophila* follicular epithelium, organelles (such as endosomes, ER, Golgi and mitochondria) might occupy distinct subcellular domains and function as a platform for the local translation of functionally related mRNAs whose activity might be needed *in situ* for protein turnover, local signaling or macromolecular assembly. This hypothesis is supported by recent studies in vertebrate axons, which reported that nuclear-encoded mitochondrial RNAs are targeted and translated at the mitochondrial surface (Lesnik et al., 2015); moreover, translating ribosomes were found in the mitochondrial outer membrane (Zhang et al., 2016; Gold et al., 2017). Finally, several mRNAs were found to be associated with other organelles (such as endosomes and lysosomes) and transported through hitch-hiking, although the functional significance of this association is not well understood (Liao et al., 2019; Cioni et al., 2019). Transport through organelle hitch-hiking and local translation of mRNAs functionally linked to organelle-specific functions might be a widespread phenomenon that merits further investigation.

smFISH validation of 21 apically- or basally- enriched mRNAs showed a spectrum of localization patterns. I could identify two categories of mRNAs on the basis of their distribution: the first category includes those mRNAs which are present almost exclusively in one domain and excluded from the other (*CG33129*, *BicD*, *Bsg25D*, *qtc*, *CG3308*, *baz*); the second category comprises mRNAs that are enriched in one of the two domains, but are present in both (*egl*, *Imp*, *zip*, *Sara*, *vkg*, *Fkbp14*, *Dlic*, *tud*, *rho-4*, *CycG*, *AdipoR*, *msps*, *Cortactin*, *SerRS*, *Rtnl1*). These different localization patterns might reflect different modes of RNA localization. Indeed, the

localization of some RNAs that display a gradient-like distribution in the apical domain (*Imp*, *msps*, *crb*, *CG33129*, *qtc*) are dependent on dynein (Dhc64C) and Egalitarian (Egl) activity, suggesting that they are localized through the dynein/BicD/Egl RNA transport machinery, which was previously shown to be active in the follicular epithelium (Karlin-McGinness et al., 1996; Vazquez-Pianzola et al., 2017). On the other hand, *BicD* mRNA appears more closely associated with the apical membrane and its localization is Egl-independent. These observations suggest that the different degrees of apical enrichment might result from the involvement of different mechanisms in apical RNA localization. It is likely that different RNA localization mechansism may also explain the variety of localization patterns observed in basally-localizing mRNAs.

***Apical and basal RNA localization depends on dynein and kinesin-1***

The follicular epithelium is characterized by a polarized array of MTs organized in parallel bundles along the A/B axis of the cell, with MT minus ends concentrated apically and plus ends basally. Therefore, I hypothesized that MT-based transport could be responsible for subcellular localization of apical and basal RNAs identified by spatial transcriptomics. To test this hypothesis, I analyzed changes in the distribution of 4 apical (*crb*, *msps*, *qtc*, *CG33129*) and 4 basal (*Fkbp14*, *CG3308*, *Rtnl1*, *zip*) mRNAs after knocking down components of known RNA transport complexes or regulators.

The knock-down of components of the minus end-directed dynein/BicD/Egl RNA transport complex disrupted the localization of all apical mRNAs; in contrast, basal mRNAs were mostly unaffected, although *Dhc64C* RNAi caused mild changes in basal mRNA localization. In contrast to Egl, which to date is the sole dynein cargo adapter known to be specifically involved in RNA transport, Dhc64C participates in the transport of other cellular cargoes, including Egl-containing RNPs, vesicles, mitochondria, and other organelles. In addition, disrupting the activity of Dhc64C was reported by previous studies to cause polarity phenotypes in the follicular epithelium (Li et al., 2008; Horne-Badovinac and Bilder, 2008). Taken together, these results indicate that the dynein/BicD/Egl complex is exclusively involved in the transport of RNAs to the apical domain; the changes in basal localization observed in *Dhc64C* RNAi can be ascribed to a disruption in the cytoskeletal network and cell polarity, probably due to the involvement of Dhc64C in several cellular processes. Previous

studies have shown that the dynein/BicD/Egl machinery is responsible for apical transport of follicle cell mRNAs, such as *upd* in the border cells and *CG33129* (which I used as a positive control in *egl* RNAi experiments), *Uba1*, and *egl* itself in the main body follicle cells (Van De Bor et al., 2011; Vazquez-Pianzola et al., 2017). However, RNA transport through the dynein/BicD/Egl machinery is clearly not the sole mechanism cells use to achieve apical mRNA localization in this tissue. Indeed, the apical localization of *BicD* mRNA in both *egl* RNAi and $egl^{NULL}FC$ background is unchanged, indicating that other mechanisms can drive the apical localization of some mRNAs in the follicular epithelium. Taken together, my results together with previous reports indicate that the dynein/BicD/Egl machinery is the predominant, albeit not the only, mechanism mediating apical mRNA localization in this tissue.

MT plus end-directed transport of RNAs is poorly characterized. The best model of plus end-directed transport is represented by *oskar* (*osk)* mRNA localization to the posterior of the oocyte. *osk* is transported to the posterior pole by kinesin-1 and localization of the mRNA is dependent on EJC deposition upon splicing of the first intron (Brendza et al., 2000; Zimyanin et al., 2008; Ghosh et al., 2012). The basal domain of the follicular epithelium is enriched in MT plus ends, and and with respect to polarity, it is considered analogous to the oocyte posterior pole (Clark et al., 1997). For this reason, I hypothesized that basal RNA localization might be achieved through MT-based RNA transport directed towards MT plus ends. To test this hypothesis, I knocked down the expression of kinesin-1 (*Khc*) by RNAi. Results showed that the localization of all basally-localized RNAs was affected by *Khc* RNAi, while none of the apically-localized RNAs showed any difference in their localization compared to that in wild-type cells. In addition, *KhcRNAi* cells did not show morphological defects as was the case in *Dhc64CRNAi* cells, suggesting that, contrary to dynein, kinesin-1 is not crucially involved in establishing or maintaining cell polarity in this tissue. These results indicate that plus end-directed RNA localization in the follicular epithelium is likely directly dependent on kinesin-1, similarly to the localization of *osk* mRNA to the posterior pole. In addition to *Khc*, I analyzed the requirement of the EJC in regulating follicle cell plus end-directed RNA transport. To this end, I expressed the EJC-disrupting protein ΔC-Pym-GFP, which was shown to dissociate the EJC from mRNAs (Ghosh et al., 2014). Upon ΔC-Pym expression, the basal enrichment of *Fkbp14* and, to a lesser extent, *zip* and *CG3308* was disrupted, suggesting that the EJC

deposition regulates the basal localization of these mRNAs. However, the localization pattern of *Rtnl1* (basal mRNA), *crb* and *CG33129* (apical mRNAs) was identical to that in wild-type cells. This indicates that the EJC is involved in the localization of a subset of basal mRNAs, directly or indirectly. This is consistent with the current model in which EJC deposition is necessary to achieve the posterior localization of *osk*, but does not affect its transport from the nurse cells to the oocyte, which involves the dynein/BicD/Egl machinery and is directed towards the MT minus ends.

***The interplay between the dynein/BicD/Egl machinery and kinesin-1***

Interestingly, the knock-down of RNA transport components has different effects on localizing mRNAs, depending on whether they are apically or basally enriched. Disruption of components of the dynein/BicD/Egl transport machinery causes apical mRNAs to be ubiquitously distributed within the cell; in contrast, disruption of Khc and, in some cases, EJC displacement, mislocalizes basal mRNAs to the apical domain. This suggests that basal mRNAs might be bound to both dynein and kinesin motors pulling the mRNA in opposing directions, a phenomenon previously observed in the context of the transport of lipid droplets and neuronal granules, and called “tug of war” (Hancock, 2014). In the tug-of-war model, the two motors engage in a mechanical competition pulling in opposite directions, with one of the two winning over the other, thus resulting in the net movement of the cargo in one direction. According to this model, basal mRNAs tested would be bound by both dynein and kinesin-1 motors, with kinesin-1 winning the competition and determining the net direction of transport of the mRNA towards the plus end. Knocking down the expression of kinesin-1 through *Khc* RNAi would leave only the dynein complex on the mRNA, resulting in a switch of transport towards the MT minus ends. However, more than one model can explain the switch of transport direction. In the case of *osk* mRNA transport, the anterior accumulation of *osk* mRNAs observed in *Khc* loss-of-function mutants was hypothesized to occur through a coordinated regulation of dynein and kinesin-1 motors. According to the model, the dynein/BicD/Egl complex transporting *osk* into the oocyte must be inhibited to allow a switch to kinesin-dependent transport towards the posterior (Zimyanin et al., 2008).

To discriminate between these two possibilities, I knocked down components of the dynein and kinesin-1 transport machineries in single and double knock-down experiments, and evaluated the change in the localization of a basal mRNA, *zipper*

(*zip*). The apical localization of *zip* mRNA observed upon *Khc* RNAi led me to hypothesize that it might depend on the activity of the dynein/BicD/Egl machinery, the only RNA transport machinery known to date to be responsible for minus end-directed transport of mRNAs in *Drosophila*. The simultaneous knock-down of *Khc* and *egl* by RNAi caused a significant change in localization of *zip* mRNA, which lost most of its apical enrichment observed in single *KhcRNAi* cells, suggesting that the dynein/BicD/Egl machinery is responsible for apical mislocalization of *zip* mRNA when Khc is lacking. However, in cells where only the expression of Egl was down-regulated, the localization of *zip* mRNA was indistinguishable from wild-type cells. Taken together, these results argue against a tug-of-war model to explain the RNA localization phenotype of *zip* mRNA upon *Khc* RNAi; indeed, if both motors were simultaneously bound to *zip* mRNA and pulling in opposite directions, *zip* mRNA should have become more basally enriched upon *egl* RNAi, gaining a higher B/A signal intensity ratio. For this reason, I propose that the basal localization of *zip* mRNA is achieved only through kinesin-1, which plays a double function: first, it transports *zip* mRNA to the basal domain; second, it inhibits the binding or the activity of dynein/BicD/Egl complex to *zip* mRNA, preventing its mislocalization to the apical domain. Therefore, when kinesin-1 is absent, the dynein/BicD/Egl complex is uninhibited and can transport *zip* mRNA to the apical domain. Interestingly, the uniform distribution of apical mRNAs resulting from *egl* or *Dhc64C* RNAi suggests that the dynein- and kinesin-dependent transport complexes do not compete for binding to the same localization element on the mRNA. Indeed, if this were the case, apical mRNAs would become basally enriched upon *egl* or *Dhc64C* RNAi, being recognized by kinesin-driven transport complexes. However, more studies are needed to elucidate this phenomenon.

In the case of *osk*, the dynein/BicD/Egl machinery is needed for the first step of RNA localization, when it is recognized by the dynein/BicD/Egl machinery through the OES and is transported from the nurse cells into the oocyte during early oogenesis. Once in the oocyte, the dynein/BicD/Egl machinery must be inhibited in order for the RNA to undergo the second step of transport, towards the posterior pole. In contrast, *zip* mRNA is never found apically enriched in the follicular epithelium; its RNA localization pattern gradually switches from ubiquitous to basally enriched around stage 9 of oogenesis, when the epithelium becomes columnar (data not shown). In

addition, the dynein/BicD/Egl machinery recognizes an RNA zipcode that adopts a specific conformation (A'-form) that is necessary and sufficient for transport of many maternal and pair-rule mRNAs mediated by this complex (Bullock et al., 2010). Therefore, it is puzzling that the down-regulation of Khc causes a switch in *zip* RNA localization to the apical domain through the dynein/BicD/Egl machinery, as it suggests that *zip* might contain a stem-loop structure recognized specifically by the minus end-directed machinery. This would also apply to the other basal mRNAs that displayed an apical enrichement upon *Khc* knock-down (*Rtnl1*, *Fkbp14,* and, to a lesser extent, *CG3308*), and possibly to many other RNAs that were not tested.

*zip* (as well as *CG3308*, *Rtnl1*, *Fkbp14*) mRNA is not found apically enriched in the follicular epithelium at any stage of oogenesis in flies maintained under optimal laboratory conditions. It is possible, however, that a switch to apical localization of *zip* occurs under stress conditions, through regulation of the balance of dynein versus kinesin transport. According to this hypothesis, application of a stressor (heat, reduced nutrient availability, etc.) might result in downregulation of kinesin-1 activity and cause a switch to a dynein-mediated transport of the RNAs. The switch to apical localization might be necessary to effectively respond to the stressor, for example if the apical domain functioned as an mRNA storage compartment or, conversely, allowed more efficient translation of mRNAs .

Alternatively, another scenario might be possible. A previous study in the blastoderm embryo has shown that ubiquitously distributed mRNAs occasionally undergo directed transport through the recruitment of the dynein/BicD/Egl machinery and that the complex is not highly selective. Consistent with this, mild overexpression (2- 2.5-fold increase) of components of the machinery causes the apical localization of ubiquitous mRNAs (Bullock et al., 2006). Considering these results, it is possible that, in the follicular epithelium, the down-regulation of Khc through RNAi causes an upregulation in activity or abundance of Egl protein; this, in turn, would increase the non-specific binding of Egl to mRNAs that do not contain an apical localization element and result in their apical localization. In this case, the apical localization of basal mRNAs upon Khc disruption might reflect a biological meaning, as well as being a side effect of non-physiological Egl upregulation.

**BicD *is apically localized independently of the dynein/BicD/Egl complex***

While screening for apical mRNAs whose localization is disrupted upon *egl* RNAi, I found that the apical localization of *BicD* mRNA does not depend on the dynein/BicD/Egl machinery. This result was confirmed by looking at the localization of *BicD* mRNA in an *egl* null background, whose germline expression was rescued to allow completion of oogenesis and screening of mid-stage egg-chambers. An *egl*-independent apical RNA localization of *BicD* mRNA was surprising, because until now it was though that the dynein/BicD/Egl machinery was responsible for the localization of minus end-localized mRNAs in *Drosophila*. For this reason, I decided to investigate in greater detail the mechanisms behind the apical localization of *BicD* RNA. Depolymerization of the MT cytoskeleton with colchicine caused *BicD* to become ubiquitously localized in the cell, indicating that microtubules are required for apical localization of the mRNA, whether be it for transport or for anchoring. In addition, expression of a transgene containing only the *BicD* CDS fused in-frame with GFP was sufficient to achieve an apical localization pattern indistinguishable from that of endogenous *BicD* mRNA. This indicates that *BicD* RNA localization is MT-dependent and does not require *BicD* 3'or 5'UTRs.

Considering these results, several mechanisms described to date could account for *BicD* apical RNA localization. The dependence on MTs demonstrated by the effect of acute colchicine treatment and the absence of cytoplasmic streaming in follicular epithelial cells argue against mechanisms other than *BicD* mRNA transport, such as facilitated diffusion or selective protection from degradation. On the other hand, three modes of RNA transport described to date could account for apical localization of *BicD* RNA: 1) active transport of *BicD* by an RNA transport machinery distinct from the dynein/BicD/Egl complex; 2) hitch-hiking on trafficking vesicles; 3) co-translational transport of *BicD* mRNA while BicD protein is being translated.

Interestingly, early studies of BicD expression using genetic mutants carrying loss-of-function alleles showed that *BicD* mRNA localization in the oocyte is dependent on BicD protein activity (Suter and Steward, 1991). Assuming that the same phenomenon occurs in the follicular epithelial cells, the directed RNA transport or vesicle hitch-hiking would involve a dynein/BicD complex bound by either an RNA-binding protein distinct from Egl or a protein that links the motor/adaptor complex with vesicles. Several studies have shown that the C-terminus domain of BicD (CTD)

can interact with several cargo-binding proteins, such as Egl, Rab6, Chc, Lam, and Fmr1 (Dienstbier et al., 2009; Li et al., 2010; Stuurman et al., 1999; Bianco et al., 2010), and, at least in some cases, it seems that their binding to the BicD CTD is mutually exclusive. Fmr1 and its mammalian ortholog FMRP are RNA-binding proteins with a conserved neuronal role in RNA translational regulation, and in both *Drosophila* and mammals Fmr1 was linked to RNA transport (Estes et al., 2008; Davidovic et al., 2007). Expression levels of Fmr1 in the apical and basal datasets indicate that Fmr1 is expressed in the follicular epithelium. It is therefore conceivable that an RNA transport complex consisting of dynein/BicD/Fmr1 might act in parallel with the dynein/BicD/Egl machinery in apical transport of mRNAs, and be specifically responsible for apical localization of *BicD* RNA. Alternatively, a complex composed of dynein/BicD and Rab6 might be responsible for the transport of *BicD* mRNA by hitch-hiking to exocytic vesicles during vesicle trafficking to the apical domain.

The finding that apical localization of *BicD* mRNA does not require the 3' or 5'UTR, and that the *BicD* CDS is sufficient for its apical transport, opens the exciting possibility that *BicD* mRNA might be co-translationally transported to the apical domain together with nascent BicD protein. In this regard, the apical localization of *BicD* RNA would reflect a mechanism in which the nascent N-terminal domain of BicD protein produced by actively translating ribosomes is bound by the dynein/dynactin complex; therefore, BicD protein would associate co-translationally with the dynein/dynactin complex, while the motor is moving towards the MT minus ends. The N-terminal region of mammalian BICD1/2 encompassing coiled-coil domain 1 (CC1) and part of CC2 was shown to bind to dynein, while the C-terminal domain (CC3) interacts with cargo-binding proteins (Hoogenraad et al., 2001). All 3 coiled coil domains are conserved in *Drosophila*, and the functional homology of BicD CTD in binding cargoes was demonstrated in several studies. This suggests that the binding of the BicD N-terminal domain with dynein/dynactin is conserved in *Drosophila*, although this has not been demonstrated. Moreover, *in vitro*-translated BicD is auto-inhibited, with the C-terminal CC3 domain interacting with the N-terminal CC1/2 domains, a regulatory mechanism that is conserved between *Drosophila* and mammal *BicD* (Liu et al., 2013). Although the release of auto-inhibition was shown to occur upon cargoes binding to BicD CTD *in vitro*, it is also conceivable that *in vivo* the autoinhibition of BicD would be overcome upon

dynein/dynactin binding to the nascent N-terminal domain of BicD. In support of this hypothesis, studies in mammalian cells showed that the N-terminal portion of BICD2 promotes formation of stable ternary complex with purified mammalian dynein and dynactin (Splinter et al., 2012). A similar mechanism of co-translational transport of a dynein-interacting protein has been described recently for *pericentrin* (PCNT) in HeLa cells and zebrafish embryos (Sepulveda et al., 2018).

Finally, it is interesting to note that mRNAs encoding components of the dynein/BicD/Egl machinery such as *Dlic*, *BicD*, and *egl* are all apically localized in follicle cells. Apical localization of *egl* was previously reported, and the mRNA is likely to be transported by the dynein/BicD/Egl machinery itself, as hypomorphic *BicD* alleles disrupt *egl* mRNA apical localization and the mRNA co-immunoprecipitates with Egl protein (Vazquez-Pianzola et al., 2017). Due to their participation in the same protein complex, I speculate that the apical transport of *BicD* and *egl*, and possibly of other mRNAs encoding components of the dynein complex such as *Dlic*, might be important for their assembly into the dynein/BicD/Egl complex in the apical domain.

### *Egl-dependent RNA localization promotes the formation of an A/B gradient of Imp protein*

To gain some insight into the functional significance of apical RNA localization, I investigated the spatial distribution of the protein products encoded by apically localizing RNAs. I found that the distribution of *Imp* mRNA, which shows a gradient-like localization pattern along the A/B axis of follicle cells, is mirrored by the distribution of Imp protein, suggesting that apical RNA localization might serve to concentrate Imp protein in the apical domain. Knock-down of Egl resulted in reduction of the apical accumulation of both *Imp* mRNA and protein. Measurement of the total apical and basal GFP fluorescence showed that Imp protein amount was unchanged, indicating a redistribution of *Imp* mRNA and protein within the cell, rather than apical degradation or reduced translation. This results suggest that *Imp* is not translationally silent while transported by Egl, and that the perturbation of *Imp* mRNA localization causes the protein to be translated ectopically in the cell, abolishing its graded distribution along the A/B axis. Considering that the majority of localized mRNAs are translationally repressed while in transport, this phenomenon is surprising and might reflect the structural characteristics of the follicular epithelium. Indeed, RNAs

transported in the germline travel long distances and undergo changes in direction before reaching their final destination, and their tight translational repression prevents ectopic protein expression and emergence of deleterious phenotypes in the ovary or embryo. The epithelial follicle cells are small (~10 µm) and the A/B orientation of the MT might be useful to achieve a local concentration of proteins through RNA localization where they are most needed, or to target mRNAs to specialized subcellular compartments for specific post-translational modifications. A similar phenomenon was observed for *wingless* (*wg*) apical RNA localization in *Drosophila* embryonic epithelium. There, the disruption of *wg* apical localization causes a redistribution of Wg protein in the cell, rather than reduced Wg expression; nevertheless, this results in a decrease in Wg signalling activity (Simmonds et al., 2001). Therefore, the authors hypothesized that the apical localization of *wg* may help target the mRNA to a specialized apical compartment for efficient Wg signalling activity. A similar scenario might apply to Imp, which plays several roles in *Drosophila*, including modulation of axonal regrowth by promoting subcellular mRNA targeting (Medioni et al., 2014), spermatogenesis (Fabrizio et al., 2008), and counteracting aging in the stem-cell niche of the testis by protecting mRNAs from degradation (Toledano et al., 2012). In stage 6 follicle cells, Imp activity is required for the apical localization of Kuzbanian, an ADAM metallopeptidase involved in the cleaving of Notch. Therefore, it is possible that the apical enrichment of Imp protein by Egl-mediated localization of *Imp* mRNA might be important to achieve efficient apical activity of Imp for downstream signaling.

In addition to *Imp*, the apical localization of other mRNAs expressed in the columnar follicle cells is disrupted upon the dynein/BicD/Egl knock-down. These include *crb*, *qtc*, *msps* (this study) and *Uba1*, *CG33129*, *egl* (Vazquez-Pianzola et al., 2017). I investigated the general role of Egl-dependent apical mRNA localization by knocking down Egl expression by driving *egl* RNAi in the follicle cells using the follicle-cell specific driver *traffic jam* (*tj*), and assessing the resulting phenotype by measuring the hatching rate of eggs. The follicular epithelium plays fundamental roles during oogenesis such as in reciprocal signalling with the oocyte leading to its polarization, contributing to vitellogenesis, and producing the eggshell structures. Therefore, I reasoned that if Egl has any role in these events, disruption of its activity should result in morphological defects in the egg and inability of embryos to hatch.

Preliminary results indicate that the absence of Egl in the follicle cells causes a small reduction in the hatching rate, suggesting that Egl activity in the somatic component of the ovary is not strictly necessary under normal laboratory conditions. This might be explained by the fact that, as exemplified by Imp protein distribution upon Egl knock-down, Egl plays a role in creating an A/B gradient of proteins by enriching the encoding mRNAs apically; however, disruption of apical localization does not result in a decrease expression of the protein, which might still have a residual function; this, in turn, might explain the reduced effects seen in the hatching rate experiment. Alternatively, Egl function might be important in flies maintained under less optimal laboratory conditions that mimic life in the wild, including under diverse stress conditions. In this regard, it was recently shown that follicle cells play a role in the activation of the germline starvation response upon protein-poor diet (Burn et al., 2015). Therefore, it might be that the apical localization of mRNAs by the dynein/BicD/Egl complex is not required under optimal growth conditions, but rather is essential for follicle cell-mediated responses to stressors. Testing if this hypothesis is correct will require subjecting *egl* follicle cell-mutant flies to various stress conditions and evaluate the state of the eggshell and egg hatching rate.

# Bibliography


Afgan, E. *et al.* The Galaxy platform for accessible, reproducible and collaborative biomedical analyses: 2018 update. *Nucleic Acids Res.* **46**, W537–W544 (2018).

Aguilar-Aragon, M., Fletcher, G. & Thompson, B. J. The cytoskeletal motor proteins Dynein and MyoV direct apical transport of Crumbs. *Dev. Biol.* **459**, 126–137 (2020).

Amrute-Nayak, M. & Bullock, S. L. Single-molecule assays reveal that RNA localization signals regulate dyneing-dynactin copy number on individual transcript cargoes. *Nat. Cell Biol.* **14**, 416–423 (2012).

An, J. J. *et al.* Distinct Role of Long 3′ UTR BDNF mRNA in Spine Morphology and Synaptic Plasticity in Hippocampal Neurons. *Cell* **134**, 175–187 (2008).

Andreassi, C. & Riccio, A. To localize or not to localize: mRNA fate is in 3′UTR ends. *Trends Cell Biol.* **19**, 465–474 (2009).

Andrews, S. FASTQC. A quality control tool for high throughput sequence data.(2010) http://www.bioinformatics.babraham.ac.uk/projects/fastqc/.

Babu, K., Cai, Y., Bahri, S., Yang, X. & Chia, W. Roles of Bifocal, Homer, and F-actin in anchoring Oskar to the posterior cortex of Drosophila oocytes. *Genes Dev.* **18**, 138–143 (2004).

Bacallao, R. *et al.* The subcellular organization of Madin-Darby canine kidney cells during the formation of a polarized epithelium. *J. Cell Biol.* **109**, 2817–2832 (1989).

Bashirullah, A. *et al.* Joint action of two RNA degradation pathways controls the timing of maternal transcript elimination at the midblastula transition in Drosophila melanogaster. *EMBO J.* **18**, 2610–2620 (1999).

Baumann, S., Pohlmann, T., Jungbluth, M., Brachmann, A. & Feldbrügge, M. Kinesin-3 and dynein mediate microtubule-dependent co-transport of mrnps and endosomes. *J. Cell Sci.* **125**, 2740–2752 (2012).

Bianco, A., Dienstbier, M., Salter, H. K., Gatto, G. & Bullock, S. L. Bicaudal-D regulates fragile X mental retardation protein levels, motility, and function during neuronal morphogenesis. *Curr. Biol.* **20**, 1487–1492 (2010).

Bilder, D., Li, M. & Perrimon, N. Cooperative regulation of cell polarity and growth by Drosophila tumor suppressors. *Science.* **289**, 113–116 (2000).

Birsoy, B., Kofron, M., Schaible, K., Wylie, C. & Heasman, J. Vg1 is an essential signaling molecule in Xenopus development. *Development* **133**, 15–20 (2006).

Blower, M. D., Feric, E., Weis, K. & Heald, R. Genome-wide analysis demonstrates conserved localization of messenger RNAs to mitotic microtubules. *J. Cell Biol.* **179**, 1365–1373 (2007).

Bobola, N., Jansen, R. P., Shin, T. H. & Nasmvth, K. Asymmetric accumulation of Ash1 in post anaphase nuclei depends on a myosin and restricts yeast mating type switching to mother cells. *Cell* **84**, 699–709 (1996).

Bolger, A. M., Lohse, M. & Usadel, B. Trimmomatic: A flexible trimmer for Illumina sequence data. *Bioinformatics* **30**, 2114–2120 (2014).

Brand, A. H., Manoukian, A. S. & Perrimon, N. Ectopic expression in Drosophila. *Methods Cell Biol.* **44**, 635–654 (1994).

Brendza, R. P. *et al.* A Function for Kinesin I in the Posterior Transport of oskar mRNA and Staufen Protein. *Science.* **289**, 2120–2122 (2000).

Brendza, R. P., Serbus, L. R., Saxton, W. M. & Duffy, J. B. Posterior localization of dynein and dorsal-ventral axis formation depend on kinesin in Drosophila oocytes. *Curr. Biol.* **12**, 1541–1545 (2002).

Bullock, S. L., Nicol, A., Gross, S. P. & Zicha, D. Guidance of Bidirectional Motor Complexes by mRNA Cargoes through Control of Dynein Number and Activity. *Curr. Biol.* **16**, 1447–1452 (2006).

Bullock, S. L., Ringel, I., Ish-Horowicz, D. & Lukavsky, P. J. A′-form RNA helices are required for cytoplasmic mRNA transport in Drosophila. *Nat. Struct. Mol. Biol.* **17**, 703–709 (2010).

Bullock, S. L. *et al.* Differential cytoplasmic mRNA localisation adjusts pair-rule transcription factor to cytoarchitecture in dipteran evolution. *Development* **131**, 4251–4261 (2004).

Bullock, S. L., Zicha, D. & Ish-Horowicz, D. The Drosophila hairy RNA localization signal modulates the kinetics of cytoplasmic mRNA transport. *EMBO J.* **22**, 2484–2494 (2003).

Bullock, S. L. & Ish-Horowicz, D. Conserved signals and machinery for RNA transport in Drosophila oogenesis and embryogenesis. *Nature* **414**, 611–616 (2001).

Burn, K. M. *et al.* Somatic insulin signaling regulates a germline starvation response in Drosophila egg chambers. *Dev. Biol.* **398**, 206–217 (2015).

Carlson, M. org.Dm.eg.db: Genome wide annotation for Fly. (2019) R package version 3.8.2.

Castagnetti, S., Hentze, M. W., Ephrussi, A. & Gebauer, F. Control of oskar mRNA translation by Bruno in a novel cell-free system from Drosophila ovaries. *Development* **127**, 1063–1068 (2000).

Chartrand, P., Meng, X. H., Singer, R. H. & Long, R. M. Structural elements required for the localization of ASH1 mRNA and of a green fluorescent protein reporter particle in vivo. *Curr. Biol.* **9**, 333–338 (1999).

Chekulaeva, M., Hentze, M. W. & Ephrussi, A. Bruno acts as a dual repressor of oskar translation, promoting mRNA oligomerization and formation of silencing particles. *Cell* **124**, 521–533 (2006).

Chen, E., Sharma, M. R., Shi, X., Agrawal, R. K. & Joseph, S. Fragile X Mental Retardation Protein Regulates Translation by Binding Directly to the Ribosome. *Mol. Cell* **54**, 407–417 (2014).

Chen, J. *et al.* Spatial transcriptomic analysis of cryosectioned tissue samples with Geo-seq. *Nat. Protoc.* **12**, 566–580 (2017).

Cioni, J. M. *et al.* Late Endosomes Act as mRNA Translation Platforms and Sustain Mitochondria in Axons. *Cell* **176**, 56–72 (2019).

Clark, A., Meignin, C. & Davis, I. A Dynein-dependent shortcut rapidly delivers axis determination transcripts into the Drosophila oocyte. *Development* **134**, 1955–1965 (2007).

Clark, I. E., Jan, L. Y. & Jan, Y. N. Reciprocal localization of nod and kinesin fusion proteins indicates microtubule polarity in the Drosophila oocyte, epithelium, neuron and muscle. *Development* **124**, 461–470 (1997).

Cohen, R. S., Zhang, S. & Dollar, G. L. The positional, structural, and sequence requirements of the Drosophila TLS RNA localization element. *RNA* **11**, 1017–1029 (2005).

Condeelis, J. & Singer, R. H. How and why does β-actin mRNA target? *Biol. Cell* **97**, 97–110 (2005).

Conesa, A. *et al.* A survey of best practices for RNA-seq data analysis. *Genome Biol.* **17**, 13 (2016).

Corradi, E. *et al.* Axonal precursor miRNAs hitchhike on endosomes and locally regulate the development of neural circuits. *EMBO J.* **39**, 1–24 (2020).

Cosker, K. E., Pazyra-Murphy, M. F., Fenstermacher, S. J. & Segal, R. A. Target-derived neurotrophins coordinate transcription and transport of Bclw to prevent axonal degeneration. *J. Neurosci.* **33**, 5195–5207 (2013).

Courchesne, S. L., Karch, C., Pazyra-Murphy, M. F. & Segal, R. A. Sensory neuropathy attributable to loss of Bcl-w. *J. Neurosci.* **31**, 1624–1634 (2011).

Cox, R. T., Kirkpatrick, C. & Peifer, M. Armadillo is required for adherens junction assembly, cell polarity, and morphogenesis during Drosophila embryogenesis. *J. Cell Biol.* **134**, 133–148 (1996).

Dahanukar, A., Walker, J. A. & Wharton, R. P. Smaug, a novel RNA-binding protein that operates a translational switch in Drosophila. *Mol. Cell* **4**, 209–218 (1999).

Darnell, J. C. *et al.* FMRP stalls ribosomal translocation on mRNAs linked to synaptic function and autism. *Cell* **146**, 247–261 (2011).

Davidovic, L. *et al.* The fragile X mental retardation protein is a molecular adaptor between the neurospecific KIF3C kinesin and dendritic RNA granules. *Hum. Mol. Genet.* **16**, 3047–3058 (2007).

Davis, I. & Ish-Horowicz, D. Apical localization of pair-rule transcripts requires 3′ sequences and limits protein diffusion in the Drosophila blastoderm embryo. *Cell* **67**, 927–940 (1991).

Delanoue, R. & Davis, I. Dynein anchors its mRNA cargo after apical transport in the Drosophila blastoderm embryo. *Cell* **122**, 97–106 (2005).

Delanoue, R., Herpers, B., Soetaert, J., Davis, I. & Rabouille, C. Drosophila Squid/hnRNP Helps Dynein Switch from a gurken mRNA Transport Motor to an Ultrastructural Static Anchor in Sponge Bodies. *Dev. Cell* **13**, 523–538 (2007).

Dictenberg, J. B., Swanger, S. A., Antar, L. N., Singer, R. H. & Bassell, G. J. A Direct Role for FMRP in Activity-Dependent Dendritic mRNA Transport Links Filopodial-Spine Morphogenesis to Fragile X Syndrome. *Dev. Cell* **14**, 926–939 (2008).

Diehn, M., Bhattacharya, R., Botstein, D. & Brown, P. O. Genome-scale identification of membrane-associated human mRNAs. *PLoS Genet.* **2**, 39–50 (2006).

Dienstbier, M., Boehl, F., Li, X. & Bullock, S. L. Egalitarian is a selective RNA-binding protein linking mRNA localization signals to the dynein motor. *Genes Dev.* **23**, 1546–1558 (2009).

Dietzl, G. *et al.* A genome-wide transgenic RNAi library for conditional gene inactivation in Drosophila. *Nature* **448**, 151–156 (2007).

Ding, D., Parkhurst, S. M., Halsell, S. R. & Lipshitz, H. D. Dynamic Hsp83 RNA localization during Drosophila oogenesis and embryogenesis. *Mol. Cell. Biol.* **13**, 3773–3781 (1993).

Dix, C. I. *et al.* Lissencephaly-1 promotes the recruitment of dynein and dynactin to transported mRNAs. *J. Cell Biol.* **202**, 479–494 (2013).

Dobens, L. L. & Raftery, L. a. Integration of Epithelial Patterning and Morphogenesis in. *Dev. Dyn.* **218**, 80–93 (2000).

Dobin, A. *et al.* STAR: Ultrafast universal RNA-seq aligner. *Bioinformatics* **29**, 15–21 (2013).

dos Santos, G., Simmonds, A. J. & Krause, H. M. A stem-loop structure in the wingless transcript defines a consensus motif for apical RNA transport. *Development* **135**, 133–143 (2008).

Doyle, M. & Kiebler, M. A. A numbers game underpins cytoplasmic mRNA transport. *Nat. Cell Biol.* **14**, 333–335 (2012).

Driever, W., Siegel, V. & Nüsslein-Volhard, C. Autonomous determination of anterior structures in the early Drosophila embryo by the bicoid morphogen. *Development* **109**, 811–820 (1990).

Drummond-Barbosa, D. & Spradling, A. C. Stem cells and their progeny respond to nutritional changes during Drosophila oogenesis. *Dev. Biol.* **231**, 265–278 (2001).

Duhart, J. C., Parsons, T. T. & Raftery, L. A. The repertoire of epithelial morphogenesis on display: Progressive elaboration of Drosophila egg structure. *Mech. Dev.* **148**, 18–39 (2017).

Duncan, J. E. & Warrior, R. The cytoplasmic dynein and kinesin motors have interdependent roles in patterning the Drosophila oocyte. *Curr. Biol.* **12**, 1982–1991 (2002).

Dunst, S. *et al.* Endogenously Tagged Rab Proteins: A Resource to Study Membrane Trafficking in Drosophila. *Dev. Cell* **33**, 351–365 (2015).

Echeverri, C. J., Paschal, B. M., Vaughan, K. T. & Vallee, R. B. Molecular characterization of the 50-kD subunit of dynactin reveals function for the complex in chromosome alignment and spindle organization during mitosis. *J. Cell Biol.* **132**, 617–633 (1996).

Eckley, D. M. *et al.* Analysis of dynactin subcomplexes reveals a novel actin-related protein associated with the Arp1 minifilament pointed end. *J. Cell Biol.* **147**, 307–319 (1999).

Ephrussi, A., Dickinson, L. K. & Lehmann, R. Oskar Organizes the Germ Plasm and Directs Localization of the Posterior Determinant Nanos. *Cell* **66**, 37–50 (1991).

Ephrussi, A. & Lehmann, R. Induction of germ cell fate by oskar. *Nature* **358**, 387–392 (1992).

Erdélyi, M., Michon, A. M., Guichet, A., Glotzer, J. B. & Ephrussi, A. Requirement for Drosophila cytoplasmic tropomyosin in oskar mRNA localization. *Nature* **377**, 524–527 (1995).

Estes, P. S., O'Shea, M., Clasen, S. & Zarnescu, D. C. Fragile X protein controls the efficacy of mRNA transport in Drosophila neurons. *Mol. Cell. Neurosci.* **39**, 170–179 (2008).

Fabrizio, J. J. *et al.* Imp (IGF-II mRNA-binding protein) is expressed during spermatogenesis in Drosophila melanogaster. *Fly (Austin).* **2**, 47–52 (2008).

Ferrandon, D., Koch, I., Westhof, E. & Nüsslein-Volhard, C. RNA-RNA interaction is required for the formation of specific bicoid mRNA 3' UTR-STAUFEN ribonucleoprotein particles. *EMBO J.* **16**, 1751–1758 (1997).

Forrest, K. M., Clark, I. E., Jain, R. A. & Gavis, E. R. Temporal complexity within a translational control element in the nanos mRNA. *Development* **131**, 5849–5857 (2004).

Forrest, K. M. & Gavis, E. R. Live Imaging of Endogenous RNA Reveals a Diffusion and Entrapment Mechanism for nanos mRNA Localization in Drosophila. *Curr. Biol.* **13**, 1159–1168 (2003).

Frohnhöfer, H. G. & Nüsslein-Volhard, C. Organization of anterior pattern in the Drosophila embryo by the maternal gene bicoid. *Nature* **324**, 120–125 (1986).

Gagnon, J. A. & Mowry, K. L. Molecular motors: Directing traffic during RNA localization. *Crit. Rev. Biochem. Mol. Biol.* **46**, 229–239 (2011).

Gáspár, I., Sysoev, V., Komissarov, A. & Ephrussi, A. An RNA-binding atypical tropomyosin recruits kinesin-1 dynamically to oskar mRNPs. *EMBO J.* **36**, 319–333 (2016).

Gáspár, I., Wippich, F. & Ephrussi, A. Enzymatic production of single-molecule FISH and RNA capture probes. *RNA* **23**, 1582–1591 (2017).

Gatfield, D., Unterholzner, L., Ciccarelli, F. D., Bork, P. & Izaurralde, E. Nonsense-mediated mRNA decay in Drosophila: at the intersection of the yeast and mammalian pathways. *EMBO J.* **22**, 3960–3970 (2003).

Gavis, E. R. & Lehmann, R. Translational regulation of nanos by RNA localization. *Nature* **369**, 315–318 (1994).

Ghosh, S., Marchand, V., Gáspár, I. & Ephrussi, A. Control of RNP motility and localization by a splicing-dependent structure in oskar mRNA. *Nat. Struct. Mol. Biol.* **19**, 441–449 (2012).

Ghosh, S., Obrdlik, A., Marchand, V. & Ephrussi, A. The EJC Binding and Dissociating Activity of PYM Is Regulated in Drosophila. *PLoS Genet.* **10**, e1004455 (2014).

Glotzer, J. B., Saffrich, R., Glotzer, M. & Ephrussi, A. Cytoplasmic flows localize injected oskar RNA in Drosophila oocytes. *Curr. Biol.* **7**, 326–337 (1997).

Gold, V. A., Chroscicki, P., Bragoszewski, P. & Chacinska, A. Visualization of cytosolic ribosomes on the surface of mitochondria by electron cryo-tomography. *EMBO Rep.* **18**, 1786–1800 (2017).

González-Reyes, A., Elliott, H. & St Johnston, D. Polarization of both major body axes in drosophila by gurken-torpedo signalling. *Nature* **375**, 654–658 (1995).

González-Reyes, A. & St. Johnston, D. Patterning of the follicle cell epithelium along the anterior-posterior axis during Drosophila oogenesis. *Development* **125**, 2837–2846 (1998).

Gonzalez, I., Buonomo, S. B. C., Nasmyth, K. & Von Ahsen, U. ASH1 mRNA localization in yeast involves multiple secondary structural elements and ASH1 protein translation. *Curr. Biol.* **9**, 337–340 (1999).

Grooms, S. Y. *et al.* Activity bidirectionally regulates AMPA receptor mRNA abundance in dendrites of hippocampal neurons. *J. Neurosci.* **26**, 8339–8351 (2006).

Guichet, A., Peri, F. & Roth, S. Stable anterior anchoring of the oocyte nucleus is required to establish dorsoventral polarity of the drosophila egg. *Dev. Biol.* **237**, 93–106 (2001).

Gumy, L. F. *et al.* Transcriptome analysis of embryonic and adult sensory axons reveals changes in mRNA repertoire localization. *RNA* **17**, 85–98 (2011).

Gutierrez, N. *et al.* The β-actin mRNA zipcode regulates epithelial adherens junction assembly but not maintenance. *RNA* **20**, 689–701 (2014).

Hachet, O. & Ephrussi, A. Drosophila Y14 shuttles to the posterior of the oocyte and is required for oskar mRNA transport. *Curr. Biol.* **11**, 1666–1674 (2001).

Hachet, O. & Ephrussi, A. Splicing of oskar RNA in the nucleus is coupled to its cytoplasmic localization. *Nature* **428**, 959–963 (2004).

Hafen, E., Kuroiwa, A. & Gehring, W. J. Spatial distribution of transcripts from the segmentation gene fushi tarazu during Drosophila embryonic development. *Cell* **37**, 833–841 (1984).

Hancock, W. O. Bidirectional cargo transport: Moving beyond tug of war. *Nat. Rev. Mol. Cell Biol.* **15**, 615–628 (2014).

Hengst, U., Deglincerti, A., Kim, H. J., Jeon, N. L. & Jaffrey, S. R. Axonal elongation triggered by stimulus-induced local translation of a polarity complex protein. *Nat. Cell Biol.* **11**, 1024–1030 (2009).

Heym, R. G. & Niessing, D. Principles of mRNA transport in yeast. *Cell. Mol. Life Sci.* **69**, 1843–1853 (2012).

Hoogenraad, C. C. & Akhmanova, A. Bicaudal D Family of Motor Adaptors: Linking Dynein Motility to Cargo Binding. *Trends Cell Biol.* **26**, 327–340 (2016).

Hoogenraad, C. C. *et al.* Mammalian golgi-associated Bicaudal-D2 functions in the dynein-dynactin pathway by interacting with these complexes. *EMBO J.* **20**, 4041–4054 (2001).

Hoogenraad, C. C. *et al.* Bicaudal D induces selective dynein-mediated microtubule minus end-directed transport. *EMBO J.* **22**, 6004–6015 (2003).

Horne-Badovinac, S. & Bilder, D. Dynein regulates epithelial polarity and the apical localization of stardust A mRNA. *PLoS Genet.* **4**, 0040–0051 (2008).

Houston, D. W. & King, M. Lou. A critical role for Xdazl a germ plasm-localized RNA, in the differentiation of primordial germ cells in Xenopus. *Development* **127**, 447–456 (2000).

Huang, F., Chotiner, J. K. & Steward, O. Actin polymerization and ERK phosphorylation are required for Arc/Arg3.1 mRNA targeting to activated synaptic sites on dendrites. *J. Neurosci.* **27**, 9054–9067 (2007).

Hughes, J. R., Bullock, S. L. & Ish-Horowicz, D. inscuteable mRNA Localization Is Dynein-Dependent and Regulates Apicobasal Polarity and Spindle Length in Drosophila Neuroblasts. *Curr. Biol.* **14**, 1950–1956 (2004).

Hüttelmaier, S. *et al.* Spatial regulation of β-actin translation by Src-dependent phosphorylation of ZBP1. *Nature* **438**, 512–515 (2005).

Igreja, C. & Izaurralde, E. CUP promotes deadenylation and inhibits decapping of mRNA targets. *Genes Dev.* **25**, 1955–1967 (2011).

Jambhekar, A. & Derisi, J. L. Cis-acting determinants of asymmetric, cytoplasmic RNA transport. *RNA* **13**, 625–642 (2007).

Jambor, H., Brunel, C. & Ephrussi, A. Dimerization of oskar 3′ UTRs promotes hitchhiking for RNA localization in the Drosophila oocyte. *RNA* **17**, 2049–2057 (2011).

Jambor, H., Mueller, S., Bullock, S. L. & Ephrussi, A. A stem-loop structure directs oskar mRNA to microtubule minus ends. *RNA* **20**, 429–439 (2014).

Jambor, H. *et al.* Systematic imaging reveals features and changing localization of mRNAs in Drosophila development. *Elife* **4**, 1–22 (2015).

Jankovics, F., Sinka, R., Lukácsovich, T. & Erdélyi, M. MOESIN crosslinks actin and cell membrane in Drosophila oocytes and is required for OSKAR anchoring. *Curr. Biol.* **12**, 2060–2065 (2002).

Jansen, R.-P., Dowzer, C., Michaelis, C., Galova, M. & Nasmyth, K. Mother Cell–Specific HO Expression in Budding Yeast Depends on the Unconventional Myosin Myo4p and Other Cytoplasmic Proteins. *Cell* **84**, 687–697 (1996).

Januschke, J. *et al.* Polar transport in the Drosophila oocyte requires Dynein and Kinesin I cooperation. *Curr. Biol.* **12**, 1971–1981 (2002).

Jeffery, W. R., Tomlinson, C. R. & Brodeur, R. D. Localization of actin messenger RNA during early ascidian development. *Dev. Biol.* **99**, 408–417 (1983).

Karlin-mcGinness, M., Serano, T. L. & Cohen, R. S. Comparative Analysis of the Kinetics and Dynamics of KIO, bicoid, and oskar mRNA Localization in the Drosophila Oocyte. *Dev. Genet.* **19**, 238–248 (1996).

Karpova, N., Bobinnec, Y., Fouix, S., Huitorel, P. & Debec, A. Jupiter, a new Drosophila protein associated with microtubules. *Cell Motil. Cytoskeleton* **63**, 301–312 (2006).

Khanal, I., Elbediwy, A., de la Loza, M. del C. D., Fletcher, G. C. & Thompson, B. J. Shot and Patronin polarise microtubules to direct membrane traffic and biogenesis of microvilli in epithelia. *J. Cell Sci.* **129**, 2651–2659 (2016).

Kilchert, C. & Spang, A. Cotranslational transport of ABP140 mRNA to the distal pole of S. cerevisiae. *EMBO J.* **30**, 3567–3580 (2011).

Kim-Ha, J., Kerr, K. & Macdonald, P. M. Translational regulation of oskar mRNA by Bruno, an ovarian RNA-binding protein, is essential. *Cell* **81**, 403–412 (1995).

Kim-Ha, J., Smith, J. L. & Macdonald, P. M. oskar mRNA is localized to the posterior pole of the Drosophila oocyte. *Cell* **66**, 23–35 (1991).

Kislauskis, E. H. & Singer, R. H. Determinants of mRNA localization. *Curr. Opin. Cell Biol.* **4**, 975–978 (1992).

Kislauskis, E. H., Zhu, X. C. & Singer, R. H. β-Actin messenger RNA localization and protein synthesis augment cell motility. *J. Cell Biol.* **136**, 1263–1270 (1997).

Kislauskis, E. H., Zhu, X. & Singer, R. H. Sequences responsible for intracellular localization of β-actin messenger RNA also affect cell phenotype. *J. Cell Biol.* **127**, 441–451 (1994).

Kloc, M. & Etkin, L. D. Two distinct pathways for the localization of RNAs at the vegetal cortex in Xenopus oocytes. *Development* **121**, 287–297 (1995).

Koch, E. A. & Spitzer, R. H. Multiple effects of colchicine on oogenesis in Drosophila: Induced sterility and switch of potential oocyte to nurse-cell developmental pathway. *Cell Tissue Res.* **228**, 21–32 (1983).

Kopylova, E., Noé, L. & Touzet, H. SortMeRNA: Fast and accurate filtering of ribosomal RNAs in metatranscriptomic data. *Bioinformatics* **28**, 3211–3217 (2012).

Krauss, J., López de Quinto, S., Nüsslein-Volhard, C. & Ephrussi, A. Myosin-V Regulates oskar mRNA Localization in the Drosophila Oocyte. *Curr. Biol.* **19**, 1058–1063 (2009).

Kugler, J. M. & Lasko, P. Localization, anchoring and translational control of oskar, gurken, bicoid and nanos mRNA during drosophila oogenesis. *Fly (Austin).* **3**, 15–28 (2009).

Lai, F., Zhou, Y., Luo, X., Fox, J. & King, M. Lou. Nanos1 functions as a translational repressor in the Xenopus germline. *Mech. Dev.* **128**, 153–163 (2011).

Larsen, K. S., Xu, J., Cermelli, S., Shu, Z. & Gross, S. P. BicaudalD actively regulates microtubule motor activity in lipid droplet transport. *PLoS One* **3**, e3763 (2008).

Lécuyer, E. *et al.* Global Analysis of mRNA Localization Reveals a Prominent Role in Organizing Cellular Architecture and Function. *Cell* **131**, 174–187 (2007).

Lehmann, R. & Nüsslein-Volhard, C. Abdominal segmentation, pole cell formation, and embryonic polarity require the localized activity of oskar, a maternal gene in drosophila. *Cell* **47**, 141–152 (1986).

Lesnik, C., Golani-Armon, A. & Arava, Y. Localized translation near the mitochondrial outer membrane: An update. *RNA Biol.* **12**, 801–809 (2015).

Leung, K. M. *et al.* Asymmetrical β-actin mRNA translation in growth cones mediates attractive turning to netrin-1. *Nat. Neurosci.* **9**, 1247–1256 (2006).

Li, P., Yang, X., Wasser, M., Cai, Y. & Chiat, W. Inscuteable and staufen mediate asymmetric localization and segregation of prospero RNA during drosophila neuroblast cell divisions. *Cell* **90**, 437–447 (1997).

Li, X. *et al.* Bicaudal-D binds clathrin heavy chain to promote its transport and augments synaptic vesicle recycling. *EMBO J.* **29**, 992–1006 (2010).

Li, Z., Wang, L., Hays, T. S. & Cai, Y. Dynein-mediated apical localization of crumbs transcripts is required for Crumbs activity in epithelial polarity. *J. Cell Biol.* **180**, 31–38 (2008).

Liao, G., Simone, B. & Liu, G. Mis-localization of Arp2 mRNA impairs persistence of directional cell migration. *Exp. Cell Res.* **317**, 812–822 (2011).

Liao, Y. C. *et al.* RNA Granules Hitchhike on Lysosomes for Long-Distance Transport, Using Annexin A11 as a Molecular Tether. *Cell* **179**, 147–164 (2019).

Liao, Y., Smyth, G. K. & Shi, W. FeatureCounts: An efficient general purpose program for assigning sequence reads to genomic features. *Bioinformatics* **30**, 923–930 (2014).

Liberzon, A. *et al.* The Molecular Signatures Database Hallmark Gene Set Collection. *Cell Syst.* **1**, 417–425 (2015).

Lie, Y. S. & Macdonald, P. M. Apontic binds the translational repressor Bruno and is implicated in regulation of oskar mRNA translation. *Development* **126**, 1129–1138 (1999).

Lin, A. C. & Holt, C. E. Function and regulation of local axonal translation Andrew. *Curr. Opin. Neurobiol.* **18**, 60–68 (2008).

Link, W. *et al.* Somatodendritic expression of an immediate early gene is regulated by synaptic activity. *Proc. Natl. Acad. Sci. U. S. A.* **92**, 5734–5738 (1995).

Liu, Y. *et al.* Bicaudal-D uses a parallel, homodimericcoiled coil with heterotypic registry tocoordinate recruitment of cargos to dynein. *Genes Dev.* **27**, 1233–1246 (2013).

Liu, Z., Xie, T. & Steward, R. Lis1, the Drosophila homolog of a human lissencephaly disease gene, is required for germline cell division and oocyte differentiation. *Development* **126**, 4477–4488 (1999).

Loiseau, P., Davies, T., Williams, L. S., Mishima, M. & Palacios, I. M. Drosophila PAT1 is required for Kinesin-1 to transport cargo and to maximize its motility. *Development* **137**, 2763–2772 (2010).

Love, M. I., Huber, W. & Anders, S. Moderated estimation of fold change and dispersion for RNA-seq data with DESeq2. *Genome Biol.* **15**, 1–21 (2014).

Lu, W., Winding, M., Lakonishok, M., Wildonger, J. & Gelfand, V. I. Microtubule-microtubule sliding by kinesin-1 is essential for normal cytoplasmic streaming in Drosophila oocytes. *Proc. Natl. Acad. Sci. U. S. A.* **113**, E4995–E5004 (2016).

Macdonald, P. M., Kerr, K., Smith, J. L. & Leask, A. RNA regulatory element BLE1 directs the early steps of bicoid mRNA localization. *Development* **118**, 1233–1243 (1993).

Macdonald, P. M. & Kerr, K. Redundant RNA recognition events in bicoid mRNA localization. *RNA* **3**, 1413–1420 (1997).

Macdonald, P. M. & Struhl, G. Cis- acting sequences responsible for anterior localization of bicoid mRNA in Drosophila embryos. *Nature* **336**, 595–598 (1988).

MacDougall, N., Clark, A., MacDougall, E. & Davis, I. Drosophila gurken (TGFα) mRNA localizes as particles that move within the oocyte in two dynein-dependent steps. *Dev. Cell* **4**, 307–319 (2003).

Mach, J. M. & Lehmann, R. An Egalitarian-BicaudalD Complex Is Essential for Oocyte Specification and Axis Determination in Drosophila. *Genes Dev.* **11**, 423–435 (1997).

Mahowald, A. P., Caulton, J. H., Edwards, M. K. & Floyd, A. D. Loss of centrioles and polyploidization in follicle cells of Drosophila melanogaster. *Exp. Cell Res.* **118**, 404–410 (1979).

Markussen, F. H., Michon, A. M., Breitwieser, W. & Ephrussi, A. Translational control of oskar generates short OSK, the isoform that induces pole plasm assembly. *Development* **121**, 3723–3732 (1995).

Martin, K. C. & Ephrussi, A. mRNA Localization: Gene Expression in the Spatial Dimension. *Cell* **136**, 719–730 (2009).

Martin, M. *et al.* Cytoplasmic Dynein, the Dynactin Complex, and Kinesin Are Interdependent and Essential for Fast Axonal Transport. *Mol. Biol. Cell* **10**, 3717–3728 (1999).

Matanis, T. *et al.* Bicaudal-D regulates COPI-independent Golgi-ER transport by recruiting the dynein-dynactin motor complex. *Nat. Cell Biol.* **4**, 986–992 (2002).

Mayr, C. Evolution and Biological Roles of Alternative 3'UTRs. *Trends Cell Biol.* **26**, 227–237 (2016).

Mazumdar, A. & Mazumdar, M. How one becomes many: Blastoderm cellularization in Drosophila melanogaster. *BioEssays* **24**, 1012–1022 (2002).

McClintock, M. A. *et al.* RNA-directed activation of cytoplasmic dynein-1 in reconstituted transport RNPs. *Elife* **7**, e36312 (2018).

McGrail, M. & Hays, T. S. The microtubule motor cytoplasmic dynein is required for spindle orientation during germline cell divisions and oocyte differentiation in Drosophila. *Development* **124**, 2409–2419 (1997).

Medioni, C., Mowry, K. & Besse, F. Principles and roles of mRNA localization in animal development. *Development* **139**, 3263–3276 (2012).

Medioni, C., Ramialison, M., Ephrussi, A. & Besse, F. Imp promotes axonal remodeling by regulating profilin mRNA during brain development. *Curr. Biol.* **24**, 793–800 (2014).

Meignin, C. & Davis, I. Transmitting the message: intracellular mRNA localization. *Curr. Opin. Cell Biol.* **22**, 112–119 (2010).

Micklem, D. R., Adams, J., Gruenert, S. & St. Johnston, D. Distinct roles of two conserved Staufen domains in oskar mRNA localization and translation. *EMBO J.* **19**, 1366–1377 (2000).

Miki, H., Okada, Y. & Hirokawa, N. Analysis of the kinesin superfamily: Insights into structure and function. *Trends Cell Biol.* **15**, 467–476 (2005).

Mili, S., Moissoglu, K. & Macara, I. G. Genome-wide screen reveals APC-associated RNAs enriched in cell protrusions. *Nature* **453**, 115–119 (2008).

Miller, S. *et al.* Disruption of dendritic translation of CaMKIIα impairs stabilization of synaptic plasticity and memory consolidation. *Neuron* **36**, 507–519 (2002).

Mingle, L. A. *et al.* Localization of all seven messenger RNAs for the actin-polymerization nucleator Arp2/3 complex in the protrusions of fibroblasts. *J. Cell Sci.* **118**, 2425–2433 (2005).

Mohr, S. E., Dillon, S. T. & Boswell, R. E. The RNA-binding protein Tsunagi interacts with Mago Nashi to establish polarity and localize oskar mRNA during Drosophila oogenesis. *Genes Dev.* **15**, 2886–2899 (2001).

Moor, A. E. *et al.* Global mRNA polarization regulates translation efficiency in the intestinal epithelium. *Science.* **357**, 1299–1303 (2017).

Moore, M. J. From birth to death: The complex lives of eukaryotic mRNAs. *Science.* **309**, 1514–1518 (2005).

Morin, X., Daneman, R., Zavortink, M. & Chia, W. A protein trap strategy to detect GFP-tagged proteins expressed from their endogenous loci in Drosophila. *Proc. Natl. Acad. Sci.* **98**, 15050–15055 (2001).

Mowry, K. L. & Melton, D. A. Vegetal messenger RNA localization directed by a 340-nt RNA sequence element in Xenopus oocytes. *Science.* **255**, 991–994 (1992).

Nagaoka, K., Udagawa, T. & Richter, J. D. CPEB-mediated ZO-1 mRNA localization is required for epithelial tight-junction assembly and cell polarity. *Nat. Commun.* **3**, (2012).

Nakamura, A., Sato, K. & Hanyu-Nakamura, K. Drosophila Cup is an eIF4E binding protein that associates with Bruno and regulates oskar mRNA Translation in Oogenesis. *Dev. Cell* **6**, 69–78 (2004).

Navarro, C., Puthalakath, H., Adams, J. M., Strasser, A. & Lehmann, R. Egalitarian binds dynein light chain to establish oocyte polarity and maintain oocyte fate. *Nat. Cell Biol.* **6**, 427–435 (2004).

Neisch, A. L., Avery, A. W., Li, M. G. & Hays, T. S. *Drosophila cytoplasmic dynein: Mutations, tools, and developmental functions*. *Dyneins: The Biology of Dynein Motors: Second Edition* (Elsevier Inc., 2017). doi:10.1016/B978-0-12-809471-6.00021-8

Nelson, M. R., Leidal, A. M. & Smibert, C. A. Drosophila Cup is an eIF4E-binding protein that functions in Smaug-mediated translational repression. *EMBO J.* **23**, 150–159 (2004).

Neuman-Silberberg, F. S. & Schüpbach, T. The Drosophila Dorsoventral Patterning Gene gurken Produces a Dorsally Localized RNA and Encodes a TGFalpha-Iike Protein. *Cell* **75**, 165–174 (1993).

Newmark, P. A. & Boswell, R. E. The mago nashi locus encodes an essential product required for germ plasm assembly in Drosophila. *Development* **120**, 1303–1313 (1994).

Nichterwitz, S. *et al.* Laser capture microscopy coupled with Smart-seq2 for precise spatial transcriptomic profiling. *Nat. Commun.* **7**, 12139 (2016).

Palacios, I. M., Gatfield, D., St. Johnston, D. & Izaurralde, E. An eIF4AIII-containing complex required for mRNA localization and nonsense-mediated mRNA decay. *Nature* **427**, 753–757 (2004).

Palacios, I. M. & St Johnston, D. Kinesin light chain-independent function of the Kinesin heavy chain in cytoplasmic streaming and posterior localisation in the Drosophila oocyte. *Development* **129**, 5473–5485 (2002).

Patel, V. L. *et al.* Spatial arrangement of an RNA zipcode identifies mRNAs under post-transcriptional control. *Genes Dev.* **26**, 43–53 (2012).

Picard. http://broadinstitute.github.io/picard/

Picelli, S. *et al.* Full-length RNA-seq from single cells using Smart-seq2. *Nat. Protoc.* **9**, 171–181 (2014).

Pickering, B. M. & Willis, A. E. The implications of structured 5′ untranslated regions on translation and disease. *Semin. Cell Dev. Biol.* **16**, 39–47 (2005).

Pignoni, F. & Zipursky, S. L. Induction of Drosophila eye development by decapentaplegic. *Development* **124**, 271–278 (1997).

RStudio Team. RStudio: Integrated Development for R. RStudio, Inc., Boston, MA (2015) http://www.rstudio.com/

Radford, H. E., Meijer, H. A. & de Moor, C. H. Translational control by cytoplasmic polyadenylation in Xenopus oocytes. *Biochim. Biophys. Acta - Gene Regul. Mech.* **1779**, 217–229 (2008).

Ran, B., Bopp, R. & Suter, B. Null alleles reveal novel requirements for Bic-D during Drosophila oogenesis and zygotic development. *Development* **120**, 1233–1242 (1994).

Rongo, C., Gavis, E. R. & Lehmann, R. Localization of oskar RNA regulates oskar translation and requires Oskar protein. *Development* **121**, 2737–2746 (1995).

Rook, M. S., Lu, M. & Kosik, K. S. CaMKIIα 3' untranslated region-directed mRNA translocation in living neurons: Visualization by GFP linkage. *J. Neurosci.* **20**, 6385–6393 (2000).

Roth, S. & Lynch, J. A. Symmetry breaking during Drosophila oogenesis. *Cold Spring Harb. Perspect. Biol.* **1**, (2009).

Roth, S., Shira Neuman-Silberberg, F., Barcelo, G. & Schüpbach, T. cornichon and the EGF receptor signaling process are necessary for both anterior-posterior and dorsal-ventral pattern formation in Drosophila. *Cell* **81**, 967–978 (1995).

Sallés, F. J., Lieberfarb, M. E., Wreden, C., Gergen, J. P. & Strickland, S. Coordinate initiation of Drosophila development by regulated polyadenylation of maternal messenger RNAs. *Science.* **266**, 1996–1999 (1994).

Saxton, W. M. Microtubules, motors, and mRNA localization mechanisms: Watching fluorescent messages move. *Cell* **107**, 707–710 (2001).

Schindelin, J. *et al.* Fiji: An open-source platform for biological-image analysis. *Nat. Methods* **9**, 676–682 (2012).

Schisa, J. A. *New Insights into the Regulation of RNP Granule Assembly in Oocytes*. *International Review of Cell and Molecular Biology* **295**, (Elsevier Inc., 2012).

Schnorrer, F., Bohmann, K. & Nusslein-Volhard, C. The molecular motor dynein is involved in targeting swallow and bicoid RNA to the anterior pole of Drosophila oocytes. *Nat. Cell Biol.* **2**, 185–190 (2000).

Schotman, H., Karhinen, L. & Rabouille, C. dGRASP-Mediated Noncanonical Integrin Secretion Is Required for Drosophila Epithelial Remodeling. *Dev. Cell* **14**, 171–182 (2008).

Schüpbach, T. & Wieschaus, E. Female sterile mutations on the second chromosome of Drosophila melanogaster. II. Mutations blocking oogenesis or altering egg morphology. *Genetics* **129**, 1119–1136 (1991).

Semotok, J. L. *et al.* Smaug Recruits the CCR4/POP2/NOT Deadenylase Complex to Trigger Maternal Transcript Localization in the Early Drosophila Embryo. *Curr. Biol.* **15**, 284–294 (2005).

Semotok, J. L. *et al.* Drosophila Maternal Hsp83 mRNA Destabilization Is Directed by Multiple SMAUG Recognition Elements in the Open Reading Frame. *Mol. Cell. Biol.* **28**, 6757–6772 (2008).

Sepulveda, G. *et al.* Co-translational protein targeting facilitates centrosomal recruitment of PCNT during centrosome maturation in vertebrates. *Elife* **7**, 1–28 (2018).

Serano, J. & Rubin, G. M. The Drosophila synaptotagmin-like protein bitesize is required for growth and has mRNA localization sequences within its open reading frame. *Proc. Natl. Acad. Sci. U. S. A.* **100**, 13368–13373 (2003).

Serano, T. L. & Cohen, R. S. A small predicted stem-leap structure mediates oocyte localization of Drosophila K10 mRNA. *Development* **121**, 3809–3818 (1995).

Shepard, K. A. *et al.* Widespread cytoplasmic mRNA transport in yeast: Identification of 22 bud-localized transcripts using DNA microarray analysis. *Proc. Natl. Acad. Sci.* **100**, 11429–11434 (2003).

Shimada, Y., Burn, K. M., Niwa, R. & Cooley, L. Reversible response of protein localization and microtubule organization to nutrient stress during Drosophila early oogenesis. *Dev. Biol.* **355**, 250–262 (2011).

Simmonds, A. J., DosSantos, G., Livne-Bar, I. & Krause, H. M. Apical localization of wingless transcripts is required for wingless signaling. *Cell* **105**, 197–207 (2001).

Sladewski, T. E. *et al.* Recruitment of two dyneins to an mRNA-dependent bicaudal D transport complex. *Elife* **7**, e36306 (2018).

Smibert, C. A., Lie, Y. S., Shillinglaw, W., Henzel, W. J. & Macdonald, P. M. Smaug, a novel and conserved protein, contributes to repression of nanos mRNA translation in vitro. *RNA* **5**, 1535–1547 (1999).

Smith, W. B., Starck, S. R., Roberts, R. W. & Schuman, E. M. Dopaminergic stimulation of local protein synthesis enhances surface expression of GluR1 and synaptic transmission in hippocampal neurons. *Neuron* **45**, 765–779 (2005).

Splinter, D. *et al.* BICD2, dynactin, and LIS1 cooperate in regulating dynein recruitment to cellular structures. *Mol. Biol. Cell* **23**, 4226–4241 (2012).

St Johnston, D., Beuchle, D. & Nüsslein-Volhard, C. staufen, a gene required to localize maternal RNAs in the Drosophila egg. *Cell* **66**, 51–63 (1991).

St. Johnston, D., Driever, W., Berleth, T., Richstein, S. & Nüsslein -Volhard, C. Multiple steps in the localization of bicoid RNA to the anterior pole of the Drosophila oocyte. *Development* **107**, 13–19 (1989).

Steward, O., Wallace, C. S., Lyford, G. L. & Worley, P. F. Synaptic activation causes the mRNA for the leg Arc to localize selectively near activated postsynaptic sites on dendrites. *Neuron* **21**, 741–751 (1998).

Steward, O. & Worley, P. F. Selective targeting of newly synthesized Arc mRNA to active synapses requires NMDA receptor activation. *Neuron* **30**, 227–240 (2001).

Stuurman, N. *et al.* Interactions between coiled-coil proteins: Drosophila lamin Dm0 binds to the Bicaudal-D protein. *Eur. J. Cell Biol.* **78**, 278–287 (1999).

Sundell, C. L. & Singer, R. H. Requirement of Microfilaments in Sorting of Actin Messenger RNA. *Science.* **253**, 1275–1277 (1991).

Suter, B. & Steward, R. Requirement for phosphorylation and localization of the Bicaudal-D protein in Drosophila oocyte differentiation. *Cell* **67**, 917–926 (1991).

Swan, A., Nguyen, T. & Suter, B. Drosophila Lissencephaly-1 functions with Bic-D and dynein in oocyte determination and nuclear positioning. *Nat. Cell Biol.* **1**, 444–449 (1999).

Swan, A. & Suter, B. Role of Bicaudal-D in patterning the Drosophila egg chamber in mid-oogenesis. *Development* **122**, 3577–3586 (1996).

Tanentzapf, G., Smith, C., McGlade, J. & Tepass, U. Apical, lateral, and basal polarization cues contribute to the development of the follicular epithelium during Drosophila oogenesis. *J. Cell Biol.* **151**, 891–904 (2000).

Tekotte, H. & Davis, I. Intracellular mRNA localization: Motors move messages. *Trends Genet.* **18**, 636–642 (2002).

Tepass, U. & Knust, E. Crumbs and stardust act in a genetic pathway that controls the organization of epithelia in Drosophila melanogaster. *Developmental Biology* **159**, 311–326 (1993).

Theurkauf, W. E., Alberts, B. M., Jan, Y. N. & Jongens, T. A. A central role for microtubules in the differentiation of Drosophila oocytes. *Development* **118**, 1169–1180 (1993).

Theurkauf, W. E., Smiley, S., Wong, M. L. & Alberts, B. M. Reorganization of the cytoskeleton during Drosophila oogenesis: Implications for axis specification and intercellular transport. *Development* **115**, 923–936 (1992).

Thio, G. L., Ray, R. P., Barcelo, G. & Schüpbach, T. Localization of gurken RNA in Drosophila oogenesis requires elements in the 5' and 3' regions of the transcript. *Dev. Biol.* **221**, 435–446 (2000).

Thurmond, J. *et al.* FlyBase 2.0: The next generation. *Nucleic Acids Res.* **47**, D759–D765 (2019).

Toledano, H., D'Alterio, C., Czech, B., Levine, E. & Jones, D. L. The let-7-Imp axis regulates ageing of the Drosophila testis stem-cell niche. *Nature* **485**, 605–610 (2012).

Tongiorgi, E., Righi, M. & Cattaneo, A. Activity-dependent dendritic targeting of BDNF and TrkB mRNAs in hippocampal neurons. *J. Neurosci.* **17**, 9492–9505 (1997).

Trcek, T. & Lehmann, R. Germ granules in Drosophila. *Traffic* **20**, 650–660 (2019).

Trovisco, V. *et al.* bicoid mRNA localises to the Drosophila oocyte anterior by random Dynein-mediated transport and anchoring. *Elife* **5**, :e17537 (2016).

Van De Bor, V., Hartswood, E., Jones, C., Finnegan, D. & Davis, I. gurken and the I factor retrotransposon RNAs share common localization signals and machinery. *Dev. Cell* **9**, 51–62 (2005).

Van De Bor, V., Zimniak, G., Cérézo, D., Schaub, S. & Noselli, S. Asymmetric localisation of cytokine mRNA is essential for JAK/STAT activation during cell invasiveness. *Development* **138**, 1383–1393 (2011).

Van Eeden, F. J. M., Palacios, I. M., Petronczki, M., Weston, M. J. D. & St. Johnston, D. S. Barentsz is essential for the posterior localization of oskar mRNA and colocalizes with it to the posterior pole. *J. Cell Biol.* **154**, 511–523 (2001).

Vanzo, N. F. & Ephrussi, A. Oskar anchoring restricts pole plasm formation to the posterior of the Drosophila oocyte. *Development* **129**, 3705–3714 (2002).

Vazquez-Pianzola, P. *et al.* The mRNA transportome of the BicD/Egl transport machinery. *RNA Biol.* **14**, 73–89 (2017).

Veeranan-Karmegam, R., Boggupalli, D. P., Liu, G. & Gonsalvez, G. B. A new isoform of Drosophila non-muscle Tropomyosin 1 interacts with Kinesin-1 and functions in oskar mRNA localization. *J. Cell Sci.* **129**, 4252–4264 (2016).

Vendra, G., Hamilton, R. & Davis, I. Dynactin suppresses the retrograde movement of apically localized. *RNA* **13**, 1860–1867 (2007).

Wagner, E. & Lykke-Andersen, J. mRNA surveillance: The perfect persist. *J. Cell Sci.* **115**, 3033–3038 (2002).

Walker, R. A., Salmon, E. D. & Endow, S. A. The Drosophila claret segregation protein is a minus-end directed motor molecule. *Nature* **347**, 780–782 (1990).

Wang, C., Dickinson, L. K. & Lehmann, R. Genetics of nanos localization in Drosophila. *Dev. Dyn.* **199**, 103–115 (1994).

Wang, D. O. *et al.* Synapse- and stimulus-specific local translation during long-term neuronal plasticity. *Science.* **324**, 1536–1540 (2009).

Webster, P. J., Liang, L., Berg, C. A., Lasko, P. & Macdonald, P. M. Translational repressor bruno plays multiple roles in development and is widely conserved. *Genes Dev.* **11**, 2510–2521 (1997).

Weil, T. T., Forrest, K. M. & Gavis, E. R. Localization of bicoid mRNA in Late Oocytes Is Maintained by Continual Active Transport. *Dev. Cell* **11**, 251–262 (2006).

Welshhans, K. & Bassell, G. J. Netrin-1-induced local β-actin synthesis and growth cone guidance requires zipcode binding protein 1. *J. Neurosci.* **31**, 9800–9813 (2011).

Welte, M. A., Gross, S. P., Postner, M., Block, S. M. & Wieschaus, E. F. Developmental regulation of vesicle transport in Drosophila embryos: Forces and kinetics. *Cell* **92**, 547–557 (1998).

Wickham, H. ggplot2: Elegant Graphics for Data Analysis. Springer-Verlag New York (2016). ISBN 978-3-319-24277-4, https://ggplot2.tidyverse.org.

Wilk, R., Hu, J., Blotsky, D. & Krause, H. M. Diverse and pervasive subcellular distributions for both coding and long noncoding RNAs. *Genes Dev.* **30**, 594–609 (2016).

Wilkie, G. S. & Davis, I. Drosophila wingless and pair-rule transcripts localize apically by dynein-mediated transport of RNA particles. *Cell* **105**, 209–219 (2001).

Willis, D. E. *et al.* Extracellular stimuli specifically regulate localized levels of individual neuronal mRNAs. *J. Cell Biol.* **178**, 965–980 (2007).

Xu, X., Brechbiel, J. L. & Gavis, E. R. Dynein-dependent transport of nanos RNA in drosophila sensory neurons requires Rumpelstiltskin and the germ Plasm organizer Oskar. *J. Neurosci.* **33**, 14791–14800 (2013).

Yao, J., Sasaki, Y., Wen, Z., Bassell, G. J. & Zheng, J. Q. An essential role for β-actin mRNA localization and translation in Ca2+-dependent growth cone guidance. *Nat. Neurosci.* **9**, 1265–1273 (2006).

Yisraeli, J. K., Sokol, S. & Melton, D. A. A two-step model for the localization of maternal mRNA in Xenopus oocytes: involvement of microtubules and microfilaments in the translocation and anchoring of Vg1 mRNA. *Development* **108**, 289–298 (1990).

Yoon, Y. J. *et al.* Glutamate-induced RNA localization and translation in neurons. *Proc. Natl. Acad. Sci. U. S. A.* **113**, E6877–E6886 (2016).

Yu, G., Wang, L. G., Han, Y. & He, Q. Y. ClusterProfiler: An R package for comparing biological themes among gene clusters. *Omi. A J. Integr. Biol.* **16**, 284–287 (2012).

Zaessinger, S., Busseau, I. & Simonelig, M. Oskar allows nanos mRNA translation in Drosophila embryos by preventing its deadnylation by Smaug/CCR4. *Development* **133**, 4573–4583 (2006).

Zhang, J. *et al.* The role of maternal VegT in establishing the primary germ layers in Xenopus embryos. *Cell* **94**, 515–524 (1998).

Zhang, Y., Chen, Y., Gucek, M. & Xu, H. The mitochondrial outer membrane protein MDI promotes local protein synthesis and mt DNA replication . *EMBO J.* **35**, 1045–1057 (2016).

Zimyanin, V. L. *et al.* In Vivo Imaging of oskar mRNA Transport Reveals the Mechanism of Posterior Localization. *Cell* **134**, 843–853 (2008).

Zimyanin, V., Lowe, N. & St Johnston, D. An Oskar-Dependent Positive Feedback Loop Maintains the Polarity of the Drosophila Oocyte. *Curr. Biol.* **17**, 353–359 (2007).

# List of Figures

# Appendix A – Supplementary Figures

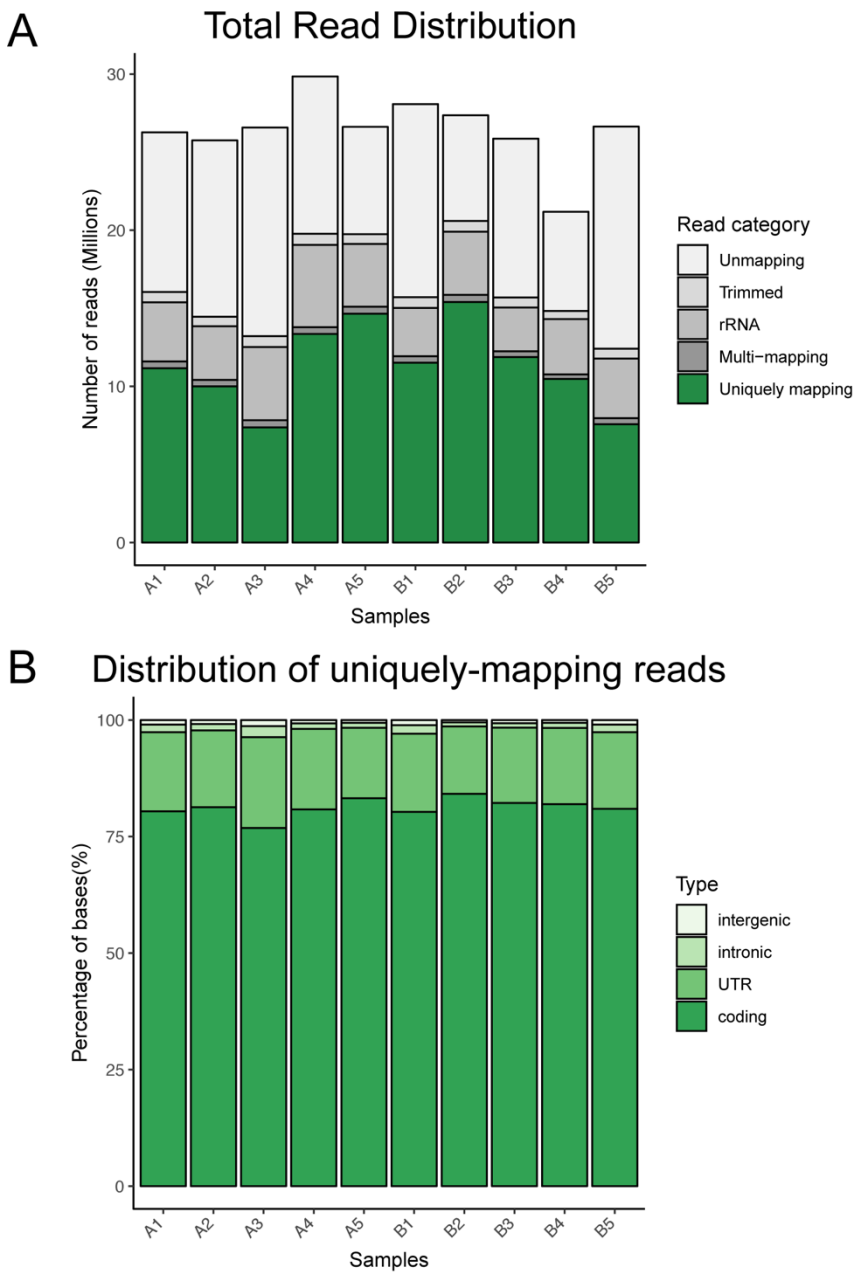


**Supplementary Figure 1 - Total read distribution (A) and distribution of uniquely-mapping reads (B) of apical (A1-A5) and basal (B1-B5) sequencing libraries.**

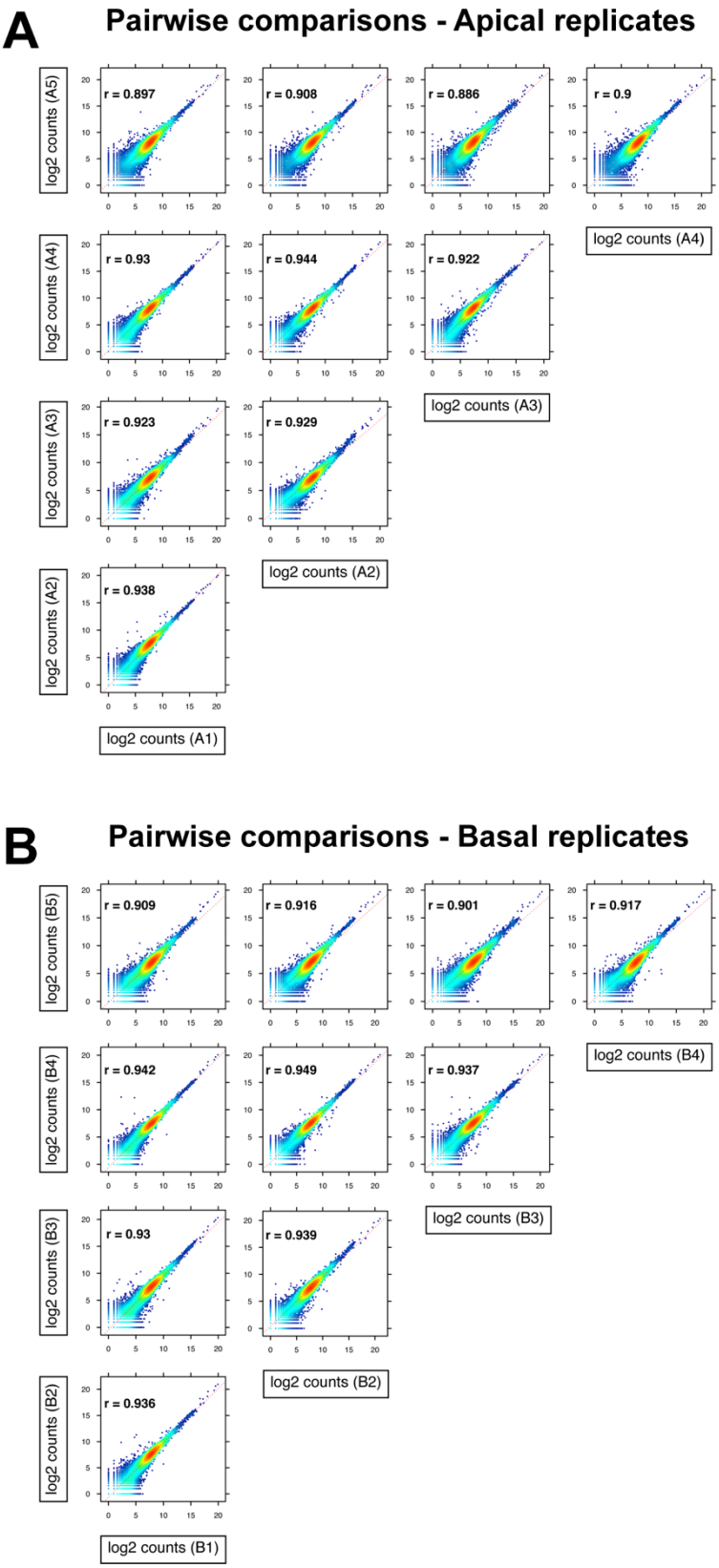


**Supplementary Figure 2 - Pairwise comparison between replicates of the apical (A1-A5) and basal (B1-B5) groups.**
r = Pearson correlation coefficient.

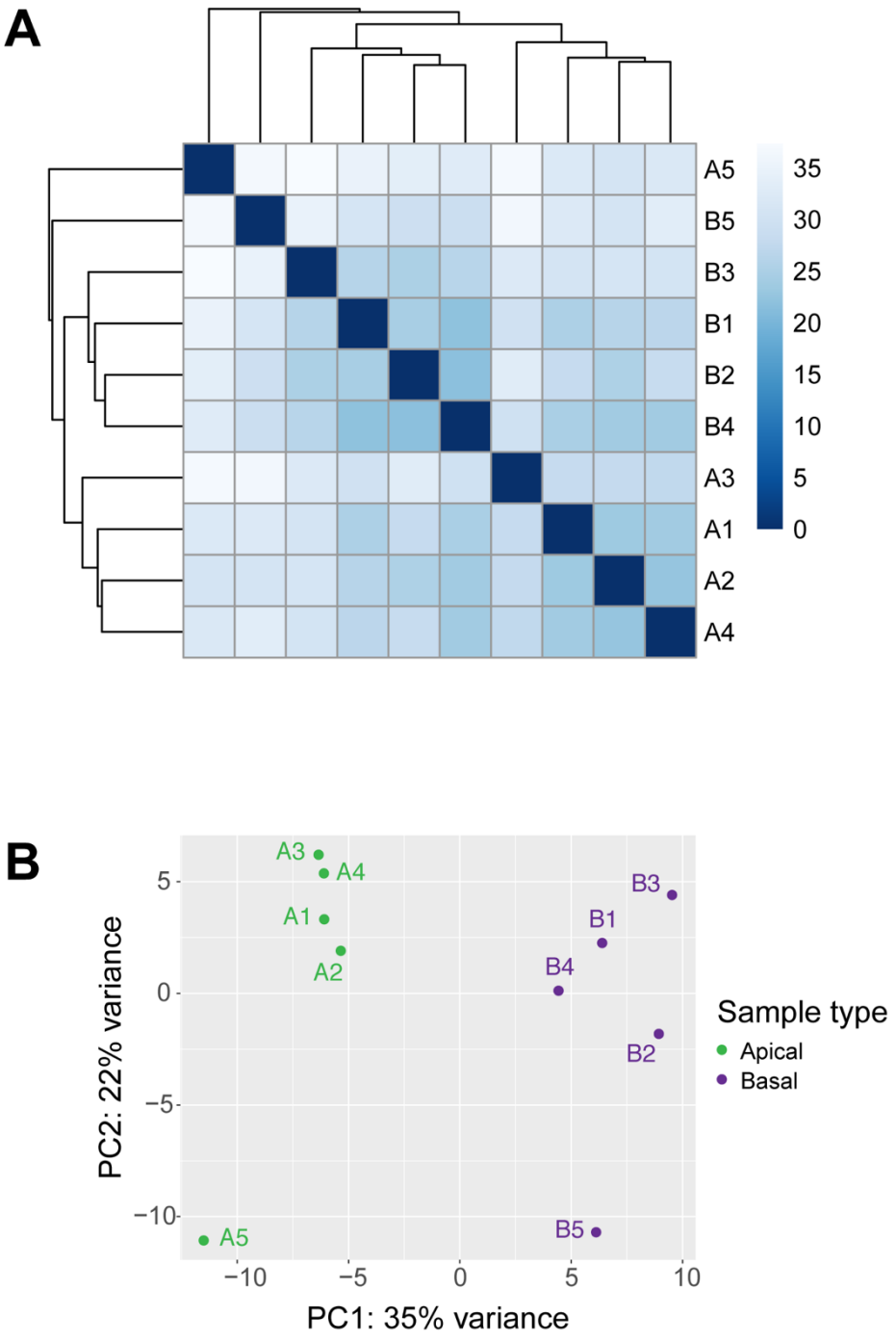


**Supplementary Figure 3 – A) Euclidean distances between apical (A1-A5) and basal (B1-B5) replicates. B) PCA plot of all 10 samples.** PC = principal component.

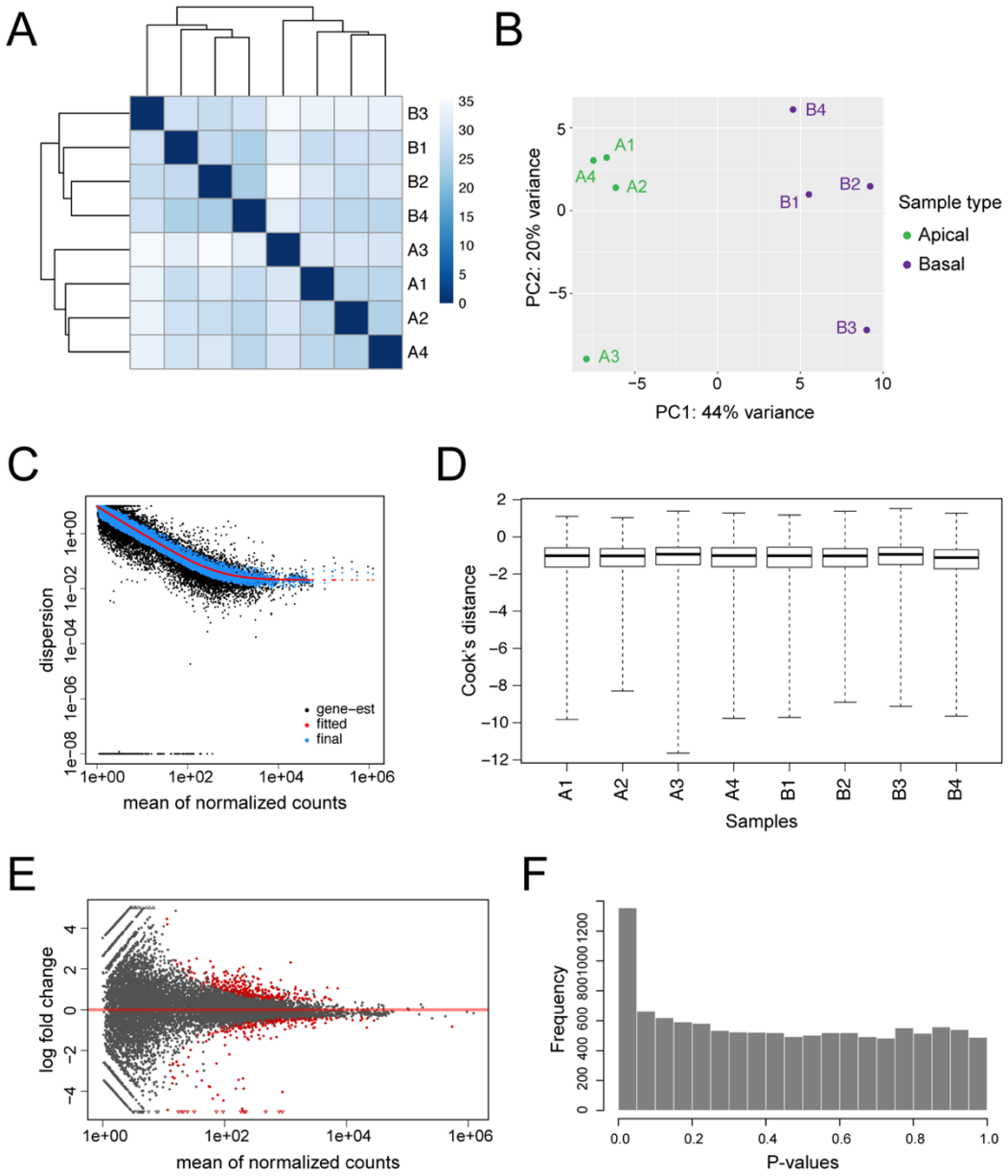


**Supplementary Figure 4 - Quality control plots of differential gene expression analysis after outlier removal in apical (A1-A4) and basal (B1-B4) samples. A) Euclidean distances; B) PCA plot (PC = principal component); C) Dispersion estimates; D) Cook's distances; E) MA plot; F) Frequency of p-values.**

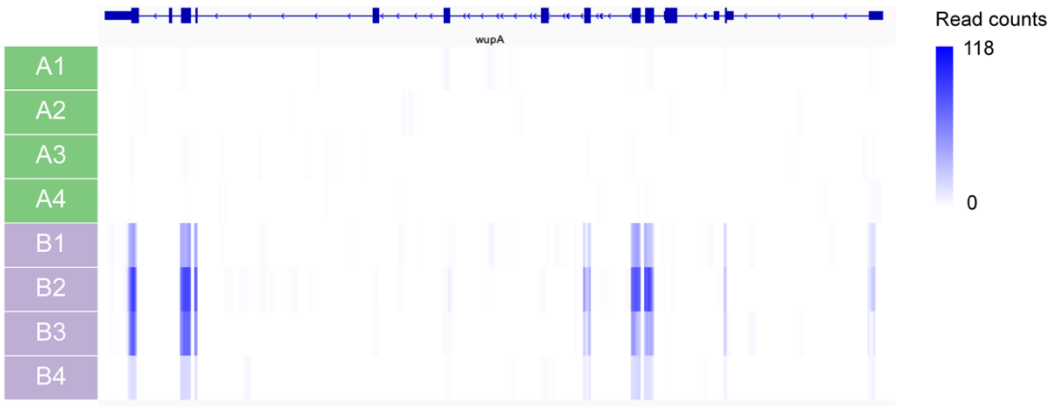


**Supplementary Figure 5 – Transcript read distribution along a representative contaminant mRNA (*wupA*) from the circular muscles surrounding the egg chamber.** The apical samples are almost devoid of reads aligning to the gene.

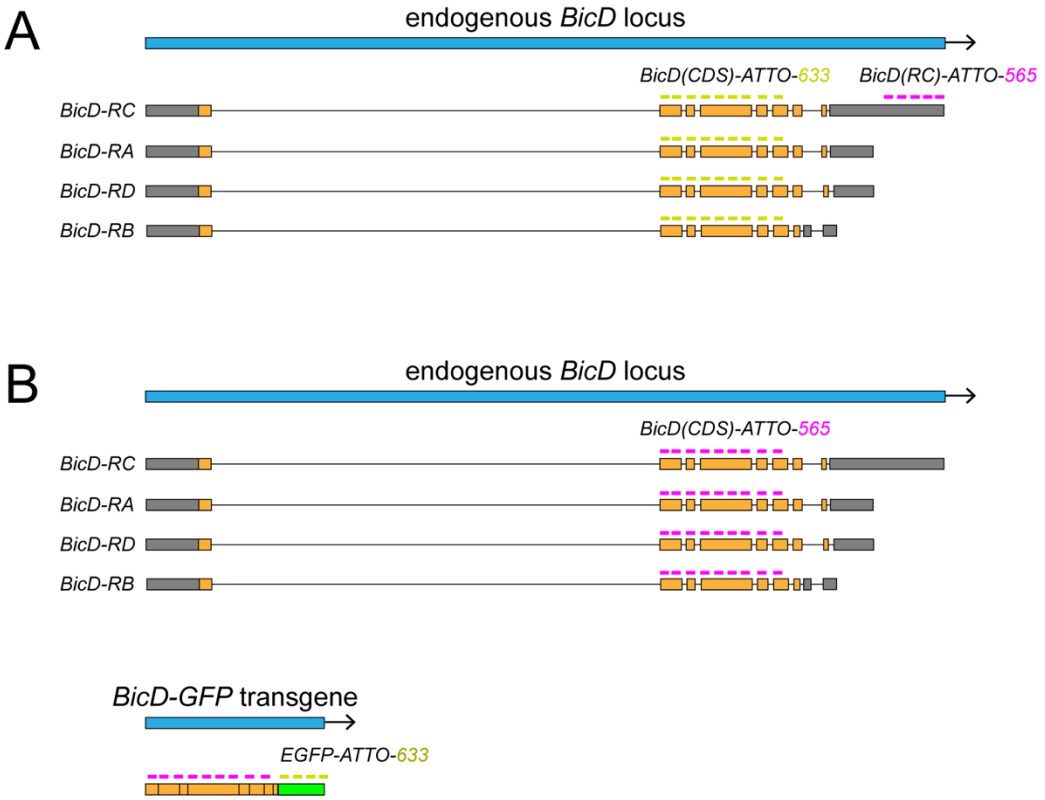


**Supplementary Figure 6 – Probe design strategies for double smFISH experiments.** A) Oligos recognizing *BicD(RC)* isoform were designed on the portion of *BicD(RC)* 3'UTR that does not overlap with other isoforms and labelled with ATTO-565. To recognize all *BicD* RNA isoforms, oligos were designed in *BicD* CDS and labelled with ATTO-633. B) Oligos recognizing the transgenic *BicD-3xEGFP* RNA were designed on the *EGFP* sequence and labelled with ATTO-633. *BicD(CDS)* oligos were labelled with ATTO-565 and anneal to *BicD* CDS both in the endogenous and the transgenic RNA. Grey boxes: UTRs; orange boxes: CDS; green box: EGFP tag.

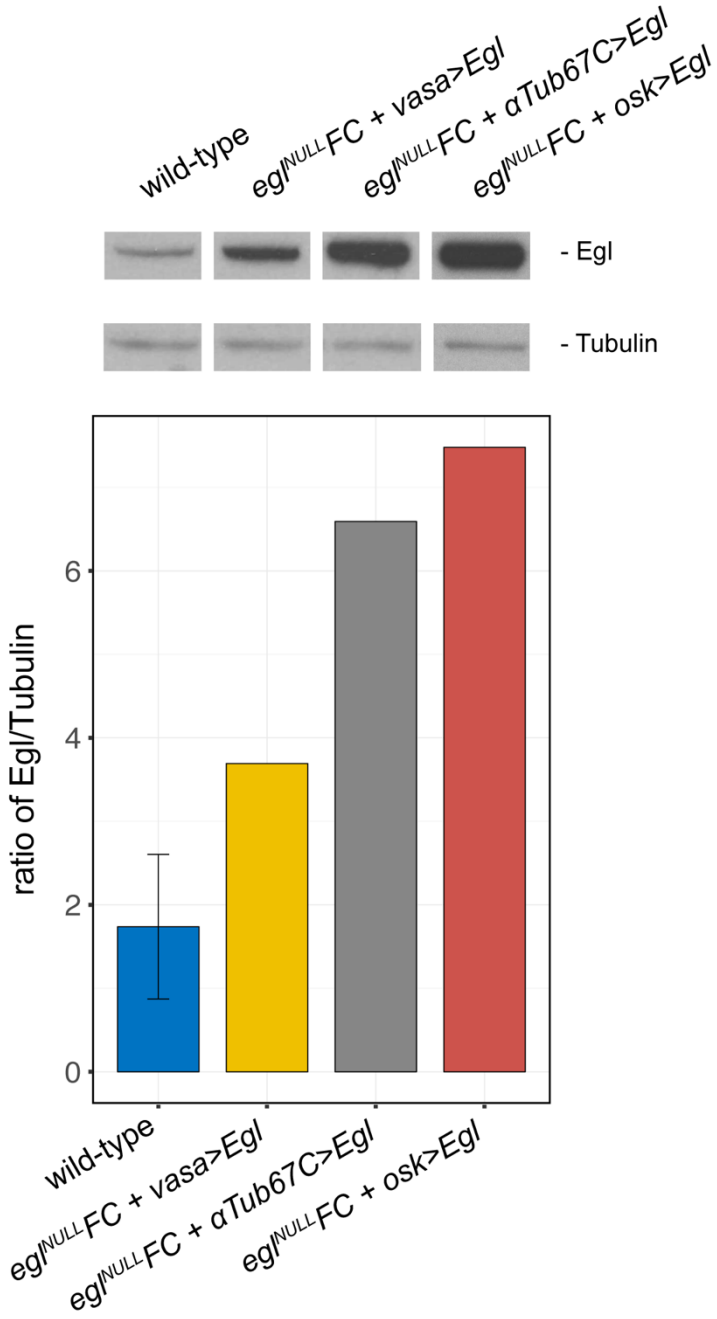


**Supplementary Figure 7 - Western blot quantification of Egl protein expressed under the control of different Gal4 drivers.** For full genotypes see Material and Methods.

# Appendix B - Supplementary Tables

**Supplementary Table 1 - Amount of sequencing reads distributing to each class.**

| Sample | Multi-mapping | | rRNA | | Trimmed | | Uniquely mapping | | Unmapping | | Total |
|---|---|---|---|---|---|---|---|---|---|---|---|
| A1 | 429185 | 1.63% | 3791232 | 14.43% | 658710 | 2.51% | 11163587 | 42.49% | 10229656 | 38.94% | 26272370 |
| A2 | 418912 | 1.63% | 3431877 | 13.33% | 607881 | 2.36% | 10001139 | 38.83% | 11293715 | 43.85% | 25753524 |
| A3 | 453857 | 1.71% | 4689508 | 17.64% | 698304 | 2.63% | 7378464 | 27.76% | 13358051 | 50.26% | 26578184 |
| A4 | 435796 | 1.46% | 5265209 | 17.64% | 713480 | 2.39% | 13359623 | 44.76% | 10075128 | 33.75% | 29849236 |
| A5 | 449427 | 1.69% | 4014627 | 15.08% | 631901 | 2.37% | 14654892 | 55.06% | 6867669 | 25.80% | 26618516 |
| B1 | 416769 | 1.48% | 3090792 | 11.01% | 686305 | 2.44% | 11518272 | 41.02% | 12367042 | 44.04% | 28079180 |
| B2 | 457836 | 1.67% | 4041466 | 14.77% | 684915 | 2.50% | 15406803 | 56.31% | 6769115 | 24.74% | 27360135 |
| B3 | 366575 | 1.42% | 2800887 | 10.83% | 649349 | 2.51% | 11881388 | 45.94% | 10166718 | 39.31% | 25864917 |
| B4 | 295962 | 1.40% | 3537628 | 16.70% | 518877 | 2.45% | 10476773 | 49.46% | 6354507 | 30.00% | 21183747 |
| B5 | 382670 | 1.44% | 3817049 | 14.33% | 630769 | 2.37% | 7582220 | 28.47% | 14224228 | 53.40% | 26636936 |

**Supplementary Table 2 - Composition of uniquely-mapping reads throughout genomic features.**

| Sample | Coding | Intergenic | Intronic | UTR |
|---|---|---|---|---|
| A1 | 80,42% | 0,99% | 1,63% | 16,96% |
| A2 | 81,30% | 0,86% | 1,38% | 16,47% |
| A3 | 76,86% | 1,31% | 2,35% | 19,48% |
| A4 | 80,84% | 0,71% | 1,19% | 17,26% |
| A5 | 83,23% | 0,61% | 1,06% | 15,10% |
| B1 | 80,31% | 1,09% | 1,84% | 16,76% |
| B2 | 84,16% | 0,52% | 0,85% | 14,47% |
| B3 | 82,22% | 0,67% | 0,95% | 16,16% |
| B4 | 81,94% | 0,60% | 1,10% | 16,36% |
| B5 | 80,95% | 1,00% | 1,61% | 16,44% |

# Appendix C - Supplementary Material

## *smFISH probe sets*

### *AdipoR*

| | | |
|---|---|---|
| CAAATGCTCCCCAAACGC | GGACAAAAGCGGCCGCAA | CCATCTCTACAGAATGACAGC |
| TCGCTATACATGACGCGG | CTTTCCAGGGAACCAGCG | GATGTGATTGACCCCAAATGTC |
| GAATGTAGAGGAGGCCCA | CCGTGTGCACGCGGAAAA | TGGCTGAACCAGCCCTCCA |
| AGACCACGATGGAGAGGA | ATCCTGCAGCCACTTGGG | ACACCCGACAGGCCAAAGC |
| AGCAGCGCAATTCCACAG | GGCGGCATTGTGTGCCAA | TCAACCGAGGGACGCGAGA |
| AGTGGCACACTTTCCAGC | ACTTCCGTCATCTCCGCC | ATGGCCGCGGTGTAGGAAG |
| CAGACCTTGCGCACAAAC | AGTGGACAACCGGCGTCA | ATCGGAGAGAACTCCGGCC |
| TCCTCGACCAACTCATCG | GTCGCTTGCGCAGGATCA | ATGGCTCCCGCCACTCACA |
| TGTCCAGATCATTGGGGC | TCGCCGGTAGCATGTCCT | GGTTATTGGTTCGATGGGAACAG |
| CTTGGCATCCACTTCAGCA | GTCCATGCCGAAAGTGGC | CCAGAATGCTAACAACGGATAGG |
| GGCCATTTCAGAGATGCCA | TGGGTGGTTACCTCCACC | AACACGGAGGGCGTACAGCAG |
| GCTCCGAAAACTTGTCCCA | CCCTGTTGCTCGAGGAGA | ATGCCACGCCGATGAAGGCGA |
| CAAGGCACAAAGGAACCCA | GTGGCCGAATCCATGGTC | TAAGCTGTGTGTCCTCCGGGG |
| GAACCTTCTCTACGCAAGG | CGATCCCGCGGATTCGTT | GCGAATGAGAATCCTAGGCACACAA |
| CCTTTGGCTGGTAATGACAG | CACTCGAAAGTCGCGCAG | CCGATAAAGAAGGCGCCAAAAACGA |
| GCCAAGAAGATGTGTCCAGA | AGGCCCAGGAGTCAACAC | AATTAGCCATCCCAGACTGGCGCGGC |
| GCACCTGCTCAAAGATATCC | GTGTGACTGCAAGCGCGA | AATACGCCAGCGCGCAAGGGACGAAG |
| CTGCACTTGCTTCAATTGCG | GGTTGCATTGTAAAACTGCGC | TAAAGCACGCACGGAAAGAGGGGAGCGG |

### *baz*

| | | |
|---|---|---|
| AATCATCCGGATCGAGGATG | CGTGGCAGGATATTCTTGAT | TACCAGGCACGGTATTTATG |
| GTCATCAAAGTGCGCCAATA | GTTTGTGTTTTACCAGTCAT | GAGGAGTAGGTGGCATCAAA |
| TGGTGGGATCGCGAAAGATG | AGTGAACAGAGAACGTGCGC | GTAACTTCTTATTCCGCTGA |
| CTTGTCAAGAAACAGGCGCT | ACGAATATACCCAAGTCACC | CTCAATGGAACCACCATACA |
| TTAGCTGATGACTGGGATCG | CACCGCCATGAATTACATTC | TATATCCCGAAAACTGGGCA |
| TTGCCATCGCCAAGAAATTG | GTTGATCATTCATCCGCAAG | CGATACTGGATGCAGTCTTG |
| GGCTGATTCTGAAGTTTCTC | TTACTGTGGTCCAGAATGTC | CAACGACGAGGACTTCTTCA |
| GATGAGAACCCTGCTGATAT | ATTGCTATGGCTATGACTGT | CGTTCAGGGAACTCTGGAAC |
| CTGATGGATTCATATGCCTG | CGCTACCATTTGAATTGCTG | TTGCCAAAGCGGAACATGTG |
| GTACTCGTTGATGATCAGCA | CATTCGAGCTGCTATTGTTG | GTAGGGGGCGAAATGTTTAC |
| ATCTCCAAGATGCGATCATC | AAATATATGACCGTGGCTCC | TCGTTCTGATGGATACCATT |
| GATTCGGTGAGTCCTATTAG | ATCTATTCATCTCATTGCCA | CGTAGTTGGCATAATGCTGA |
| CCCTTCTTGAGCATAATTTC | TAGGCGATCCAAAACGGGAT | |
| CGCGTGTTGTGACCGAAAAG | AGTCATTAAGTGCATCTGCG | |

### *BicD*

| | | |
|---|---|---|
| GAAGTTTACGCTGCACGC | CTGTAAGGTCTCTAGCGC | CAGCGATATGTTCTCCTCC |
| TGGATTCCTGCTCGAAGG | CTTCAGTGAGACGACGGA | CTGGGCGGAATCTTTTCGA |
| CGGTCCATTTCCATCTCC | GTCTCCCGGAACTTAAGG | CCGTTTGAATGCGAACGTG |
| TCCACCTGGGTCACATAC | CTCTTGTCCCGCCCAAAA | GTGTGTGTGTGGAATGGTA |
| CACGCAGGCTTGAGAATG | AGTTCTCCTGCAGCATCC | CTTTCGTTCGCTGGCAAAG |

| | | |
|---|---|---|
| ACCTCAGCGGTTTGCTTG | AACTCATGGCGCAGTTGC | GTCGTCGATGGAGTCGAAA |
| GCTTCACGGACAGCAAAC | TGAAACTTGGTCAGCGCC | CACTCACCGCGCTAAATTAG |
| GACTATCTGCTCCTGCAG | AGGTCTTGCACGGATTGG | CTTGGCAATGTTTGTGACGG |
| TGGTATGCTCAACAGCCG | GATGGATGGATGGTGTCC | CGGGTTGGCCAATTAATGCA |
| CGAAGCTCATGTCATCGG | TGCGGGTTTTCTCCTCTC | CAGATCAAACCAATCAGGCG |
| GTGTCTCTCCGTTGACTG | AAAACGCAGCGCAGGAAG | GTAGTTGGATACAGCTGGGA |
| TGATACAGCTGCGCCAGA | ACGACTGCTCTTCGCGTA | GAATGGATTGGCGTTACTGC |
| CGCTTAAGGCCACCAATG | TGTCCGCAATCACGTCGA | GTCTTTTTCTCCTCCTCTGC |
| CCAGCGTTTTGCGAGATG | GTTCAATGGCTGCAAGCCA | CGCTGACAATGATCTTCTCG |
| TGAACATCGCTCTGCAGG | GACAAGTACGCCATTGGTG | CCATCTCCTCTGTGTTAACC |
| TGGTGGCGTCCGTATAGT | CTCTCATTTCCGCAGGAAC | GATCACTGACTGTATCCACG |
| AGCTGCTGCTCCAGTTCA | CTCCAATTGGCGGTTGAGA | GTTCCGTAGCAAGAAGCTTG |
| TTCTTCTGGCCACCTTCC | GCATCCTCCTTAAGAAGCC | CAGTCTTAAGGCCATCGATC |
| CCTGCTCCTTCACATCGA | CGTACTGCGAGATTAACGC | CACTTTCCATGCTCTCCAAC |
| GAAGAGCCAGACGAGACA | CTGCAGCTCGTTTTGTGAC | CTCCGAGTATTCGCTAAGCA |
| TCCAGACTCGTCTGAGCT | GAGATCACATTTGGTGCCG | CTCGTTGTTGCTGTTGATGC |
| TTCGCCGTCAGATGAGTC | CAGACGCTTAAGAGCCAGA | GCCGCACTGTTTTGTTGTAC |
| TGCTGGCGTTGTCTTCCA | GTGGTACATAGACTCACGG | |
| AAGTGGCCATCCAGTTCC | GGCACCTTCAAATTCCACC | |

*Bsg25D*

| | | |
|---|---|---|
| TGAGATCGTCTCCAATTGCT | GGTTGAGCTTAATGTTCTGT | CTCATCTTCGTAGATCTGTC |
| CAGGCTTCCATAATGCTATG | CAATGCTGCTCGACGTTTGG | ATCAGCTCGGTGAACTTCTT |
| TGCGAGTGTTGGGAATGCTG | TTCTCGGTCGCAATGGACTG | CATATCGCGCTCATCAATGG |
| AATCCCAGGACGTGAAGTAG | GTTCTCCATTTGAAGAGCAG | AATTCCGAGTACTGCTGTTC |
| AATGCCTTAGTTAGCTGCTG | ATTTCGATGGTCAGTTCGTC | TGAATGGAACTCGAGCGCAG |
| AGCGCGCAACATATTCGATT | TAGTTCCACATTTAAGCTCT | TTGCAGTGAACTGATTTCCT |
| ATAGGCAAGTCTGTAGTTGC | TTTTAGCCTTGGTTTTCGAG | AATCTCTGTCGCAAATCCTC |
| CACTTCCACGGCAAGCAAAG | TGTTTCTCCTGTTTTTCTTG | TGAGGATCTCAACGCTCTCA |
| ACCTGCTTCTTGGAGTTATC | TCCTCTGTTAGATGTGTTTT | AGAGGTAGCTGATGGGTGAG |
| TTATTTCACGCACCATGCTG | AGTTTAGAGCCAACCAATCT | TGGAATCGGCAAGCGATTTC |
| TGATCGCGGTCATTAGTCAT | TGGCTTTGACTTCTTTGCAG | CGAGCAATTCGATGGCACTG |
| CTGCTCAAGCGATTTAAGCT | TGTCTAAGGCTTGTTAGCTC | CTGTCTTGTGCGATGGTGAG |
| TTCAAGTTCCGTTCTCAGAC | ATTTGCTCTAGACTGGTCTC | CTCATCTTCGTAGATCTGTC |
| AGCTCTGTGATTTGGATGTG | CTAAGTTTCGTTTGCCAGTA | ATCAGCTCGGTGAACTTCTT |

*CG3308*

| | | |
|---|---|---|
| GTGTCTGTGTGCGGACAA | CTTGCTCGATTTGACCGAAG | CAGGCTAACAGAGACACAAAC |
| TTTCGCATGCAATGGGGG | CGATCAGGTTCTCAAAGCAG | GGATAAGCGCTTCATCCTGAA |
| TGTGTGTATGTGTGGGGA | GTCCATGTTCTGGATCGGAA | GCAGAGGTTTATTTAGCCGGA |
| CGTTCAGTTCCATGTGGC | GCCGTGAAATGTGGATCTAC | CACGGCTATACTTCTTGTTGG |
| CTACAATGGCGGGCAAAC | GGCTAGAGTTGAACAACGTC | AAGCTGCTGGGTGGCACAC |
| AGTCTTCACGTGTTGCGG | TTATGCAACCTCCGCGGG | TCCTTGCACAGGTAGCCCG |
| GAAGCCCTTGTGTTTGGG | TATCGCTTCGGGAGCGAG | TGCGGGTGAATGCCAGCAG |
| CTGATGTAGAACCTCCGG | CGAATCCGGAGTCGACGT | TCCTGGGGCGTCTGTTGAC |
| AGGTACTTAAGCGCCTCC | CACCACCTTGGCACCGTT | GGCACATAGGTATGAGTCTATCG |
| CGGTGCCCATAAAACCTC | GCTCGTTGCGTTGGAAGG | GGAAGAGTTGACCAATTCGGCAA |
| AGCTTATGACGCAGGCGA | AGCATCCGTCTCCACCAG | TTGCACCTTTACGGCAGGGGG |

| | | |
|---|---|---|
| CCCGACACGAACTACAAC | TCTAGCGGCAATGTGCCG | AAGGCAGTGGCCAAAGCCACC |
| GGGCTTTTGTTCGTTTGGG | GCGAACGCCAGTATCCGA | AAATCGAGCTGAGCCGACCGC |
| GCCAAACAGTTTCAGGGCA | GCAGCTGCTTGGCGAAGA | CGTGAACCATTAGTTTCTGGACACC |
| GATCACAGGCGGAAGATTC | CCAATCGCCACACACTCC | GGCTCGTTGAATCTATAGAGTTACGGG |
| GTCCAATTCCAGCTGATCC | TGGGCGATGTGCTCCAGA | TTCTGGGCGTCCGGTTCGGAGAAG |
| CGTCATCGTCGCAACAAGAA | GGCTCTTCCACGATGGAC | ATAGATGCGCGAAAGGCGCAGCGC |
| CAAAAGACAAGCTGCAGCAC | GCTCTCTGCACCACGGAA | GGGTACTCGAGTAAATAAAGCAATTGCTCGG |
| CTAGACCCTGCAAACTTCGA | GATTCGCACCCACGTCGA | TTTTTGAGGGCGCAAGGAAACGCGACGGCGG |
| CTTTTCTTCATGAAGGCGGC | ATTGCTGGGCTGCGACTG | |
| GTACAACAATGAGCGTTCGG | CTTCGAGGCGTGAAGTGCA | |

*CG33129*

| | | |
|---|---|---|
| GCAAGTATTGGGGAGGAG | TAGCCTGCCACTGTCTGA | CGACCACAAACTTGGTGTAC |
| GTTTGCATCTGCTGCAGC | ATGCTATCCAGCAGGGAG | CGATCAACTGTAGGATGAGC |
| TTGAGCTTGGCGTATGCG | GGTTTTGTTCGCCCACAC | CAGACACCTTCTTGTCCAGA |
| TAGCTGCTGGCGGCTAAA | GCAGTCATAGGACAAGGC | GTCTGGTTCAGCGCCTGA |
| CCAAAGTATCCCTTGCCG | GCATTCTTTGCGGTGTGC | AGACGGCCAACAAGCACC |
| ATGACCGTGTACCAGGAC | GCTGTTCGAGAAGTAAGCG | TTGATGAGCGCTGCAGCC |
| AGTACAGAGCTCCGGCAA | GCTTCAGACTTTGCTGCCA | AACGCCAGCGGCAAAAGC |
| GGGCGATGATGAAGATGC | CTGGTTGATCTGCAGAGGA | CCAGACGAATTGGGCACG |
| CAAGGTCCACTTGCAGCA | GCTACGGTTCTGATAGGAG | CTTTGCCACAACGGGCCA |
| TTTTTTTCTGCCGCGGCC | CTCCAGTTGGGCAGCAAAA | TAAGCGTTGCAGGCCGCA |
| CTTCCCTGCAGTTCTTCG | GATGTTTCTCAAGGCCAGC | GCTTCCACAGGTCACAGG |
| ACAGTCGACGTAGCCAAC | GACGTGGTCCTTTTTTGGG | GTACGGCGGCACATTCAC |
| TGGGTAGACGTGGTCCAA | GTTGCTGCTGCCGAACAAA | TCTTCTTCTGCTGCGCGC |
| CCGGAAGAGCGTAAGGAA | CATCGCCACAAAAAACGCAC | AGTTCATGCGCCACACCC |
| GAAGCAACAAACGCGCAC | CGGCATCCACAAAGATTTGC | GGCAATCATCTCTGCCGC |
| GGACTGATAGCCACCTTG | CTTGGACGCTCAACAAAACC | TGGCATGCCTCACAGGAC |
| ACAGGATGCTCAGGCAGA | GAAGCAGTAGACTAGGCAAC | |

*Cortactin*

| | | |
|---|---|---|
| TCACCTGACACGGGAAAC | CCCGATGACTAACTCCTAC | GCTGCCGTCGATCGTCTT |
| GGTTCTTGCACAATCCCC | CCAAATTGTCTGAGTTCGCG | TCACGAAGTCCGGATCCG |
| ACCACCCATCGTCGATCT | CTTCAACTACTGGCTCAGGA | CTGCACTGGTGGCCTGAA |
| GGTAGTCGTACAGGGCAA | CTATTTTAACAGGCTGCGCC | CGGCACTTGCCTTCCACA |
| ATTCCGGTGTCCTCCAGA | CCTCGGAGTTTTTAGCCAGA | CGTTGCACATAATTTGGAGGG |
| CCACGGTCTCAACCTCAA | GAGACCAACAAACGGGAAAC | GGATCAAAGGATATCTCGTCG |
| GTTGTACTTGCCGTTGGC | GAGTTCTGTCCCACCACC | GATAATGGGTTCCTTTCGTGC |
| GCACGCAAATTGGAAGGC | ACTCGGAGCAACAGCCTC | GAACTTATGATCTGATGCCGC |
| TCCTCCTGAACGCCAAAC | GGCCTGGTTCTGGTACAG | CCACGGTTACTTTAAGTGCTAG |
| CTTGCGATCCTCTTGCAC | TTGAGGTTGCGGCTCAGG | ATTGCCTCCTCGGGAACGG |
| TTCCCCCAAAACCATCGC | TTGGACTTGGGCGTGGAC | TTTGGAGGCGGTGCTTCCG |
| ACCTTGCCCTGGTAGTCA | AGGCGTCGGCACATACAC | TTCCTCCCGATCCCGCTTG |
| TGATCCTTCAGCAGCTGC | CACATCTGGTGGTGGAGC | ACCTTGTGGTCCACCTGGC |
| TTCTTGTCCAGATCGGCC | CTTGGCCACTGGAGCTGT | TCCGAAGCCGGTGGCGTAA |
| TGCTCCTGCTCACTGACA | AGTAGGAGCAACCGCAGC | TCCTTCTGCGAGGCGTGCT |
| TTACCGGTTTCTGGTCGC | CATTGCCAATGCCACCGG | TCCTCGCGCAGCTTGTCCA |

| | | |
|---|---|---|
| TTTCTGGGAGGAGAAGGG | GAGTGTTCTCGGCCACAG | ATCCCACCGCGGACTTGTCCT |
| CAATGGATGGGAAATGGGC | TTGGCCTCACGGAGACGT | ATTGCGGCTCACTTCTGGGAGGCG |
| CGTAGTTGGCTGGAAAGAG | GCACCTTCGATGACTGGC | TGTTCCTCGGCCCGCTTACGTGAC |
| GATGTGGGTGATCACGTCA | TGCTTCTGCGGAGCCTCT | ATGTGATCCCAGCCCACGGCGGAT |
| GGTTTCAGAAACAGGCGAC | GACTCGTGCTTCTCCACC | ATTCGTTGGTGGCAAGGGCGAGGCAGCCT |
| GCCAAAGCCCTTGGAGTAA | TTCTGGGAGGCGTGCTTC | TTTTCGACGTGGTCCCAGCCCACGGCAGACT |
| GATCGGACTGCACTCCAAA | CCACAGCCGACTTGTCCA | |
| GTCCTTCTCAACGCCAAAC | CCGTATCCGTATCCTGCG | |

*crb*

| | | |
|---|---|---|
| GTGCCACCGTTCAAACAC | GACGTAATTTGAGCTGCGC | GGGTCCAGCCAGTGAGAT |
| ACACTGGCAGGTGTACCA | GTTGTTGTGGTCGTTGCTG | TGTACTGCTGGGCGAGGA |
| CACGGATTCTTGTCGCAC | CTGCTTGCCGCTGTTTTTG | TGGTGAGGCGGAGGTAAG |
| GCTGCAATCGCAGCTGAA | GGAAAGGGTTGCTTTTGGC | CCACTGAGGCGACATCTG |
| TGGCCCATACAGGGATCA | CATTCTCCCTTCTCTCTGC | TCGTGCGGTCTCGACTTC |
| AGTTGTCTGGCAGTCGAG | GCACTTGGCTTAGAACAGG | ACACACACACGCGCGCAA |
| CCCAGTATCAAGATGGCG | GACAGTGACCAAAGACCACA | AGCGCCGAAGACTTGGCT |
| AATATGCTTGCCGCGCGA | GTAGCCAATGTCCTGGTTAG | CACCGTCGAGTTGTTCACAAA |
| CGTACTTGAACTGCAGCG | CATGCAGGTAGAGATTTCCG | CATGATCGCTGATTTGTTGGC |
| GGCACGAGCGGAAACTAA | GTATCCATTGAGGCGACGAA | GAGATTCCACTTTGAGCCAAC |
| ATGGCGCGCTTGAGCAAA | CGCGAGCAACCAATAAAACG | CAAAACGGGGCGAAAAAAACG |
| TTCTACTGATGCCGCCAC | GCAGAAAGTCATTGAGCACTG | AATCTCGCCGCCCCAACCA |
| ACAGTGACGCATTGGCGA | TGGAAGCCGATGGGCTTG | ATCGAAGCATCTGCCGCCG |
| AACTTTCGCACGCGACAC | CGTCTGGCATGTCATGGG | ACCTGGCACCAGCGTATCC |
| TTTCTTCCCAGGCCACGA | CGGTCTATGCAGCTTCCG | TTTGGCACACGGCGAGCCA |
| CCAACACACACACACACA | ACACTCGCAGGTGAGTGC | TGCCGTGCACCGACATTCG |
| AAGAGAGGTGCGCTGTTC | GCCGCCAATCACCACACA | TCTGGACTGGACGAGCAGG |
| GTCGCTGCCCTTTTGAAC | CCATTGTTCAGGCAGGGG | CCTTCTGGCAATTTTTTCCCGAG |
| AAGATCGTGATCGCTGCAG | TCTGGCAGAGTGGGTGGA | TTCTCCAGGCAGGAACCACCG |
| GTTGGGATCACAGAAGCAC | TCTCGCAGTGCTGACCAC | ATTCGTCTGGCAGAACGCACCCG |
| CTGACTGTTGTACGTGGAG | AGGCAACCGGAGAAGGAG | TTCTGACACGGCTGTGAGGCGCAC |
| GAGTGATCCCAAATGGGCA | CAGCGGTTGTCCAGCAGT | ACACACACGCGCGCGCACACACAT |
| GCCATTAAAGTACGCCTCC | AGCTTGACATCCAGCCGG | |

*CycG*

| | | |
|---|---|---|
| GTTCTAGAACGCAGGCCA | CTGGTAGTGCTGGTATTGC | AGCACGTAGGCGGATCCA |
| TGGGGATGCCTTCCTCAA | GCTGTTGCAAGTGCAACTG | GGCAGTAACCTCACGCCT |
| CGCGATCAGGAATCCTCA | CCCGTTGTAATGGGACAGAA | CCTCGTCCGCAATCCTCA |
| TCGAAGACGTGCTTCAGC | CCTTGAGGGTTTCGTACAAC | GGCATCTCTGCATTGCGG |
| GGGTGTACGACTCCTTGA | CGAGTCCGATGTTGTTGTTG | GCTCGTCGTCGACCAGAA |
| CCAGTTCCTCCAGCTTGA | ATGGGTGAAGTGGGCCAG | TGATGCTGTGGGCGTCCA |
| TGAAAAAGTCGCCGCCGA | CCTCCTCCTCGGAGCTAA | TCCGTTCAAAAGGGCGGC |
| GCAGGTAGCTCACAGAAG | TGCTTGTAGGGCGCCTTG | GCGATATCCTGCTCCCGT |
| AACTTGTCCTGCAGGACG | AGTCCAGGTGCAGGCAGA | CAATCAACTTCGGCGGCG |
| TGCAGCTGATCCTCTAGC | GCGTGATCACCGTGGTCT | TTGTTGCTGGCTCCACCGA |
| ACCGATAGCACCACCCAA | ATCAGGATCTCCAGGCGG | AATGCCGTTGGCCAGCTTG |
| GCATAACCGACGACGACA | AAGTTGCGGAAGAGGGCG | GTTTCAAGTCCAGCTGCTTGA |
| GTCCTCTGCTGCATCAAC | CCAGCGGTACAACCACAC | AGGTCGGAGGAGAAGCGGT |

| | | |
|---|---|---|
| GCCTGCAACTGGCAATAG | AGGCCATGTGCTTCGGCT | AGCGTGCGACTGGACAGCT |
| TGCTGTTGCAGAGTGCTC | ATGCGATCCAGGAAGCGG | ACGATGCTGAAGCCGCAGG |
| AGCGTACAGGGACAGACA | ATGGCCGAGAACAGGACG | AATCACGCCGGCCATGCGT |
| CTGCTGCAGGAAGAGAATG | AGGGCAGCTCGTACCACA | |

*Dlic*

| | | |
|---|---|---|
| GCGTCATTACTGCATCCG | CAATATCGCCGACCATAGG | CCCAAACGCCTAAACGCG |
| CGCATCCTTCTCAACGAC | GTTTGCGTCCCACTGTTCA | GTTTAGCTGCTCCAGCCAG |
| TCCTCGTCGATCGAGTTG | GCAGCAGCGAGTTAAAGAAG | CTCTTTTTTCACACTGCGCGA |
| AGCTGCAGGCTATCGATG | GTTCTTGTCTTCCTTGACGC | GTAAAGGATGATGTCAGCGCA |
| CCGAGGACCTTGATCCAA | GCTGGATGAAGTCAAAGTGC | TACCCGGACTGCCCGACTT |
| TGAGTGTCGTCTTTCCGG | CACGATACTCGTACTCCTTC | TGCTGGCGTCAGCTTGGGA |
| GGAAGTTTTGTGCTGCCC | GTTCGGGGTCCGCTCTTA | TTGGGCGAACTCTGTCCGG |
| CAACACTCACTCTGCGACA | TGCGATCGCAGTGGTGAC | TGCACTTCCGCCTCGCGAT |
| CCTTTCTAGTTGGTGGCGA | GGTCGCCCTGCTTTAGGA | TCGCCCACCTCACAGTAGC |
| CGTACGGAATGGTAGACCA | GCCAGGAATGCCTGCTCA | ATACTCCAGGCCGGAACCC |
| GTAGAAGAGCGAAGTGCCA | GTGTAGGGATTCTCGGCC | ATCCTCGACGCCCTGCAGT |
| CGCAGGCAGAAGTTACGTA | TATCCCAGCCAGCCGGAA | TTTTCCGCGGCCGCATCCT |
| GATGACGAGTGTGTGTGCA | GCGTGGTCATGTAGTCCG | GCGTCAGATACTTGTAGAGGACA |
| CGTTTCGTTGAGCGCATAG | ACGATGTCGAGGCCCAGA | ATCTGTGCGCACGGCCAGCTT |
| CAGGTTTGTGTGTCCTGGA | GCCTCCTTCTCTTTGGCG | TTGACGGGGGAGCCTGGATCCAGA |
| GTCGTCTCTGTACTCATCC | GCTGCGTCATCGAAACGG | TTAGTGCATCCTCCGTCAGCGGCAGCAGG |

*egl*

| | | |
|---|---|---|
| AAGAGCAACGTCATGTTGCG | CCAATCTCAATCAGGGTGAT | TATGCGATCCATTGACTTGT |
| AGAAATATGGCCGGGTACTG | AGGACTGCACGTCGAACAAG | AATTTGTTCACATGGCAGCG |
| GCAGCATCTTGTTCTTGAAG | CGTGTATAACCTTGATCACC | CCTAATTGCTCTTGCATAGA |
| AAGTCGGTGAACTCCTTGAT | AGGATGCCGAATTGCAGATA | TGCTCGTCCTGGAAGAATAT |
| TTGAGGAATGAGCTCAGGTC | CTCCTGATACTGCAAGATGG | GCGCTTTGTTTGTTAGGAAT |
| TGACTAGATTGGCCTGTATG | TGCTTCAACTGATCCTTGAT | CAAGCCCCTCAACTGTAAAA |
| TGGCACTGTTGTTATTGTTC | CACAGCTCTGAGAAGAGAGC | CGGGGCGAGTAGTTAACAAT |
| TTTAGCTTGAAGTTTGGGCA | TTGGGTTTGATCTGCATGAG | AGGGATTCGGTAAGATTGCA |
| CACCCATCACATTCGAAACG | CTTCTGTTTGAGATCGGACA | GTCCGTAGACATTTTCTGAG |
| TAGTTGTTCTCGCACAGATT | GATTGGAGAGCACAATGCTC | TTAGTTTTGTTTGGAGCTGC |
| CGTATAACCAGGGTGTTGAT | GAGTCACTTTGATCTTTGCT | ATTGGTCCAACGCAGATTTA |
| TGGTTCGAACTCGAATTGGC | AAACTGGGAAAGGCGTCGTT | TCTTCCGATATGGCGACAAA |
| GTTGCTATTGGCGTTATTTG | GAAGCGTGGCGAAAATGTGC | |
| ACTTCAGTATGATGTCGGTC | GAGAATCTCTTCCAGCATTT | |

*Fkbp14*

| | | |
|---|---|---|
| CTTAAGCACTCGTGTCCC | GGTCTTCCACAGACGGATA | CGGCGCCCAATTGGAATG |
| GCAAACCAAGAACCCCCA | GAAGTGCAAACACGTCCGA | CGTGCTGATCACCTCCAC |
| TTGGGTCCCGAGAACTCA | GACTTCGTCTTGAGAGTGTG | GGACCAGGCTGTTGCTGA |
| TGTCGTTCTCAGCCAGCA | GCACTCCTCTAATGTGTTGG | CCAGCAGAAGGCACGAGA |
| TTCAGCTCCTCGGAATCC | GATGCAGATGCAGATGCTGA | CGAAGTGCGGGCGAGAAA |
| GGGCATTGCCGATGTTGA | CACTCGATTTATTGCTCGGC | GAGATTGGATTTCGACATGGC |
| CACATGTTGAGCAGACCC | CTCCTTGAACACATTGGTGG | CGATGGGTCTAAAAATCGTCAC |
| TCCCAACCCTTAATCACC | CCCGCAGCCGACACAAAA | TCCACGGCGGTCATCTGCT |

| | | |
|---|---|---|
| GTCGAAGCTCGAGTCGAA | CTACGTCTAGTACCGGGG | TCGCTGACCTCTTCGCGAC |
| GACATCGGGAAGCATTTGG | GAGCACTACAGCTCGTCG | TTGCCATCGGCCTGCAGAG |
| CTCGTGCTGAAAGATCTCC | CCACATCGAAGAGGAGGG | GCGAGATGAAACCGTTCTTATCC |
| CTGCTTGTCGGCATTATCG | CCTTGGGCGGTATCACGT | AACACGCGAGCAAACGGCGGA |
| GTAGTGCATGGTGAGGGAA | TGGTCACCATAGCCCAGC | |
| GGACTTTTGTTCGCACACC | GGAATGGTCAGCTTGCGC | |

*Imp*

| | | |
|---|---|---|
| GGGCTGTCCTAAAGCTTG | GGTTGTAAATTGTGGTGGG | TGCTTCTGCTGCTGCTGC |
| TTCGATTTTTGGGCGGGG | CCTCCTTACTGTTGTGAGC | CCGGCTCTCCTTTAACGG |
| CTATGAACGATAGCGCGC | GAAAGCATCATGGCTCGGA | CGCAGTTGCATTGCCAGG |
| CTTGCTGTGTGACTGCTG | GAAGATCATGTACTGCGCC | TGAGATGGCGACTGTGGC |
| TAGAGCTCTTCACGCAGC | GGTATGTAGAGATAGGTGG | GCTGGGCAGACTGTACAC |
| TTGATGTGGTGGTTCCCC | CGTATTGAAGACCATGCCG | CGCACATTTTGGCCACCC |
| CTTACTTTTGCCGTCGCC | GGTGTCGACATCATTGCCA | CCAATGATACGGCCCACC |
| TGCTGCTGCTGCTGCTTT | CATAACTTCCAGGATGCGC | GAGCTGGCCACAAGCAAC |
| TTGGTTATTGGCGGCGGA | CACGATCCTCCTTTGAGAG | CATCGTCCGTGCCACACA |
| CTCTTCATCTCCACCGGA | CGCTTCTTGTTGGCTTTGAG | CCTCCGGTGTGCCAACAA |
| AAGGGCATGTTCGGGCAA | GCCGCTCAAAAAGGTTTTCG | CACCTTGCGCTCCGTTTG |
| AGCCTTCTTCGCGCATCT | CTCCTACTGCCTTGAAAACG | TTCGGATATGCGAGCCCC |
| ATGCGTTCGAGAAGCGCA | GCTTATGTTACTGCTCCAGG | ATAATGGCGCCGACAGCG |
| AGAATGCGCAGCGGAAAG | GGGTCTTGGGGTATTGAATC | GTCATTGGGGAAGACCGG |
| CAACAGCAGCTCTTGAGG | CAACAGTAGAAAACCCTGCC | ACCACACTAGCCGGAGTC |
| AGCACCTTCCAACTGCTG | GCTATTTTTGGCGCTTTCGC | GATGGAGACCGGGGAACA |
| GTCGGCGAATTGATCCAG | CCTTGACCGTAATGATTCGC | CCATCGCCTGCAGATCGT |
| GCCTGACTGAAACCGAAG | CAGTGATCTTCGTATCGGTG | GGTTCTCAGCACGCGACA |
| CCGAGTCGAAACTTTCGC | CCTTATTCGTAGAGATGGCC | CAGGCGTTGGTGCAGTTC |
| ACCGGTGTGAAAGAAGCG | CATTCTCCTTACGATGGACG | GAGCACGGCTCTGTTGTG |
| TTCACGGGTCTTCGCAAC | GTCTTCGTTTAACTCCTGCC | CAATGATGGCGCCCACCA |
| CTTGGTTGTGCGTTGCGA | GTTTTTGGTGTCAATTGGGCC | GGCATACCCGGATACGGA |
| CTCGTCCTTTTTGTGGGC | GGTGTGCTGTGGAGGTAG | |
| CAGTTTAGGCGGTACCGAA | TGCTGCTGCTGCTGCTGA | |

*msps*

| | | |
|---|---|---|
| TGGAGATGCTGCAAGCGA | CGTACGGAATTATCCCGG | GCCATTTCGAACAGCATCC |
| GGTGACATGTCCCGCTTT | AAATCGCAGCGTCAGCCA | CTTGTTATCACCCAGAGCG |
| ATTCCGTTCAGGCAGAGG | AGATTACACACCAGCGCC | GCGAGTTTTCCAGTCCTTG |
| TCCATCGTCTGCTGAACG | TACCAGCCAGATCTTCGC | CATCTCCTTCAGCAATGCC |
| AGGCGGTCCATCCAGAAA | CGGCGATGTGTCGATATC | GTGGAGCAATATCAACGCG |
| AAGAACGAGTAGCTGCCG | CTTCGGCTCCTCAGGTAT | CCTGGATCTGGGACTTTAG |
| CCCTCCTCGATGTACTTG | AGAGCGCGGTTCATTGCA | GCTGCAATTGGAAGCCGAA |
| TCCCCTTCACCTTTGCCA | ATAATGCCCAACACCGCC | GTGTTTGGTGCGAAATTCGC |
| ACTCGTGCACCTCGAGAA | TTTTTCCGGACATCGGCG | CAATTCCTGAAGCAGAGCCA |
| GCGTCATAGTTCAGCTCG | CGATCGCAGATGTGAGCA | CTGGTTGAGATGCTGCAGAA |
| CTTCGTTCGGGTAGCATC | GCGGCACCATTGAATGGA | GAATGGATAATAGCGGCTGG |
| ACGTTGCGCCATATGCAC | CTTTAGAGCTGGGGATCC | GTTGTCGAGAAATCAGCCGA |
| CGGACAAGTCTCCCGTAA | TCAGGGCATCGGCTATCA | GCATTGAGAGGTCCTTTTCG |
| TTTTGATGCAGGCCACGC | TGGCAAGCTGCTCGCAAA | CCATCACATAGCCAAAGACC |

| | | |
|---|---|---|
| TCTCTGGAGCCTCGATGA | TGCAGCTTAGTCAGACCC | CAGATGTGGGACAAAACTGC |
| TTTACCAGCTGCGGATCG | ACCGCTGCTACGTTGAAC | GCTCGATGACTTTCAAGTGG |
| AACTTCTCCTGCGGGTAG | TCTAACAGGCTTGGGTGG | CGTTTGCGGTCATCATTTGG |
| CTACGTTCAGTAGCGGCT | GATTCCTCTCAATCTCGGC | CGAGTGCTGCAAGTATATCC |
| TCGCTGATTACCTGCGAG | GTATGTAGCTCCGAGTGTG | CAAGTGTCGTTTGGGCAATC |
| TGGGCCTGCTGTTGTAAC | GTCTGTAAACTTCGGCAGC | CATTGGAATCTACCAGACGG |
| TGCTGGAGTAGAAGCAGC | CAACTACGGATTGAGCCGA | CAGCCATATTAATGGGCTCC |
| AAGGTGCCTGGTCGAAAG | CCCGGACAAAAAGAAGACC | CGCCCACATTCTTGTCAAAC |
| TCATCTGGTGGTGGAAGC | GGGACAGATGTTCATGCCA | |
| ATGCAGTTGAGTGCTGCG | GGTTAACTCGTCAAGGCAC | |

*qtc*

| | | |
|---|---|---|
| AGTATGCTCTCGATGGCC | ACACGGGCGCCTGCAAAA | GCGAACTGAGCGATGCCT |
| TCTTGAGGAACTGCAGCG | TTCGATTGGCGGCGCTGA | AGACGCAGCAGCTCCGTA |
| TACTGCCGCACTCTCTCA | TCTGCTTCTCGGCATCGG | GCGGAGTCCTCGGAGAAA |
| TGCACTCTGATGCGCGTA | AGATGGCCCTGGGAGTTC | CTCGTGCAGCGTGGAAAG |
| ACGCTGTGCCAAATCCAG | GGATCCACATGGGTGCGA | TGGTTGGCCTTGACGCAG |
| TGCGTGGGCGTCAGATAA | CCAGCAGGCGGCGATAAA | CTGCCGAATGCAGCTGTG |
| GAGCAATGCACGACGTAC | TCTCCAACTCGTCCTGCG | CTCTGCCACAGATGCAGC |
| TCTTGCGACCACTGAAGG | TCCGCTCGAGAAATGCGC | TTTGTGGCGTCTGCGGTG |
| TTCCTGGCCACATAGGGA | CCTGTCCCTGCTGGTACA | TGGGGGACGACTCCTTGT |
| GCGAACGAGTACATCGAG | TCCTCGTGCTCGATCAGC | AGGTGCCACTGCTGCTGA |
| GTCCAGATAGGTACTGGG | CGCTGCAAATCCTCCAGC | CTTGGCGCGCGAACTGAA |
| GGCCTAAATTGCACCAGC | GCTCATAGTCGGGCACCA | TCAGCCCGTAAACCGAGC |
| ACGCGTTTCGAGACTGGA | GGGATCGCTTCAGATCGC | CGGGATGTGGAATGCGTG |
| AATTGTGTGGAGTGCGCG | CGCTGTCCTGACTCCGAA | TCGGCGGAATCGTTGTCC |
| TGGAGGCGAGCGACAAAA | TCCTCGATCCGATGCTCG | GGCTACGCTTGCGGCAAA |
| GTAACGACGAACAAGGACC | TCTGCGTCTGCGAGTCCT | CGTACTAGTATGCCTTAAGCC |
| CTGCAACTGATGCAGTAGC | AGTGCACCGACGACATGG | CTTCGTTGCCAAAGAGAGAAC |
| CGAGTACCTGGTATTGCAC | TCCTCGAAATGGCCGGAG | GAAATTAATGCCGCCAGCCAA |
| GCTTATCAGTTCCTGTCGC | GCGTAGGAGCTCTGCATC | CGCGAACCAAAATCGTAGACA |
| GCTCATTTTGGCGTGCAATC | CATCTGCATGGCCTGCAG | CGCCAAGTACCCACAAAGAAA |
| GTCCGTGAGGAAGTAGAAGA | TGCTGCTGGCGGCTTAGA | CCGTTCAACTGGAGAGACAAA |
| GCAGGTACATCTTGTTCTGC | GTGGACTGCCCTTTGCGT | CTCCACTGAAACTCCACAAAAC |
| CTCGTAGTTCTCCAGATTGC | CGTCCACCATGTCGACGA | |
| GAGCACAACGTTTAACCAAGC | GAGACATCCTGCGAGGTC | |

*rho-4*

| | | |
|---|---|---|
| ACGACATGCTTGCACCAC | GCTAGAAAGATGCGAGGAC | CTTATGTGCTACGTGGCTATG |
| ACTGTGCGTACTGCAACC | CTCATAGCGCTTGTACGGA | GGATTGGGAATGAAGCTGACA |
| TGGGGCTAGTTGTACTCC | GAATTCCTCGAAGTCCAGG | CATGTAGCTAACAAAGCGCCA |
| GTGGTCATGAGGGCAAAG | GATCAGTTCCTTCAGCTCG | CGATAATCGAGAAGAGCACCA |
| GCGTACTCCATTTCCGAG | GTGTTGATCAGCCCATCTC | GTCTGATTGAGCGGTATTTCC |
| TATCGTGGCAATGTGGGC | GCTCTGAGTTTTGTTCTCCG | CTTCGAATGAATTCGCTTTGCG |
| TGCGTATACTCCACCCGA | GAAGTGCACTTTGGACATGG | TTGATCTGCGCGAGAGCGC |
| AGATGCATGATGCCCACG | CCACATAGCCAATCTGATCG | TGCCTGCCTAGTGTCTGGG |
| CGATCCTGGTAGTTGGGA | ACATTTCGTTGCGCCGCG | ACGGCGACCCACCAGAGAA |
| TGACGTCCACGAGGAACA | GCAGCTGGCATAGGCACA | AAGTGGCGGTACACCGAGG |

| | | |
|---|---|---|
| TCAGCATGTTGCGCACCA | TAGGGCTAGGGCTAGAGC | AGATGAACAGGGTGGCCGC |
| CGTCGTTATCCTGATCGC | CATCGCCGCACCTCCAAA | ATCCTCTGGCTCCTGGCTG |
| ATGTCCCGGCAATAGCCA | ACCAGAAAGGCCAGCAGC | ATGGTGTCCTGTCGCAGCG |
| GCGTCATGTGGATCGAGAA | CACCAGTGATGCACCAGC | AAACCGGCGACGGCACCGGACAAA |
| GGCTTAAGTGGATGCGCAA | GGGCGATGCCCAGAAAGA | TTCTCGTAGGCACCGTCGGGCTCA |
| GTAGTCGGGAACAAACACG | TCCACTTGTGCTCTCGCC | CAGAGTCGTGCTTGTCAAATATCTCGTGCA |
| ACGACATGCTTGCACCAC | GGCGGGCAGATGGACATT | AACAAGGAATCGATACGGCGGACCACCGCGG |
| ACTGTGCGTACTGCAACC | GGCACAACGTAGCGACAG | |
| TGGGGCTAGTTGTACTCC | ACTTGTGGCGCAGGGACA | |

*Rtnl1*

| | | |
|---|---|---|
| TTCTCTTGCTAGTGCGGG | GTGAGTGTCGATCGATTGC | CGCTGATCACCGAGAAGC |
| GCGAGACAAAGGCCAAGA | CGGAAATTGCGTGGAACTCA | AGATGGCCGCCAGTGTGA |
| CACAGAATGACGCCGAAC | CTTCTTGTTGCCAATGGGGA | GCCGAAGACAATGCCGGA |
| GCTCGGAGATGAAGCCAT | CTCAACAAGAAACAGACGCC | GATTCCACTGGTCCGCGT |
| TCCAGCTCCAGGTAATCC | GAAGCGGCTGAAAATTGCCA | GCTGCCGCCTGCCATTTT |
| AGATTCTGAAGGCGACGG | CAGTTAGCTTGGCGCCAAAA | ATGCAAAGCGGGCTGGAC |
| AGGGTTAGGAGCGACAAG | CCACTCGGATCTTGTCGG | GAAACTGCTACGAGTTGTTGG |
| TCACATCGCGCCAGTAGA | CGTAGACCTTGGGCAAGG | GCGTGTCTAGGCTTAATTACAGCGA |
| GTTGTTGCGTGAGTAGCG | TTGAACCAGGCACCCACG | TATGTGCCACAGCCACGCCGGCAA |
| ACGCACACACACAACCAC | CCTTTTCGTGCGACAGCG | AATGGGACGATTCGGCCGACCGTC |
| CGAGCGCAGCAAAAGAAC | AGGGGTGACCCTCGTTTG | ACTTGTCCTTCTCAGACTCGGCAGCGGCC |
| CAATTTGCTGCGCACCAGA | CACGGCCTGTGTCACAGA | |

*Sara*

| | | |
|---|---|---|
| TGGTCATCAATGGGCGAC | AATCCATTAGCCTGCCGC | ACAGCCTGATCTTGGTGC |
| TCTCACTCTGATCGTCGG | CAGACAGAGCACAAGACC | TGTTCCTTTGGCTCCACC |
| CAATGGGTCCACAGACGA | ACCTTGCCCAGATTGGCA | CGAGAAGGTGGAACAGGA |
| TTTTGGTTGCGCAACGCC | GGACTTTCCTCGTCATCC | CAGCTCCAACTCCACTGA |
| CCTCCATTTTGGCAGGCA | CTTTCTGCCTGGCAACCA | CCCCACATTGATGTCACGA |
| ACTTACCCGACAAGCCAC | TCTTGGGTTTCCAGGGCA | CTGTACCATTAGGCCATCC |
| GTTGCCAGCAAAAGCCAG | TTCCTGCCCGAAAGGGAA | CTCCAGTGATTTTCCTGGG |
| ATTACATCCTGCTGGCGG | GAGGTTGTCTCCTGCTCA | GGAGTACATCTCGGATCGA |
| TAATCACCGTCGTCTGCC | GATAGAATCCGCACCGAC | GTTTGGCGGTAGTTTGCGA |
| ACCGCAAAGGTAGCACCT | TCGTCGGGCATTTGCTGA | CTTTCGCTTTCTTTGGCCC |
| ATGAGCACGCCAACCAGA | GCCTGGTTGTCATCTGCA | CTGCACACAAACCCTAGAC |
| TCCCGGGAACCCAGAAAA | TTGCAGCATGCTGTCCAG | GTTCGGTGGCGAATTCCAA |
| GGACTGGTGAAAGCCAAC | TGTCCGAGATCTCGTCCA | CGGGTATAACACCTACTCC |
| TGATCCATCGTTGCGCAC | TCCGTTTGTACTGGCTGC | GATTCCGTGCTGCTGAAAC |
| AGATAGCAGCCTTGGGCA | CTCTTTAGGGACCGGTAC | GTCCACGTTCATCTGATCG |
| TGGAATGGAACCGCGGAA | CGGTTTCGGGTTCTCTAC | GCCGTTATTTTTGGACGCC |
| CCATCCGAACTGGAGGAA | TTTGGATTGCGTTGGCGG | |

*SerRS*

| | | |
|---|---|---|
| ACATCGTGGCGTTCAGCA | CAAAGCACAGCTTGATCCAG | CACTGACGCCACTCCGTA |
| AGCACGAGACAAGTTCCC | GCCGGCATGTACTTCTTCAA | CGATCAGGTACTTCTCATCGA |
| TATGGAATGCCCAGCGAC | AGATCAATGGGAGCGGGC | CCAGCACCATTTTAGTTACCC |
| TCCATCATCTCCCACGAC | CACCTTGATGCCCGTCTC | CAGTTTCAGTCGCGTATTAGC |

| | | |
|---|---|---|
| TGCTCCACCTTCTCGAAC | TCTCCAGGATGGCGCAGA | TGTCGTGTGGGGAGGTCAG |
| GGTAGCCATTCATCGCGA | ACATAGTCTACGGCGGCG | ACGCGGAAAATGCCGCGAG |
| TCGTCGAACTGTGACAGC | GCCTGGTAGTCCAAGCAG | TCCGCGTTCATGCCGTCGA |
| TTCGCATGAAGAAGGGCG | TGAGGGCACCGGAAACGA | ACGGACTCGTGCAGGTGGT |
| ATGAGGTCCACATGCGAG | ACTGCTCCGCATTCCCGA | ACCTCCCGCAGTGAGGTGT |
| GCTTGATCTGGTTGACGG | CTTCCTGTCGGAAGCAGG | TCGTCTGCTCGGCAAGCTC |
| GCAGTGTCTCGGCTACAA | CGATAGGCTGCTCTGAGG | ATGGCACCAACCGGCTCCT |
| ATCTTCTCGCCGATCACC | CCCACCACCTTGTAGAGC | AGTCTCCACCAGCGCCACA |
| CTGCAGACGTTCTTGACC | GCCACCTCCTGCATTACC | TCAGCTGGGCAGTGCTGGAA |
| TGATTTTCGCGCACGAGG | GCGTGCTGGATAAGAGCC | AACCAGGCCTCGAGATCCAGC |
| TCACAACGTGGCTAGGCT | AAAAGACTGCGGCTCCGG | TAGTCACGGGCGTACAGCAGG |
| CATCTTCTTAGTCTGGCCG | TTGCCGCGCTTTTCGCAG | TTCTCTCGCGTTTCGTCGGCG |
| CGGAATCTCATCCTGGAAC | GGTTCTCGTCCTCGTCGT | TTTAGGCTTAACCGGCGGCAGGG |
| CTTAATGGGCAGCGAAGAC | GTCGTCGATGAGAACGCG | TTTGCCTTTCTGCTTCTCGGCGGCGGCCAAC |
| GACTTCTGGTTCTCGGTCA | GTGAGGTCCTTGGTCACG | AAAGTAACCACGTCCGCCGGACACCACGGCTCCT |
| CTTGTCGCTGCGAAACAGA | TTCAGGTTGTCGGCACGG | |

*tud*

| | | |
|---|---|---|
| TTCCCTTGGTGGCCAGAA | ATCCTCTTGTGCAGGAGC | ATGGCGATCGATTCGCTG |
| TTGCGAATTTGGGCGCGA | AGTGGCTGGTTTTGGCAC | GCTACGTTTGTCCCAGTC |
| CTGTTCTGCATCGAGCAG | CAGGTTGTGGAGCAACAG | TTGCTTCCGCTAACGGAC |
| TGCTCTAGTGCTGGCACA | TTTTGGGCTCGCGATCCT | TGCTGCCTAACATCGACC |
| ATCTGACCACAGGAGGAC | ACAGTTTCCTTGCGACCC | CCCTTTTCCAGGGACAGA |
| GTCCAGCAGTGCGTCAAA | CCTCCTCTTCGTCCAAAG | TACGTTCAGACCATCGGG |
| CTCAAATATGGCGCTGGG | TCTTTGCCGGGTACAAGC | GCACACTAAATGTGCGCC |
| GCATATTTCGGCCACAGG | GCCGCACCTCAATCGATT | CGGTAATCTTGTCCTCGC |
| GAGCGTGAACTCTTGAGG | ATTTCCTCCGTGTTGCCG | ATTGCCTGGCGAGGCATT |
| ACCACAGTCGTATTGCCG | AAACACCTCGAAGCACGC | TGCCGCACAATCACAGAG |
| CTACTGCAGCCTTTTCCG | ACCAATTGCCATCGGAGC | TCGATGAACGACTGGAGCA |
| CGGGATGTATTCTCCACG | GCACAGATCTGTCCCACA | GAACTGCACCACAACACAG |
| GACTCCTTACTGGCTTCC | ATGGCCTGCGGTTGAACA | GGAGTTCAGCAATCAGAGG |
| AGGCGGTCGATGATGTTC | CGAGTGCTTGGAATGAGC | CTAGCAAAGCAGCAAAGGC |
| CATGATCCTGTCCTGGCT | ATGACCTGCGATCCTCCA | GACAGTGTAGAGCCAACGA |
| ACTTCGATGTGGTGGAGG | CTGTGTAGGAGCAAGTGC | GGATTAGTTTCAGCTCGGC |
| TATCGGGAATCGGGCAAC | GCCAAATATCCTCCGAGG | GATGTAGGCATCTGGCAAC |
| GCAGCCACAATCAAACCC | GATTGCATGCGGTCACAG | GCAATCTCTTCGGACAGCA |
| TCAAATCCTTCGAGGGGC | CGCAGAATGGCATTGTCC | CTAGCGCCTTTGAATCACG |
| TCCGCTGGCCAAATACTC | TGAAGTGGCTGGTGTTGC | GGTTCGATATGCGACCACA |
| TTAGCCACATCCTCGCCA | GGCAATATCACTCCCCAC | GCACCGTTTACCACGTTCA |
| GTGGCATCCGAAACGCAA | GGCTTTTGAGCATAGCCC | GGCAAAGAGGGAGACACAA |
| TTTGGCGCGATACCAGCA | CTGTTGCTAAAGCGCGCA | |
| GATAGCTGATCGATCGGG | CACTGCTGTAACTACCGG | |

*vkg*

| | | |
|---|---|---|
| GAACCCTTTGCTGGTACC | CACACAACGCAACGCGAAA | GCAAACCGTGCACCTGCT |
| GGACCAGCTAGAGTACGA | GGCATGGTTGTAAACCGCA | GGCTGGACGAACTGATCC |
| CCAGAATAAGCTCCGGCA | CTCCCTGCTCACCAATCAA | TTGCAGCGTCCATGGCCA |

| | | |
|---|---|---|
| TCGAGGCAGAACCATCTG | CGTGGTCCTTGATCACCAA | CACCGACGTTGTCCAAGG |
| GACAGTCCGGAATGGACA | CATCATCACCAGAGAGACC | ATTGCGAGTGGAGGGCGA |
| GCGTCATGGTCATTGGCA | CACGAAGTCCAATAGCTCC | TTCATGAGGTCCCTGCCC |
| GTGATGTCGCACAGCATG | CATGAAGTAACTGTAGCCGG | GTGGACAGCCAGAGACTG |
| CCTCCCATAGCAGATTCG | CGATTAGTCCATGACGACCA | TGGGCAAAGTGGCAGACG |
| TTGTCACCACGTTGTCCC | GTTGTCCAGCATAGCCAATG | ACGTTGCCCGACAGTGAG |
| GTTACACCTGGTTGACCC | GTCATCACCCTTTATGCCAC | TGAGGTACGTGGACGGAC |
| GCCTTCAGCTCCATCGAA | CCTTGTATCCAATGCCTCCA | GTGGCGGGCGAAGATGAA |
| GCCGGGAGGTCCAATAAA | CGGTTGTACTGGCGGGTA | GCTCCGGTCAAGCCCATA |
| ACGTTCACCCTGTAGACC | CCACCATGGCGAGCATAC | GATATCCGACGGCACCTC |
| ACCATCCAAGCCCACAAC | AGTTTGATGGGCCGCGAC | ACGAGTCCGTCCATGCCA |
| CGCCCTTCAGGCCATTAA | TGATCCAAGAGGAGCGCG | CACCCACCCTTCCGTTCT |
| TTGCGTCCAGCAACTCCA | CCGGCGTTAGATTCGGGA | CGGAAGTCCGGGATATCC |
| TTGCGAATCTCCAACGGG | CGGATTGGAGACCGATCC | TCGCCCTGGAAGCCGATA |
| ACCCTGCCGTCCATTGTA | TCCGGAATGCCAGCTGGA | TGCCTGCCGACAATGGCA |
| GGTCCGGTATAACCATCC | CCAGGATAAGCTCCGGCA | ACCCATGTCGCCAAGCTC |
| AGTAGACCTTGGGAGTGG | CCAGGATAAGCTCCGGCA | ATCGCACCGTTGGGTCCA |
| TTTCTACCGGGAGCTCCA | CCAGGATAAGCTCCGGCA | GCTCCCTTCTGGCCAAAG |
| CGCTCACCTTTGCTACCA | ATGACCAGGATCCGGAGC | TCCTGCTCGTCCATCGAG |
| GATCCATCCCGACCCTTT | TGGACTGAGAGCCAGGAC | |
| CTTGCTGGTAAAATCCGCC | CAGTGCGAGCCACAAAGC | |

*zip*

| | | |
|---|---|---|
| CATGTCGGCCAAAACACC | TGCTGCAAGCGCTTTTGG | AAGGCCTCCAGAATGGGA |
| GTCTCCTCTTCGAGAGAC | TCTTCTCGCAGGCCTTCT | GTTTTGCCAGCACCCGAT |
| CAATTCTTGCTGAGCGGC | GGAACTCCTGGAAGGGAA | TGCCCTTGTACCGTTCCA |
| CTAAGGTCGCGTCTAACC | TCAAGCACCAAGGGAGCA | GTTGTGCAAAACGGAGGC |
| TCTTGAATCTCGGCCAGC | GCTTCTCGTGGTTCGGTA | GCTCCTGCGAATGTTTGTG |
| ATCTACTTGTACGCGCCG | TGTTGCGCAGAGTGTCCA | CTTGAGAGCCTCTAGTTCC |
| TGCAAACGTTCCTCGAGC | ACTTAGCCAGCTGCTCCT | CCGCTTAGATCGATCAGAC |
| GAGATTGTGGCTTCGTGC | TCTGCGACTCCTCGAAAG | CATTAGTCTAGAGCGCGAC |
| TTCCTCCTCCTCAGCAAG | ATCAGGTCGATGGTAGGC | CTTAAGGTAGGCGGCACAA |
| GACAGATCGTTAGCACGC | GGTCCAACCCAAAGTCGA | GTTGGGTGTAAGGAGTTCG |
| TTTAGCGTCGAGCTGCAC | ACTCTTCCTGCTCCAGGA | GATGTTCACCACGAACGGA |
| CTTCTTCTTCGATGCGCG | CACAGCTGCTCAAAGGAG | CAAACGTCTTGTCAGTGGC |
| GTCTTCTCCACCAAAGCC | GTGCGGTCTAAAGAACGG | GGTGTGGTTAAAGAGCTGC |
| TGGTACTTGCGCTCGTAC | ATCCGGTTCACAAGCCAC | CTGTCACACTAAGTCCGAG |
| GCGTATTCTTGGCCAGAG | ATTCGCTCGTAACACGCC | GTCTGGTAGAGTTGCCTGA |
| TCCTCCTTCTGGACAAGC | TGCTCCTTTGTTTGGGCC | CATGGACTTAACCGTTGCC |
| GTAACTTCCAACAGGGGC | CCTCTGATGTCATGCCCA | |

*Act57B*

| | | |
|---|---|---|
| TCAATAGACCCCATCCGC | CAGAACGATACCGGTGGTA | GAGACACCATCACCGGAG |
| TAAGGAAACCGCGAGCGA | CGGGGAAGTTGTTAGGTTC | CCTGGATGGCGACGTACA |
| CGAACCAAGGATGACACG | CACCCAGAACCACCACAAA | TGGGTCATCTTCTCGCGG |
| AGATGAGCAGGAGACAGG | GATGGAGTTGTAGACGGTC | GCAACACGCAGCTCGTTG |
| GTGCTAGGCAACTGCAAC | GTCACGGACAATTTCACGC | ACCGTGCTCGATGGGGTA |
| TCCACATCTGCTGGAAGG | CTTCTGCATACGATCGGCAA | AGGGTGAGGATACCACGC |

| | | |
|---|---|---|
| ATGTTGGCGTACAGGTCC | GGGCAACATAGCACAACTTC | TCTGGCCCATACCGACCA |
| CGGATATCCACATCGCAC | ATGGTTGGATGGTGGTGG | CGAAACCGGCCTTGCACA |
| ATGGTGATCACCTGTCCG | TAGACCGGGTGGTGCTAG | CAAAATACATGAGGGTGTCGG |
| GGAAGCTCGTACGACTTC | AGCACTTGCGGTGGACGA | GATGGTGTTGTGTTCAGTCAG |
| GCTCGGTCAGGATCTTCA | GACTCGTCGTACTCCTCC | GCGAGTTGAAGGTCTCAAACA |
| AAATCGCGACCAGCCAGA | GGATGCCGCAGGATTCCA | CCATATCATCCCAGTTGGTGA |
| AAGGTGTGGTGCCAGATC | GAAGGCTGGAACAGGGAC | AAGTGGATGGGGATCGCGG |
| TCATCACCGACGTACGAG | GGCAACGGAAACGCTCGT | TTGCGCTCTGGGGGAGCAA |
| AACGACCAGAGCAGCAAC | GCCATCTCCTGCTCGAAG | ATGGTGGTGCCACCGGACA |
| TTTTTACGGCACCACGGG | GCGGTGGTGGTGAAAGAG | ACCGACGATGGAGGGGAAGA |
| AGTTACGGTGTGTACGGC | ATGGCATGGGGCAGAGCA | ATGGAGCCACCGATCCAGACGGAG |
| GTTGTTTTTGCCGGTGGAG | CCTCATAGATGGGGACGG | ATCTTGATGGTGGATGGGGCCAGGGAGG |

*Mhc*

| | | |
|---|---|---|
| ATTGTGGCCTAACGGACG | ACCAGATCCTGCATGCGC | TTCTGGGAGGCATCCAGC |
| CGGAATTTGCTGATGGCC | TGGTTCTTGCGGTCCTCC | CTCATGTTGTTCGGTTGAGAG |
| GCTTCGTTCAGGAGTTCG | GACTGGAAGCTCAGCTCC | GTTTTCAGGAGCAAGGTCGAA |
| GAGACTCCTCCAGTTCGT | TCGGACTTGCGCAGGTTC | GTCTTGATCTTCTGTTGCAGC |
| TGGCGTGATCCAGAGCAA | TGCCTCCTCTGCTCACCA | GTATGCTAATCGATGGTGATCG |
| AGCTCGTTGATGTCAGCC | ACGCGCTGCTCAAGCTTC | TGGTGGGAAGGCCAATCCG |
| GTGTTCTCGAACTCCTCC | ATGGCCTTCTTGCCTCCC | ACAGAACCGGCACGTCCCT |
| TCGAGCAGATCCTTGACC | CTCGAGGGCCTTCCTCAA | TCAGCCTCCTCGATCTGCC |
| TCGGCCAGGTTCTTGTTC | TCCTGGGTCTGGGCATGA | AGACGGACCTGCAGCTCCT |
| CCCTTAAGACGGAACAGC | CGGCATCGACCATAGCCT | TGCAGCTCGGACTCCAGCT |
| CATAAGCGCAGTGTGTAGC | TGGCCTTCTCCTCGGAGT | TCGGCCTGTTCCAGCAGAG |
| GTCGTCCGTAAGTCTTGTC | GCGGACACTTCGTTCAGC | TCCTCGAGGGCAGTCTGGA |
| TTCGAACTGCGGGCGACA | TTGCACGACGCTCGGAGA | AGGGCACGCTGGTGGTTCT |
| TCCGCGGGGCCTTCATTT | AGCTGCTGCTGGTAACGC | AGCCTGGAGCTCGTCCTTC |
| GGGCTCACGTTTCGCGAT | TTCTTCATGCGCAGGGCC | ACGCACAGCCTCCAACTGC |
| TACAGGTCCAGCGAGCAG | CTTCGAGGGAAGCCTGCA | ATGTTCTTCTGGGCCTCGGCG |
| CCATGGCAAATGTCGCGC | ACCTGGGACAGCTCAAGC | TTTGGCCAAGTTGAGGGCGGCGA |
| GCCTAAGTGCATCTGGCG | CGGAGCACCTTGTTCTCC | TCTTGGCAGCGGAGATGGAGGCGT |
| TTGGTGGTTTGCCTCCCG | TTGCGGGCCTTCTCGATC | TTCTCCTGGATGCGGCGGTCGATC |
| TCAAGCTCCTGCTGAGCC | GTGGAGTAGTTGCGGCAC | ATGTTGCGGCCACCCTCACCGATC |

*wupA*

| | | |
|---|---|---|
| GGCGTTCAGATGTTTGGC | CGGATCGTTGTTGATCGGA | GAGATTTGAGTGTGTCTTCGC |
| TGGACACTAGTGGACGTG | CAGTGCTTGCGATTAATGCC | GCCTTCTAAATCCACATCCAG |
| TAAGCTTCGGCCTCAACC | CAACGTTCTTCGATGATGCG | CTATGCTGTCGATCACACGAA |
| TCCTTCTTCTTCACCACC | CCCGTCCAAATCACTTCCAA | CGACACAAAAAGACTGAACGG |
| ACGAACTTGCCGCGAAGA | CCTTGGACCAGTCGGGTT | GTGGACACATATATATGGCGAG |
| TCTTCCTCTCTGGGGTCA | CGGCCTTCTTCTGCAGCT | TTCTCCTCCTCCTCCAGCG |
| TTCTTGGCCTTCTTGGCC | GGAGACCTTCTTCAGGGC | TCTTCAGCTCCTCAGCGGC |
| ACGATCCACGGCAGACTA | CGCTGAGATTCCTGGGAC | TCAGCACGCTTGCGCTCGA |
| TCGTATCGCATCGTCTCG | ACGTTCAGCCGCTTTGCG | TTCACCTTGGCATCTCCGGGC |
| GGCTCGGTTCCGTTATGT | ACGCAGCAGCAACCTGAG | TTGTTTAGGGCGGGAGTCACGGG |
| CTGGTTGCGGAAGTTGAAC | AGGCTTCCTCCATGCGCT | TCTAGCGGCTAGCCACCCAACGGA |
| CTCACCTCATCATCAGCCA | CTTGGGCATTGAGATCGTTGA | |

*BicD(CDS)*

| | | |
|---|---|---|
| GAAGTTTACGCTGCACGC | CTGTAAGGTCTCTAGCGC | CAGCGATATGTTCTCCTCC |
| TGGATTCCTGCTCGAAGG | CTTCAGTGAGACGACGGA | CTGGGCGGAATCTTTTCGA |
| CGGTCCATTTCCATCTCC | GTCTCCCGGAACTTAAGG | CCGTTTGAATGCGAACGTG |
| TCCACCTGGGTCACATAC | CTCTTGTCCCGCCCAAAA | GTGTGTGTGTGGAATGGTA |
| CACGCAGGCTTGAGAATG | AGTTCTCCTGCAGCATCC | CTTTCGTTCGCTGGCAAAG |
| ACCTCAGCGGTTTGCTTG | AACTCATGGCGCAGTTGC | GTCGTCGATGGAGTCGAAA |
| GCTTCACGGACAGCAAAC | TGAAACTTGGTCAGCGCC | CACTCACCGCGCTAAATTAG |
| GACTATCTGCTCCTGCAG | AGGTCTTGCACGGATTGG | CTTGGCAATGTTTGTGACGG |
| TGGTATGCTCAACAGCCG | GATGGATGGATGGTGTCC | CGGGTTGGCCAATTAATGCA |
| CGAAGCTCATGTCATCGG | TGCGGGTTTTCTCCTCTC | CAGATCAAACCAATCAGGCG |
| GTGTCTCTCCGTTGACTG | AAAACGCAGCGCAGGAAG | GTAGTTGGATACAGCTGGGA |
| TGATACAGCTGCGCCAGA | ACGACTGCTCTTCGCGTA | GAATGGATTGGCGTTACTGC |
| CGCTTAAGGCCACCAATG | TGTCCGCAATCACGTCGA | GTCTTTTTCTCCTCCTCTGC |
| CCAGCGTTTTGCGAGATG | GTTCAATGGCTGCAAGCCA | CGCTGACAATGATCTTCTCG |
| TGAACATCGCTCTGCAGG | GACAAGTACGCCATTGGTG | CCATCTCCTCTGTGTTAACC |
| TGGTGGCGTCCGTATAGT | CTCTCATTTCCGCAGGAAC | GATCACTGACTGTATCCACG |
| AGCTGCTGCTCCAGTTCA | CTCCAATTGGCGGTTGAGA | GTTCCGTAGCAAGAAGCTTG |
| TTCTTCTGGCCACCTTCC | GCATCCTCCTTAAGAAGCC | CAGTCTTAAGGCCATCGATC |
| CCTGCTCCTTCACATCGA | CGTACTGCGAGATTAACGC | CACTTTCCATGCTCTCCAAC |
| GAAGAGCCAGACGAGACA | CTGCAGCTCGTTTTGTGAC | CTCCGAGTATTCGCTAAGCA |
| TCCAGACTCGTCTGAGCT | GAGATCACATTTGGTGCCG | CTCGTTGTTGCTGTTGATGC |
| TTCGCCGTCAGATGAGTC | CAGACGCTTAAGAGCCAGA | GCCGCACTGTTTTGTTGTAC |
| TGCTGGCGTTGTCTTCCA | GTGGTACATAGACTCACGG | |
| AAGTGGCCATCCAGTTCC | GGCACCTTCAAATTCCACC | |

*BicD(RC)*

| | | |
|---|---|---|
| GTTCGCAAAAAGGGACGG | CCACAGTTACCACATGCAAAG | GCAACTTGTTTTGTTCGCTTGC |
| TACCGAAAGTGCTCTGGC | CCACTTTACTTCGTTTCTGGC | TCCTCGCTTTTCTGGCGCG |
| TGAACGGAAATCCGCCCA | CTTTGGCTTGTTGGATCGATG | GGACTTTTGCTTGGACACGAAAC |
| CCAAAACGATGCAACCAGG | GCAATGAATGGACGTAGTGTG | CGTTATTGGTTCAGTGAGTTGCG |
| GCAGTTTGCCGGCATTTTATC | GATTTCTCTGCGGGTTAAACG | GGTTAAGCTGCTGGTAATCACCA |
| GGGCTATCCCTTGCACAC | CATTCGTAATCCATCGTTTGGG | GGTTTTAGGCTTTTTTGAGGGTGG |

*EGFP*

| | | |
|---|---|---|
| TCTTCTGCTTGTCGGCCAT | ATGGGGGTGTTCTGCTGGT | ACGCTGCCGTCCTCGATGTT |
| CGTCCTCCTTGAAGTCGAT | CCTTCAGCTCGATGCGGTT | TCCAGCTTGTGCCCCAGGAT |
| GCGGATCTTGAAGTTCACCT | TTCAGGGTCAGCTTGCCGT | AGGGTGTCGCCCTCGAACTT |
| GACGTTGTGGCTGTTGTAGT | TTTACGTCGCCGTCCAGCT | TCGGCGCGGGTCTTGTAGTT |
| GGACTTGAAGAAGTCGTGCT | TGAACAGCTCCTCGCCCTT | TGGACGTAGCCTTCGGGCAT |
| GTCGTCCTTGAAGAAGATGGT | TAGGTCAGGGTGGTCACGA | AGCTTGCCGGTGGTGCAGAT |
| CGAACTCCAGCAGGACCAT | AGCTCGTCCATGCCGAGAGT | TCGCCGGACACGCTGAACTT |
| GACTGGGTGCTCAGGTAGT | ATCGCGCTTCTCGTTGGGGT | TCATGTGGTCGGGGTAGCGGCTGAAGCACT |